

Department of Chemistry
Thesis

**Reactions of some rhodium complexes in
imidazolium ionic liquids**

Maira Hernández Guzmán

This PhD project has been funded by the National Council of Science and Technology, (Consejo Nacional de Ciencia y Tecnología, CONACyT), Mexico. Scholarship 113454.

A la memoria de mi madre

Agradecimientos

Acknowledgements

Gracias a la Universidad de Sheffield por aceptarme en el Doctorado. Al Prof. B. E. Mann por permitirme trabajar en su proyecto y por su enorme paciencia.

Un especial agradecimiento a mis amigos de Sheffield, por todos los buenos momentos compartidos.

A los compañeros del lab. D28, por su apoyo y confianza. En especial a la Dra. Castro por su agradable compañía y al Dr. Johnson por sus clases de “ingles común” y sus correcciones.

A mis compañeros de Cardiff por todos sus festejos y el buen trato que he recibido.

A todas las personas que de alguna u otra manera han contribuido a la realización de este trabajo.

A mi familia por su apoyo incondicional y por la fortaleza e inspiración que han fundado en mi. Gracias a mi Padre, Carmelita, Zayra, Agustin y Arturo.

Finalmente gracias a Dios por darme vida y salud para realizar el sueño mas grande de mi vida.

Index

Abbreviations	v
List of complexes	vii
Abstract	1
1. Introduction	3
1.1. Chemistry and Society	3
1.2. Green Chemistry	4
1.3. Alternatives to organic solvents	6
1.4. Ionic liquids	9
2. Background	15
2.1. Ionic Liquids	15
2.2. Synthesis of ionic liquids	16
2.3. Characteristic properties of ionic liquids	18
2.3.1. <i>Melting points</i>	19
2.3.2. <i>Viscosity and thermal stability</i>	20
2.3.3. <i>Solvation strength and solubility characteristics</i>	21
2.4. Ionic liquids as solvents and catalysts	22
2.4.1. <i>Ionic liquids in reactions: Hydrogenation</i>	24
2.4.2. <i>Hydroformylation</i>	25
2.4.3. <i>Polymerization</i>	26
2.4.4. <i>Alkylation and C-C bond forming</i>	26
2.4.5. <i>Diels-Alder reaction and Friedel-Craft acylation</i>	27
2.5. Chloroaluminate (III) ionic liquids: Chemical properties	28
2.5.1. <i>Reactions in chloroaluminate (III) ionic liquids:</i> <i>Friedel Craft acylation</i>	31
2.5.2. <i>Transition metal catalysed reactions in</i> <i>chloroaluminate (III) ionic liquids</i>	33
2.5.3. <i>Hydrogenation in chloroaluminate (III) ionic liquids</i>	33

2.5.4. <i>Dimerization in chloroaluminate (III) ionic liquids</i>	33
2.6. Catalytic hydrogenation with rhodium complexes	35
2.6.1. <i>Wilkinson's catalyst: [RhCl(PPh₃)₃]</i>	35
2.6.2. <i>Monocationic Rhodium-olefin catalyst for hydrogenation</i>	40
2.7. Interaction of [SnCl ₃] ⁻ with metallic centres	43
2.8. Interaction of metallic centres with weak coordinating anion	45
2.9. Summary	45
2.10. Aim of the work	46
2.11. Bibliographic references	47
3. Experimental	52
3.1. Instrumentation	52
3.2. Synthesis of ionic liquids	54
3.3. Synthesis of [Rh(Cl)(PPh ₃) ₃] and its reactions in [emim][Al ₂ Cl ₇]	54
3.4. Synthesis of [RhCl(CO)(PR ₃) ₂] compounds	57
3.5. Reaction of [emim][Al ₂ Cl ₇] with [RhCOCl(PR ₃) ₂]: formation of Rh(I) carbonyls from Rh(III) complexes by carbonylation	60
3.6. Synthesis of chlorostannate diphosphine rhodium complexes in [bmim][Sn ₂ Cl ₅]	62
3.7. Synthesis of [Rh(diolefin)(Ph ₂ P(CH ₂) _n Ph ₂)]X, [Rh(PPh ₃) ₃][PF ₆] and their reaction with H ₂ in [bmim][BF ₄] and [emim][PF ₆]	63
3.8. Hydrogenation of cyclohexene in biphasic conditions: ionic liquid/hexane	65
3.9. Bibliographic references	64
4. Results and discussion: Solution in [emim][Al₂Cl₇]	67
4.1. [RhCl(PPh ₃) ₃] in [emim][Al ₂ Cl ₇]	67
4.1.1. <i>A vacant site</i>	72
4.1.2. <i>The coordination of nitrogen or the formation of a carbene</i>	74
4.1.3. <i>[AlCl₄]⁻ as ligand</i>	74
4.2. Solution of [Rh(Cl)(PPh ₃) ₃] in [emim][Al ₂ Cl ₇]/Al ⁰	76
4.2.2. <i>Interaction with the imidazolium ring to give Rh(I) hydride</i>	77
4.2.1. <i>Al⁰ as a reductive agent</i>	80

4.3.	Hydrogenation of $[\text{Rh}(\text{Cl})\{(\mu\text{-Cl})\text{AlCl}_3\}(\text{PPh}_3)_2]^-$ in $[\text{emim}][\text{Al}_2\text{Cl}_7]$, $x_{\text{AlCl}_3} = 0.67$	81
4.4.	Summary	86
4.5.	References	86
5.	Results and discussion:	
	Solution of $[\text{RhCl}(\text{PPh}_3)_3]$ in CH_2Cl_2 with AlCl_3	93
5.1.	$[\text{RhCl}(\text{PPh}_3)_3]$ in $\text{CH}_2\text{Cl}_2/\text{AlCl}_3/\text{HCl}$	93
5.2.	Reaction of $[\text{RhCl}(\text{PPh}_3)_3]$ in CH_2Cl_2 and toluene with 10-fold excess of AlCl_3	102
5.3.	References	105
6.	Results and discussion:	
	Carbonylation of rhodium complexes in $[\text{emim}][\text{Al}_2\text{Cl}_7]$	106
6.1.	Carbonylation of $[\text{RhCl}\{(\mu\text{-Cl})\text{AlCl}_3\}(\text{PPh}_3)_2]^-$ in $[\text{emim}][\text{Al}_2\text{Cl}_7]$	106
6.2.	Reaction of $[\text{Rh}(\text{Cl})(\text{CO})(\text{PPh}_3)_2]$ in $[\text{emimCl}]\text{AlCl}_3$, $x_{\text{AlCl}_3} = 0.67$	108
	6.2.1. <i>Solution of $[\text{Rh}(\text{Cl})(\text{CO})(\text{PR}_3)_2]$ in $[\text{emim}][\text{Al}_2\text{Cl}_7]$</i>	109
	6.2.2. <i>Alternative of Rh(III) for 38</i>	113
	6.2.3. <i>Solution of $[\text{Rh}(\text{Cl})(\text{CO})(\text{PR}_3)_2]$ in $[\text{emim}][\text{Al}_2\text{Cl}_7]$</i>	118
	6.2.3. <i>^{103}Rh {INEPT} NMR data</i>	125
6.3.	Carbonylation of $[\text{Rh}(\text{Cl})\{(\mu\text{-Cl})_2\text{AlCl}_2\}(\text{CO})(\text{H})(\text{PPh}_3)]$, 39, in $[\text{emim}][\text{Al}_2\text{Cl}_7]$, $x_{\text{AlCl}_3} = 0.67$	129
	6.3.1. <i>Hexacoordinated Rh(III) complex, an alternative for 37</i>	135
	6.3.2. <i>Rh(I) centre as a second alternative for 37</i>	137
6.4.	Characterization of $[\text{Rh}(\text{Cl})\{(\mu\text{-Cl})\text{AlCl}_3\}(\text{CO})_2(\text{PPh}_3)]^-$, 68; the second product of carbonylation of $[\text{Rh}\{(\mu\text{-Cl})\text{AlCl}_3\}(\text{H})(\text{PPh}_3)_2]^-$, 25 and $[\text{Rh}\{(\mu\text{-Cl})\text{AlCl}_3\}\{(\mu\text{-Cl})_2\text{AlCl}_2\}(\text{H})(\text{CO})(\text{PPh}_3)]$, 38	143
6.5.	The observation of a possible carbonyl rhodium complex in the carbonylation of $[\text{Rh}\{(\mu\text{-Cl})\text{AlCl}_3\}(\text{H})(\text{PPh}_3)_2]^-$, 25 and $[\text{Rh}\{(\mu\text{-Cl})\text{AlCl}_3\}\{(\mu\text{-Cl})_2\text{AlCl}_2\}(\text{H})(\text{CO})(\text{PPh}_3)]$, 38 in $[\text{emim}][\text{Al}_2\text{Cl}_7]$	148
	6.5.1. <i>Possibilities of Rh(III) for 74</i>	150
	6.5.2. <i>Possibilities of Rh(I) for 74</i>	151
	6.5.3. <i>Possibilities of Rh(0) for 74</i>	152

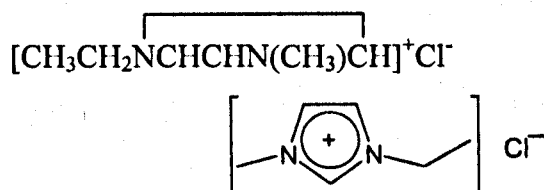
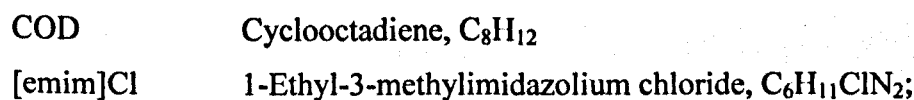
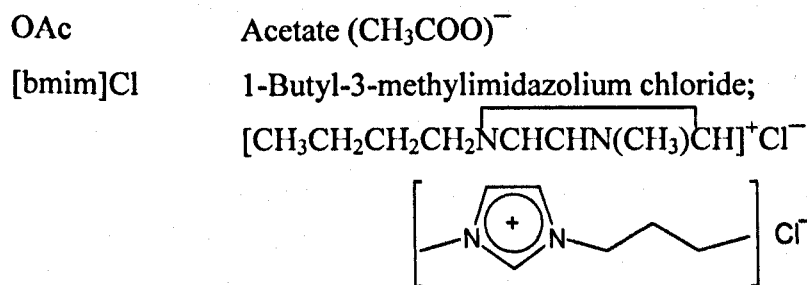
6.6. Solution of $[\text{Rh}(\mu\text{-Cl})(\text{CO})_2]_2$ in $[\text{emim}][\text{Al}_2\text{Cl}_7]$ with the addition of PPh_3	154
6.7. Carbonylation of $[\text{Rh}\{(\mu\text{-Cl})\text{AlCl}_3\}\{(\mu\text{Cl})_2\text{AlCl}_2\}(\text{H})(\text{CO})(\text{PR}_3)]$ in $[\text{emim}][\text{Al}_2\text{Cl}_7]$	160
6.8. Solution of $[\text{Rh}(\text{H})(\text{CO})(\text{PPh}_3)_3]$ in $[\text{emim}][\text{Al}_2\text{Cl}_7]$	164
6.9. Summary of the solutions of $[\text{Rh}(\text{Cl})(\text{PPh}_3)_3]$, $[\text{RhCl}(\text{CO})(\text{PR}_3)_2]$, $[\text{Rh}(\mu\text{-Cl})(\text{CO})_2]_2$ and $[\text{Rh}(\text{H})(\text{CO})(\text{PPh}_3)_2]$ in $[\text{emim}][\text{Al}_2\text{Cl}_7]$	166
6.10. References	167
7. Results and discussion:	
Solutions in $[\text{bmim}][\text{Sn}_2\text{Cl}_5]$	170
7.1. $[\text{RhCl}(\text{PPh}_3)_3]$ and $[\text{Rh}(\text{Cl})(\text{CO})(\text{PR}_3)_2]$ in $[\text{bmim}][\text{Sn}_2\text{Cl}_5]$	171
7.2. Solution of $[\text{Rh}(\text{Cl})(\text{CO})(\text{PPh}_3)_2]$ in $[\text{bmim}][\text{Sn}_2\text{Cl}_5]$	174
7.3. Solution of $[\text{Rh}(\text{Cl})(\text{CO})(\text{PR}_3)_2]$, $\text{R}_3 = \text{Et}_3, \text{MePh}_2$ in $[\text{bmim}][\text{Sn}_2\text{Cl}_5]$	177
7.4. Summary	180
7.5. References	181
8. General Conclusions	183
Appendix 1. Crystallographic data	186
Appendix 2. Spectrographic data of known rhodium complexes	196
Appendix 3. Useful graphics	202
Appendix 4. ^{31}P, ^1H and ^{103}Rh NMR spectrum of $[\text{Rh}(\text{Cl})\{(\mu\text{-Cl})_2\text{AlCl}_2\}(\text{CO})(\text{H})(\text{PR}_3)]$	210

Abbreviations

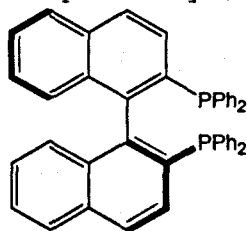
COSY	Correlation Spectroscopy
δ	Chemical shift
dd	double doublet
dt	double triplet
EXSY	Exchange Spectroscopy
eq.	Equation
fig.	Figure
Hz	Hertz
INEPT	Inductive Enhancement Polarization Transfer
NOESY	Nuclear Overhauser Effect Spectroscopy
ppm	Parts per million
TOF	Turn Over Frequency
x	molar fraction:

$$x_a = \frac{n_a}{n_a + n_b}$$

$n_a = \text{mol AlCl}_3; n_b = \text{mol [emim]Cl}$

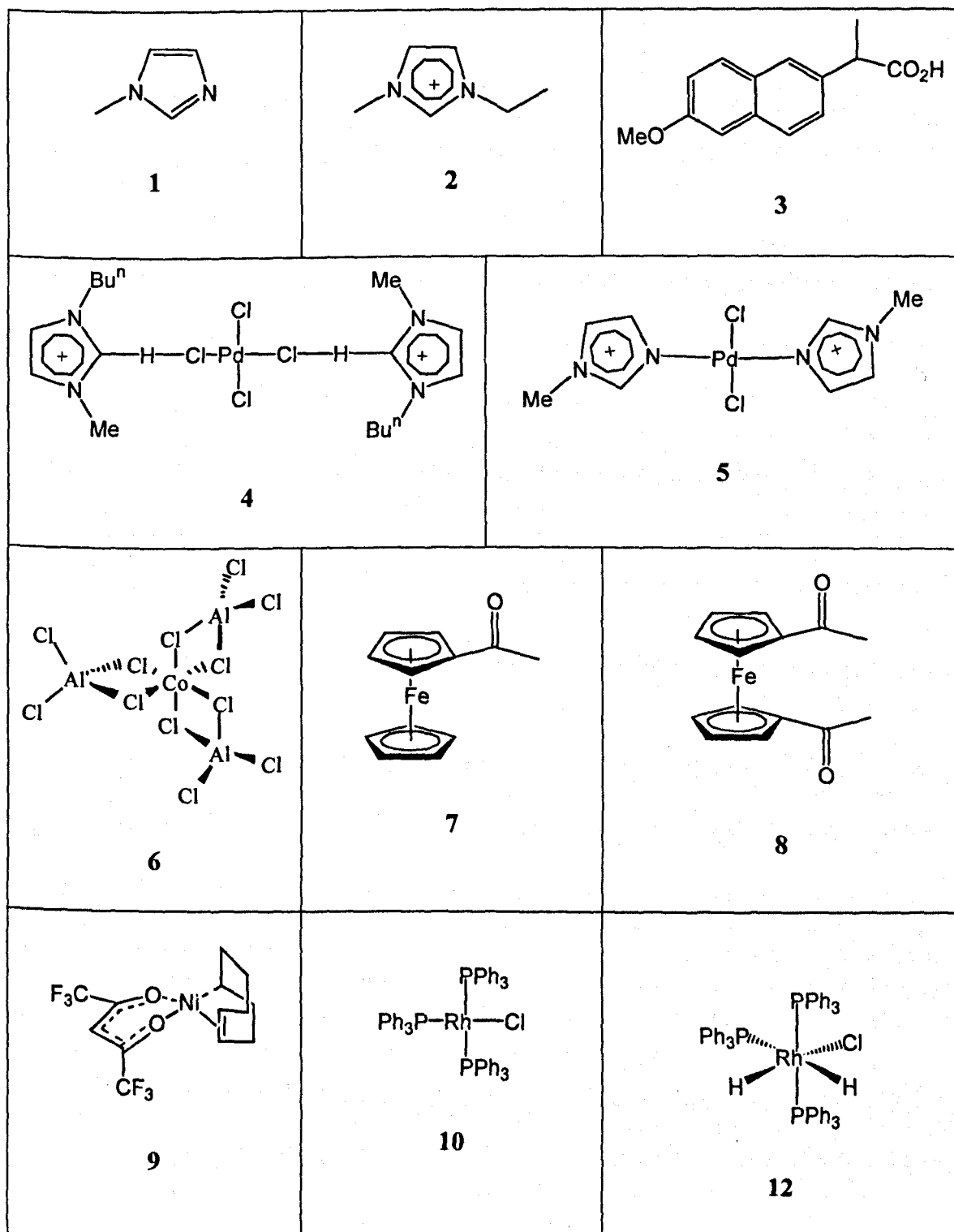


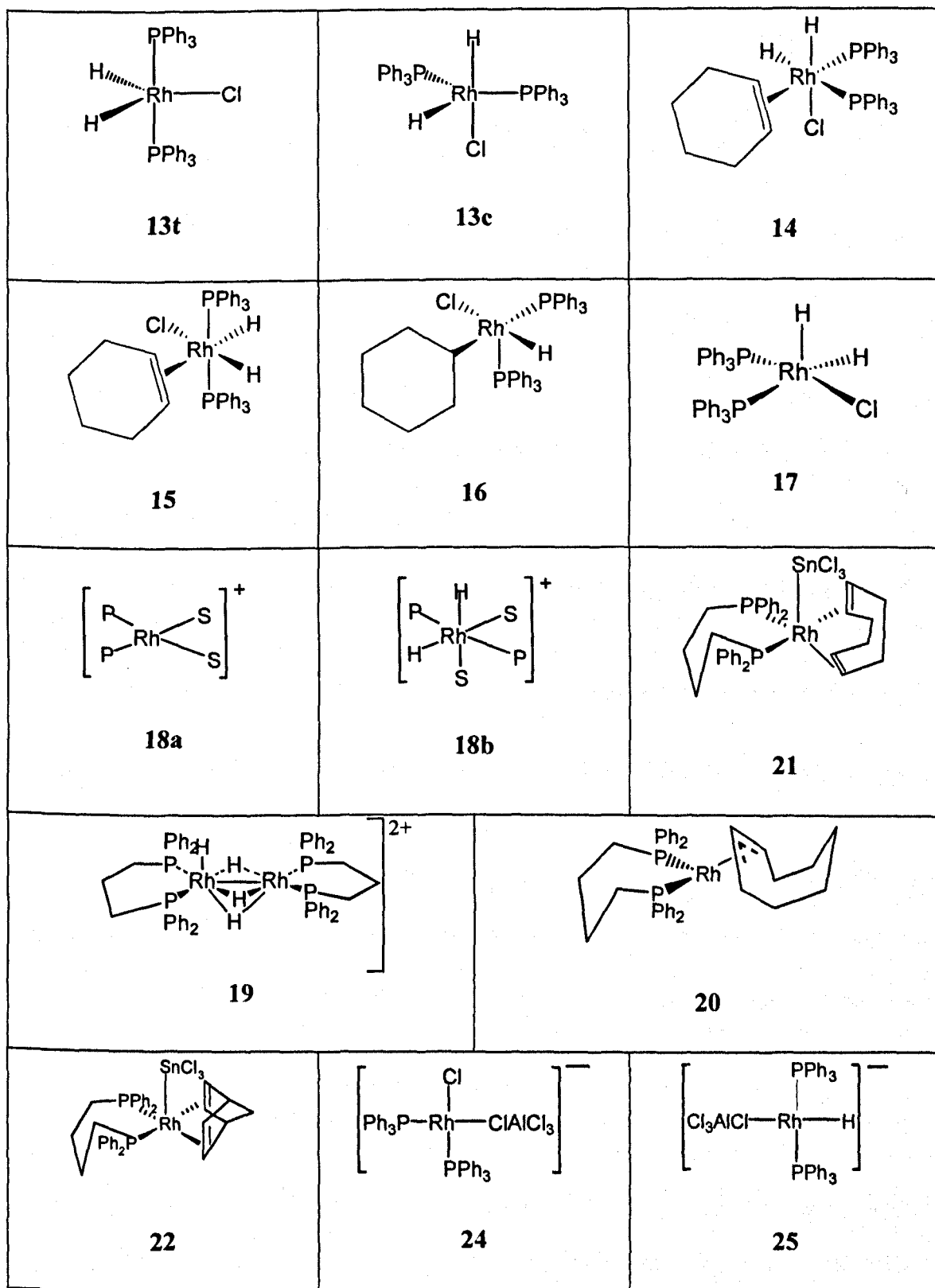
dipp	1,3-Bis-(di-isopropylphosphino)propane, $\text{Pr}'_2\text{P}(\text{CH}_2)_3\text{PPr}'_2$
dipb	1,3-Bis-(di-isopropylphosphino)butane, $\text{Pr}'_2\text{P}(\text{CH}_2)_4\text{PPr}'_2$
dppb	1,4-Bis-(diphenylphosphino)butane, $(\text{C}_6\text{H}_5)_2\text{P}(\text{CH}_2)_4\text{P}(\text{C}_6\text{H}_5)_2$
dppe	1,2-Bis-(diphenylphosphino)ethane, $(\text{C}_6\text{H}_5)_2\text{PCH}_2\text{CH}_2\text{P}(\text{C}_6\text{H}_5)_2$
dppm	1,2-Bis-(diphenylphosphino)methane, $(\text{C}_6\text{H}_5)_2\text{PCH}_2\text{P}(\text{C}_6\text{H}_5)_2$
nbd	Norbornadiene, Bicyclo[2.2.1]heptane
PCy ₃	Tricyclohexyl phosphine, $\text{C}_{18}\text{H}_{33}\text{P}$
PEt ₃	Triethylphosphine, $\text{C}_6\text{H}_{15}\text{P}$
P(OMe) ₃	Trimethylphosphite, $\text{C}_9\text{H}_{27}\text{O}_3\text{P}$
PPr ⁱ ₃	Triisopropyl phosphine, $\text{C}_9\text{H}_{21}\text{P}$
PPh ₃	Triphenyl phosphine, $\text{C}_{18}\text{H}_{15}\text{P}$
PMe ₂ Ph	Dimethylphenylphosphine, $\text{C}_8\text{H}_{11}\text{P}$
P(<i>p</i> -tol) ₃	Tris(<i>p</i> -tolyl)phosphine, $\text{C}_{21}\text{H}_{21}\text{P}$
PPN	bis(triphenylphosphino)iminium
sbp	square based pyramid
sp	square planar
(S)-BINAP	(S)-(\square)-2,2'-Bis(diphenylphosphino)-1,1'-binaphthyl; Phosphine, [1,1'-binaphthalene]-2,2'-diylbis[diphenyl]

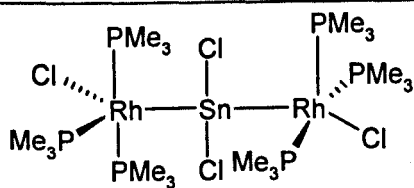


THF	Tetrahydrofuran
TMPP	Tris(2,4,6-trimethoxyphenyl)phosphine, see compound 74
TMS	Tetramethylsilane, $(\text{CH}_3)_4\text{Si}$
TMSO	Trifluoromethanesulfonate, $[\text{CF}_3\text{SO}_3]^-$, commonly known as triflate
tbp	trigonal bipyramidal
triphos	$\text{CH}_3\text{C}\{\text{CH}_2\text{P}(\text{C}_6\text{H}_5)_2\}_3$
ttp	$\text{PhP}((\text{CH}_2)_3\text{PPh}_2)_2$

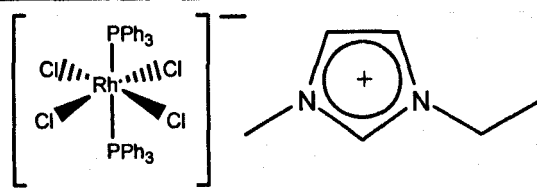
List of complexes



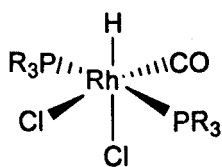




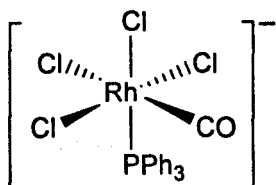
23



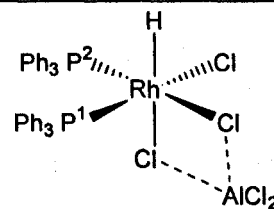
26



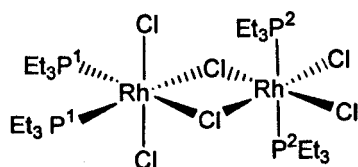
27



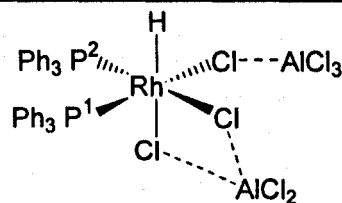
28



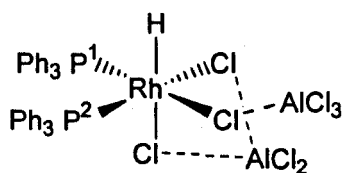
29



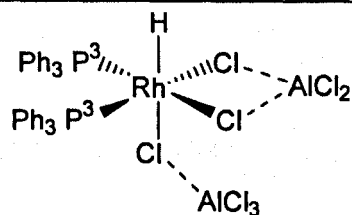
30



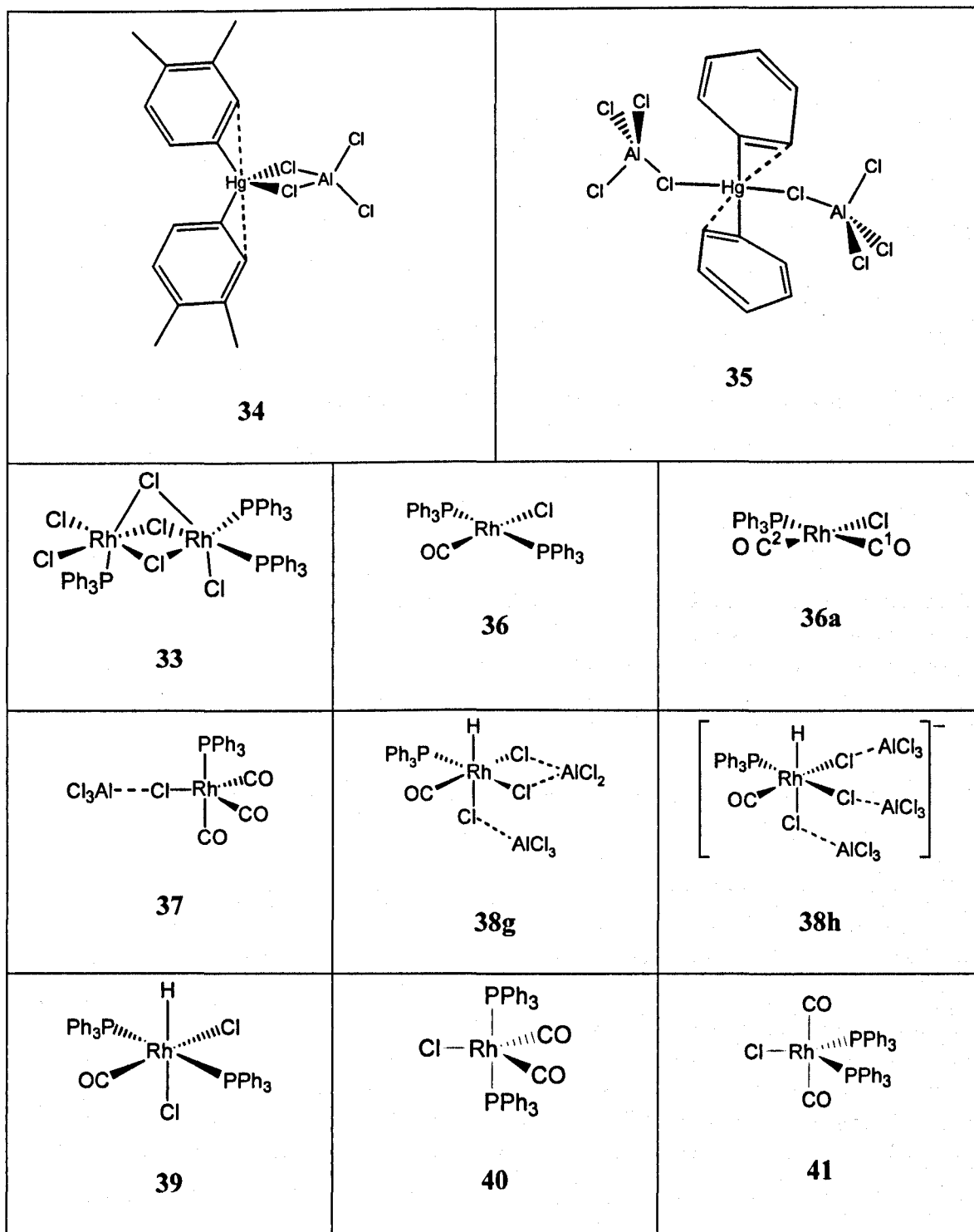
31a

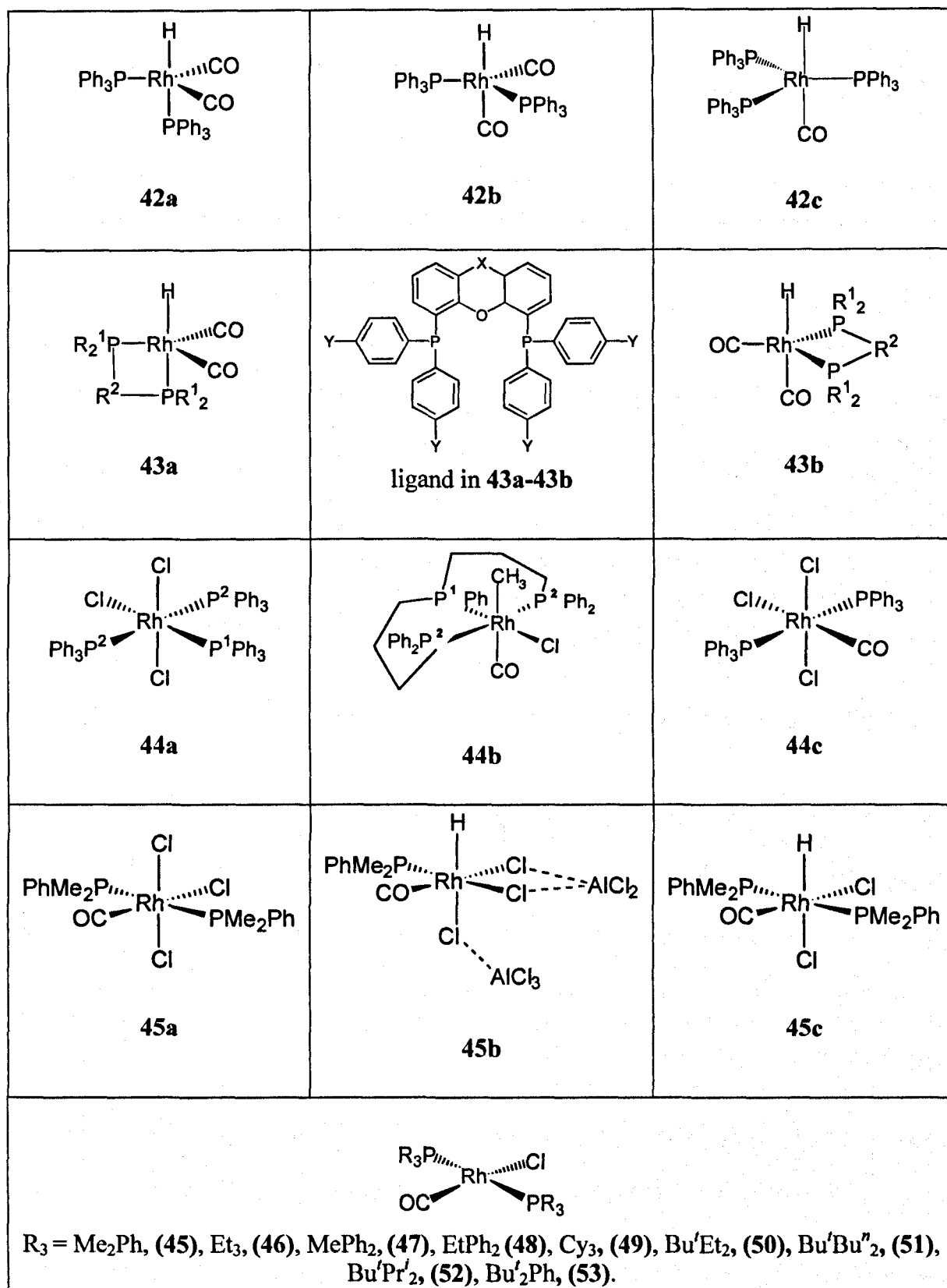


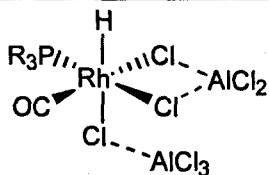
31b



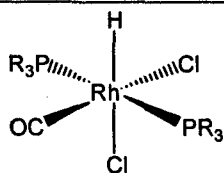
32



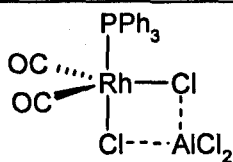




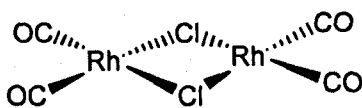
$R_3 = \text{Me}_2\text{Ph}$, (45b), Et_3 , (54), MePh_2 , (55), EtPh_2 (56), Cy_3 , (57), Bu^iEt_2 , (58), Bu^iBu^n_2 , (59), Bu^iPr^n_2 , (60), Bu^i_2Ph , (61).



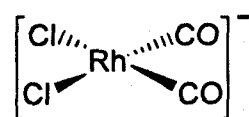
$R_3 = \text{Me}_2\text{Ph}$, (45c), Et_3 , (62), MePh_2 , (63), EtPh_2 (64), PPh_3 (38), Bu^iEt_2 , (65), Bu^iBu^n_2 , (66), Cy_3 , (67).



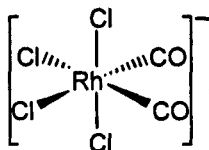
68



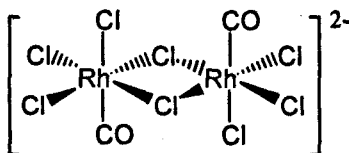
69



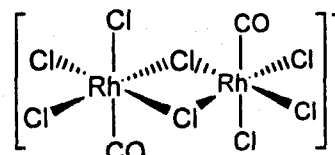
70a



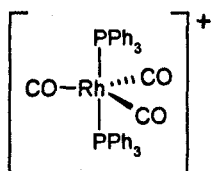
71



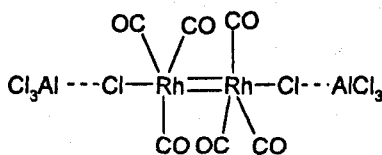
72a



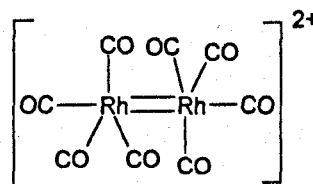
72b



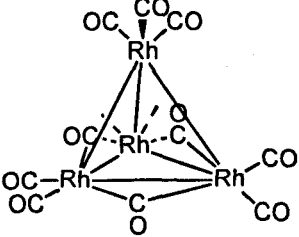
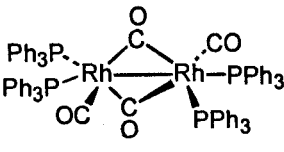
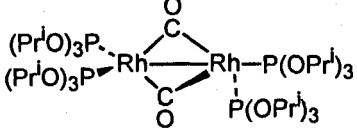
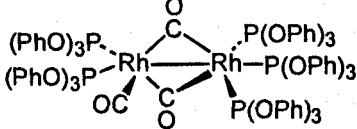
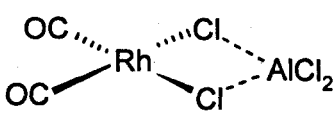
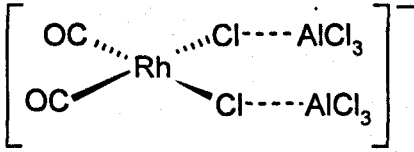
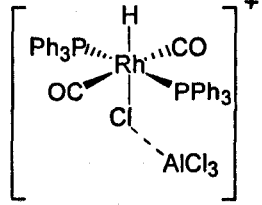

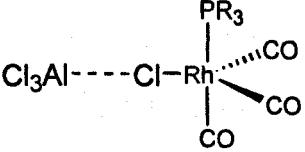
73



74a



74b

 <p style="text-align: center;">75b</p>	 <p style="text-align: center;">75c</p>
 <p style="text-align: center;">75d</p>	 <p style="text-align: center;">76</p>
 <p style="text-align: center;">77a</p>	 <p style="text-align: center;">77b</p>
 <p style="text-align: center;">78a</p>	 <p style="text-align: center;">88a</p>
 <p>R₃ = Me₂Ph, (79a), Et₃, (80a), MePh₂, (81a), EtPh₂ (82a), Bu^tEt₂, (83a), Bu^tBuⁿ₂, (84a), Bu^tPr^t₂, (85a), Cy₃, (86a), Bu^t₂Ph, (87a)</p>	

R₃ = Me₂Ph, (79b), Et₃, (80b), MePh₂, (81b), EtPh₂ (82b), Bu^tEt₂, (83b), Bu^tBuⁿ₂, (84b), Bu^tPrⁱ₂, (85b), Cy₃, (86b), Bu^t₂Ph, (87b)	
88b	89a
89b	90
R₃ = PPh₃, (91a), Et₃, (93), MePh₂, (94).	91

Abstract

Ionic liquids have been used as novel solvents in chemical reactions with higher yields than common organic solvents. The present work starts by showing an introduction where ionic liquids are discussed as a green alternative as solvents. After this the background of ionic liquids is explained, including a short review of recent results that include the use of organometallic compounds as catalysts in these solvents. Many of those works do not give details about the interaction of catalysts with the ionic solvents. After this, the experimental part is explained and the results are shown.

The first part of the results examines the chemistry of Wilkinson's catalyst $[\text{RhCl}(\text{PPh}_3)_3]$ in $[\text{emimCl}][\text{AlCl}_3]$ ionic liquids with $x_{\text{AlCl}_3} = 0.65$ (acidic). These results propose an interaction between the rhodium compound and the anionic species $[\text{AlCl}_4]^-$ of the ionic solvent. The complete dissociation of one phosphine to yield $[\text{Rh}(\text{Cl})\{\mu\text{-Cl}\}\text{AlCl}_3\}\{\text{PPh}_3\}_2]^-$, **24**, is observed. The reaction with H_2 in the ionic solvent shows the formation of one symmetric hydride, $[\text{Rh}\{\mu\text{-Cl}\}\text{AlCl}_3\}\text{H}\{\text{PPh}_3\}_2]^-$, **25**. Secondly, the study of $[\text{Rh}(\text{PPh}_3)_3\text{Cl}]$ in CD_2Cl_2 by adding AlCl_3/HCl yielded the formation of Rh(III) species that have been partially identified as three isomeric forms of $[\text{Rh}\{\mu\text{-Cl}\}_2\text{AlCl}_3\}\{\mu\text{-Cl}\}\text{AlCl}_3\}\{\text{H}\}\text{Cl}\{\text{PPh}_3\}_2]$, **31a**, **31b** and **31c**, depending on the position of $[\text{ClAlCl}_3]^-$ anion and the μ -coordination.

Thirdly, the reaction of **25** in $[\text{emim}][\text{Al}_2\text{Cl}_7]$ with CO yields a tricarbonyl as intermediate $[\text{Rh}\{\mu\text{-Cl}\}\text{AlCl}_3\}\{\text{CO}\}_3\{\text{PPh}_3\}]$, **37**, that is unstable and a biscarbonyl as final product $[\text{Rh}(\text{CO})_2\{\mu\text{-Cl}\}_2\text{AlCl}_2\}\{\text{PPh}_3\}_2]^-$, **68**. The solution of $[\text{RhCl}(\text{CO})(\text{PPh}_3)_2]$, **36**, yields a hydride of the type $[\text{Rh}\{\mu\text{-Cl}\}\text{AlCl}_2\}\{\mu\text{-Cl}\}\text{AlCl}_3\}\text{H}\{\text{CO}\}\{\text{PPh}_3\}]$, **38**, that reacts with CO to give **37** and **68** in the same way as **25**. The study of complexes with other PR_3 groups such as PMe_2Ph , **45b**, PEt_3 , **54**, PMePh_2 , **55**, PEtPh_2 , **56**, PBu^tEt_2 , **57**, PBu^tBu^n , **58**, PBu^tPr^i , **59**, PCy_3 , **60**, PBu^t_2Ph , **61** in the Vaska's type complex was compared with **36**. These showed the formation of an analogue hydride to **38** and the reaction with CO gave the formation of similar complexes to **37** and **68** in each case. Also, the solution of $[\text{Rh}(\text{CO})_2\text{Cl}]_2$ in $[\text{emim}][\text{Al}_2\text{Cl}_7]$ produced a new species that corresponds to the cleavage of the

dimer to yield $[\text{Rh}\{(\mu\text{-Cl})\text{AlCl}_3\}_2(\text{CO})_2]^-$. The addition of PPh_3 to the last solution gave the formation of $[\text{HPPH}_3]^+$, **68**, **38**, **37** and the formation of three more complexes that have been partially identified as Rh(III) species.

Finally, the study of $[\text{RhCl}(\text{CO})(\text{PR}_3)_2]$, where $\text{PR}_3 = \text{PPh}_3, \text{Me}_2\text{Ph}, \text{Et}_3, \text{MePh}_2, \text{EtPh}_2$ in $[\text{bmim}][\text{Sn}_2\text{Cl}_5]$, $x_{\text{Sn}_2\text{Cl}_5} = 0.6$ was followed by ^{31}P NMR. The $^{119/117}\text{Sn}$ coupling to phosphorus suggests the formation of *trans*- $[\text{Rh}(\text{SnCl}_3)_2(\text{PPh}_3)_2]^-$ for PPh_3 and $[\text{Rh}(\text{SnCl}_3)_2(\text{CO})(\text{PR}_3)_2]^-$ for the case of $\text{PR}_3 = \text{Me}_2\text{Ph}, \text{Et}_3, \text{MePh}_2, \text{EtPh}_2$.

The separation of resulting species has been impossible because of the high solubility of the species in ionic solvents.

1. Introduction

1.1. Chemistry and Society

The last century witnessed a new era for human beings. Drugs such as antibiotics were used to treat diseases that had ravaged mankind for millennia. A medical revolution had begun.¹

The role of chemistry in this pharmaceutical achievement was essential and the advances that emerged in this century as the application of technology, resulted in the average life expectancy rising from 47 in 1900 to 75 years in the 1990's.

Chemistry has also been important in other areas and we know that the world's food supply has seen a huge expansion in the 20th century, partly because of the development of chemicals that protect crops and enhance growth. Chemistry has been involved in the advances in transportation, communications, clothing, *etc.* resulting in an improvement in quality of life for human beings.

Unfortunately, the public image of chemistry has not been that positive. The creation of new materials has brought the synthesis of by-products that are harmful to human beings. They often use toxic materials that are dangerous and they are released into the environment in almost all cases.

The image that chemistry has to face nowadays is a negative one. Chemistry is blamed as the direct creator of pollution arising from chemical waste in factories and industry.

In the 1960's there were some incidents that helped to increase the bad reputation of chemistry.¹

- In 1962 Rachel Carson illustrated the irreparable damage that DDT can cause to some bird eggs and showed how it can spread into the food chain.²
- In 1961 the studies on thalidomide that was used to decrease the effect of nausea in pregnant women showed that it caused malformation in the embryos.¹

Over the following years, the chemical industry was partly responsible for a number of natural disasters that transformed the image of chemistry into that of a science of pollution and environmental damage:

- In 1971 Love Canal, a small town in Niagara Falls, NY, was built after a chemical and plastic company was closed and this company had been used as the channel to discard toxic and carcinogenic substances such as benzene, chlorinated hydrocarbons and dioxin. This has resulted in a high level of health effects in the region because of the exposure at Love Canal. The region was declared an official disaster area.¹
- In 1983 in Times Beach, Missouri, roads were contaminated by dioxin, a toxic chemical present in the oil that had been sprayed on the roads a decade before. Another disaster area was declared.¹

All these incidents, in the United States, resulted in an outcry in society about the use of toxic compounds. Scientists were blamed as the originators of disasters.

The Government of the United States had to think of ways to regulate the disposal of material, ways of discarding toxic material into the environment and ways to protect the environment and society by decreasing the risk of exposure. It introduced the Creation of Clean Air Act in the 1970's. In 1990, the Pollution Prevention Act (PPA) was passed by the United States Congress and this helped to control pollution and regulate the disposal of chemical substances.

Green chemistry is a particular method of pollution prevention. There are many other useful methods of decreasing pollution, however green chemistry offers an essential way to abate the level of pollution by changing the methodology of synthesis or obtaining products, by generating clean processes that reduce or eliminate the quantity of by-products, hazardous solvents or raw materials.

1.2. Green Chemistry

Anastas and Warner have defined green chemistry as “the utilization of a set of principles that reduces or eliminates the use or generation of hazardous substances in the design, manufacture and application of chemical products”.¹

Advances in chemical methodologies will help to achieve this goal. The efficiency of a synthetic method influences both the expenses and the overall quality of the process. Economic considerations have played a major role in designing syntheses that use the most available and least expensive feedstock.

Recently, new concepts have been introduced to help efficiency. ‘Specificity’

emphasises the efficiency term and 'atom economy' is a substitute for the term 'yield'. These new concepts help to describe the quality of a synthetic process whose goal is to decrease the overall risk of harm to people and the environment.

Basically, the risk can be described as a function of hazard and exposure. Using less hazardous materials during the synthesis of chemicals must decrease the risk. Therefore the reduction of toxic material makes the inevitable exposure safer for humans and the waste environmentally more benign. In practice, this is difficult to implement.

Current practice has achieved the use of less hazardous material, which correspondingly decreases the risk but does not eliminate it. Exposure will lead to risk. Clearly, decreasing hazard is better than decreasing exposure in industrial processes. Security rules concerning exposure for workers represent an economic drain to industries.

In this way, green chemistry has some tools to reduce the hazards in processes:

1. *Alternative feedstocks, starting material.* Currently, more than 90% of organic products come from petroleum oxidation, which is one of the most environmentally polluting processes. Alternatives are agricultural or biological feedstocks.
2. *Alternative reagents.* Efficiency, atom economy, availability and the effect of each step during transformation must be considered when choosing the necessary reactants.
3. *Alternative solvents.* This area has a special importance in green chemistry. About 90% of chemical syntheses are developed in solution. However, almost all used solvents are volatile organic compounds (VOC) that cause smog when released into the atmosphere. Alternatives such as aqueous systems, ionic liquids, immobilised solvents and supercritical fluids are being applied in syntheses. Present work has special interest in this area and supports the use of ionic liquids as new solvents due to their reusability.
4. *Alternative product, target molecule.* All chemical transformations have a specific molecule as a goal, with a particular group in the compound. The pharmaceutical industry is interested in producing safer medicines that reduce or eliminate secondary effects. Identifying the group which make a medicine biologically active and/or produce toxic effects can reduce the hazards. Choosing the proper molecule is a worthy challenge for synthetic research.
5. *Alternative catalyst.* The use of catalysts in processes has not only improved the efficiency and selectivity in industrial chemistry, but also brought about benefits to the

environment. However, it has been shown that heavy transition metal based catalysts are extremely toxic and their use has to be avoided.

The principle of these green alternatives is to prevent waste rather than to treat or clean up waste after it is formed. There are certainly alternatives to the traditional use of auxiliary substances, which are being pursued for the reasons that drive all the elements of green chemistry. The present chapter pays attention to alternatives to traditional organic solvents. The next section examines some of the alternatives: solvent free synthesis, use of water as solvents, use of supercritical fluids as solvents. Moreover, it provides a deeper explanation of ionic liquids, the focus of this thesis.

Exposing the advantages of the use of ionic liquids as green solvents will demonstrate their versatility as materials. Rather than just trying to convince the reader of their real advantage, this thesis will attempt to unravel their mechanistic chemistry, how they work and why they represent a good alternative to organic solvents. Moreover, it aims to encourage new researchers, eager to explore new areas in chemistry, to continue the investigation in this field that has always been a challenge since its beginning.

1.3. Alternatives to organic solvents

The last section has shown that environmental legislation has generated a pressing need for cleaner methods of chemical production. Therefore the chemical industry wishes to introduce green technologies that reduce or preferentially eliminate the generation of waste and avoid the use of toxic or hazardous reagents and solvents. Reducing the chemical waste to zero will benefit the environment, but it will also provide a more cost-effective use of starting materials. In order to achieve the zero-waste goal it will be necessary to rethink and redesign many of the chemical processes that are in use today.

The current method to evaluate the efficiency of a process is focused on chemical yield. Any trend towards green chemistry requires a change from the traditional concept of process efficiency to one that assigns economic value to eliminating waste, called atom efficiency.³

The proportion of waste is defined by the magnitude of by-products generated per kg of product, designated as the *E* factor in various segments of the chemical industry. Table 1.1 shows this proportion.

$$E = \frac{\text{weight of byproducts}}{\text{weight of products}} \quad \text{Eq. 1.1}$$

The atom efficiency, atom utilization⁴ or atom economy⁵ concept is an extremely useful tool for rapid evaluation of the amount of waste generated by alternative routes to a specific product. The theoretical *E* factor is readily derived from the atom efficiency concept.

Waste is defined as everything produced in the process except the desired product. It consists mainly of inorganic salts formed in the reaction or subsequent neutralization steps. The *E* factor increases dramatically on going from bulk to fine chemicals and specialities such as pharmaceuticals, which involve multi-step syntheses. It is also a reflection of the use of stoichiometric reagents rather than catalytic methodologies.

Table 1.1. E factor for representative industries. The higher the E factor the higher amount of waste in the transformation.³

Industry	Production/tons p.a.	<i>E</i> -factor
Oil refining	10 ⁶ -10 ⁸	0.1
Bulk chemicals	10 ⁴ -10 ⁶	1-5
Fine chemicals	10 ² -10 ⁴	5-50
Pharmaceuticals	10 ¹ -10 ³	25-100

This means that oil refining and bulk chemicals have low waste production, while fine chemical syntheses are inefficient and dirty, even though they are performed on a smaller scale. However, even oil refining and bulk chemicals processes produce huge amounts of waste products because the processes are on such a large scale.⁶ Industries that do not answer quickly to the need of introducing cleaner technologies will die.

One of the main sources of chemical waste is without doubt the use of organic solvents in industrial reactions. Both petrochemical and pharmaceutical processes use organic solvents during transformations. Many of these solvents are harmful to the environment and present problems of disposal.

Therefore, looking for new alternatives to undesirable solvents is one of the main interests of the chemical industry and a main concern in academia. Perhaps the latter is the source of solutions to problems in the industry and a starting point for building new, green technologies. Alternatives ranging from industrial application to solutions in current research are described below:

- *Supercritical fluids.* This state is reached when compressible gases are compressed at a specific temperature, which is called critical temperature, and the fluid shows special characteristics between the two possible states of liquid and gas. Ethane (C_2H_6) and ammonia (NH_3) are cheap gases and possible supercritical fluid solvents.⁷ The use of supercritical carbon dioxide as a substitute for organic solvents already represents an important tool for waste reduction in the chemical industry and related areas. Coffee decaffeination, hops extraction, and essential oil production, as well as waste extraction/recycling and a number of analytical procedures already use this non-toxic, non-flammable, renewable, and inexpensive compound as a solvent.⁸ The extension of this approach to chemical production, using CO_2 as a reaction medium, is a promising approach to pollution prevention. Of the wide range of supercritical carbon dioxide reactions that have been explored, asymmetric catalytic reductions, particularly hydrogenations and hydrogen transfer reactions, have shown exceptional promise.⁹ They can be carried out in supercritical carbon dioxide with selectivity comparable or superior to that observed in conventional organic solvents.
- *Solventless reactions.* They have the most obvious advantages for human health and the environment as far as hazard is concerned. Many companies and scientists in academia are developing methods where the reagents and feedstock serve as the solvents as well. There is also some innovative work being carried out where reactions take place in solid surfaces such as specialised clays. Unfortunately, all these approaches need auxiliary substances (solvents) to be used in the process.¹⁰

- *Aqueous reaction.* Obviously water is the most innocuous substance on Earth and is therefore the safest solvent possible. A brilliant reaction recently published demonstrated a Grignard reaction with the element indium in aqueous media.¹¹ It has been particularly useful in the synthesis of carbohydrates and their analogues.¹² However, one has to be careful of the amounts of contamination in the remaining water. It is possible that waste water can contain larger amounts of contaminants than common organic solvents.¹³
- *Immobilization.* This consists of making a solvent soluble in the solid phase, hence there is no exposure of humans or the environment to the hazards of the substance. The solid phase can consist of a polymer phase and the solvent is introduced into the molecular layer.¹⁴

These advantages represent attractive options to industrial application in many cases. Some of these options are, in specific cases, being studied at present. With the exception of sc-CO₂, their actual development can be very different from real applications. There are also a few other examples that are used as alternatives today. Nevertheless, ionic liquids have been proposed as an outstanding new replacement for solvents for many organic and inorganic transformations.

This option has been mentioned at the end for obvious reasons. The present work shows the significant alternatives that these novel solvents represent in industrial applications, their advantages over organic solvents and their actual research in laboratory reactions. The next section explains the definition of these substances and the development of their chemistry.

1.4. Ionic liquids

Firstly, we have to understand the definition of ionic liquids. These substances are made entirely from ions. One example is molten sodium chloride (NaCl) with a melting point of 803°C.¹⁵ There are other examples, which contain only inorganic ions, whose melting points are higher than room temperature (LiCl, 610°C; KCl, 772°C, etc.). In addition, there are salts that are liquids at room temperature, called *room temperature ionic liquids*. The first reported example of such compounds was [EtNH₃][NO₃], which was synthesized in 1914 and has a melting point of 12°C.¹⁶ Nevertheless, these kinds of

compounds were not seriously examined until 1951, when Hurley and Wier reported the syntheses of some alkylpyridinium chloroaluminates (Fig. 2.1) as materials with new electrochemical properties and applications.¹⁷ After this, many kinds of ionic liquids were synthesized.

In 1967, Swain described the use of tetra-n-hexylammonium benzoate as a solvent for kinetic and electrochemical investigations. It contained a quantitative determination of the ionization strength of the ionic medium.¹⁸

The most widely studied ionic liquids have been the ones that contain imidazolium and pyridinium cations and halogenoaluminate (III) anions, because of their application as new electrolytes. Moreover, their preparation is easy and cheap.¹⁹ Seddon and Hussey began to use chloroaluminates as non-aqueous polar solvents in 1983 for investigations concerning transition metal complexes (section 2.5).²⁰

The first study of homogeneous transition metal catalysis in an ionic liquid was the hydroformylation of ethene catalysed by platinum (II) in tetraethylammonium trichlorostannate in 1972.²¹ This ionic liquid has a melting point of 78°C but at the time of the report, it was described as a molten salt. This report seems to have been ignored as all subsequent studies were focused on ionic liquids containing cyclic cations. All of these studies concerned chemical physics and electrochemical properties until Osteryoung and coworkers reported the first organic reaction using them as solvents and catalysts in 1976.²²

In fact, there are many special properties of ionic liquids that make them attractive as solvents:²³

- They have a liquid range of 300°C, allowing tremendous kinetic control.
- They are outstandingly good solvents for a wide range of inorganic, organic and polymeric materials.
- They are relatively cheap and easy to prepare.
- They have no effective vapour pressure.
- They exhibit Brønsted, Lewis and Franklin acidity, as well as superacidity.
- Their water sensitivity does not restrict their industrial applications.
- They are often composed of poorly coordinating ions, so they have the potential to be

highly polar yet non-coordinating solvents. This can strongly affect the rate-enhancing effect on reactions involving cationic intermediates.

- They are immiscible with a number of organic solvents and provide a non-aqueous, polar alternative for two-phase systems.
- The solubility with gases such as H₂, CO, O₂ is generally good which makes them attractive solvents for catalytic hydrogenation, carbonylations, hydroformylations and aerobic oxidations.
- They have been described as ‘designer solvents’. This means that the polarity and hydrophilicity/lipophilicity of the ionic environment can be adjusted with a suitable choice of cation/anion.

All these advantages have increased the importance of ionic liquids and their applications in syntheses. For example, chloroaluminate ionic liquids have been used as solvents and catalysts in reactions such as Friedel-Craft acylation²⁴ and phosphonium halide melts were used successfully in nucleophilic aromatic substitution reactions.²⁵

Many other reactions such as Diels-Alder reactions (section 2.4.5), alkylations, olefin dimerisation and oligomerisation (sections 2.4.3, 2.4.4) have also been reported. In addition, ionic liquids have been mixed with coordination compounds like [Ni(acac)₂] for the dimerization of propene, first reported in 1990.²⁶ Around the same time, ethylene polymerization with Ziegler-Natta catalysts using chloroaluminates melts was studied. Examples with [NiCl₂(PCy₃)₂] in the dimerization of olefins using the same ionic solvents are described in Section 2.5.4.²⁷

Halogenoaluminate ionic liquids were the main focus of attention among molten salts until the 1980’s, but because of their water sensitivity, they did not represent a good option for important applications. In 1992, Wilkes described the synthesis of tetrafluoroborate ionic liquids that are water stable.²⁸ In contrast to chloroaluminates, tetrafluoroborates represent a better option for future industrial application, especially for transition metal catalysis.

Section 2.4.1 illustrates some examples of organometallic catalysts such as the use of [H₄Ru₄(η⁶-C₆H₆)₄][BF₄]₂ for hydrogenation. Examples of the Heck reaction and

hydroformylation using Pd^{II} complexes in tetrafluoroborates are described in sections 2.4.3, and 2.4.4.

Before all of this research, the known chemistry of ionic liquids was mainly limited to chloroaluminates. The use of tetrafluoroborates and other ionic liquids as solvents in catalysis is relatively new and they have only been studied over the last decade.

Despite all this new research into catalysts in ionic liquids, there has been little research into the interactions of the catalyst with these solvents and how such interaction could increase the catalyst activity in comparison with organic solvents. In fact, there has been only one paper where a partially evident intermediate is reported, which included the use of [Rh(NBD)(PPh₃)₂] as catalyst.²⁹ The intermediates reported for Heck reaction in [emim][BF₄] illustrated the formation of carbenes that are already known in palladium chemistry.³⁰ This means that there are many aspects of the chemical properties of ionic liquids that continue to be unclear. Some questions which can be asked are:

- What happens to a solute in an ionic liquid? What interactions occur between the solute and the ionic liquid?
- What does the ionic liquid do to the reactivity of a solute?
- Do solutes such as MCl_n ionize significantly to give [MCl_{n-1}] and hence generate a vacant site for the coordination of an organic substrate and catalysis?
- How important is the structure of the ionic liquid for the higher activity of the catalyst?
- Is it possible that poor coordinating cations can not interact with the metallic centre at all leaving available places for the coordination and transformation of substrates to products?
- How important is hydrogen bonding?

There are many useful techniques that can help us understand what is happening with the interactions in ionic solution, such as electrochemistry or UV-vis spectroscopy. However, nuclear magnetic resonance (NMR) spectroscopy is one of the strongest, and can provide more detailed information about structures in solution.

The mechanism of alkene hydrogenation by Wilkinson's catalyst is well known in non-coordinating organic solvents. By replacing the solvent media with ionic liquids of interest, it is expected that behavioural changes will be observed. These may provide sufficient clues to determine the nature of the interaction. Other compounds that have a known chemistry for catalytic hydrogenation generally contained coordinated dienes such as $[\text{Rh}(\text{COD})\{\text{Ph}_2\text{P}(\text{CH}_2)_n\text{PPh}_2\}]\text{X}$, where COD = cycloocta-1,5-diene, $n = 2, 3, 4$, $\text{X} = [\text{BF}_4]^-$, $[\text{Cl}]^-$ or $[\text{PF}_6]^-$.

In this situation NMR continues to be one of the best tools to give detailed information about solutions. Take, for example, the $^{31}\text{P}\{^1\text{H}\}$ NMR spectra of Wilkinson's catalyst in an ionic liquid:

- Chemical shifts give information concerning charge distribution.
- Intensity lends data about how many species in solution are present.
- Coupling constants can give us information about the oxidation state of the rhodium centre, the bonding and the conformation. $^{31}\text{P}\{^1\text{H}\}$ NMR gives information about the configuration in Wilkinson's catalyst (*cis* or *trans*) while the reaction is occurring.

In addition, multinuclear NMR can give information. ^{27}Al -NMR, in the case of chloroaluminates, can provide information about the formed aluminate species. ^{19}F and ^{11}B NMR may be useful tools in the case of $[\text{BF}_4]^-$ and $[\text{PF}_6]^-$ anions. Also ^{103}Rh NMR can corroborate the number of phosphorus and hydrogen atoms attached to the metal centre.

So, it is proposed by using Rh based catalytic complexes and multinuclear NMR, we can elucidate coordinating or non-coordinating features of ionic liquids, their preference to dissolve some complexes and the way that they react. It may provide new details or reinforce existing information about special intermediates.

1.5. References

- ¹ P. T. Anastas and J. C. Warner, *Green Chemistry, Theory and Practice*, Oxford, London, 1st edn., 2000, ch 1.
- ² R. Carlson, *Silent Spring*, Houghton Mifflin Co., 1st edn, New York, 1962.
- ³ R. A. Sheldon, *Pure Appl. Chem.*, 2000, **72**, 1233.
- ⁴ R. A. Sheldon in *Precision process technology: Perspectives for pollution prevention*, ed. M. Weijnen and A. Dreinkenburg, Kluwer, Amsterdam, 1st edn., 1993, pp. 125.

- ⁵ R. A. Sheldon in *Industrial Environmental Chemistry*, ed. D. T. Sawyer and A. E. Martell, Plenum, New York, 1992, pp. 99.
- ⁶ B. Trost, *Science*, 1991, **254**, 1471.
- ⁷ K. Zosel, *Angew. Chem. Int. Ed. Engl.*, 1978, **17**, 702.
- ⁸ P. Hubert and G.O. Vitzhum, *Angew. Chem. Int. Ed. Eng.*, 1978, **17**, 710.
- ⁹ M. J. Burk, *J. Am. Chem. Soc.*, 1991, **113**, 8518; M. J. Burk, F. Nuget and R. L. Harlow, *J. Am. Chem. Soc.*, 1993, **115**, 10125; K.J. Burk, S. Feng, M. F. Gross and W. J. Tumas, *J. Am. Chem. Soc.*, 1995, **117**, 4423.
- ¹⁰ R. S. Varma, *Tetrahedron*, 2002, **58**, 1235; R. S. Varma, *Pure Appl. Chem.*, 2001, **73**, 193.
- ¹¹ Y. Yang and T. Hang-Chan, *J. Am. Chem. Soc.*, 1999, **121**, 3228.
- ¹² Taken from ref. 11: S. K. Choi, S. Lee and G. M. Whitesides, *J. Org. Chem.*, 1996, **61**, 8739.
- ¹³ U. M Lindström, *Chem. Rev.*, 2002, **102**, 2751.
- ¹⁴ T. R. Jones, *Clay Miner.*, 1983, **18**, 399.
- ¹⁵ *Handbook of Chemistry and Physics*, McGraw Hill, United States, 77th edn., 1995, section 4, pp. 37.
- ¹⁶ Taken from ref. 24: P. Walden, *Bull. Acad. Imper. Sci.*, St. Petersburg, 1914, 1800; S. Sugden and H. Wilkins, *J. Chem. Soc.*, 1929, 1291.
- ¹⁷ F. H. Hurley and T. P. Wier, *J. Electrochem. Soc.*, 1951, **98**, 203.
- ¹⁸ R. Brown, T. Maugh, D. K. Roe, A. Ohno and C. G. Swain, *J. Am. Chem. Soc.*, 1967, **89**, 2648.
- ¹⁹ S. Wilkes, J. Levinsky, R. Wilson and C. Hussey, *Inorg. Chem.*, 1982, **21**, 1263.
- ²⁰ P. D. Armitage, C. L. Hussey, C. M. Kear, T. B. Scheffler and K. R. Seddon, *Inorg. Chem.*, 1983, **22**, 2099; C. L. Hussey, K. R. Seddon, I. W. Sun, J. E. Turp and E. H. Ward, *Inorg. Chem.*, 1987, **26**, 2140.
- ²¹ G. W. Parshall, *J. Am. Chem. Soc.*, 1972, **94**, 8716.
- ²² R. Gale and A. Osteryoung, *Inorg. Chem.*, 1979, **18**, 1603 and reference therein.
- ²³ T. Welton, *Chem. Rev.*, 1999, **99**, 2071.
- ²⁴ J. A. Boon, J. A. Levinsky, J. L. Flug and J. S. Wilkes, *J. Org. Chem.*, 1986, **51**, 480.
- ²⁵ S. E. Fry and N. J. Pienta, *J. Am. Chem. Soc.*, 1985, **106**, 6399.
- ²⁶ Y. Chauvin, B. Gilbert and I. Guibard, *J. Chem. Soc., Chem Commun.*, 1990, 1715.
- ²⁷ K. Dietrich, J. Dupont, S. Einloft and R. De Souza, *Polyhedron*, 1996, **15**, 3257; Y. Chauvin, B. Gilbert and I. Guibard, *J. Chem. Soc., Chem. Commun.*, 1990, 1715.
- ²⁸ J. Wilkes and M. Zaworotko, *J. Chem. Soc., Chem. Commun.*, 1992, 965.
- ²⁹ Y. Chauvin, L. Mussman and H. Olivier, *Angew. Chem. Int. Ed. Engl.*, 1995, **34**, 2698.
- ³⁰ W. Chen, J. Xiao and L. Xu, *Organometallics*, 2000, **19**, 1123.

2. Background

2.1. Ionic Liquids

Until recent years room temperature ionic liquids were considered to be rare, but it is now known that many salts form liquids at or close to room temperature. Invariably, these ionic liquids are either organic salts or mixtures consisting of at least one organic component. The most common salts in use are those with alkylammonium, alkylphosphonium, *N,N*-dialkylpyridinium, and *N,N*-dialkylimidazolium cations (Fig. 2.1).

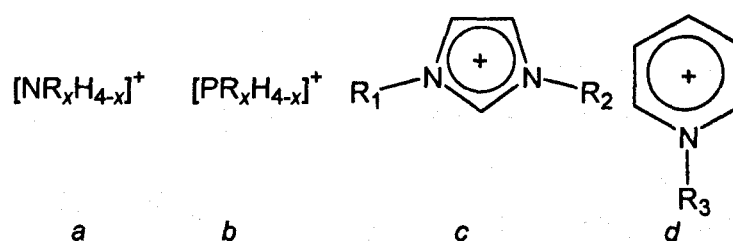


Fig. 2.1. a) alkylammonium; b) alkylphosphonium; c) *N,N*-dialkylimidazolium; d) *N*-alkylpyridinium cations.

Salts with different anions can be obtained by many routes. The ionic liquids used in this work focus on choice *c*, *N,N*-dialkylimidazolium cations. The next section shows common methods to synthesise this organic cyclic cation (*c*, Fig. 2.1), gives examples of common anions in these ionic salts and compares some properties of the cations with alkylammonium and alkylphosphonium (*a* and *b* respectively, Fig. 2.1) cations. After the synthetic procedure, important characteristic properties such as melting points, solubility and their relationship with different anions or cations are mentioned.

Finally, applications of ionic liquids as solvents in catalytic reactions are discussed as examples of the advances that have been made in this area.

Table 2.1. Examples of ionic liquids that can be formed by direct quaternization.

Ionic liquid	Alkylation reagent	M.p.	Ref.
[Emim][CF ₃ SO ₃] ^a	Methyl triflate	-9	9
[Bmim][CF ₃ SO ₃]	Methyl triflate	16	9
[Ph ₃ POc][OTs] ^b	(Oc)OTs	70-71	10
[Bu ₃ NMe][OTs]	(Me)OTs	62	5
[Bmim]Cl	Chlorobutane	65-69	5

Emim = ethylmethylimidazolium;

bmim = butylmethylimidazolium;

a) CF₃SO₃ = triflate anion.

b) OcOTs = H₃CC₆H₄SO₂ = octyl tosyl.

Table 2.2. Examples of ionic liquids that can be generated by the reaction of a halide with a Lewis acid.

Ionic liquid	Established anion	Ref.
[emim]Cl/AlCl ₃	Cl ⁻ , [AlCl ₄] ⁻ , [Al ₂ Cl ₇] ⁻ , [Al ₃ Cl ₁₀] ⁻	5,11
[emim]Cl/AlEtCl ₂	[AlEtCl ₃] ⁻ , [Al ₂ Et ₂ Cl ₅] ⁻	12
[emim]Cl/BCl ₃	Cl ⁻ , [BCl ₄] ⁻	13
[emim]Cl/CuCl	[CuCl ₂] ⁻ , [Cu ₂ Cl ₃] ⁻ , [Cu ₃ Cl ₄] ⁻	14
[emim]Cl/SnCl ₂	[SnCl ₃] ⁻ , [Sn ₂ Cl ₅] ⁻	15

Alternatively, a halide imidazolium and an acid or metal salt which contains the desired anion (*iii*, *iv*, Fig. 2.3) can be mixed giving the youngest family of ionic salts. These are frequently stable in air, which make them more attractive for applications. In this method, the dialkylimidazolium chloride is commonly used as starting material when other anions such as [BF₄]⁻¹⁶ and [PF₆]⁻ are required. Other salts prepared by anion exchange are: [emim]SbF₆, [NR₄][NO₃], [cation][CH₃CO₂]¹⁷, [cation][HSO₄] and [cation][BEt₃Hex]¹⁸ where cation refers to any option given in Fig. 2.1.

Seddon has summarised ionic liquids in two main categories, namely simple salts (made of a single anion and cation) and binary ionic liquids (salts where an equilibrium is involved). For example, [emim][BF₄] is a simple salt while mixtures of aluminium (III) chloride with [emim]Cl contain several different ionic species (binary ionic liquid

system), and their physical and chemical properties depend upon the mole fraction of the aluminium (III) chloride and 1,3-dialkylimidazolium chloride present.

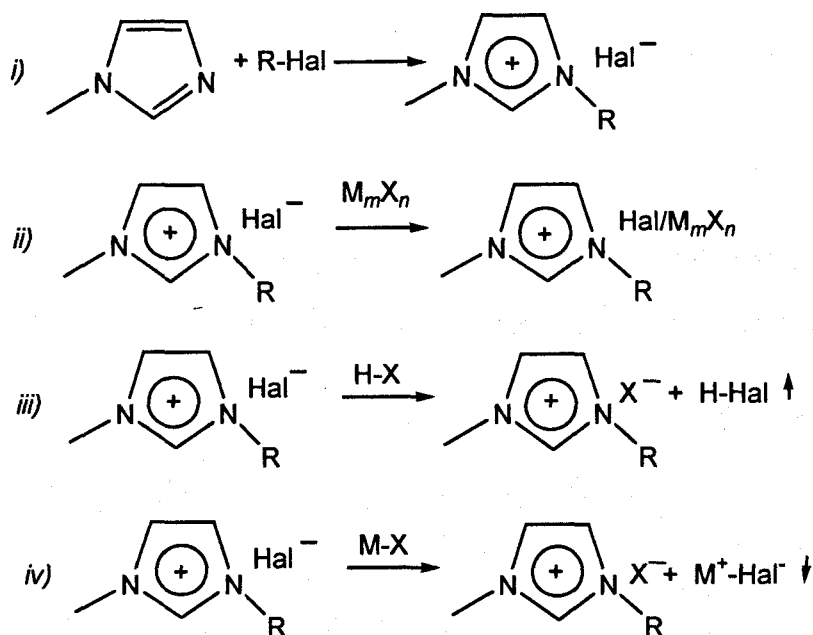


Fig. 2.3. Review: Synthesis of imidazolium ionic liquids: i) alkylation of the ring by direct quaternization, yielding an imidazolium halide; ii) Addition of Lewis acid to an imidazolium halide to decrease the melting point; iii) Metathesis of the halide salt with the desired anion; iv) Metathesis by precipitation with metal halide, often Ag^+ .

2.3. Characteristic properties of ionic liquids

This section illustrates the relationship between the structural features of an ionic liquid and its important physical and chemical properties. It compares melting points or solvation strength and their relationship with the structure of cations or anions in the ionic solvents.

2.3.1. Melting points

This characteristic is the key criterion for giving the name of ionic liquid to a salt. Evaluating melting points of different chloride salts illustrates the influence of the cation. Alkali metal chlorides have high melting points, whereas chlorides with big organic cations melt at temperatures near room temperature (Table 2.3).

Recent publications have reported there is no reliable way to predict the precise melting point of inorganic salts. However, the study of substituents in imidazolium ionic liquids has showed the longer chains are, the lower melting points they have,¹⁹ as ionic liquids consist of a salt where one or both ions are large, and the cation has a low degree of symmetry.²⁰ Other features such as distribution of charge in the cation²¹ and weak intermolecular interactions (such as the avoidance of hydrogen bonding points)²² are related to low-melting salts.

Table 2.3. Melting points of some chlorides.

Salt	M.P. (°C)
NaCl	803
KCl	772
1-R-3-R'-imidazolium chloride:	
R = R'=methyl ([mmim]Cl)	125
R=methyl, R'=ethyl	87
R = methyl, R'=n-butyl	65

The melting point of binary ionic salts is affected by the molar ratio of reactants. The presence of several anions in mixtures with chloroaluminates (III) (such as $[\text{AlCl}_4]^-$ and $[\text{Al}_2\text{Cl}_7]^-$) decreases the melting point, while the maximum temperature is observed at an exact 1:1 stoichiometry, where only the $[\text{AlCl}_4]^-$ anion exists (Fig. 2.4).

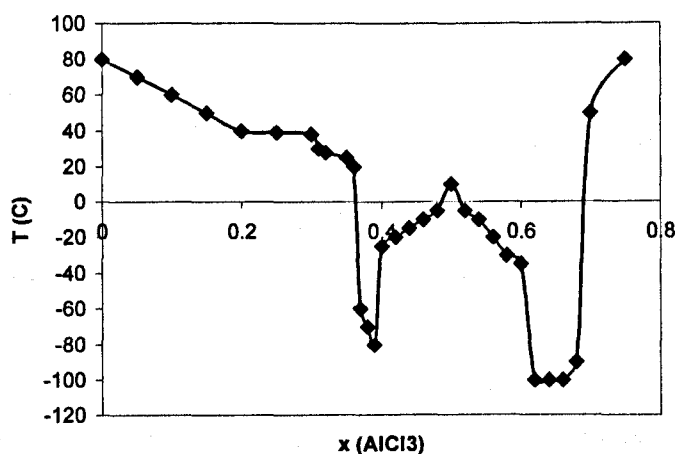


Fig. 2.4. Experimental phase diagram in the system $[emim]Cl/AlCl_3$.

Welton²³ has pointed out that salts which have melting points of 20°C and 30°C are similar in their structures and interionic interactions. Another effect of the alkyl substitution in these rings is the increasing lipophilicity, decreasing hydrophilicity and acidity or stability of H⁺ abstraction.²⁴

2.3.2. Viscosity and thermal stability

Hydrogen bonds determine the viscosity of ionic liquids. The comparison of the viscosity of chloroaluminates (III) with different compositions shows clearly that the absence or presence of hydrogen bonds causes this property to vary. At the same temperature basic mixtures, where the presence of chloride can produce interaction with imidazolium ring hydrogens, show higher viscosity. Acidic mixtures, where $[AlCl_4]^-$ and $[Al_2Cl_7]^-$ are present, have lower viscosity due to a better charge distribution and weaker interaction with hydrogen in the ring.²⁵⁻²⁶

The other property that has to be noted is the maximum working temperature for ionic salts. While 150°C has to be considered as this maximum in ammonium chloride salts, $[emim][BF_4]$ salts are stable up to 300°C. $[Emim][(CF_3SO_2)_2N]$ is even stable to above 400°C.²⁶

2.3.3. Solvation strength and solubility characteristics

Changing the substitution in the imidazolium ring can dissolve specific organic substances, depending on how long or short the substituted chain is. Non-miscibility of some ionic salts with water has been used in liquid-liquid extraction.

In recent years, the use of ionic liquids as solvents for extraction has increased considerably. Rogers and co-workers have showed that the extraction of organic components from water into [bmim][PF₆] is ten times larger than with the use of octan-1-ol,²⁷ also the addition of a metal to coordinate the organic substrate increases the solubility in the ionic phase.²⁸ The option of extraction with ionic liquids is an interesting candidate in separation processes, especially if they represent a decrease in the use of volatile organic solvents.

Further studies of solubility of supercritical CO₂ in [bmim][PF₆] have shown that the sc-CO₂ is soluble in [bmim][PF₆] but the latter is insoluble in the supercritical fluid. This property has been very useful and has been applied to extract naphthalene from the ionic part by using sc-CO₂ with success. The extraction is quantitative without contamination of the fluid by the ionic salt.²⁹

The next table shows the coordinating ability of the anions in common ionic liquids that have been proposed by Wasserscheid and Keim,³⁰ based on results of Chauvin and Olivier-Bourbigou.¹⁴

Table 2.4. Coordinative characteristics of various anions.

Basic/Strongly coordinating	Neutral/weakly coordinating	Acidic/non-coordinating
Cl ⁻	[AlCl ₄] ⁻	[Al ₂ Cl ₇] ⁻
[AcO] ⁻	[CuCl ₂] ⁻	[Al ₃ Cl ₁₀] ⁻
[NO ₃] ⁻	[SbF ₆] ⁻	[Cu ₂ Cl ₃] ⁻
[SO ₄] ²⁻	[BF ₄] ⁻	[Cu ₃ Cl ₄] ⁻
	[PF ₆] ⁻	

2.4. Ionic liquids as solvents and catalysts

The use of ionic liquids as solvents and catalysts has been widely studied in the last decade because of their application in homogeneous catalytic reactions. Nowadays it is believed that the homogeneous catalyst is the best option for “atom economy” in the synthesis of fine chemicals and pharmaceuticals. This means trying to maximise the number of atoms that are converted from reactants to products. As the number of catalytic centres involved in the reaction during homogeneous catalysis is larger in comparison with the heterogeneous one, it makes the transformation more effective.

In order to have the advantages of atom economy, high activity, high selectivity and good reproducibility, along with those characteristics of a heterogeneous catalyst, *i.e.* long lifetime and ease of separations, the “heterogenization” (immobilization or anchoring) of homogeneous catalysts has been proposed.

Biphasic media (two-phase technique) is one procedure to heterogenize a homogeneous reaction. It uses a homogeneous catalyst, dissolved in water or organic solvent, as a “mobile” phase or support. The reaction mixture, catalyst and reactants/products are separated after the reaction, approximately at the same temperature. This procedure has the advantage of homogeneous catalysis and it is supplemented by immediate separation after reaction without the addition of any chemical but only temperature. Ruhr Chemie Rhone-Poulenc’s oxo process³¹ and Shell’s SHOP process³² are important industrial applications which use this system.

Table 2.5 shows the advantages and disadvantages of biphasic media that have been proposed as a heterogenization of homogeneous reactions.³³

The problem with the extraction of the products from the ionic liquids can be solved in many cases by using an organic solvent. Although it could seem paradoxical, using ionic liquids to increase the atom efficiency and reduce the atmospheric emissions,

Table 2.5. Biphasic media options for the heterogenization of homogeneous catalyst.

Biphasic media	Advantage	Disadvantage
Water-Organic solvents	High effectiveness for industry	Difficulties to remove the organic traces from water. Insolubility and instability of many expensive catalysts
Fluorous-organic solvents	Permit the use of water sensitive materials	Specially and expensively prepared catalysts
Ionic liquids-organic solvents	Wide solubility of many materials.	Separations continue being a problem in some cases

they can increase the total yield of the transformation having an environmental benefit (as was discussed in the introduction). In addition there are other scenarios using ionic liquids in catalysis:³⁴

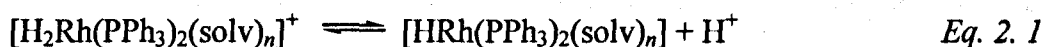
- Monophasic systems in which the catalyst and substrate are dissolved in the ionic liquid (section 2.5.3).
- Monophasic systems in which the ionic liquid acts as both the solvent and the catalyst, e.g. Friedel–Craft catalysis (sections 2.4.5 and 2.5.1).
- Biphasic systems in which the catalyst resides in the ionic liquid and the substrate/product in the second phase or *vice-versa* (section 2.4.1).
- Mono or biphasic systems in which the anion of the ionic liquid acts as a ligand for the homogeneous catalyst (section 2.4.2).
- Triphasic systems comprising of an ionic liquid, water and an organic phase in which the catalyst resides in the ionic liquid, the substrate and product in the organic phase and the salts formed in the reaction are extracted into the aqueous solution (Heck reaction, section 2.4.4).

The use of ionic liquids in biphasic media has opened an interesting area of research. For example the hydrogenation of 2-(6-methoxy-2-naphthyl)acrylic acid to give

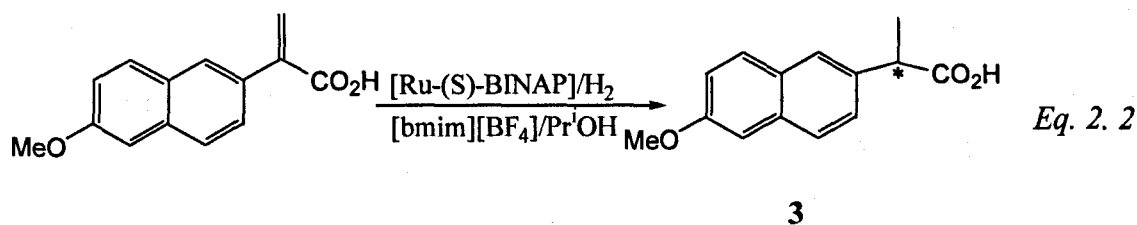
quantitatively (*S*)-Naproxen (see next section) using bmim[BF₄] and methanol in the reaction mixture proposes the use of ionic salts in biphasic media in important organic syntheses. The next section provides some examples of catalytic reactions in biphasic media with ionic salts but it focuses on the general use of the ionic liquids as novel media for catalysis.

2.4.1. Ionic liquids in reactions: Hydrogenation

Because of its industrial application, the first reaction that caught the attention of many research groups was the hydrogenation of C=C bonds, catalysed by transition-metal complexes. Initial experiments using [Rh(nbd)(PPh₃)₂][PF₆] (nbd = norbornadiene) for hydrogenation of pent-1-ene in [bmim][BF₄], [bmim][PF₆] and [bmim][SbF₆] showed five times higher activity than in acetone (TOF: 0.55 vs. 2.54) with 98% selectivity and 96% conversion in the case of [bmim][SbF₆].³⁵ The ³¹P-NMR spectrum of an ionic solution of Rh compound and H₂ gas showed a doublet at δ 40.6 ppm with ¹J(¹⁰³Rh-³¹P) 103 Hz. As ionic liquids are known to stabilize preferably cationic species, the formation of a symmetrical Rh-hydride during the reaction is proposed, with two free coordination sites (eq. 2.1). Similar behaviour was observed when Wilkinson's catalyst, [RhCl(PPh₃)₃], was dissolved in [emimCl][AlCl₃] (chapter 4).



Another important investigation involves the asymmetric hydrogenation of 2-(6-methoxy-2-naphthyl)acrylic acid to give quantitatively (*S*)-Naproxen (**3**) in 80% ee in bmim[BF₄] (eq. 2.2). This yield is slightly higher than in the homogeneous media. The reaction is carried out at 75 atm, room temperature for 20 h. and the catalyst is [{(*S*)-BINAP}Ru(OAc)₂]. The catalyst is "immobilized" in the ionic liquid and can be separated from the products.³⁶



$[\text{RuCl}_2(\text{PPh}_3)_3]$ and $\text{K}_2[\text{Co}(\text{CN})_5]$ in the same ionic liquid have been used to catalyse the hydrogenation of hexene and cyclohexene with 100% conversion. However, the latter gives $[\text{bmim}]_2[\text{Co}(\text{CN})_5]$ after the first catalytic reaction. This species is inactive because of the strong hydrogen bonds between $[\text{Co}(\text{CN})_5]^{2-}$ and $[\text{bmim}]^+$.³⁷

The use of clusters such as $[\text{H}_4\text{Ru}_4(\eta^6\text{-C}_6\text{H}_6)_4][\text{BF}_4]_2$ in $[\text{bmim}][\text{BF}_4]$ has hydrogenated 91% of benzene at 60 atm H_2 , 90°C in 2.5 h, while the same reaction in water gives 88% conversion. The same active catalyst in both media is proposed but conditions in the ionic phase are much milder than in the industrial process.³⁸ In addition, the separation of reactants and products is easier in the ionic phase.

2.4.2. Hydroformylation

Another kind of reaction widely studied is hydroformylation. One example is the conversion of hex-1-ene to heptanal and 2-methylhexanal in the presence of $[\text{Rh}_2(\text{OAc})_4]$ in phosphonium-tosylates as ionic solvents (Fig. 2.5). This study offers the advantage of easy separation and recovery of the catalyst after its use because of the high melting point of the ionic liquid. Moreover, the authors propose the formation of $[(\text{PPh}_3)_3\text{Rh}(\text{CO})\text{H}]$ as the active catalyst.³⁹

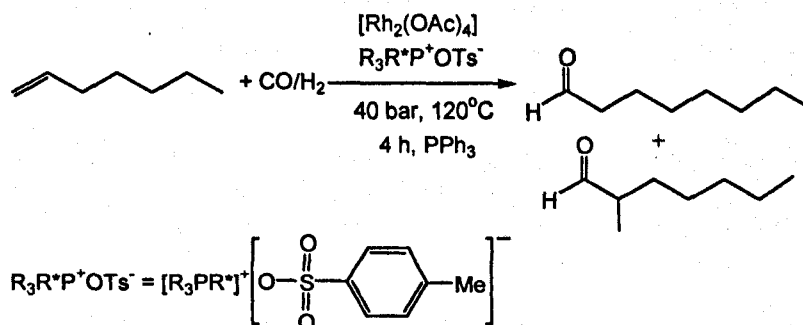


Fig. 2.5. Hydroformylation of hex-1-ene with rhodium. The solvent is a new phosphonium ionic liquid whose synthesis was reported in 1999.¹⁰

2.4.3. Polymerization

Another interesting reaction is the hydrodimerization of 1,3-butadiene by $[\text{bmim}]_2[\text{PdCl}_4]$ (**4**) in $[\text{bmim}][\text{BF}_4]$.⁴⁰ The new catalyst is completely soluble in the ionic phase and it is obtained by the addition of PdCl_2 to $[\text{bmim}]\text{Cl}$. The IR spectrum of this compound shows bands associated with a $\text{C-H}\cdots\text{Cl}$ interaction, characteristic of hydrogen bonding.⁴¹ This species reacts with H_2O in the ionic liquid to undergo β -elimination affording but-1-ene, HCl and **5** (Fig. 2.6). The authors propose the ionic liquid as an ionizing agent which can stabilize the palladium species involved in this process. Moreover, the use of **5** in the hydrodimerization is the same as **4**. So, the true catalyst is **5**. Unfortunately the authors did not mention the importance of the cleavage of the $\text{C}_{\text{alkyl}}\text{-N}$ bond in the imidazolium ring.

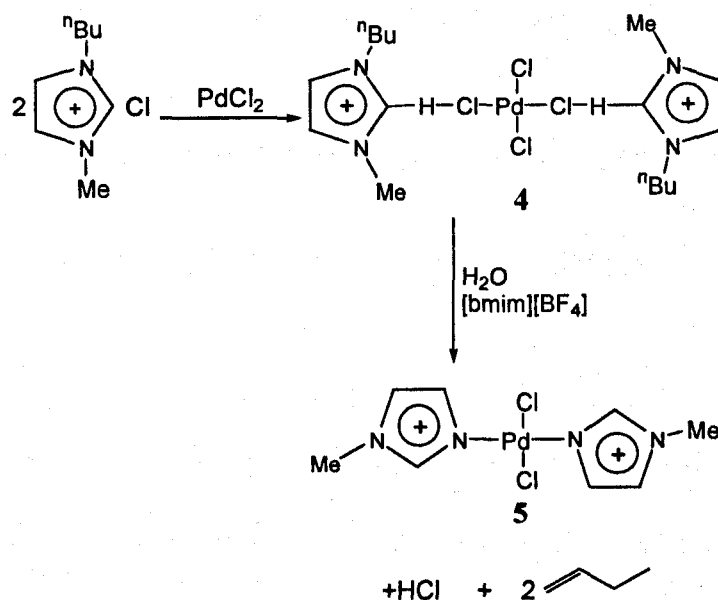


Fig. 2.6. The use of $[(\text{bmim})\text{PdCl}_4]$ in ionic liquids gives a new catalyst **5** which is active for the hydrodimerization of but-1-ene.¹²

2.4.4. Alkylation and C-C bond formation

Xiao⁴² and coworkers, have reported the use of $[\text{Pd}(\text{OAc})_2]$ in $[\text{bmim}][\text{BF}_4]$ in the allylic alkylation and amination of some malonate derivatives (Fig. 2.7). Total conversion was obtained when the proportion of free PPh_3 was four times greater than $[\text{Pd}(\text{OAc})_2]$.

Other palladium catalysts have been used with great success in the synthesis of C-C bonds as Suzuki cross-coupling⁴³ and Trost-Tsuji coupling⁴⁴ reaction in [bmim][BF₄].

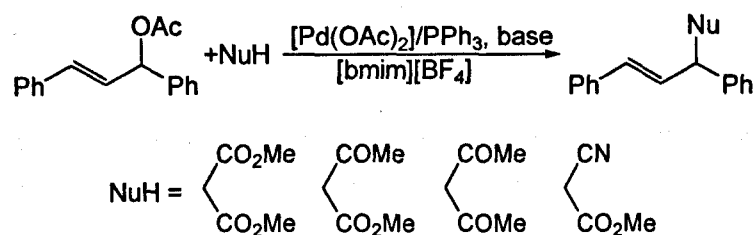


Fig. 2.7. Synthesis of malonate derivatives using Pd compound as catalyst.

The study of Heck reaction in [bmim][BF₄] and [bmim]Br using Pd(OAc)₂ resulted in C-C bond formation between aryl halides and acrylates.⁴⁵ The formation of palladium carbenes has been identified as the active species in this kind of formation (Fig. 2.8).

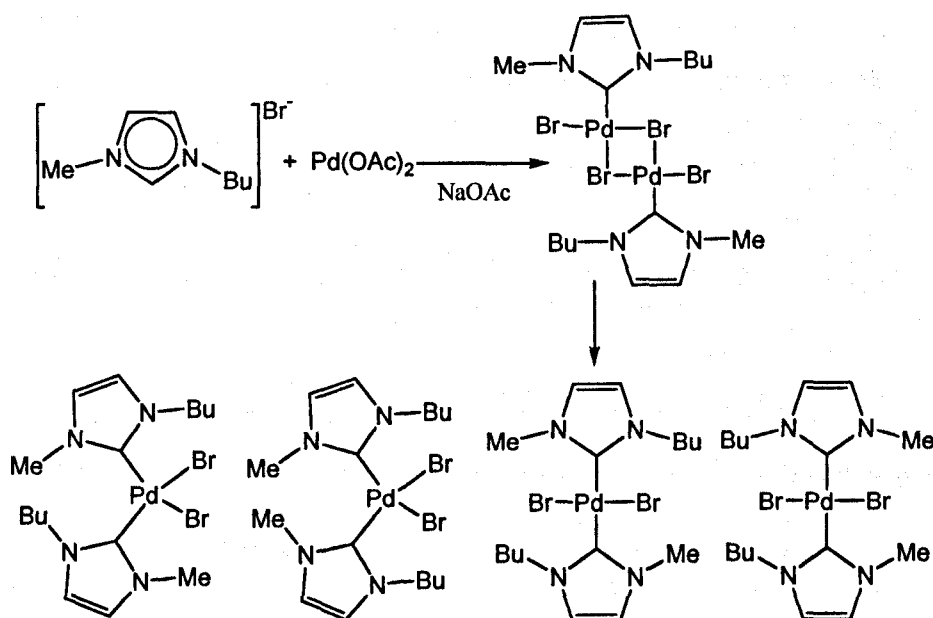


Fig. 2.8. All isomeric carbenes observed in [bmim]Br due to the coordinating characteristic of Br⁻. These kind of species were not observed when [bmim][BF₄] was used.

2.4.5. Diels-Alder reaction and Friedel-Craft acylation

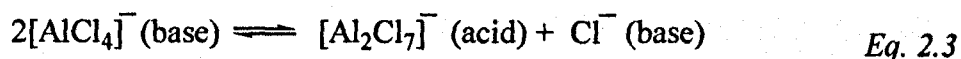
It is necessary to emphasise the use of ionic liquids like [bmim][TfMS], (TfMS = trifluoromethanesulfonate), as solvents in Diels-Alder reactions.⁴⁶ This medium offers an

alternative possibility to the lithium perchlorate-diethyl ether system, which is now used in the industry. In addition, the alkylation of naphthalene and its derivatives has also been reported.^{47, 48}

Another example, which uses the same ionic salt, is the Friedel-Craft alkylation of benzene with alkenes. In this case the conversion is more than 99% and the ionic salt can be recovered and reused.⁴⁹ Trifluoromethanesulfonate ionic liquids have been used to synthesise benzoxazine in a one-pot reaction. The yield is more than 90%, the recovered ionic liquid yield is almost 99% and this can be reused without a decrease in the yield in the second and third cycles.²⁶

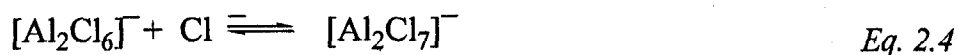
2.5. Chloroaluminate (III) ionic liquids: Chemical properties

Because of their historical importance, these kinds of ionic salts have to be mentioned in a separate section than the rest of the ionic liquids. Despite their sensitivity to the air, halogenoaluminates have been the most largely studied of the ionic liquids, especially 1-methyl-3-ethylimidazolium chloroaluminate ([emim]Cl/AlCl₃) and (1-butyl)pyridinium chloroaluminate (III) ([bupy]Cl/AlCl₃) which are easy to prepare.⁵⁰ Both ionic liquids can be made to exhibit a wide range of Lewis acidity and solvation characteristics at room temperature simply by varying the relative amount of AlCl₃ and organic salt. The acid-base properties of these solvents are well established. Mixtures that contain a molar excess of AlCl₃ are designated as “acidic” ($x_{AlCl_3} > 0.5$) while those containing a molar excess of the organic salt are denoted as “basic” ($x_{AlCl_3} < 0.5$).⁵¹ In addition, those mixtures at the compound formation point are called neutral. Over much of the liquid range, the anions present in significant quantities are Cl⁻, [AlCl₄]⁻ and [Al₂Cl₇]⁻ and their relative amounts are controlled by the equilibrium shown below.⁵²



The equilibrium constant for this reaction is in the order of 10⁻¹⁶ at ambient temperature,⁵³ hence, in melts containing more than a slight excess of AlCl₃, the concentration of Cl⁻ is very small. Thus, the [Al₂Cl₇]⁻ anions are powerful Cl⁻ acceptors and are the source of high Lewis acidity. In addition to eq. 2.3, there are two more

equilibria to be considered in the ionic liquid. They are shown in eq. 2.4 and 2.5. The equilibrium constant for eq. 2.5 is $2.09 \pm 0.06 \times 10^{-3}$ at 40°C .⁵⁴



The high moisture sensitivity of chloroaluminates has led to many studies of their behaviour with water. The first work that showed this chemistry was published by Zawodzinski and Osteryoung.⁶ They proposed the formation of one hydroxo and at least two O-bridged chloroaluminate or oxochloroaluminate species in acidic solutions, where both "Al-O" showed a higher chemical shift than "Al-OH" in ^{17}O -NMR (Fig. 2.9).

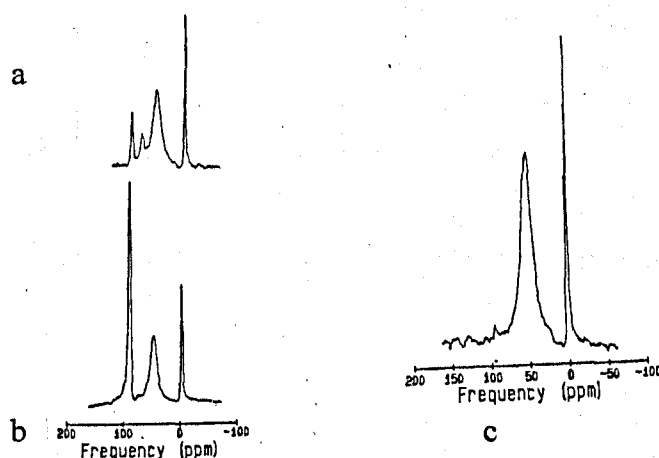
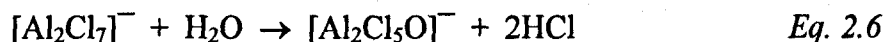


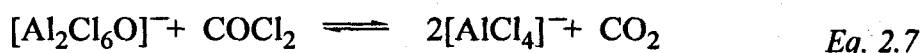
Fig. 2.9. ^{17}O -NMR spectra of 50mM of H_2O in a) $\text{emimCl}/\text{AlCl}_3$ with $x_{\text{AlCl}_3} = 0.45$ or $[\text{emim}][\text{AlCl}_4]$; b) $\text{emimCl}/\text{AlCl}_3$ with $x_{\text{AlCl}_3} = 0.54$ or $[\text{emim}][\text{Al}_2\text{Cl}_7]$; c) the same solution as 'a' after HCl is bubbled through it.⁶

A more detailed work has been reported by Seddon and coworkers. Basically, the results by ^{17}O -NMR and FAB mass spectra showed the formation of $[\text{Al}_2\text{Cl}_5\text{O}]^-$ ions. No evidence for $[\text{AlCl}_3(\text{OH})]^-$ ions was observed. Seddon suggests that the reaction in equation 2.6 is most favoured. The negative fast atom bombardment mass spectrometry showed the presence of ions $[\text{Cl}]^-$, $[\text{Cl}_2]^-$, $[\text{AlCl}_4]^-$, $[\text{Al}_2\text{Cl}_5\text{O}]^-$, $[\text{Al}_2\text{Cl}_6(\text{OH})]^-$, $[\text{Al}_2\text{Cl}_7]^-$, $[\text{Al}_3\text{Cl}_6\text{O}_2]^-$, $[\text{Al}_3\text{Cl}_7\text{O}(\text{OH})]^-$, $[\text{Al}_3\text{Cl}_8\text{O}]^-$, and $[\text{Al}_4\text{Cl}_9\text{O}_2]^-$.⁵⁵ This study was compared to that reported by Zawodzinski and Osteryoung. The first-formed hydroxide-containing species is the $[\text{Al}_2\text{Cl}_6(\text{OH})]^-$ ion, and it became dominant as the level of oxide

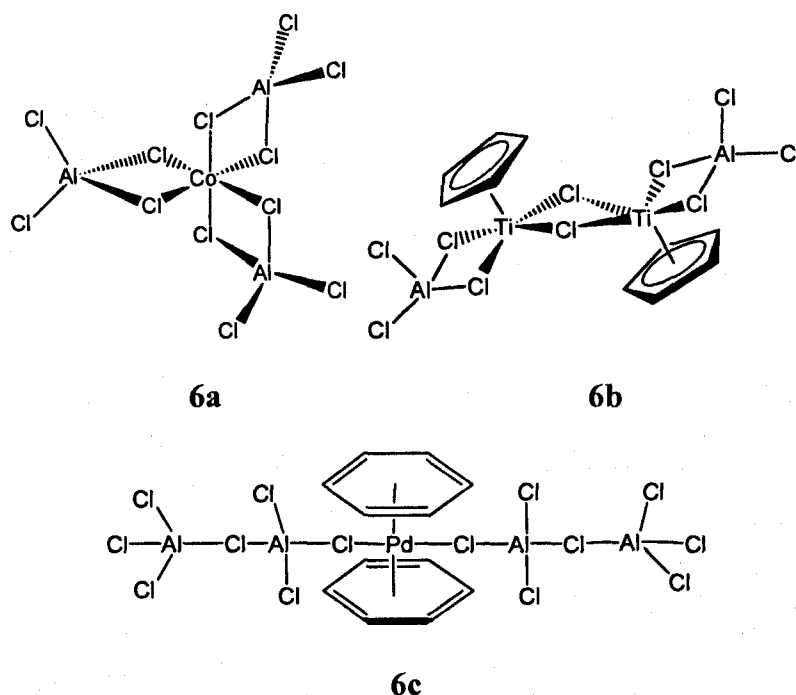
impurities increases. Clearly, this is the species detected in the ^{17}O -NMR spectrum of acidic emim[Al₂Cl₇] ionic liquids at δ 49.7 ppm. Perhaps oxo-species shown in the FAB as [Al₂Cl₅O]⁻ and [Al₃Cl₈O]⁻ are responsible for the previously reported NMR signals at δ 91.8 and 73.8 ppm respectively.⁶



Highly purified chloroaluminate (III) ionic liquids are produced by using phosgene. Seddon and coworkers reported the removal of oxide contamination by passing this poison stream through the ionic solution. The reaction to eliminate the impurities is summarised in eq. 2.7.



Also, the electrochemistry of transition metal halide complexes in chloroaluminate (III) ionic liquids has been widely studied and reviewed.⁵⁶ The use of this technique together with electronic spectroscopy has established the interaction of chlorometalates in acidic chloroaluminate (III) ionic mixtures. Initial studies with oxochlorouranate⁵⁷ ions and oxochloromolybdates⁵⁸ determined a change in the $E_{1/2}$ of the complex in the organic and the acidic ionic solvents but did not indicate any direct interaction with [AlCl₄]⁻ ions. Some oxochlorometalates have shown larger stability in acidic [emim][Al₂Cl₇] than in common organic solvent and such is the case for oxoiridium ions.⁵⁹ Later reports suggest an interaction of the chlorides of the metal and the [AlCl₄]⁻ ions by comparison of the electrochemistry between chloride complexes derived from clusters in CH₃CN and [emim][Al₂Cl₇], such as {Ta₆Cl₁₂}^{z+} (z = 5, 4, 3) and {Nb₆Cl₁₂}^{y+} (y = 2, 3, 4).⁶⁰⁻⁶¹ In the case of tantalum, it has been proposed that there is a replacement of the chlorides in the initial cluster when it is dissolved in [emim][Al₂Cl₇]. The difference in the $E_{1/2}$ goes from 1.160 V in the ionic liquid to -0.274 V in CH₃CN for the redox couple [Ta₆Cl₁₂]^{4+/3+}. This clearly suggests the interaction of the cluster with the environment and the partial or complete replacement of the peripheral Cl⁻ with [ClAlCl₃]⁻ in the tantalum cluster.⁶⁰ Similar results are observed with niobium.⁶¹ In addition, acidic ionic liquids have shown the existence of tetrachloroaluminate (III) as a ligand by EXAFS, even if it has not been completely accepted (6a).⁶² However, in basic ionic liquids, chlorometalate species form well-defined halogenometalate species.⁶³



Acidic mixtures of chloroaluminates, where $[\text{Al}_2\text{Cl}_7]^-$ and $[\text{Al}_3\text{Cl}_{10}]^-$ are present, were considered as non-coordinating anions by Chauvin,¹⁵ but there have been crystal structures where $[\text{Al}_2\text{Cl}_7]^-$ and $[\text{AlCl}_4]^-$ are ligands on metallic centres such as Pd⁶⁴ and Hg.⁶⁵ The last species have not been isolated from any chloroaluminate (III) ionic liquid but they have been synthesised from AlCl_3 and metal chlorides in aromatic solvents; such as **6b** and **6c**. Section 4.4 describes two more examples of these kinds of complexes and with these examples it is clear that the interaction of $[\text{AlCl}_4]^-$ ions with metals has been well documented since the 1970's and it had been considered rare until the 1980's.⁶⁶

2.5.1. Reactions in chloroaluminate (III) ionic liquids: Friedel Craft acylation

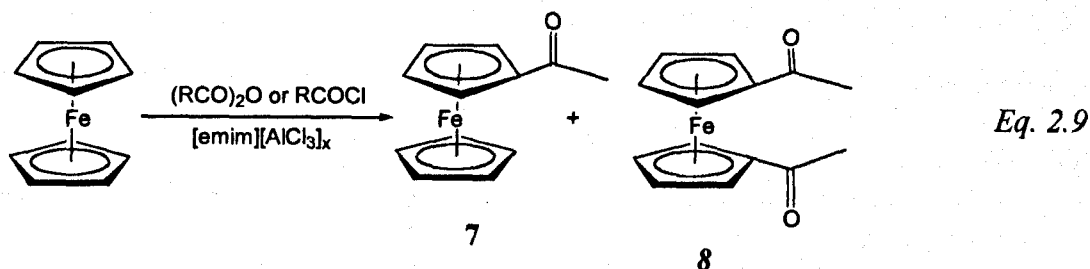
Because of their possible function as both catalyst and solvents, these ionic liquids were first used in organic chemistry for Friedels-Craft acylation. Lauer and Bartak demonstrated that the acidic ion $[\text{Al}_2\text{Cl}_7]^-$ could extract a Cl^- from alkyl carbons and give the carbonium ion. For example, the formation of the triphenylmethyl carbonium ion (eq. 2.8) in acidic ionic liquids from the respective halogen was performed.⁶⁷



Another example is the cyclopentadiene/methyl acrylate Diels Alder reaction. It should be noted that acidic mixtures of chloroaluminate ionic liquids have given better results for this reaction than many others. In this reaction, acidic melts offer a better media for the hydrophobic association of reactants and hydrogen bonding to the activating group of the dienophile. The yield is far superior in this solvent than in water or ethyl ammonium nitrate (EAN). Unlike EAN, chloroaluminates are not potentially explosive. Furthermore, unlike water, many organic molecules are very soluble in ionic liquids. This means that reactions can be performed at synthetically useful scales in chloroaluminate ionic liquids.⁶⁸

Other organic reactions performed in these solvents have included the alkylation of many organic substances such as isobutane,⁶⁹ benzene,²⁴ naphthalene⁷⁰ and the polymerization of olefins such as ethene, propene or ethylbenzene.⁷¹

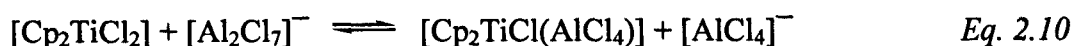
Nevertheless, the first acylation of organometallic compounds was reported a few years ago with the study of ferrocene in $[\text{emimCl}][\text{AlCl}_3]$ (eq. 2.9). The mono (7) and diacetylation (8) is perfectly controlled and a higher yield is obtained with the addition of toluene and the formation of a clathrate.⁷² The AlCl_3 catalyzes the replacement of one cyclopentadiene with arenes in ferrocene. Chloroaluminate ionic liquids have been used as solvents and catalysts for these reactions.



For example, the substitution of Cp in ferrocene by cyclophane was reported some years ago. This study included the kinetic chemistry followed by $^1\text{H-NMR}$. The advantage of the use of ionic liquids is the high purity in the final compounds, which do not need chromatographic separation.⁷³

2.5.2. Transition metal catalysed reactions in chloroaluminate (III) ionic liquids

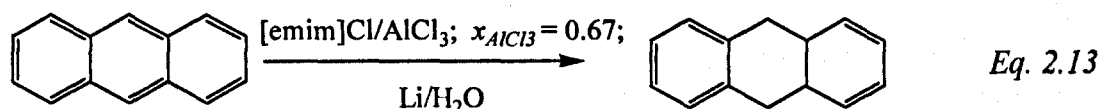
Another important example of the use of organometallic compounds in this solvent is the reductive carbonylation of $[\text{Cp}_2\text{TiCl}_2]$ to $[\text{Cp}_2\text{Ti}(\text{CO})_2]^+$ by forming a Ti(III) intermediate which has the labile ligand $(\text{AlCl}_4)^-$. This is a labile species that is easily replaced by CO (equations 2.10-2.12).⁷⁴



The reduction of the carbonyl Ti(III) leads to the precipitation of $[\text{Cp}_2\text{Ti}(\text{CO})_2]$.

2.5.3. Hydrogenation in chloroaluminate (III) ionic liquids

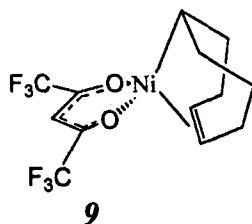
The catalytic hydrogenation of aromatic rings in chloroaluminate (III) ionic liquids has been reported. The stereoselective hydrogenation of aromatic compounds like anthracene and pyrene with $[\text{emim}][\text{AlCl}_3]/\text{Li}/\text{H}_2\text{O}$ in very gentle conditions (eq. 2.13), have been reported before.⁷⁵ This contrasts with the catalytic hydrogenation used in industry, which requires high temperatures, high pressures and usually gives rise to isomeric mixtures.⁷⁶



2.5.4. Dimerization in chloroaluminate (III) ionic liquids

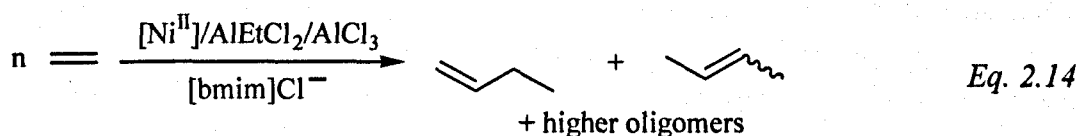
Linear dimerisation of but-1-ene to give C_8 -olefins has been reached by using square planar Ni-O,O' chelating systems. For example, complex 9 is active in organic solvents but its combination with expensive ligands has prevented industrial development. Using chloroaluminates with this catalyst increases the yield and makes the separation of

reactants and products easier. The ionic liquid used was (bmim)X/AlCl₃/AlEtCl₂, and the acidic mixture gave much higher yields than basic mixtures.⁷⁷



AlEtCl₂ transfers an ethyl group to the Ni at temperatures higher than -10°C and destroys the Ni-X-Y chelating system which is known to be responsible for the desired high linearity.⁷⁸

The dimerization of ethene with [Ni(MeCN)₆][BF₄]₂ in [bmim]Cl/AlEtCl₂/AlCl₃ (eq. 2.14) shows the same yield as [NiCl₂(PPR¹₃)₂] in [bmim]Cl/AlCl₃.⁷⁹



These results provide a very advantageous technological alternative to the industrial IFP Dimersol X process operating world-wide nowadays.⁸⁰

As we can see, ionic liquids have been widely studied in organic and catalytic reactions. In most cases the syntheses have been improved in the new ionic solvents, hence they represent an alternative route to industrial processes. As their applications in industrial processes have been emphasised, the analysis of species involved during transformations has not been the focus of all these works. Nowadays, the understanding of the mechanistic routes has contributed to developing and improving the processes which are now used. We can now understand the importance of clarifying the principal steps during catalytic reactions in ionic liquids.

The next section gives an introduction to rhodium chemistry as a catalyst for the hydrogenation of olefins using [RhCl(PPh₃)₃]. Because of its historic importance, it has been chosen as a good starting point to study its catalytic chemistry in ionic liquids. The advantage of having a phosphine ligand attached to 100% NMR active metal centre

(^{103}Rh), is that it permits the use of NMR spectroscopy as a tool to understand the chemistry in solution. Other compounds such as $[\text{Rh}(\text{diolefin})(\text{diphosphine})]$, (diolefin = NBD, COD; diphosphine = $\text{PR}_2\text{P}(\text{CH}_2)_n\text{PR}_2$), which have been studied for catalytic hydrogenation are also discussed. The mechanism for both complexes, Wilkinson's and diphosphine compounds, are briefly explained.

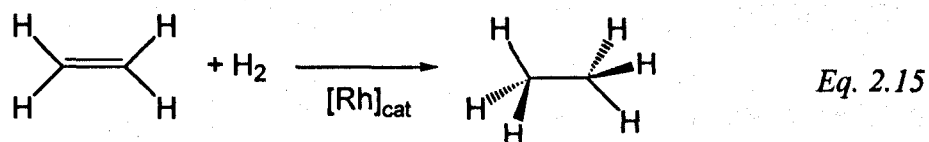
2.6. Catalytic hydrogenation with rhodium complexes

2.6.1. Wilkinson's catalyst: $[\text{RhCl}(\text{PPh}_3)_3]$

Rhodium was discovered by William Hyde Wollastone in 1803. The first rhodium complexes were synthesised and studied at the beginning of that century. All those compounds were basically coordination complex types, but a totally new field of rhodium chemistry was opened up by the discovery of the remarkable catalytic properties of $[\text{RhCl}(\text{PPh}_3)_3]$ by Wilkinson's group in the 1960's.⁸¹ This work showed that $[\text{RhCl}(\text{PPh}_3)_3]$ accelerated the hydrogenation of olefins in homogeneous media.⁸²

The importance of the chemistry of rhodium increased after this report, and many new rhodium compounds were synthesized for sophisticated reactions. This achievement certainly marked a great step forward in the chemistry of this metal and contributed to the development of the chemistry of the transition metals. Before the Wilkinson paper, it was known that an iridium complex worked as a catalyst for the hydrogenation of olefins at 40-60°C, but it was slower than $[\text{RhCl}(\text{PPh}_3)_3]$ catalyst.⁸³ Hence, there was an increasing interest in Wilkinson's catalyst $[\text{RhCl}(\text{PPh}_3)_3]$, its involvement in the mechanism of hydrogenation and the general chemistry of the compound.

The general reaction for catalytic hydrogenation is described by eq. 2.15.



Tolman reported a study of hydrogenation of olefins with Wilkinson's catalyst in 1974.⁸⁴ He described the initial formation of the dihydride $[\text{Rh}(\text{H})_2\text{Cl}(\text{PPh}_3)_3]$ from $[\text{RhCl}(\text{PPh}_3)_3]$ and H_2 . More studies were published in order to explain the intriguing mechanism by which this complex works but there were some differences in the kinetic constants. A widely accepted mechanism in the 1970's is outlined in Fig. 2.10, but certainly it did not give any specific details.

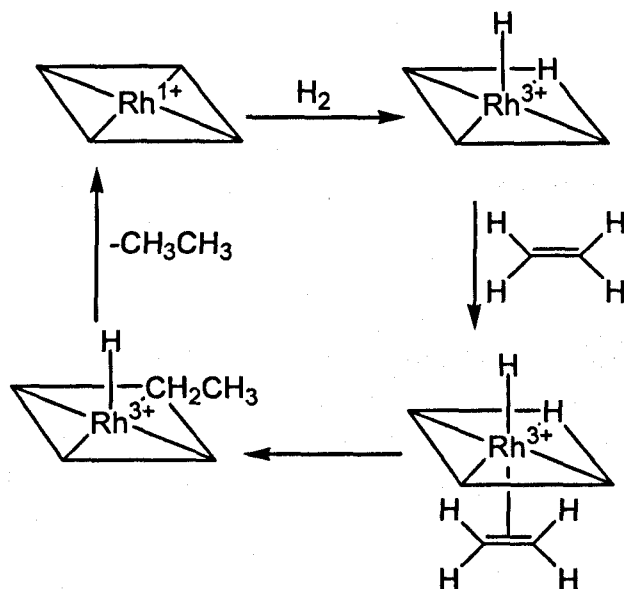


Fig. 2.10. Catalytic hydrogenation of olefins: mechanism accepted in the 1970's.⁷⁵

The complexity of the mechanism lies both in its multistep character and also in the lability of dissociation of each ligand, phosphine or olefin, in each proposed intermediate and in the olefin insertion or substitution processes.

Halpern reported a complete cycle for the hydrogenation using $[\text{RhCl}(\text{PPh}_3)_3]$ in the 1980's (Fig. 2.11).⁸⁵ The catalytic cycle involves 16 and 18 electron rhodium species. This mechanism describes two routes: the initial coordination of hydrogen or of the olefin to $[\text{RhCl}(\text{PPh}_3)_3]$. In both cases the rate-determining step is the insertion of alkene into the $\text{Rh}-\text{H}$ bond. These intermediates were proposed by kinetic studies using direct measurements on the individual stages of the reaction. In addition, recent theoretical calculations agree with the experimental results: the insertion of the olefin is the rate determining step in the whole cycle.⁸⁶

In addition, the catalytic mechanism depends upon the olefin used. For example, catalytic hydrogenation of styrene includes an additional pathway with the observation of a monophosphine bis-olefin complex $[\text{RhCl}(\text{H})_2(\text{PPh}_3)(\text{PhHC}=\text{CH}_2)_2]$, while for cyclohexene the formation of the mono-olefin intermediate $[\text{Rh}(\text{Cl})(\text{H})_2(\text{PPh}_3)_2(\text{C}_6\text{H}_{10})]$ is seen (Fig. 2.11, inner or outer cycle). Different kinetic rates for cyclohexene and styrene arise from this difference.⁸⁵

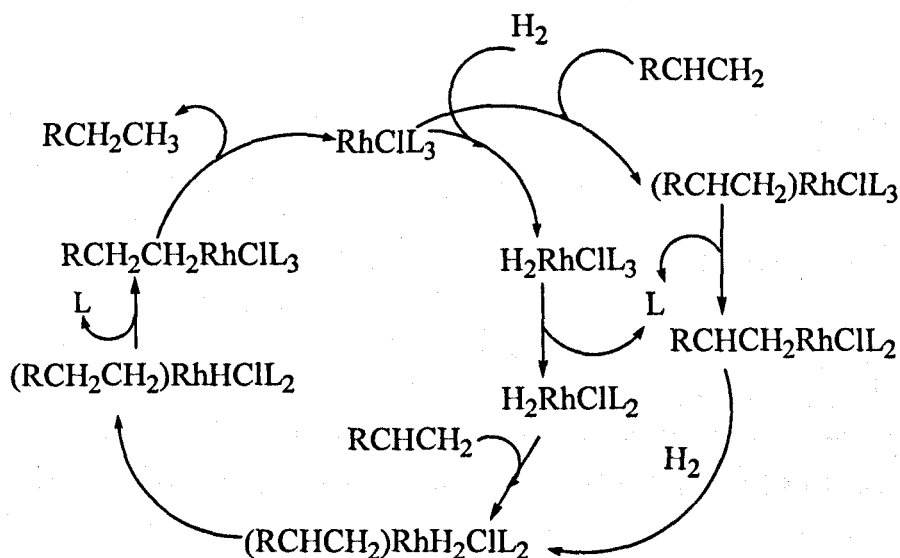


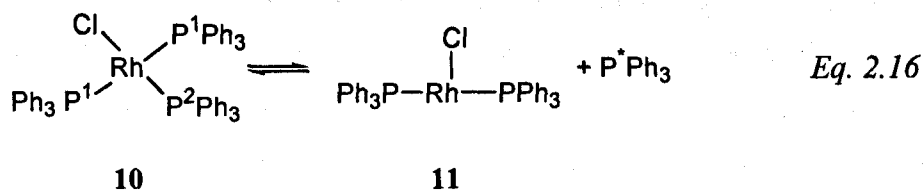
Fig. 2.11. Catalytic cycle proposed by Halpern in 1981.⁸⁵

Brown and co-workers used ^{31}P NMR and molecular modelling to study some proposed intermediates, Fig. 2.12.⁸⁷ The DANTE pulse NMR sequence was used to elucidate some dynamic aspects that had not been clear earlier.

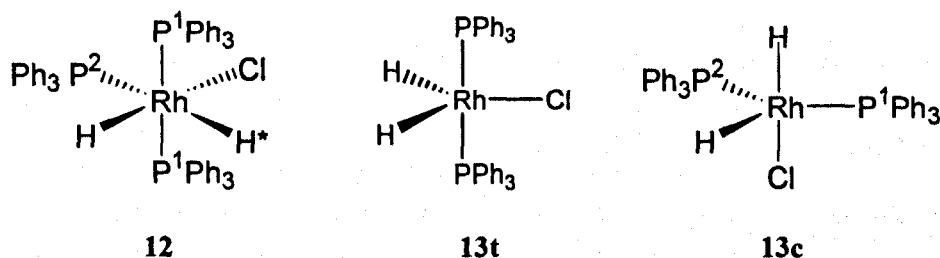
Firstly, the dissociation of one phosphine from $[\text{RhCl}(\text{PPh}_3)_3]$ (**10**), to yield $[\text{RhCl}(\text{PPh}_3)_2]$ (**11**), is required in order to add H_2 to the catalyst and form $[\text{Rh}(\text{H}_2)\text{Cl}(\text{PPh}_3)_3]$ (**12**). The structure of the intermediate **11** is unknown but it is well recognised that three possible geometrical isomers can exist, the geometry is 'T'-shaped and 'Y'-shaped.⁸⁸ Compounds of general type $[\text{Rh}(\text{X})(\text{P})_2]$ are 'T'-shaped with phosphines in the *trans* position, maybe due to steric constraints, because all known examples have bulky phosphines.

The DANTE spin saturation was recorded in order to determine which phosphine dissociates more rapidly in **10**. The saturation of P^1 in a solution of **10** with free PPh_3

showed fast magnetisation transfer from P^1 to P^2 and a much more slow magnetisation transfer from P^1 to free PPh_3 , eq. 2.16. This important result shows a fast exchange rate between P^1 and P^2 , which makes the phosphine sites equivalent without dissociation.



The second part of Brown's study was the dissociation of PPh_3 in the hydride $[\text{Rh}(\text{H}_2)\text{Cl}(\text{PPh}_3)_3]$ **12**. It is well established that **12** releases a PPh_3 in order to form the bis(PPh_3) pentacoordinate complex **13** which traps olefin in the catalytic pathway. The structure of complex **13** is unknown. Previous to Brown's paper, studies had proposed the formation of the *trans*-axial $\text{bi}(\text{PPh}_3)_2$ **13t** instead of *cis*-equatorial $\text{bi}(\text{PPh}_3)$ **13c** due to higher steric hindrance in **13c**. The use of magnetization transfer in ^{31}P and ^1H NMR and molecular modelling in Brown's study suggested that: H and H^* in **12** exchanged rapidly, with the same rate as the P^1 and P^2 exchange in **12**. The dissociation of $P^1\text{Ph}_3$ may give the formation of **13c** but the exchange rate between P^1 and P^2 in **13c** is faster than the coordination of free $P^1\text{Ph}_3$. This coordination of $P^1\text{Ph}_3$ is *trans* to a hydride and occurs through an intermediate with C_{2v} symmetry that may be **13t**, where both phosphines are equivalent. The formation of **13t** is due to the exchange in **13c**.



Brown's results suggest the existence of a detailed mechanism depicted in Fig. 2.12. The existence of a bis(phosphine) **13c** is possible in the TOF hydrogenation rate. This complex **13c** may be more important in the catalytic cycle due to the formation of a more constrained bis(phosphine)(mono-olefin) **14** instead of the less constrained **15**. Hence, the migration of the hydride in **14** to give **16** might be very fast and the determining step in the

whole cycle. Recent theoretical calculations have revealed that the isomerization of **13t** to **13c** has a large activation barrier of 113 kJ mol^{-1} in Brown's mechanism vs the barrier of the insertion of the olefin in Halpern's mechanism of $60\text{-}70 \text{ kJ mol}^{-1}$. In general, theoretical calculation agrees that when the insertion of the olefin is the determining step of the cycle, Halpern's mechanism is the most likely pathway, while theoretical results of Brown's mechanism suggest that the rate determining step is the reductive elimination of the olefin and the last mechanism could only be a possibility when bulky olefins are used.⁵ In any case, theoretical studies at the beginning of the 1980's have discussed the possibility of a square based pyramid such as **17** instead of the bipyramidal trigonal geometry, due to the lower energy state of the PH_3 complex instead of the PPh_3 . Clearly PH_3 as a model of the PPh_3 may not give rise to the same steric effect.⁸⁹ The last report did not calculate activation energies of any route, hence the proposal of the existence of species such as **17** in the cycle cannot be conclusive.

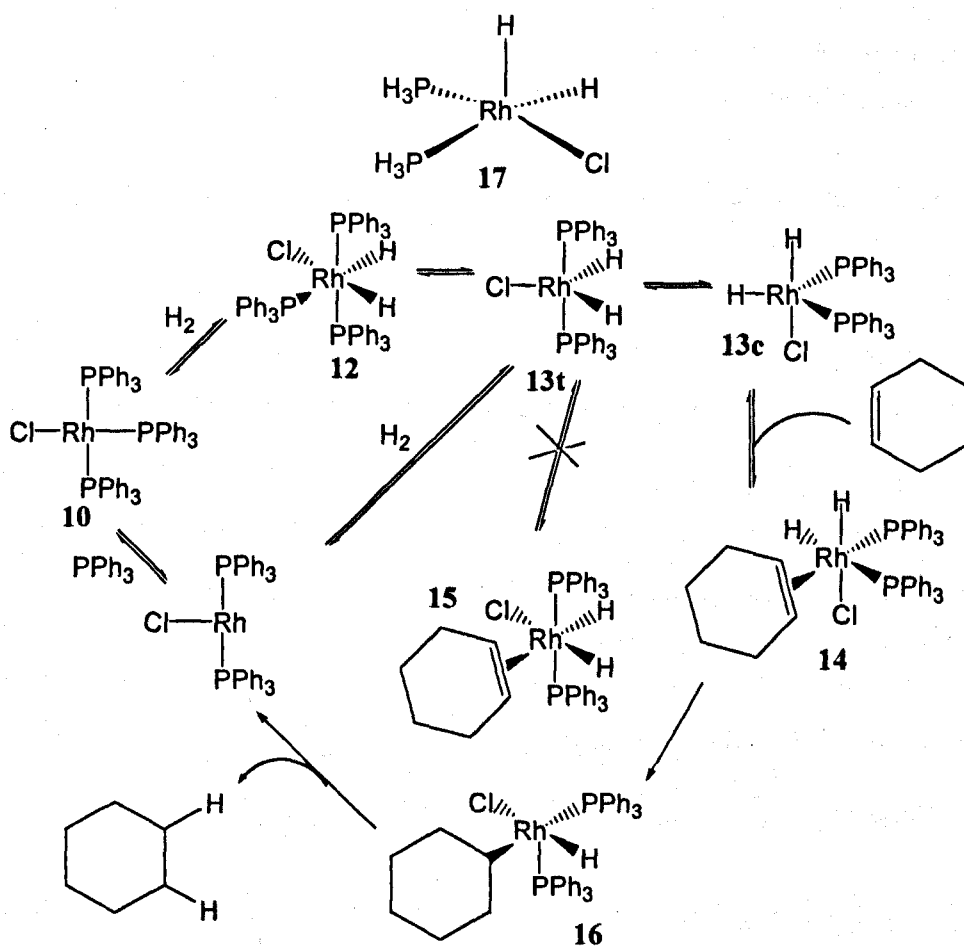


Fig. 2.12. Mechanism proposed by Brown from the DANTE sequence pulse (NMR).⁵ This proposal is based on the original study by Halpern, Fig. 2.11.

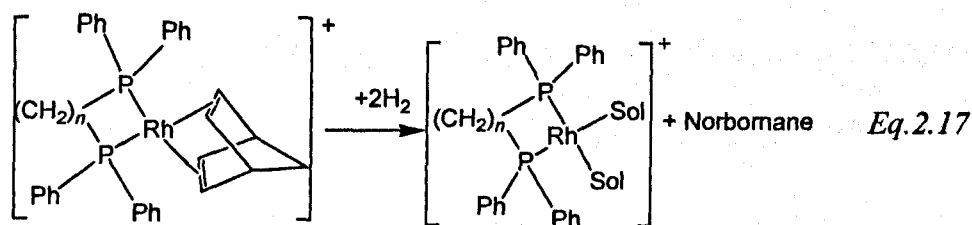
The last study shows the power of NMR spectroscopy as a technique to elucidate mechanisms where fast inter-conversions are involved. Studies on catalytic hydrogenation with Wilkinson's catalyst have cleared up many aspects of the mechanism and have been used to understand other catalytic transformations. Finally, it is worth noting that the proposed intermediates have not been isolated. Only have **12** and similar compounds to **16** been directly observed by NMR. The rest have been proposed on the basis of results of multinuclear NMR studies.

The present work reports the results of the chemistry of Wilkinson's catalyst in [emim][Al₂Cl₇] ionic liquids. It shows a different chemistry (chapter 4) from the well-known behaviour reported before.

2.6.2. Monocationic Rhodium-olefin catalyst for hydrogenation

As has been said, following the report of the Wilkinson's catalyst in homogeneous media, the chemistry of rhodium compounds increased hugely. Some reports following these complexes included the syntheses of compounds of the type [Rh(diolefin)(L₂)]X. The diolefin is either 1,5-cyclooctadiene (COD) or 2,5-norbornadiene (NBD). L₂ is either (PPh₃)₂, (PMePh₂)₂, 1,2-bisdiphenylphosphinoethane, (dppe);⁹⁰ 1,3-bisdiphenylphosphinopropane, (dppp); 1,4-bisdiphenylphosphinobutane, (dppb). The counterion is either [Cl]⁻, [BF₄]⁻ or [PF₆]⁻.

The complexes are active as hydrogenation catalysts of olefins. Osborn and Shrock reported on only a few studies in 1967. They proposed a cycle, based on the formation of a solvated intermediate, which is an air and oxygen sensitive active species (eq. 2.17).⁹¹



The presence of some anions is quite important as in the case of chloride. The latter

species can enter into the coordination sphere of the rhodium centre and inhibits the hydrogenation process by blocking one position. This behaviour is not followed when $[\text{Cl}]^-$ is replaced by $[\text{BF}_4]^-$ or $[\text{PF}_6]^-$, because of the lack of coordination abilities in the last two ions.

Table 2.6. ^{31}P NMR data for solvated complexes obtained from the hydrogenation of NBD in $[\text{Rh}(\text{NBD})(\text{L}_2)][\text{BF}_4]$.

Phosphine L_2	Free phosphine	Phosphine in complex $[\text{Rh}(\text{NBD})(\text{L}_2)][\text{BF}_4]$		Solvated complex $[\text{Rh}(\text{L}_2)(\text{MeOH})_2][\text{BF}_4]$	
	δ , ppm	δ , ppm	$^1J(^{31}\text{P}-^{103}\text{Rh})$, Hz	δ , ppm	$^1J(^{31}\text{P}-^{103}\text{Rh})$, Hz
dppe	-12.3	55	157	80	203
dppp	-17.0	14	148	38	190
dppb	-15.0	26	152	52	196

The chemistry of the solvated intermediates has been well reported. Halpern,⁸⁵ Brown and Baird⁹² have observed the solvated complexes in solution in the case of bidentate phosphines.

The last works proposed more detailed mechanisms during the hydrogenation process by ^{31}P -NMR studies. All of them suggest initial formation of **18a** (Fig. 2.13) and the consequent formation of **18b**.

Those intermediates have $[\text{BF}_4]^-$ or $[\text{PF}_6]^-$ as anions and they can only coordinate to the metal centre with difficulty. In fact, there have been few reports where these kinds of anions coordinate to metal centres in solution.

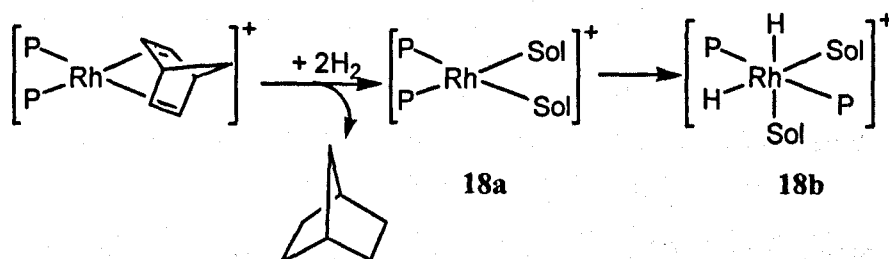
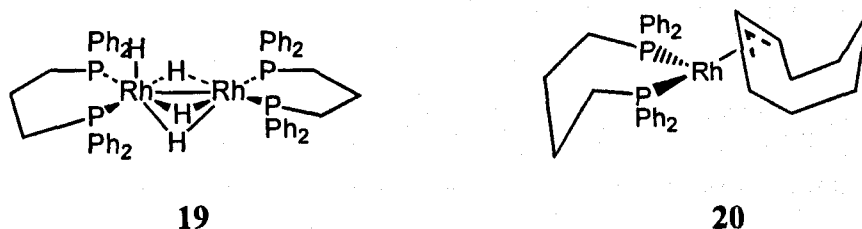


Fig. 2.13. Hydrogenation process with Osborn and Shrock complexes.⁹²

There is a study where the initial hydrogenation of the diene is examined. The same

work compares the hydrogenation rate of NBD and COD, NBD being the faster substrate to hydrogenate.⁹³

There is no mention of any addition of hydride to the active catalyst at room temperature when $L_2 = dppe, dppp$ and $dppb$ in acetone or coordinating solvents. However, the hydrogenation in CD_2Cl_2 or $CDCl_3$ has been reported and a mixture of dimeric hydrides may be formed by using $dppe$.⁹⁴ The solution of $[\{^iPr_2P(CH_2)_2P^iPr_2\}(H)Rh(\mu-H)_3Rh\{^iPr_2P(CH_2)_2P^iPr_2\}]$, **19**, is stable under a H_2 atmosphere and it has been characterized by ^{31}P NMR spectroscopy.⁹⁵ Finally, the substitution of COD in the cluster $[Rh(COD)(H)]_4$ with $dppb$ yields the formation of the η^3 -allyl complex, **20**, under H_2 atmosphere. This complex is rapidly hydrogenated and changes to $[RhH(dppb)_2]$.⁹⁶



All these compounds have been widely studied and the chemistry of hydrogenation has been well elucidated.⁹²⁻⁹⁷

2.7. Interaction of $[SnCl_3]^-$ with metallic centres

This section explains some chemical aspects of $SnCl_2$ in order to understand the chemistry of some rhodium complexes in $[bmim][Sn_2Cl_5]$, chapter 5.

In general, the structural chemistry of $Sn(II)$ halides is particularly complex, partly because of the stereochemical activity (or non-activity) of the nonbonding pair of electrons and partly because of the propensity of $Sn(II)$ to increase its coordination number by polymerisation into larger structural units such as rings or chains. For example, $SnCl_2$ in the gas phase forms bent molecules but the crystalline material has a layer structure with chain of corner-shared trigonal pyramidal $\{SnCl_3\}$ groups. $Sn(II)$ rarely adopts structures typical of spherically symmetrical ions because the nonbonding pair of electrons, which is $5s^2$ in the free gaseous ion, readily distorts in the condensed phase and this can be

described in terms of ligand-field distortion or the adoption of some 'p character'.⁹⁷ The dihydrate also has a coordinated structure with only one of the H₂O molecules directly bonded to the Sn^(II). If the aquo ligand is replaced by Cl the pyramidal [SnCl₃]⁻ ion is obtained, and has been observed in CsSnCl₃.⁹⁰

There seems little tendency to add a fourth ligand: *e.g.* the compound K₂SnCl₄·H₂O has been shown to contain pyramidal [SnCl₃]⁻ and 'isolated' Cl⁻ ions, *i.e.* K₂[SnCl₃]Cl·H₂O. Apart from its structural interest, SnCl₂ is important as a widely used mild reducing agent in acid solution. The dihydrate is commercially available for use in electrolytic tin-plating baths, as a sensitizer in silvering mirrors, in the plating of plastics and as a perfume stabilizer in toilet soaps. The anhydrous material can be obtained either by dehydration using acetic anhydride or directly by reacting heated Sn with dry HCl gas.

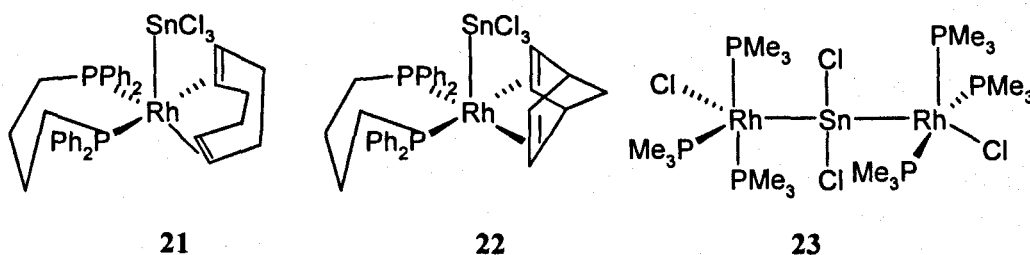
SnCl₂ can be considered as a stannylene, it is bent with a lone pair and undergoes the general type of carbene reactions to give new bonds, eq. 2.18.⁹⁸ According to this reaction SnCl₂ can break the Rh-Cl bond and it can be inserted to form Rh-SnCl₃ species. The new ligand [SnCl₃]⁻ in the metallic centre has a strong *trans*-effect due to the strong σ donation from tin to the metal and it is comparable to CN⁻ and CO.⁹⁹ The nonbonding pair in the Sn(II) can act as a donor to 'd' vacant orbitals in the metal, and the vacant 'third' 5p orbital and 5d orbitals can act as acceptors in tin.



The interest of trichlorostannato ligands was increased with the discovery of homogeneous hydrogenation of ethene and ethyne at room temperature and low H₂ pressure in solutions containing chloro(trichlorostannato)platinum (II) complex anions.¹⁰⁰ The first examples of Rh-SnCl₃ interactions were described in 1964.¹⁰¹ The observation of catalytic dehydrogenation of propan-2-ol yielding acetone and dihydrogen was reported to proceed in a propan-2-ol solution containing RhCl₃·3H₂O, SnCl₂·2H₂O and LiCl in 1970.¹⁰² The characterization of the possible active catalyst [RhH(SnCl₃)₅]₃³⁻ has been proposed by ¹¹⁹Sn and ¹H NMR.¹⁰³ The stability of the catalytic system in Pt and Rh complexes is not well understood but the [SnCl₃]⁻ ligand stabilizes Pt and Rh low valent species and its strongly 'π acid' nature labilizes the often kinetically inert complexes of the platinum group metals to ligand substitution.

Surprisingly, the interaction of SnCl_2 and platinum chloride had been documented for more than 190 years¹⁰⁴ and the interaction with Rh for more than a half century.¹⁰⁵ Remarkably, the detailed nature of the interaction of SnCl_2 with platinum group metals has only been elucidated relatively recently (1980's). Nowadays, SnCl_2 is still used as a colorimetric reagent to detect traces of Pt(II/IV) in the sub parts per million range.^{105,106}

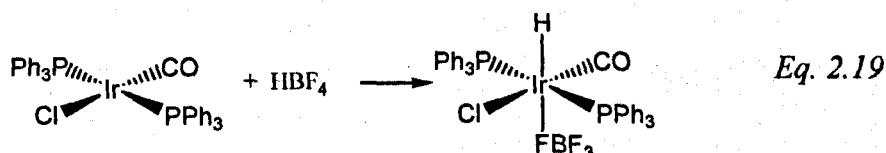
Some examples where chlorostannates (II) act as ligands in rhodium complexes have been isolated. Ligands such as $[\text{SnCl}_3]^-$,¹⁰⁷ $[\mu\text{-SnCl}_2]$,¹⁰⁸ and alkylstannates have been known in complexes such as **21-23** and they have been identified by X-ray diffraction in the 1990's and ^{31}P or ^{119}Sn NMR spectroscopy in the 1980's.¹⁰⁹⁻¹¹⁰



The interaction of Vaska's type complexes with $[\text{bmim}][\text{Sn}_2\text{Cl}_5]$ is described in chapter 7. This small review gives a general idea about the chemical behaviour of the $[\text{SnCl}_3]^-$ species in the $[\text{Sn}_2\text{Cl}_5]^-$ ionic liquid.

2.8. Interaction of metallic centres with weak coordinating anions

Finally, this section mentions the compounds where weakly coordinating anions bond to the metal. The interaction of characteristic non-coordinating anions such as $[\text{BF}_4]^-$, $[\text{PF}_6]^-$ and $[\text{OSO}_2\text{CF}_3]^-$ has been observed for such metallic centres as Ir,¹¹¹ Pt,¹¹² Re¹¹³ and Os.¹¹⁴ All these complexes are highly air and moisture sensitive and only a few crystalline structures have been reported. The coordination is shown in eq. 2.19.



Organic solvent molecules or any neutral ligand quickly replace these types of ligands. The anion remains in the complex as the counter anion. Large anions have the ability to stabilize such species that have been impossible to isolate with small anions. This is the case for carboanions, where the large anion $[1\text{-Et-CB}_{11}\text{F}_{11}]^-$ enables the isolation of the non-classical cation $[\text{Rh}(\text{CO})_4]^+$.¹¹⁵ In such a case, the interaction of fluorine with the metallic centre gives enough stability to the centre for it to be characterized by X-ray crystallography.

2.9. Summary

This section has shown the chemistry of well studied metallic compounds such as the historically important Wilkinson's catalyst $[\text{Rh}(\text{Cl})(\text{PPh}_3)_3]$, Vaska's type complexes such as $[\text{Rh}(\text{Cl})(\text{CO})(\text{PR}_3)_2]$ and diphosphine complexes $[\text{Rh}(\text{diolefin})(\text{L}_2)]\text{X}$. It is important to note that their chemistry has been studied for four decades and there is a clear mechanism understood in each case.

Any change in chemical behaviour of the complexes in the ionic liquids will be discovered when these rhodium compounds are compared with their original behaviour in the common organic solvents. The use of chloroaluminate (III) ionic liquids, which are the highest polar media known in an ionic liquid, give the best opportunity for seeing the difference between organic and ionic solvents. Chloroaluminates (III) have been tested to stabilize species that are unstable in common organic solvents and this characteristic could be crucial for explaining the enhancement of catalytic activity in this ionic medium.

The aims of the project are explained next followed by the experimental procedure of the thesis. Chapters 4-8 include the results and discussion of the chemistry of Wilkinson's catalyst and some organometallic complexes in representative ionic liquids. Chapter 4 discusses the chemistry of $[\text{RhCl}(\text{PPh}_3)_3]$ in $[\text{emim}][\text{Al}_2\text{Cl}_7]$. Chapter 5 shows the results when the same complex is dissolved in CH_2Cl_2 in the presence of different quantities of AlCl_3 . Chapter 6 takes back the chemistry of chloroaluminate ionic liquids and discusses the carbonylation of dissolutions of $[\text{Rh}(\text{Cl})(\text{CO})(\text{PR}_3)_2]$ in $[\text{emim}][\text{Al}_2\text{Cl}_7]$ giving evidence of completely new species. After that, chapter 7 shows the chemistry of the same kind of rhodium complexes in $[\text{bmim}][\text{Sn}_2\text{Cl}_5]$ and the strong ability of $[\text{SnCl}_3]^-$ to stabilize species that were difficult to isolate in common organic solvents. In

general, the results will show the behaviour of Rh species that are completely different to the established one. Solutions of organometallic complexes in the ionic liquids in this study have shown a different reactivity at the metallic centre, giving species that have been proposed as intermediates in common organic solvents.

2.10. Aim of the work

The solutions of complexes such as $[\text{Rh}(\text{Cl})(\text{PPh}_3)_3]$, $[\text{Rh}(\text{Cl})(\text{CO})(\text{PR}_3)_2]$ and $[\text{Rh}(\text{diolefin})(\text{dppb})][\text{BF}_4]$ in $[\text{Al}_2\text{Cl}_7]^-$, $[\text{Sn}_2\text{Cl}_5]^-$, $[\text{BF}_4]^-$ and $[\text{PF}_6]^-$ ionic liquids will be studied by multinuclear NMR: ^{31}P , ^{13}C and ^1H mainly. The spectroscopy data will be analysed and compared with the established in common organic solvents. The use of rhodium complexes with catalytic activity in ionic liquids can give detailed information of different reactivity of these complexes in ionic substances.

The solution of $[\text{Rh}(\text{Cl})(\text{PPh}_3)_3]$ and $[\text{Rh}(\text{Cl})(\text{CO})(\text{PR}_3)_2]$ in $[\text{Al}_2\text{Cl}_7]^-$ ionic liquids will be studied by NMR techniques of $^{103}\text{Rh}\{\text{INEPT}\}$ and ^{27}Al when necessary. Spectroscopy data will be compared with that established in common organic solvents. Chloroaluminate (III) ionic liquids with $x_{\text{AlCl}_3} = 0.67$ offers the highest acidic medium known in an ionic liquid. Hence, they have been chosen as the initial option to develop the present thesis.

The solutions of $[\text{Rh}(\text{Cl})(\text{PPh}_3)_3]$ and $[\text{Rh}(\text{Cl})(\text{CO})(\text{PR}_3)_2]$ in chlorostannate (II) ionic liquids with $x_{\text{SnCl}_2} = 0.60$ will also be studied by ^{31}P NMR and this can establish the synthesis of new species by the addition of chlorostannate anions to the metallic centre. The coordination of 'Sn' will show a highly coordinating environment. The results will give information about the reactivity of such systems in hydrogenation reactions.

2.11. References

- ¹ V. P. W. Böhm, W. A. Herrmann and T. Weskamp, *J. Organomet. Chem.*, 2000, **600**, 12.
- ² G. R. J. Artus, L. J. Goowen and W. A. Herrman, *Chem. Eur. J.*, 1996, **2**, 1627.

- ³ A. Gridven and I. M. Mihaltseva, *Synth. Commun.*, 1994, **24**, 1547.
- ⁴ J. Joule, K. Mills and G. Smith, *Heterocyclic Chemistry*, 3rd. edn., Chapman and Hall, London, 1995, pp. 370; M. Grimmet, *Adv. Heterocycl. Chem.*, 1980, **27**, 241.
- ⁵ C. Hussey, J. Levinsky, J. Wilkes and R. Wilson, *Inorg. Chem.*, 1982, **21**, 1263.
- ⁶ T. A. Zawodzinski and R. A. Osteryoung, *Inorg. Chem.*, 1987, **26**, 2920.
- ⁷ A. Abdul-Sada, A. Avent, M. Parkington, A. Ryan, K. Seddon, and T. Welton, *J. Chem. Soc., Dalton Trans.*, 1993, 3283.
- ⁸ Z. Karpinski, C. Nanjundiah and R. A. Osteryoung, *Inorg. Chem.*, 1984, **23**, 3358.
- ⁹ P. Bonhôte, P. Dias, N. Papageorgiou, K. Kalyanasundaram and M. Grätzel, *Inorg. Chem.*, 1996, **35**, 1168.
- ¹⁰ N. Karodia, S. Guise, C. Newlands and J. A. Andersen, *J. Chem. Soc., Chem. Commun.*, 1998, 2341.
- ¹¹ Z. J. Karpinski and R. S. Osteryoung, *Inorg. Chem.*, 1984, **23**, 1491; A. A. K. Abdul-Sada, A. M. Greenway, K. S. Seddon, and T. Welton, *Org. Mass. Spectrom.*, 1993, **28**, 759.
- ¹² Y. Chauvin, S. Einloft and H. Olivier, *Ind. Eng. Chem. Res.*, 1995, **34**, 1149; Y. Chauvin, F. Di-Marco-Van Tiggelen, B. Gilbert and H. Olivier, *J. Chem. Soc., Dalton Trans.*, 1995, 3867.
- ¹³ G. Mamantov, J. P. Schoebrechts, J. C. Selkirk and S. D. Williams, *J. Am. Chem. Soc.*, 1987, **109**, 2218.
- ¹⁴ Y. Chauvin and H. Olivier-Bourbigou, *CHEMTECH*, 1995, **25**, 26.
- ¹⁵ G. W. Parshall, *J. Am. Chem. Soc.*, 1972, **94**, 8716; H. Waffenschmidt and P. Wasserscheid, *J. Mol. Catal.*, 2001, 234.
- ¹⁶ J. Wilkes and M. Zaworotko, *J. Chem. Soc., Chem. Commun.*, 1992, 965; J. Dullius, J. Dupont, S. Einloft, R. de Souza and P. Suarez, *Polyhedron*, 1996, **15**, 1217.
- ¹⁷ R. Carlin, J. Fuller, D. Haworth and H. De Long, *J. Chem. Soc., Chem. Commun.*, 1994, 299.
- ¹⁸ W. Ford, D. Hart and R. Hauri, *J. Org. Chem.*, 1973, **38**, 3916.
- ¹⁹ C. Bowlas, D. Bruce and K. R. Seddon, *J. Chem. Soc., Chem. Commun.*, 1996, 1625.
- ²⁰ K. Seddon and M. Earle, *Pure Appl. Chem.*, 2000, **72**, 7, 1391.
- ²¹ H. Stegemann, A. Rhode, A. Reiche, A. Schnittke and H. Füllbier, *Electrochim. Acta*, 1992, **37**, 379.
- ²² P. Bonhôte, A. Dias, N. Papageorgiou, K. Kalanasundaram and M. Grätzel, *Inorg. Chem.*, 1996, **35**, 1168; A. Elaiwi, P. Hitchcock, K. Seddon, N. Srinivasan, Y-M Tan, T. Welton and J. Zora, *J. Chem. Soc., Dalton Trans.*, 1995, 3467.
- ²³ T. Welton, *Chem. Rev.*, 1999, **99**, 2071.
- ²⁴ J. Holbrey and K. R. Seddon, *J. Chem. Soc., Dalton Trans.*, 1999, 2133.
- ²⁵ A. A. Fanin, D. A. Floreani, L. A. King, J. S. Lander, B. J. Piersma, D. J. Stech, R. L. Vaughn, J. S. Wilkes and J. L. Williams, *J. Phys. Chem.*, 1984, **88**, 2614.
- ²⁶ P. Bonhôte, A. P. Dias, N. Papageorgiou, K. Kalyanasundaram and M. Grätzel, *Inorg. Chem.*, 1996, **35**, 1168.
- ²⁷ J. Huddleston, R. Swatloski, A. Visser, H. Willauer and R. Roger, *J. Chem. Soc., Chem.*

- Commun.*, 1998, 1765.
- ²⁸ R. Roger, R. Swatloski and A. Visser, *Abstracts of Paper of the American Chemical Society*, 1999, **218**, No. Pt1, pp. 22-IEC; S. Griffin, R. Roger, R. Swatloski and A. Visser, *Abstracts of Paper of the American Chemical Society*, 1999, **218**, No. Pt1, pp. 23-IEC; J. Huddleston, R. Rogers, R. Swatloski and A. Visser, *Abstracts of Paper of the American Chemical Society*, 1999, **217**, pp. 40-IEC; pp. 41-IEC; pp. 42-IEC; pp. 109-IEC. The abstraction of organometallic compounds once they are in the ionic liquid has been impossible.
- ²⁹ L. A. Blanchard, D. Hancu, E. J. Beckman and J. F. Brennecke, *Nature*, 1999, **399**, 28; L. A. Blanchard and L. A. Brennecke, *Ing. Eng. Chem. Res.*, 2001, **40**, 287.
- ³⁰ P. Wasserscheid and W. Keim, *Angew. Chem. Int. Ed.*, 2000, **39**, 3772.
- ³¹ B. Cornyl and E. Weibus, *Chem. Ing. Tech.*, 1994, **66**, 916; *CHEMTECH*, 1995, **25**, 33.
- ³² W. Keim, *Chem. Ing. Tech.*, 1984, **56**, 850.
- ³³ The second method that has been proposed as heterogenization of homogeneous media is the "anchor" of the metal complex catalyst in a solid "support". However, this method does not have any industrial application because it does not offer the surface contact advantage of homogeneous catalyst in some cases.
- ³⁴ R. Sheldon, *J. Chem. Soc., Chem. Commun.*, 2001, 2399.
- ³⁵ Y. Chauvin, L. Mussman and H. Olivier, *Angew. Chem. Int. Ed. Engl.*, 1995, **34**, 23, 2698.
- ³⁶ J. Dupont, A. Monteiro, R. De Souza and F. Zinn, *Tetrahedron: Asymmetry*, 1997, **8**, 2, 177.
- ³⁷ J. Dullis, J. Dupont, S. Einloft, R. De Souza and P. Suarez, *Inorg. Chim. Acta*, 1997, **255**, 207.
- ³⁸ P. Dyson, D. Ellis, D. Parker and T. Welton, *J. Chem. Soc., Chem. Commun.*, 1999, 25.
- ³⁹ J. Andersen, S. Guise, N. Karodia and C. Newlands, *J. Chem. Soc., Chem. Commun.*, 1998, 2341.
- ⁴⁰ J. E. L. Dullis, J. Dupont, S. Einloft, R. F. De Souza and P. A. Z. Suarez, *Organometallics*, 1998, **17**, 815.
- ⁴¹ P. Hichcock, K. Seddon and T. Welton, *J. Chem. Soc., Dalton Trans.*, 1993, 2639.
- ⁴² W. Chen, L. Xu, C. Chatterton and J. Xiao, *J. Chem. Soc., Chem Commun.*, 1999, 1247.
- ⁴³ C. J. Mathew, P. S. Smith and T. Welton, *J. Chem. Soc., Chem. Commun.*, 2000, 1249.
- ⁴⁴ C. Beelefon, E. Pollet and P. Grenouillet, *J. Mol. Catal. A.*, 1999, **145**, 121.
- ⁴⁵ W. Chen, J. Xiao and L. Xu, *Organometallics*, 2000, **19**, 1123.
- ⁴⁶ M. Earle, P. McCormac and K. R. Seddon, *Green Chem.*, 1999, 23.
- ⁴⁷ M. Earle, P. McCormac and K. R. Seddon, *J. Chem. Soc., Chem. Commun.*, 1998, 2245; M. Badri, J. Brunet and R. Perron, *Tetrahedron Letters*, 1992, **33**, 4435.
- ⁴⁸ T. Kitazume and F. Zulficar, *Green Chem.*, 2000, **2**, 137; T. Kitazume, F. Zulficar and G. Tanaka, *Green Chem.*, 2000, **2**, 133.
- ⁴⁹ J. H. Choi, E. J. W. H. Roh and C. E. S. Song, *J. Chem. Soc., Chem. Commun.*, 2000, 1695.
- ⁵⁰ I. Wen, S. Ward, C. Hussey, K. R. Seddon and J. Turp, *Inorg. Chem.*, 1987, **26**, 2140.
- ⁵² J. Shoenbrechts and B. Gilbert, *J. Electrochem. Soc.*, 1981, **128**, 26; Z. Karpinsky and R. Osteryoung, *Inorg. Chem.* 1984, **23**, 14; Z. Karpinsky and R. Osteryoung, *Inorg. Chem.*, 1985, **24**, 23.

- ⁵² A. Dworkin, G. Smith, R. Pagni and S. Zingg, *J. Am. Chem. Soc.*, 1989, **111**, 525.
- ⁵³ C. Hussey, T. Scheffler, J. Wilkes and A. Fannin, *J. Electrochem. Soc.*, 1986, **133**, 1389.
- ⁵⁴ L. Hermmann and W. D'Olieslager, *Inorg. Chem.*, 1985, **24**, 4704.
- ⁵⁵ T. Zawodzinski and R. Osteryoung, *Inorg. Chem.*, 1990, **26**, 2842; A. Absul-Sada, A. Greenway, K. R. Seddon and T. Welton, *Org. Mass. Spectrom.*, 1993, **28**, 759.
- ⁵⁶ C. Hussey, *Pure Appl. Chem.*, 1988, **60**, 1768.
- ⁵⁷ P. B. Hitchcock, T. J. Mohammed, K. R. Seddon, J. A. Zora, C. L. Hussey and E. H. Ward, *Inorg. Chim. Acta*, 1986, **113**, L25.
- ⁵⁸ T. B. Scheffler, C. L. Hussey, K. R. Seddon, C. M. Kear and P. D. Armitage, *Inorg. Chem.*, 1983, **22**, 2099.
- ⁵⁹ I. W. Sun, E. H. Ward, C. L. Hussey, K. R. Seddon and J. E. Turp, *Inorg. Chem.*, 1987, **26**, 2140.
- ⁶⁰ C. L. Hussey, R. Quigley and K. R. Seddon, *Inorg. Chem.*, 1995, **34**, 370.
- ⁶¹ R. Quigley, P. A. Barnard, C. L. Hussey and K. R. Seddon, *Inorg. Chem.*, 1992, **31**, 1255.
- ⁶² A. Dent, K. R. Seddon and T. Welton, *J. Chem. Soc., Chem. Commun.*, 1990, 315; A. Absul-Sada, A. Greenway, K. R. Seddon and T. Welton, *Org. Mass Spectrom.*, 1992, **27**, 648.
- ⁶³ C. L. Hussey, and T. M. Laher, *Inorg. Chem.*, 1981, **20**, 4201.
- ⁶⁴ G. Alegra, A. Immirzi, L. Porri, G. C. Tettamanti and G. Vitulli, *J. Am. Chem. Soc.*, 1970, **92**, 289.
- ⁶⁵ A. R. Barron, A.S. Borovik and S. G. Bott, *J. Am. Chem. Soc.*, 2001, **123**, 11219.
- ⁶⁶ W. Beck and K. Sünkel, *Chem. Rev.*, 1988, **88**, 1405.
- ⁶⁷ J. Boon, J. Levinsky, J. Pflug and J. Wilkes, *J. Org. Chem.*, 1986, **51**, 840.
- ⁶⁸ C. Lee, *Tetrahedron Lett.*, 1999, **40**, 2461.
- ⁶⁹ Y. Chauvin, A. H. Hirshauer and H. B. Olivier, *J. Mol. Catal.*, 1994, **92**, 155.
- ⁷⁰ A. Christopher, M. Earle, G. Roberts and K. R. Seddon, *J. Chem. Soc., Chem. Commun.*, 1998, 2245.
- ⁷¹ V. Biriss and M. Goledzinowski, *Ind. Eng. Chem. Res.*, 1993, **3**, 1795.
- ⁷² a) L. Green, R. Singer and J. Surene, *J. Chem. Soc., Chem. Commun.*, 1996, 2753; A. Stark, B. MacLean and R. Singer, *J. Chem. Soc., Dalton Trans.*, 1999, 63.
- ⁷³ P. Dyson, M. Grossel, N. Srinivasan, T. Vine, T. Welton, D. William, A. Shite and T. Zigras, *J. Chem. Soc., Dalton Trans.*, 1997, 3465.
- ⁷⁴ R. T. Carlin and J. Fuller, *Inorg. Chim. Acta*, 1997, **255**, 189.
- ⁷⁵ A. Christopher, M. Earle, G. Roberts and K. R. Seddon, *J. Chem. Soc., Chem. Commun.*, 1999, 1043.
- ⁷⁶ D. Dalling and D. Grant, *J. Am. Chem. Soc.*, 1974, **96**, 1827.
- ⁷⁷ B. Ellis, W. Keim and P. Wassercheid, *J. Chem. Soc., Chem. Commun.*, 1999, 337.
- ⁷⁸ B. Hoffman, J. Fleischhauer, W. Keim, R. Lodewick, U. Meier, M. Peukert and J. Schmitt, *J. Mol. Catal.*, 1979, **6**, 79.

- ⁷⁹ K. Dietrich, J. Dupont, S. Einloft and R. Souza, *Polyhedron*, 1996, **15**, 3257; Y. Chauvin, B. Gilbert and I. Guibard, *J. Chem. Soc., Chem. Commun.*, 1990, 1715.
- ⁸⁰ R. Friedlander, J. Nielich, R. Obenaus and D. Ward, *Neumeister Hydroc. Process*, 1986, 31.
- ⁸¹ J. A. Osborn, G. Wilkinson and J. F. Young, *J. Chem. Soc., Chem. Commun.*, 1965, 17; F. H. Jardine, J. A. Osborn, G. Wilkinson and J. F. Young, *J. Chem. Soc. A*, 1966, 1711.
- ⁸² Apparently, it was discovered independently by R. S. Coffrey at ICI. Nevertheless, Wilkinson's name has stuck.
- ⁸³ L. Vaska, R. E. Rhodes, *J. Am. Chem. Soc.*, 1965, **87**, 4970; L. Vaska, *Inorg. Nuclear Chem. Lett.*, 1965, **1**, 89.
- ⁸⁴ P. Jesson, D. Lindner, P. Meakin and C. A. Tolman, *J. Am. Chem. Soc.*, 1974, **96**, 2762; *Dynamic Nuclear Magnetic Resonance*, F. Cotton and L. Jackman, Academic Press, London, 1975, page 304.
- ⁸⁵ J. Halpern, *Inorg. Chim. Acta*, 1981, **50**, 11.
- ⁸⁶ M. Torrent, M. Sola and G. Frenking, *Chem. Rev.*, 2000, **100**, 439.
- ⁸⁷ J. E. Brown, P. Evans and A. Lucy, *J. Chem. Soc. Perkin Trans. 2*, 1987, 1589.
- ⁸⁸ R. Bau, S. Miles, C. Reed and Y. Yared, *J. Am. Chem. Soc.*, 1977, **99**, 7076; J. Huheey, *Inorganic Chemistry: Principles of structure and reactivity*, 4th ed., Harper Collins, U.S.A., 1993, page 707. The evidence for dissociation of a PPh₃ from [RhCl(Ph₃P)₃] is indirect but persuasive: i) For complexes with less sterically hindered phosphine (e.g. PEt₃), the catalytic effect disappears apparently, steric repulsion forcing dissociation is necessary; and ii) with the corresponding iridium complex in which the metal-phosphorus bond is stronger, no dissociation takes place and no catalysis is observed. This tricoordinated complex is very reactive and has not as yet been isolated, but the closely related [Rh(Ph₃P)₃]⁺, which could form from the dissociation of a chloride ion from Wilkinson's catalyst has been studied and found to have an unusual structure.
- ⁸⁹ A. Dediue, *Inorg. Chem.*, 1980, **19**, 2941.
- ⁹⁰ E. W. Abel, M. A. Bennett and G. Wilkinson, *J. Chem. Soc.*, 1959, 3178.
- ⁹¹ J. A. Osborn and R. R. Schrock, *J. Am. Chem. Soc.*, 1971, **93**, 2397.
- ⁹² M. C. Bair, I. Greveling and D. A. Slack, *Inorg. Chem.*, 1979, **18**, 3125.
- ⁹³ D. Heller and A. Börner, *Tetrahedron Lett.*, 2001, **42**, 223; M. A. Esteruelas, J. Herrero, M. Martín, L. A. Oro and V. M. Real, *J. Organomet. Chem.*, 2000, **599**, 178.
- ⁹⁴ I. R. Butler, W. R. Cullen, B. E. Mann and C. R. Nurse, *J. Organomet. Chem.*, 1985, **280**, C47.
- ⁹⁵ F. W. B. Einstein, M. D. Fryzuk, T. Jones and W. E. Piers, *Can. J. Chem.*, 1989, **67**, 883.
- ⁹⁶ E. Dinjus, F. Gassner, H. Görls and W. Leitner, *Organometallics*, 1996, **15**, 2078.
- ⁹⁷ N. N. Greenwood and A. Earnshaw, *Chemistry of the Elements*, Pergamon, Oxford, 2nd edn. 1997, ch. 10.
- ⁹⁸ F. A. Cotton, G. Wilkinson, C. A. Murillo and M. Bochmann, *Advanced Inorganic Chemistry*, John Wiley & Sons, New York, 6th edn., 1999, pp. 260.
- ⁹⁹ R. H. Crabtree, *The organometallic chemistry of the transition metals*, Wiley-Interscience, U.S.A., 2001, pp. 11.
- ¹⁰⁰ R. D. Cramer, E. L. Jenner, R. V. Jr. Linday, and U. G. Stolberg, *J. Am. Chem. Soc.* 1963, **85**,

- 1691; K. F. G. Brackenbury, L. Jones, I. Nel, K. R. Koch and J. M. Wyrley-Birch, *Polyhedron*, 1987, **6**, 71.
- ¹⁰¹ G. Wilkinson, R. D. Gillard and J. F. Young, *J. Chem. Soc.*, 1964.
- ¹⁰² H. B. Charman, *J. Chem. Soc., B*, 1970, 584.
- ¹⁰³ T. Yamakawa, S. Shinoda, Y. Saito, H. Moriyana and P. S. Pregosin, *Magn. Res. Chem.*, 1985, **23**, 202.
- ¹⁰⁴ R. Von Wagner, *Manual of Chemical Technology*, J and A. Churchill, London, 1904, pp. 452; Taken from ref. 93b: *Gmelin, Handbuch der Anorganischen Chemie: Gold*, Vol. 62, pp. 79 and 92; *Verlag Chemie*, Weinheim 1950; A. H. Sexton, *Outlines of qualitative analysis*, C. Griffin, London, 3rd edn., 1892, pp. 45; E. A. Schneider, *Z. Anorg. Chem.* 1984, **5**, 80.
- ¹⁰⁵ F. E. Beamish and W. A. E. McBryde, *Anal. Chim. Acta*, 1958, **18**, 551; S. S. Berman and E. C. Goodhue, *Can. J. Chem.* 1959, **37**, 379.
- ¹⁰⁶ G. Shehla, *Vogel's Textbook of Macro and Semimicro Quantitative Inorganic Analysis*, Longmans, London, 5th edn, 1979, pp. 517. The tin(II) chloride spot test for traces of Pt is still one of the more sensitive tests available, 25×10^{-9} g. Pt being easily detectable.
- ¹⁰⁷ M. Garralda, E. Pinilla and M. A. Monge, *J. Organomet. Chem.*, 1992, **427**, 193; V. Garcia, M. A. Garralda, R. Hernandez, M. A. Monge and E. Pinilla, *J. Organomet. Chem.*, 1994, **476**, 41.
- ¹⁰⁸ T. B. Marder and D. M. T. Chan, *Angew. Chem. Int. Ed. Engl.*, 1988, **27**, 442.
- ¹⁰⁹ A. R. Sanger, *Inorg. Chim. Acta*, 1992, **191**, 81.
- ¹¹⁰ V. Garcia and M. A. Garralda, *Inorg. Chim. Acta*, 1991, **180**, 177; M. Kretschmer, P. S. Pregosin and M. Garralda, *J. Organomet. Chem.*, 1983, **244**, 175.
- ¹¹¹ H. Bauer, W. Beck, H. Lobermann, U. Nagel and B. Olgemöller, *Chem. Ber.*, 1982, **115**, 2271; W. Beck and B. Olgemöller, *Inorg. Chem.*, 1983, **997**, 22.
- ¹¹² W. Beck, B. Olgemöller and L. Olgemöller, *Chem. Ber.*, 1981, **114**, 2971.
- ¹¹³ R. Mews, *Angew. Chem. Int. Ed. Engl.*, 1975, **14**, 640.
- ¹¹⁴ K. R. Laing, S. D. Robinson and M. F. Uttley, *J. Chem. Soc. Dalton Trans.*, 1973, 2713.
- ¹¹⁵ O. P. Andersen, M. D. Havighurst, A. J. Lupinetti and S. H. Strauss, *J. Am. Chem. Soc.*, 1999, **121**, 11920.

3. Experimental

3.1. Instrumentation

Compounds and solutions were prepared and handled under an argon atmosphere, using Schlenk line techniques. All the solvents were dried and freshly distilled before use. Johnson Matthey supplied $\text{RhCl}_3 \cdot 3\text{H}_2\text{O}$. Aldrich supplied AlCl_3 , AgBF_4 , GaCl_3 , PCy_3 , PEt_3 , PMePh_2 , PMe_2Ph and TIPF_6 , which were used without further purification. The complexes $[\text{Rh}(\text{CO})(\text{Cl})(\text{PR}_3)_2]$ where $\text{PR}_3 = \text{P}^i\text{Bu}^t\text{Bu}^n$, $\text{P}^i\text{Bu}^t\text{Et}_2$, $\text{P}^i\text{Bu}^t\text{Ph}_2$, $\text{P}^i\text{Bu}^t\text{Pr}^i_2$, were kindly donated by Prof. Shaw from the University of Leeds. ^1H , ^{19}F and ^{31}P NMR were recorded on a Bruker AMX-250 MHz, at 249.9, 234.9 and 100.9 MHz respectively for compounds that were already reported. ^1H , ^{31}P , ^{13}C , ^{27}Al and ^{103}Rh NMR for new compounds in solution were recorded on a Bruker AMX-400, at 399.8, 161.8, 100.5, 103.8, 12.6 MHz respectively. A capillary tube with toluene- d_8 was used to lock the NMR equipment when ionic liquids were used as solvents. Infrared spectra were recorded on a Paragon-1000 Perkin-Elmer Spectrometer, using a 0.2mm CaF_2 solution cell or KBr for solids. The synthesis of $[\text{emim}]\text{Cl}$ was performed in an autoclave or a Fisher-Porter reaction vessel. The catalytic reaction products were analyzed by GC on a HP5890 instrument, with a 50m A-1 capillary column. The temperature programming was isothermally for 10 min at 373K (100°C). The composition of the cyclohexane produced and the remaining cyclohexene were compared to a standard solution of 5% of each component (cyclohexene and cyclohexane) in hexane.

Table 3.1. Desiccant agents used for each solvent. ^a Using benzophenone.

Solvent and reactants	Desiccant agent
Acetonitrile	P_2O_5
Dichloromethane	CaH_2 or CaCl_2
Diethylether ^a	Na
1-methylimidazole	CaH_2
Hexane	Na
Tetrahydrofuran ^a	Na
Toluene	Na



Fig. 3.1. Bruker AMX-400 NMR Magnet.

3.2. Synthesis of Ionic liquids

3.2.1. Purification of AlCl_3

20 g of commercial AlCl_3 was sublimed three times at 140°C in an argon stream. NaCl was added in the final sublimation and the white free-flowing crystal powder sublimed was transferred and kept in a glove box.¹

3.2.2. Synthesis of 1-ethyl-3-methylimidazolium chloride, $[\text{emim}]\text{Cl}$

Freshly distilled 1-methyl imidazole (130 mL, 1.636 mol) was added to ethylchloride (141.0 mL, 1.964 mol) at -32°C in an autoclave. The container was filled with nitrogen at 1 bar. The mixture was heated to 80°C for 72 h. This yellow-white product was transferred to a Schlenk tube and dissolved in acetonitrile. The viscous oil was allowed to stand at 4°C for 8 hours. The white crystals were removed from the solution and washed with acetonitrile at 4°C . The solid was dried at 40°C under vacuum for 96 hours. Yield = 85-90%.² ^1H NMR, CDCl_3 , δ , ppm: 10.12 (s, NCHN), 7.65, (s) 7.82 (s), 4.24 (c, NCH_2 , $^3\text{JHH} = 7.32$ Hz), 3.89 (s, NCH_3), 1.41 (t, $\text{NCH}_2\text{CH}_2\text{CH}_2\text{CH}_3$, $^3\text{JHH} = 7.32$).

3.2.3. Synthesis of 1-butyl-3-methylimidazolium chloride [bmim]Cl

Freshly distilled 1-methyl imidazole (50 mL, 0.545 mol) was added to a 250 mL three neck round bottomed flask with 50 mL of dry toluene. 1.2 equivalents of n-butylchloride (61.5 mL, 0.654 mol) was added and the mixture was heated at 90°C for 48 hours. The mixture was allowed to cool to room temperature and left at 4°C for 12 hours. The toluene was eliminated by filtration and the white powder was dried under vacuum for 42 hours. The product was quite pure and ready to be used in the next synthesis. Yield 89-92%.² ¹H NMR, CDCl₃, δ, ppm: 9.84 (s, NCHN), 8.75, 8.70 (d, NCHCHN ³J_{HH} = 1.57 Hz), 5.38 (t, NCH₂, ³J_{HH} = 7.32 Hz), 5.10 (s, NCH₃), 2.98 (p, NCH₂CH₂, ³J_{HH} = 7.32 Hz), 2.43 (h, NCH₂CH₂CH₂, ³J_{HH} = 7.32 Hz), 2.00 (t, NCH₂CH₂CH₂CH₃, ³J_{HH} = 7.32).

3.2.4. Synthesis of 1-ethyl-3-methylimidazolium chloroaluminate (III) acidic, ionic liquid, [emim][Al₂Cl₇]

[emim]Cl (7 g, 0.047 mol) was mixed with AlCl₃ (12.90 g, 0.097 mol). The inorganic salt was added slowly taking care that the mixture does not exceed 80°C because the organic part can decompose. The mixture was made in a glove box, avoiding any contact with water and air.^{2,3,4} ¹H NMR, CDCl₃, δ, ppm: 8.30 (s, NCHN), 7.60, 7.20 (d, NCHCHN ³J_{HH} = 1.57 Hz), 4.30 (t, NCH₂, ³J_{HH} = 7.32 Hz), 3.80 (s, NCH₃), 0.90 (t, NCH₂CH₃, ³J_{HH} = 7.32).

3.2.5. Synthesis of 1-butyl-3-methylimidazolium trichlorostannate (II) acidic ionic liquid, [bmim][Sn₂Cl₅]

SnCl₂ (5 g, 0.026 mol) was mixed slowly with [bmim]Cl (3.06 g, 0.017 mol) avoiding the high temperature that comes from the exothermic reaction. After 5 minutes the colourless liquid was left under vacuum for 8 hours. The final mixture has $x_{\text{SnCl}_2} = 0.6$. ¹H NMR, CDCl₃, δ, ppm: 8.51 (s, NCHN), 7.15, 7.09 (d, NCHCHN), 3.85 (s, NCH₂), 3.55 (s, NCH₃), 1.38 (s, NCH₂CH₂), 0.83 (s, NCH₂CH₂CH₂), 0.35 (s, NCH₂CH₂CH₂CH₃).

3.2.6. Synthesis of 1-butyl-3-methylimidazolium trichlorostannate (IV), [bmim][Sn₂Cl₉]

The mixture tin (IV) chloride follows the same procedure as in 3.2.5 but using SnCl₄ (5 g, 0.019 mol) with [bmim]Cl (2.22 g, 0.012 mol). The final mixture has $x_{\text{SnCl}_4} = 0.6$. ¹H NMR, CDCl₃, δ , ppm: 7.87 (s, NCHN), 6.80, 6.76 (d, NCHCHN), 3.55 (s, NCH₂), 3.31 (s, NCH₃), 1.23 (s, NCH₂CH₂), 0.70, 0.68, (NCH₂CH₂CH₂), 0.65 (s, NCH₂CH₂CH₂CH₃).

3.2.7. Synthesis of 1-ethyl-3-methylimidazolium tetrafluoroborate ionic liquid [emim][BF₄]

3.2.7.1. Method a: Metathesis of the chloride

Dry [emim]Cl (20 g, 136.5 mmol, with 50°C as melting point) was dissolved in 5 mL of water (minimum quantity). NaBF₄ (1.5 eq, 22.52 g, 204.77 mmol) was dissolved in H₂O (5 eq, 18 ml) and was added to the solution of [emim]Cl/H₂O. The solution was stirred for 8 hours at room temperature under nitrogen. Finally, the [emim][BF₄] was extracted into CH₂Cl₂. The organic extracts were combined, washed with water and put into the fridge for one hour to allow complete separation of phases. The washing was repeated at least 3 times. The ionic liquid was dried over MgSO₄ for 8 hours and filtered through a plug of celite. The solvent was removed under vacuum while the ionic liquid was heated at 100°C for 8 hours. This procedure gave 50% yield but with a significant amount of a Cl⁻ impurity.⁵

3.2.7.2. Method b: Metathesis by precipitation

Dry [emim]Cl (5 g, 34.12 mmol) was dissolved in water (5 mL). Ag₂O (9.46 g, 40.95 mmol) and HBF₄ (4.33 mL, 54% by weight in Et₂O) were added and stirred for 5 hours, protected from light. The colourless solution was filtered and concentrated under vacuum. The mixture reaction was left under vacuum for 24 hours to allow the precipitation of AgCl. This solution was filtered three times more through celite to remove all of the silver residues. This procedure gave a 20% yield of a highly pure [BF₄]⁻ ionic liquid with low Cl⁻ impurities. The [emim][BF₄] ionic liquid must be heated at 100°C under nitrogen

for an hour every time before use, to avoid traces of moisture. ^1H NMR, CDCl_3 , δ , ppm: 8.76 (s, NCHN), 7.27, 7.22 (d, NCHCHN $^3\text{J}_{\text{HH}} = 1.57$ Hz), 4.11 (c, NCH_2 , $^3\text{J}_{\text{HH}} = 7.41$ Hz), 3.89 (s, NCH_3), 0.90 (t, NCH_2CH_3 , $^3\text{J}_{\text{HH}} = 7.41$).

3.2.8. Synthesis of 1-ethyl-3-methylimidazolium hexafluorophosphate ionic liquid, [emim][PF₆]

Dry [emim]Cl (5 g, 34.15 mmol, with 50°C as melting point) was dissolved in water (3 mL, minimum quantity). HPF₆ (1.2 eq, 8.3 g, 40.95 mmol, 60 % weight in water) was added drop wise to the emimCl/H₂O solution. During the addition the reaction mixture was cooled in an ice bath with vigorous stirring. After the addition the cloudy reaction mixture was left for 1 hour with stirring. The yellow solution was then left to stand for one hour to allow the separation of the phases. The upper phase contains the aqueous HPF₆ with some HCl as a by-product. The bottom phase, which contains the ionic liquid, was recovered by decantation and washed twice with 5 cm³ CH₂Cl₂ to eliminate traces of [emim]Cl. The ionic liquid phase was dried with MgSO₄ with stirring for 8 hours. It was left to stand for 24 hours and filtered through celite. It was dried under vacuum at 100°C for 24 hours to remove the CH₂Cl₂. This procedure gives a 50% yield. ^1H NMR, CDCl_3 , δ , ppm: 8.37 (s, NCHN), 7.32, 7.29 (d, NCHCHN $^3\text{J}_{\text{HH}} = 1.31$ Hz), 4.10 (c, NCH_2 , $^3\text{J}_{\text{HH}} = 6.83$ Hz), 3.85 (s, NCH_3), 0.87 (t, NCH_2CH_3 , $^3\text{J}_{\text{HH}} = 7.01$).

3.3. Syntheses of tris(triphenylphosphine)chloride rhodium [Rh(Cl)-(PPh₃)₃] and its reactions in [emim][Al₂Cl₇]

3.3.1. Chlorobis(triphenylphosphine)rhodium (I), [RhCl(PPh₃)₃], 10

This compound was synthesized using an Inorganic Synthesis method.⁶ RhCl₃·3H₂O (0.200 g, 0.5 mmol) was dissolved in 3.5 mL of ethanol. 1.5 g of phosphine PPh₃ (15 mmol) was dissolved in 30 mL of ethanol and added to the Rh solution slowly. The mixture was heated at reflux for two hours under argon. The red powder was filtered and washed five times with 3 mL of dried ether. The powder was dried under vacuum. M.P.

148 °C. $^{31}\text{P}\{\text{H}\}$ NMR: $\delta \text{P}^1 = 23$ ppm, $^1J(^{103}\text{Rh}-^{31}\text{P}^1) = 145$ Hz, $^2J(^{31}\text{P}^1-^{31}\text{P}^2) = 28$ Hz; $\delta \text{P}^2 = 48$ ppm, $^1J(^{103}\text{Rh}-^{31}\text{P}^2) = 196$ Hz.

3.3.2. Solutions of $[\text{RhCl}(\text{PPh}_3)_3]$, (10) in $[\text{emim}][\text{Al}_2\text{Cl}_7]$, synthesis of $[\text{Rh}(\text{Cl})\{(\mu\text{-Cl})\text{AlCl}_3\}(\text{PPh}_3)_2]^-$, 24

The solution was prepared by dissolving 40 mg of **10** in 1 mL of $[\text{emim}][\text{Al}_2\text{Cl}_7]$ ($x_{\text{AlCl}_3} = 0.65$) and waiting for 30 minutes until complete dissolution has occurred. The solution was reddish-brown. The separation of the observed compound **24**, as was reported by Dupont *et.al.*, proved impossible.⁷

3.3.3. Reaction of 24 with hydrogen in $[\text{emim}][\text{Al}_2\text{Cl}_7]$, synthesis of $[\text{Rh}\{(\mu\text{-Cl})\text{AlCl}_3\}(\text{H})(\text{PPh}_3)_2]^-$, 25

H_2 was bubbled through a solution of $[\text{RhCl}(\text{PPh}_3)_3]$ in $[\text{emim}][\text{Al}_2\text{Cl}_7]$ at 1 atm of pressure for 5 minutes. The solution changes from reddish-brown to light brown.

3.3.4. Reaction of 10 with AlCl_3 in dichloromethane. Determination of three isomers of $[\text{Rh}\{(\mu\text{-Cl})\text{AlCl}_3\}\{(\mu\text{-Cl})_2\text{AlCl}_2\}(\text{H})(\text{PPh}_3)_2]$, 31a, 31b, 32

Freshly sublimed AlCl_3 (10 mg, 0.075 mmol) was dissolved in 1 mL of CH_2Cl_2 , 10 mL of HCl was bubbled in this solution and finally $[\text{RhCl}(\text{PPh}_3)_3]$ (20 mg, 0.021 mmol) was added. ^1H , $^{31}\text{P}\{^1\text{H}\}$, and ^{27}Al NMR spectra of the final solution were recorded at room temperature and at 257, 241, and 225 K (-16°C , -32°C and -48°C).

3.3.5. Reaction of 10 in dichloromethane and excess of AlCl_3 , Observation of 25

Freshly sublimed AlCl_3 (10 mg, 0.075 mmol) was dissolved in 1 mL of CH_2Cl_2 , 10 mL HCl was bubbled through the solution and then $[\text{RhCl}(\text{PPh}_3)_3]$ (20 mg, 0.021 mmol) was added. ^1H , $^{31}\text{P}\{^1\text{H}\}$, and ^{27}Al NMR spectra of final solution were recorded at room temperature.

3.3.6. Reaction of 10 in toluene and excess of AlCl_3 . Observation of 25

AlCl_3 (10 mg, 0.075 mmol) was dissolved in 1 mL of toluene and stirred for 5 minutes. The solution becomes slightly yellow. $[\text{RhCl}(\text{PPh}_3)_3]$ (25 mg, 0.027 mmol) was added. The solution changes initially to deep yellow and while the raw materials were dissolved, a brown-oil appears. After 30 minutes of heating at 80°C the solution changes to orange with an orange oil. The oil was separated and characterized by ^1H , ^{31}P and ^{27}Al NMR. The upper part contains Al_2Cl_6 in toluene, ^{27}Al NMR = 90.8 ppm, 350 Hz of width (literature 91 ppm, 300 Hz width)⁸, while the oil in the bottom shows ^{27}Al NMR at 102 ppm with a linewidth of 2200 Hz.

3.3.7. Reaction of 38 with carbon monoxide in $[\text{emim}][\text{Al}_2\text{Cl}_7]$. Synthesis of $[\text{Rh}\{(\mu\text{-Cl})\text{AlCl}_3\}(\text{CO})_3(\text{PPh}_3)]$, 37

CO was bubbled through a solution of $[\text{RhCl}(\text{PPh}_3)_3]$ in $[\text{emim}][\text{Al}_2\text{Cl}_7]$ at 1 atm of pressure for 5 minutes. The solution changed from reddish-brown to a light brown colour.

3.4. Synthesis of chloride monocarbonyl bis(trialkylphosphine) rhodium compounds, $[\text{RhCl}(\text{CO})(\text{PR}_3)_2]$

3.4.1. Tetracarbonyl μ_2 -dichloro dirhodium, $[\text{Rh}(\mu\text{-Cl})(\text{CO})_2]_2$

$\text{RhCl}_3 \cdot 3\text{H}_2\text{O}$ (5 g, 18.97 mmol) was mixed with 5 g of acid sand. The mixture was put in a tube with sintered glass on the bottom that was connected to CO . The upper part was connected to a bubbler with $\text{NaOH}/\text{H}_2\text{O}$ 20%. The mixture was heated at 100°C for one hour in a stream of CO , or until all water has been released. Then, it was heated at 120°C for 5 hours in CO . The solid mixture was sublimed under argon at 120°C . The red-orange sublimed needles were separated and kept under argon. The product was water sensitive.⁹

3.4.2. Synthesis of enriched tetracarbonyl μ_2 -dichloro dirhodium ^{13}C , $[\text{RhCl}(^{13}\text{CO})_2]_2$, 69

$[\text{Rh}(\mu\text{-Cl})(\text{CO})_2]_2$ (100 mg, 0.257 mmol) was dissolved in 10 mL of dry pentane and stirred under an atmosphere of ^{13}CO for 2 h.

3.4.3. Chloride carbonyldiphosphine rhodium (I), $[\text{RhCl}(\text{CO})(\text{PR}_3)_2]$, 36, 45-49

The respective phosphine (3.904 mmol) was added to a solution of $[\text{Rh}(\mu\text{-Cl})(\text{CO})_2]_2$ (0.10 g, 0.976 mmol) in 5 mL of methanol under argon. Reaction time and ^{31}P -NMR data for products were specified in Table 3.2 for each phosphine. NMR samples were prepared under an argon atmosphere.^{10,11}

Table 3.1. Properties of Chloridecarbonyldiphosphine rhodium (I) complexes, NMR data in CDCl_3 .

Phosphine	Reaction Time (h)	δ ^{31}P -NMR, ppm ^a , free	δ ^{31}P -NMR, ppm complex	$^1J(^{103}\text{Rh}-^{31}\text{P})$ Hz
45 PMe_2Ph	12, r.t.	-47.5	-1.1	117.7
46 PEt_3	24	-20.1	23.6	116.1
47 PMePh_2	24	-27.6	14.2	122.4
48 PEtPh_2	12	12.3	27.0	123.3
36 PPh_3	24	-9.9	29.1	126.2
49 PCy_3	24	37.2	37.1	118.2

3.4.4. Oxidative addition of HCl to $[\text{Rh}(\text{Cl})(\text{CO})(\text{PPh}_3)_2]$ in CDCl_3 , 38, 45c, 62-67

$[\text{Rh}(\text{Cl})(\text{CO})(\text{PPh}_3)_2]$ (20 mg) was dissolved in 1 mL of CDCl_3 and HCl was bubbled through the solution for 1 min. The yellow solution was transferred to an NMR tube. ^{31}P $\{^1\text{H}\}$ NMR and ^1H NMR spectra were recorded and shown in Table 3.2. Discussion appears in chapter 6.

Table 3.2. ^{31}P $\{^1\text{H}\}$ and $\{^1\text{H}\}$ NMR spectra parameters for $[\text{Rh}(\text{Cl})_2(\text{H})(\text{CO})(\text{PR}_3)_2]$ in CDCl_3 . $\text{P}^t\text{Bu}_2\text{Ph}$ and $\text{P}^t\text{Bu}^n\text{Pr}^d$ did not react with HCl .

Phosphine	δ $^{31}\text{P}\{^1\text{H}\}$ -NMR, ppm ^a complex	$^1J(^{103}\text{Rh}-^{31}\text{P})$	δ ^1H NMR	$^1J(^{31}\text{P}-^1\text{H})$	$^2J(^{103}\text{Rh}-^1\text{H})$
45c PMe_2Ph	3.5	80.2	-13.39	Broad signal	Broad signal
62 PEt_3	26.5	80.1	-13.42	9.9	9.9
63 PMePh_2	18.7	84.0	-12.31	Broad signal	Broad signal
64 PEtPh_2	25.1	82.9	-12.67	9.9	15.1
38 PPh_3	25.3	85.9	-12.05	9.9	13.9
65 $\text{P}^t\text{Bu}^i\text{Et}_2$	44.6	80.0	-13.49	15.1	8.9
66 $\text{P}^t\text{Bu}^i\text{Bu}^n_2$	40.6	79.9	-13.50	15.1	8.2
67 Pcy_3	35.0	79.3	-14.75	9.9	13.9

Compounds **63**, **66**, **38** and **67** were isolated from the CDCl_3 solution by evaporating the solvent and drying under vacuum. Yellow products were isolated and dissolved in the corresponding ionic liquid. The rest lose HCl gradually and cannot be isolated pure.

3.4.5. Synthesis of hydride monocarbonyl tris(triphenylphosphine) rhodium (I)

A solution of rhodium trichloride 3-hydrate (0.26 g, 1.0 mmol) in ethanol (20 mL) was added to a vigorously stirred, boiling solution of triphenylphosphine (2.64 g, 10 mmol) in ethanol (100 mL). After a delay of 15 s, aqueous formaldehyde (10 mL, 40 % w/v solution) and a solution of potassium hydroxide (0.8 g) in hot ethanol (20 mL) were added rapidly and successively to the vigorously stirred, boiling reaction mixture. The mixture was heated under reflux for 10 min and then allowed to cool to room temperature. The bright yellow, crystalline product was removed by filtration, washed with ethanol, water, ethanol, and pentane, and dried under vacuum. Yield was 80% based on $\text{RhCl}_3 \cdot 3\text{H}_2\text{O}$.¹²

3.5. Reaction of chloroaluminate (III) ionic liquids with rhodium carbonyl chloride bis(trialkylphosphine) $[RhCOCl(PR_3)_2]$: formation of rhodium (I) carbonyls from rhodium (III) complexes by carbonylation

3.5.1. Solutions of $[RhCl(CO)(PR_3)_2]$ in $[emim][Al_2Cl_7]$, formation of $[Rh\{(\mu-Cl)_2AlCl_2\}\{(\mu-Cl)AlCl_3\}(H)(CO)(PR_3)]$ 39, 45b, 54-61

These complexes were prepared by dissolving 40 mg of the compound in 1 mL of $[emim][Al_2Cl_7]$ ($x_{AlCl_3} = 0.67$) and waiting for 30 minutes until complete solubilization. The solutions range from brown to orange, depending on the phosphine. They were transferred to an NMR tube to run $^{31}P\{^1H\}$ and 1H NMR spectra. The separation of the observed compound was impossible in all the solutions.

3.5.2. Solutions of $[Rh(H)(CO)(PPh_3)_3]$ in $[emim][Al_2Cl_7]$, formation of 39 and 37

$[Rh(H)(CO)(PPh_3)_3]$ (30 mg, 0.032 mmol) was dissolved in 0.7 mg of $[emim][Al_2Cl_7]$. The ^{31}P and 1H NMR spectra of the solution were recorded at room temperature and the results were shown in section 6.6.

3.5.3. Addition of CO to $[Rh\{(\mu-Cl)_2AlCl_2\}\{(\mu-Cl)AlCl_3\}(H)(CO)(PR_3)]$ in $[emim][Al_2Cl_7]$. Formation of 68, 45h-l, 54a,b-61a,b

$[RhCl(ClAlCl_3)(H)(CO)(PR_3)_2]$ in 1 mL of $[emim][Al_2Cl_7]$ ($x_{AlCl_3} = 0.67$) solution was subjected to a CO stream for 20 min. The colour of the solution lightens and was transferred to an NMR tube to run $^{31}P\{^1H\}$ and 1H NMR spectra.

3.5.4. Addition of ^{13}CO to $[Rh\{(\mu-Cl)AlCl_3\}(H)(CO)(PPh_3)]$ in $[emim][Al_2Cl_7]/CH_2Cl_2$, 1:1. Formation of $[Rh\{(\mu-Cl)AlCl_3\}(CO)_3(PR_3)]$, 37

$[RhCl\{(\mu-Cl)AlCl_3\}(H)(CO)(PPh_3)_2]$ (40 mg) in 1 mL of $[emim][Al_2Cl_7]$ ($x_{AlCl_3} = 0.67$) solution was put in a Shlenk tube that was previously filled with ^{13}CO . The reaction was stirred for 1, 5 and 20 minutes until the colour changes slightly. This solution was transferred to an NMR tube and $^{31}P\{^1H\}$, 1H and ^{13}C spectra were run at room temperature.

The temperature decreases during the NMR experiment and the spectrum was run every 10°C from 0°C to -30°C (273K to 243K).

3.5.5. Synthesis of isotopic enriched ^{13}C $[\text{Rh}(\text{Cl})(^{13}\text{CO})(\text{PPh}_3)_2]$, **36**

This synthesis follows the same procedure as complex **16** by using ^{13}CO 60% isotopically enriched $[\text{Rh}(\mu\text{-Cl})(^{13}\text{CO})_2]_2$.

3.5.6. Addition of ^{13}CO to **36** to obtain ^{13}CO $[\text{Rh}\{(\mu\text{-Cl})\text{AlCl}_3\}\{(\mu\text{-Cl})\text{AlCl}_3\}(\text{H})(^{13}\text{CO})(\text{PPh}_3)]$, **37** in $[\text{emim}][\text{Al}_2\text{Cl}_7]/\text{CD}_2\text{Cl}_2$

Compound $[\text{RhCl}(\text{CO})(\text{PPh}_3)_2]$, **36** (40 mg, 0.057 mmol) was dissolved in $[\text{emim}][\text{Al}_2\text{Cl}_7]$ (0.3 mL) in a 5 mL Schlenk flask. The container was filled with ^{13}CO and the solution reacted with the gas for 1 min. The solution was transferred to an NMR tube where CD_2Cl_2 (0.4 mL) was added. The NMR tube was closed under N_2 and $^{31}\text{P}\{^1\text{H}\}$, $^{13}\text{C}\{^1\text{H}\}$ with 2D-COSY $^{13}\text{C}\{^1\text{H}\}$ NMR spectra were recorded at 223K, (-50°C) and 2D-EXSY $^{13}\text{C}\{^1\text{H}\}$ NMR was recorded at 230K (-43°C).

3.6. Synthesis of chlorostannate diphosphine rhodium complexes using 1-butyl-3-methylimidazolium chlorostannate (II) ionic liquid, **90, 91, 93, 94**

$[\text{RhCl}(\text{CO})(\text{PR}_3)_2]$ (40 mg, 0.107 mmol) was dissolved in 1 mL CH_2Cl_2 . 0.2 mL of $[\text{bmim}][\text{Sn}_2\text{Cl}_5]$ were added while stirring. The red solution was transferred to an NMR tube and ^{31}P , ^1H NMR spectra were recorded. For the case of $[\text{Rh}(\text{SnCl}_3)_2(\text{CO})(\text{PPh}_3)_2]$ the ^{31}P NMR was recorded at 250K, -23°C.

3.7. Synthesis of $[Rh(\text{diolefin})(Ph_2P(CH_2)_nPh_2)]X$, diolefin = cyclooctadiene, norbornadiene; $n = 4$; $X=[BF_4]^-$, $[PF_6]^-$; $[Rh(PPh_3)_3(\text{solvent})]PF_6$ and their reaction with H_2 in 1-butyl-3-methylimidazolium tetrafluoroborate ionic liquid $[bmim][BF_4]$ and 1-ethyl-3-methylimidazolium hexafluorophosphate ionic liquid $[emim][PF_6]$

3.7.1. Synthesis of dicyclooctadiene-di- μ -chloride-dirhodium, $[Rh(COD)Cl]_2$

$RhCl_3 \cdot 3H_2O$ (0.20 g, 0.759 mmol) was dissolved in 2 mL of a solution 5:1 of ethanol:water. 0.5 ml of cyclooctadiene (4.62 mmol) was added. After 18 hours of stirring and refluxing, the yellow-orange powder was dried under vacuum and washed with pentane (3 mL) and methanol:water 1:5 (2 mL each time) until no more chloride was present. The filtered liquid was tested with 0.1 mM of $AgBF_4$ until no more cloudiness occurs. It was dried under vacuum. Yield: 67%, M.P. 220°C (with decomposition).¹³

3.7.2. Synthesis of bisnorbornadiene-di- μ -chloride-dirhodium, $[Rh(NBD)Cl]_2$

This synthesis follows the same procedure as 3.7.1, but the reaction time was for 6 h only.

3.7.3. Synthesis of cyclooctadiene- η^2 -1,4-(1,2-bis(diphenylphosphino)butane) rhodium (I) tetrafluoroborate, $[Rh(COD)(dppb)]-[BF_4]$

$[RhCl(PPh_3)_3]$ (50 mg, 0.101 mmol) and $AgBF_4$ (20.3 mg, 0.105 mmol) were dissolved and heated in 5 mL of dry acetone. After 30 min of stirring the reaction was filtered. $Dppb$ (43 mg, 0.101 mmol) in 20 cm³ of THF was added slowly to the filtered liquid. The mixture was stirred at room temperature for 30 minutes more. The colour changes from yellow to slightly orange. The filtered solution was concentrated to 30% of the original volume and ethyl ether was added until complete precipitation was reached. The orange solid was filtered and dried under vacuum. Yield: 80%. ³¹P-NMR $\delta = 56$ ppm, $^1J(^{103}Rh-^{31}P) = 146$ Hz.^{14,15}

The synthesis of cyclooctadiene- η^2 -1,4-(1,2-bis(diphenylphosphino)propano)rhodium (I) tetrafluoroborate, $[\text{Rh}(\text{COD})(\text{dppp})]\text{BF}_4$,¹⁴ follows the same procedure. A solution of dppp (44.5 mg, 0.101 mmol) in dry acetone (15 mL) was used.

The procedure using NBD (norbornadiene) was the same. However the addition of the phosphine must be slower, avoiding the complexation of two bisphosphines.

3.7.4. ^{31}P NMR determination of η^2 -1,4-(1,2-bis(diphenylphosphino)butane) bis(solvent) rhodium (I) tetrafluoroborate, $[\text{Rh}(\text{COD})(\text{dppb})][\text{BF}_4]$ in acetone and CH_2Cl_2

30 mg of $[\text{Rh}(\text{COD})(\text{dppb})][\text{BF}_4]$ was dissolved in 1 mL of acetone $\text{CH}_3\text{COCH}_3/\text{CD}_3\text{COCD}_3$ 10%. H_2 was bubbled for 30 min through the solution. $^{31}\text{P}\{^1\text{H}\}$ NMR was recorded for this solution. The same procedure was followed for the dissolution in $\text{CH}_2\text{Cl}_2/\text{CD}_2\text{Cl}_2$ 10%. In the last case, ^1H and ^{31}P were recorded.

3.7.5. ^{31}P NMR determination of rhodium tris(triphenylphosphine)-(solvent) hexafluorophosphate. $[\text{Rh}(\text{PPh}_3)_3(\text{solvent})][\text{PF}_6]$ in CH_2Cl_2 and $[\text{bmim}][\text{PF}_6]$

40 mg (0.043 mmol) of $[\text{RhCl}(\text{PPh}_3)_3]$ were mixed with TIPF_6 (15.4 mg, 0.043 mmol) in 5 mL CH_2Cl_2 , stirring for 30 min and filtered. The liquid was concentrated until dry. The yellow powder was characterized by NMR at 250K using $^{31}\text{P}\{^1\text{H}\}$. 49.3 ppm, dt $^1J(^{103}\text{Rh}-^{31}\text{P}^1) = 244$ Hz, $^2J(^{31}\text{P}^1-^{31}\text{P}^2) = 30.5$ Hz; 31.0 ppm, dd, $^1J(^{103}\text{Rh}-^{31}\text{P}^2) = 133$ Hz. Coalescence temperature at 300K (broad peak) at 36 ppm.¹⁶

3.7.6. Reaction of cyclooctadiene- η^2 -1,4-(1,2-bis(diphenylphosphino)butane) rhodium (I) tetrafluoroborate, $[\text{Rh}(\text{COD})(\text{dppb})][\text{BF}_4]$ with H_2 in 1-butyl-3-methylimidazolium tetrafluoroborate ionic liquid $[\text{bmim}][\text{BF}_4]$

30 mg of $[\text{RhCl}(\text{COD})_2]_2$ were dissolved in 1 mL of $[\text{bmim}][\text{BF}_4]$. Hydrogen was bubbled through the solution for 30 min. ^1H and ^{31}P NMR were recorded. Identification of $[\text{Rh}(\text{dppb})(\text{S})_2][\text{BF}_4]$, $[(\text{H})(\text{dppb})\text{Rh}(\mu_2\text{-H})_3\text{Rh}(\text{dppb})(\text{H})]$ and $[\text{Rh}(\text{dppb})]_3^+$ was performed by ^{31}P NMR.

3.8. Hydrogenation of cyclohexene by using biphasic conditions: ionic liquid/hexane. $[RhCl(PPh_3)_3]$ in $[emim][Al_2Cl_7]$ $x_{AlCl_3}=0.67$ /hexane; $[Rh(NBD)(dppb)]BF_4$ or $[Rh(COD)(dppb)][BF_4]$ in $[bmim][BF_4]$ /hexane

$[RhCl(PPh_3)_3]$ (46 mg, 0.05 mmol) was dissolved in 2 mL of $[emim][Al_2Cl_7]$ $x_{AlCl_3}=0.67$. 3 mL of hexane and 0.46 mL of cyclohexene (5 mmol) were added. The biphasic mixture was heated at 40°C, with H_2 at 1 atm for 24 h. At the end of this time, the products in the organic phase were quantified by gas chromatography. The inorganic mixture, which contains the ionic liquid and the coordination catalyst, was characterised by $^{31}P\{^1H\}$ -NMR spectroscopy.

Table 3.3. Parameters for the hydrogenation of cyclohexene by using $[Rh(Cl)(PPh_3)_3]$ in $[emim][Al_2Cl_7]$ and $[Rh(COD)(dppb)]$ in $[emim][BF_4]$ and $[emim][BF_6]$.

	Time (h)	Temperature (°C)	mg/mmol Rh	mL, g, mmol cyclohexene	mL hexane	[Rh] in ionic liquid M
$[emim][Al_2Cl_7]$ $x_{AlCl_3}=0.67$ 1mL	24	40	23.5/0.0254	0.2/0.162/1.978	1.5	0.0127
$[bmim][BF_4]$ 1mL	19	40	35/0.0483	0.42/0.34/4.153	1.5	0.0483
	19:30	r.t.		0.1/0.081/0.989	1.5	
	20	r.t.		0.3/0.243/2.967	1.5	
$[bmim][PF_6]$ 1mL	20:30	30	30/0.0414	0.1/0.081/0.989	1.5	0.0414
	20	r.t.		0.3/0.243/2.967	1.5	

3.9. References

- ¹ D. Seegmiller, G. Rhodes and L. King, *Inorg. Nucl. Chem. Lett.*, 1970, **6**, 885.
- ² S. Wilkes, J. Levinsky, R. Wilson and C. Hussey, *Inorg. Chem.*, 1982, **21**, 1263.
- ³ A. Abdul-Sada, A. Avent, M. Parkington, A. Ryan, K. R. Seddon and T. Welton, *J. Chem. Soc., Dalton Trans.*, 1993, 3283.
- ⁴ R. Osteryoung, and T. Zawodzinski, *Inorg. Chem.*, 1987, **26**, 2920.
- ⁵ J. D. Holbrey and K. R. Seddon, *J. Chem. Soc., Dalton Trans.*, 1999, 2133.

- ⁶ R. Angelici, *Inorg. Synth.*, **28**, 76.
- ⁷ K. Dietrich, J. Dupont, S. Einloft and R. De Souza, *Polyhedron*, 1996, **15**, 3257.
- ⁸ D. E. O'Reilly, *J. Chem. Phys.*, 1960, **32**, 1007; D. E. O'Reilly, C. P. Poole, R. F. Belt and H. Scott, *J. Polymer Sci.*, 1964, **A2**, 3257.
- ⁹ R. Angelici, *Inorg. Synth.*, **28**, 88.
- ¹⁰ B. E. Mann, C. Masters and B. Shaw, *J. Chem. Soc.*, A, 1971, 1104.
- ¹¹ H. Jardine, A. Osborn, G. Wilkinson and F. Young, *J. Chem. Soc.*, A., 1965, 1711.
- ¹² R. Angelici, *Inorg. Synth.*, **28**, 82.
- ¹³ R. Angelici, *Inorg. Synth.*, **28**, 89.
- ¹⁴ C. J. Elsevier, W. G. J. Lange and J. M. Ernsting, *Magn. Reson. Chem.*, 1991, **29**, S118.
- ¹⁵ D. H. M. W. Thewissen, J. W. Marsman, J. G. Noltes and K. Timmer, *Inorg. Chim. Acta*, 1985, **97**, 143.
- ¹⁶ F. Barrière and W. E. Geiger, *Organometallics*, 2001, **20**, 2133.

4. Results and discussion:

Solution in [emim][Al₂Cl₇]

This chapter discusses the different behaviour found in chloroaluminate ionic liquids when the complex [RhCl(PPh₃)₃] is dissolved in acidic [emim][Al₂Cl₇], with AlCl₃ molar fraction $x_{AlCl_3} = 0.67$. The molar fraction is given by equation 4.1 and refers to the quantity of AlCl₃ added to [emim]Cl.

$$x_{AlCl_3} = \frac{n_{AlCl_3}}{n_{AlCl_3} + n_{emimCl}} \quad \text{Eq. 4.1}$$

All the rhodium complexes are insoluble in neutral or basic chloroaluminate ($x_{AlCl_3} \leq 0.5$). Hence all the work reported here is based on acidic mixtures of [emim][Al₂Cl₇].

4.1. [RhCl(PPh₃)₃] in [emim][Al₂Cl₇]

Fig. 4.1 shows the ³¹P{¹H}-NMR spectrum of Wilkinson's catalyst dissolved in [emim][Al₂Cl₇] $x_{AlCl_3} = 0.67$. Three signals are observed (details in Table 4.1).

Table 4.1. 162 MHz ³¹P{¹H} NMR data for Fig. 4.1. Couplings are in Hz and chemical shifts in ppm.

Nuclei	Chemical shift	Integration ^a	multiplicity	² J(³¹ P- ³¹ P)	¹ J(¹⁰³ Rh- ³¹ P)
P ₁	45.5	1	dd	37	216
P ₂	43.7	1	dd	37	201
P ₃	6.8	1	s	--	--

^a Without Nuclear Overhauser Effect (NOE). Integration with NOE is 1.6 for P² + P¹ and 1 for the singlet in 6.8 ppm.

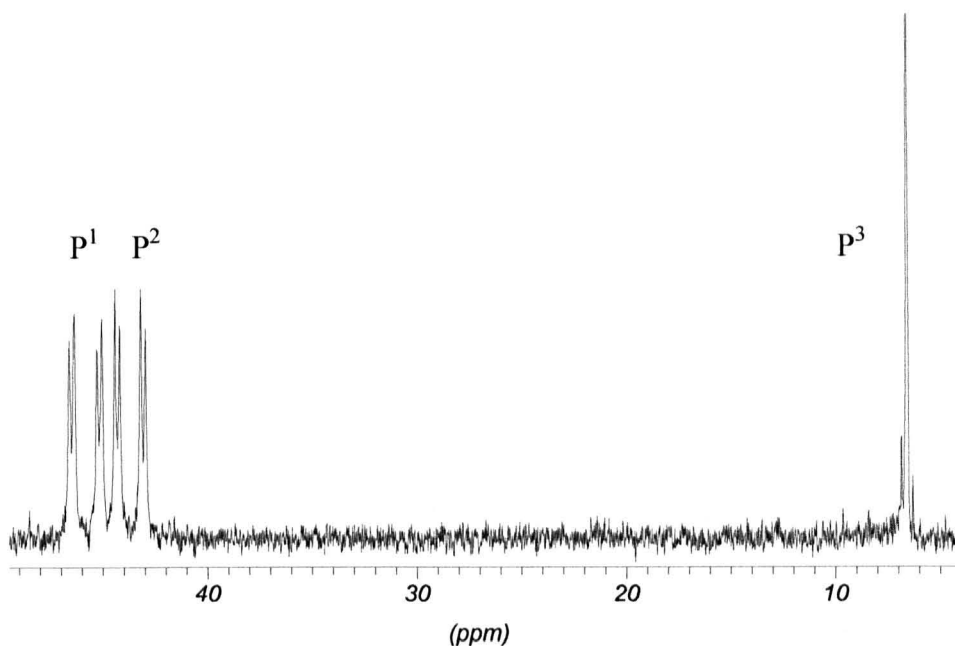


Fig.4.1. 162 MHz $^{31}P\{^1H\}$ NMR of $[RhCl(PPh_3)_3]$ in $[emimCl][Al_2Cl_7]$.

The singlet at low frequency does not show Rh-P coupling and its integration is one, which means that one PPh_3 is no longer attached to the metal. The spectrum of this signal without H decoupling showed a doublet with coupling constant of 504 Hz (Fig. 4.2). This coupling constant is consistent with a P-H interaction and is assigned to $[HPPH_3]^+$.¹ It is well known that strong acids such as fluorosulfuric acid are able to protonate PR_3 to form species such as $[HPR_3]^+$. Table 4.2 shows the NMR parameters of protonated PR_3 that have been reported before and the values of coupling $^1J(^{31}P-^1H)$ are quite large due to a direct interaction of protons with the phosphorus.² The large coupling $^{31}P-^1H$ for all the $[HPR_3]^+$ in Table 4.2, are in the same order of magnitude as the coupling observed for $[HPPH_3]^+$ in $[emim][Al_2Cl_7]$. The protonation of PPh_3 in chloroaluminate ionic liquid may be due to the presence of H^+ species in the ionic medium. It is known that $AlCl_3$ and any chloroaluminate (III) anion reacts with traces of H_2O (present during the synthesis of the organic cation) to produce HCl , $[Al_2OCl_6]^-$ and other chlorooxoaluminate (III) species. Also, the presence of HCl in an ionic medium gives a superacidity to the ionic liquid³ where PPh_3 is easily protonated. The counterion of $[HPPH_3]^+$ may be $[AlCl_4]^-$ or any oxochloroaluminate (III) anion that has been studied by Osteryoung and Seddon's group (section 2.6).⁴

The signals at high frequency in Fig. 4.1 correspond to two different phosphorus nuclei that are still attached to rhodium. There are eight lines, where each four lines

correspond to each phosphorus atom and are a result of ^{103}Rh - ^{31}P coupling and ^{31}P - ^{31}P coupling, for the two phosphorus atoms. The expansion of this region appears in Fig. 4.3.

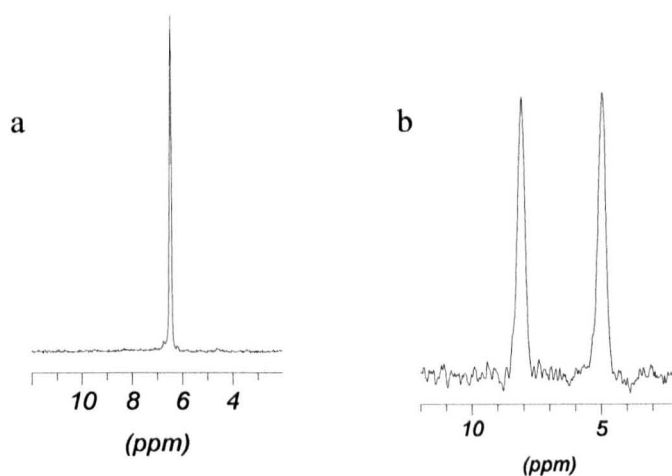


Fig. 4.2. 162 MHz ^{31}P NMR spectrum $[RhCl(PPh_3)_3]$ in $[emim][Al_2Cl_7]$. a) Signal at low frequency in Fig. 4.1, 1H decoupled; b) The same signal but with 1H coupling, $^1J(^{31}P-^1H)$ 504 Hz.

Table 4.2. NMR spectral parameters for protonated PR_3 with fluorosulfuric acid.²

PR_3	δ free PR_3 ppm	δ ^{31}P NMR of $[HPR_3]^+$ ppm	δ 1H NMR in $[HPR_3]^+$ ppm	$^1J(^{31}P-^1H)$ Hz
PH_3	-238	-101	2.2	548
PMe_3	-62	-3	6.3	497
PEt_3	-19	22	5.9	471
PPr^i_3	19	44	5.5	448
PBu^i_3	61	58	5.4	436
PBu^n_3	32	13	6.0	470
PPr^n_3	32	13	6.0	465

The analysis of the $^{31}P\{^1H\}$ NMR signals gives $\delta(P^1)$ 45.5 ppm, $^1J(^{103}Rh-^{31}P^1)$ 216 Hz; $^2J(^{31}P^2-^{31}P^1)$ 37 Hz; $\delta(P^2)$ 43.5 ppm, $^1J(^{103}Rh-^{31}P^2)$ 201 Hz. It is worth noting that line 1 and 3 in Fig. 4.3 have slightly different intensities than 2 and 4. In the same manner signal 6 and 8 have less intensities than 5 and 7. This ‘lean’ of the signals of P^1 and P^2 is indicative of spin-coupling between them that was corroborated by $^{31}P\{^1H\}$ -COSY NMR (Fig. 4.4). The small coupling constant P^2-P^1 is consistent with a *cis* conformation at the metal. Large coupling constants $^1J(^{103}Rh-^{31}P)$ of both phosphorus nuclei to the rhodium centre suggest a Rh(I) centre.

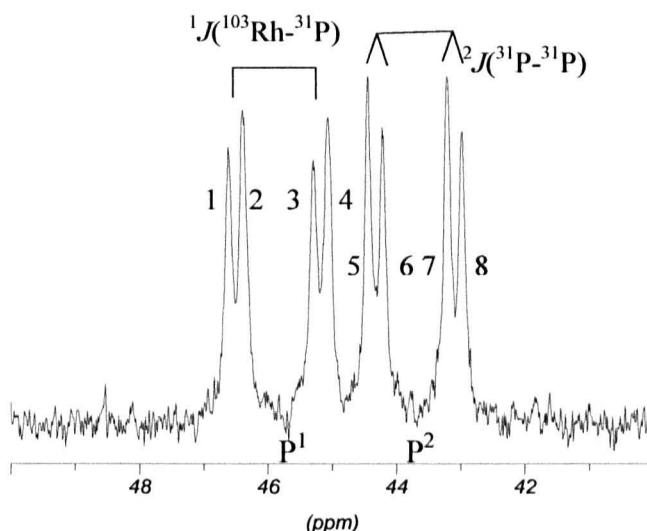


Fig. 4 3. Expansion of high frequency region in Fig. 4.1. Each phosphorus shows a double doublet, with a large coupling to ^{103}Rh and a smaller $^{31}P-^{31}P$ coupling.

In addition, these large couplings suggest a similar weak *trans*-influence ligand. For comparison, in the case of Wilkinson’s catalyst (Fig. 4.5, **10**) P^1 , which is *trans* to chlorine, has $^1J(^{103}Rh-^{31}P)$ 192 Hz, while for the P^2 atoms, which are mutually *trans* to each other, $^1J(^{103}Rh-^{31}P^2)$ is 146 Hz.

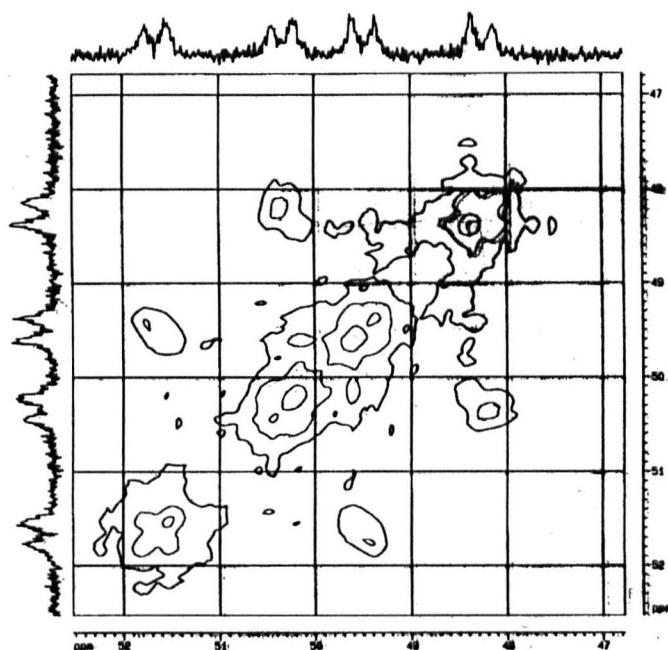


Fig. 4.4. 162 MHz ^{31}P COSY-NMR of $[\text{RhCl}(\text{PPh}_3)_3]$ in $[\text{emim}][\text{Al}_2\text{Cl}_7]$, 241 K. $^2J(^{31}\text{P}-^{31}\text{P})$ 35 Hz suggests a *cis* stereochemistry. $^1J(^{103}\text{Rh}-^{31}\text{P}^1)$ 216 Hz and $^1J(^{103}\text{Rh}-^{31}\text{P}^2)$ 201 Hz.

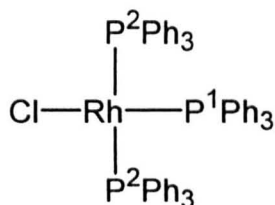


Fig. 4.5. Wilkinson's catalyst, **10**.

Considering the values $^1J(^{103}\text{Rh}-^{31}\text{P}^1)$ 216 Hz and $^1J(^{103}\text{Rh}-^{31}\text{P}^2)$ 201 Hz for the solution of $[\text{RhCl}(\text{PPh}_3)_3]$ in $[\text{emim}][\text{Al}_2\text{Cl}_7]$, we can assume that in the ionic liquid each phosphorus should be *trans* to ligands 'similar' to chloride or a "solvent" molecule. Ligands with similar *trans*-influence properties produce the proposed structure in Fig. 4.6.

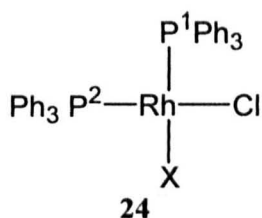


Fig. 4.6. Proposed structure for $[\text{RhCl}(\text{PPh}_3)_3]$ in $[\text{emim}][\text{Al}_2\text{Cl}_7]$ according to the results of NMR.

This structure fits with the ^{31}P -NMR spectrum. It has two *cis*- PPh_3 ligands attached to rhodium (I) and two similar *trans* ligands. In this case, X the ligand *trans* to one phosphorus, should be similar to Cl^- . The possibilities for X are:

1. A vacant site.
2. N_2 .
3. A carbene derived from the 1-ethyl-3-methyl imidazolium ion.
4. $[AlCl_4]^-$, whose co-ordination must be by chloride as a bridge between rhodium and aluminium. Other possibilities are any oxochloroaluminate (III) that can act as a ligand too. The possibilities of $[Al_2Cl_7]^-$ or $[Al_3Cl_{10}]^-$ are less likely as they are less coordinating than $[AlCl_4]^-$.⁵

4.1.1. A vacant site

Initially, the possibility of a vacant site is discussed. A tricoordinated centre in $[RhCl(PCy_3)_2]$ has been reported and the ^{31}P NMR spectrum shows both phosphorus atoms to be equivalent, with $^1J(^{103}Rh-^{31}P)$ 209 Hz.⁶ The authors do not clearly discuss any difference between 'Y' or 'T'-shape structures but the ^{31}P NMR suggests equivalence in both PCy_3 ligands due to a rapid exchange or 'Y'-shape structure. It is known that compounds such as *cis*- $[Pt(R^1)(MeOH)(PR^2)_2]$ ($R^1 = Ph, Et, Me$ and $R^2 = Et, Me$) exchange a molecule of methanol at low temperature and they rearrange to the *trans* isomer. This mechanism was deduced by 1H and $^{13}C\{^1H\}$ NMR and does not discard the possibility of a 'Y' shaped intermediate, but there is no clear evidence for this proposal.⁷ However, a 'Y' structure for **24** in Fig. 4.6 would give a simple signal (doublet) in the ^{31}P NMR spectrum, but not two different phosphorus atoms as is observed in Fig. 4.3.

On the other hand, the crystal structure of $[Rh(PPh_3)_3]ClO_4$ has been reported with a 'T'-shape structure due to the presence of a coordinating solvent such as THF.⁸ This first report does not discuss the possibility of interchange between phosphorus sites and no ^{31}P NMR parameters were reported.

More recently, the fragment $[Rh(PPh_3)_3]^+$ has been observed in $CD_2Cl_2/[NBu^t_4][PF_6]^-$ ⁹ and in CD_2Cl_2 with the anion $[7-[(1'-(closo-1',2'-C_2B_{10}H_{11})]-7,8-C_2B_9H_{11})]^-$.¹⁰ In the first case, the solution in $CD_2Cl_2/[NBu^t_4][PF_6]$ produces a clear AB_2M pattern in the ^{31}P NMR spectrum at 250K for $[Rh(PPh_3)_3]^+$: P^1 (a, Fig.4.7), doublet of triplets at 49.3 ppm, $^1J(^{103}Rh-^{31}P_1)$ 244 Hz, $^2J(^{31}P-^{31}P)$ 30.5 Hz; P^2 , doublet of doublets, 31.0 ppm, $^1J(^{103}Rh-^{31}P^2)$ 133.5 Hz,

$^2J(^{31}\text{P}_1-^{31}\text{P}_2)$ 30.5 Hz. In the second case, with the carborane as an anion, the fragment $[\text{Rh}(\text{PPh}_3)_3]^+$ gives a similar result in the ^{31}P NMR at 185K: P_1 , doublet of triplets at 48.5 ppm, $^1J(^{103}\text{Rh}-^{31}\text{P}^1)$ 244 Hz, $^2J(^{31}\text{P}^1-^{31}\text{P}^2)$ 32 Hz; P^2 , doublet of doublets at 29.9 ppm, $^1J(^{103}\text{Rh}-^{31}\text{P}^2) = 134$ Hz. The large coupling $^1J(^{103}\text{Rh}-^{31}\text{P}^1)$ 244 Hz is due to the PPh_3 with a *trans* vacant site. When the fragment $[\text{Rh}(\text{PPh}_3)_3]^+$ is dissolved in coordinating organic solvents such as acetone or CH_3CN , the coupling $^1J(^{103}\text{Rh}-^{31}\text{P}^1)$ for the PPh_3 *trans* to the solvent is reduced to 171 Hz, (b, Fig. 4.7).¹¹ It is worth noting that in $[\text{emim}][\text{Al}_2\text{Cl}_7]$ ionic liquids this coupling is not as large as 244 Hz and it is not as small as 171 Hz (208 and 216 Hz, Fig. 4.3).

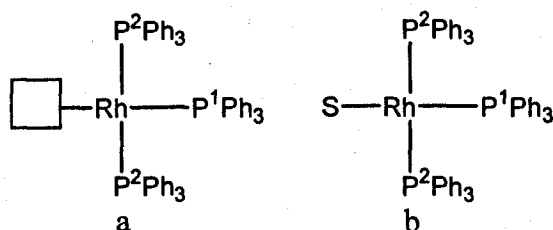


Fig. 4.7. Elimination of a Cl^- from Wilkinson's catalyst to produce: a) vacant site in non-coordinating solvents with large $^1J(^{103}\text{Rh}-^{31}\text{P}^1)$ or b) the coordination of the solvent, $\text{S} = \text{CH}_3\text{CN}$ or THF and reduction of $^1J(^{103}\text{Rh}-^{31}\text{P}^1)$.

The two examples in Fig. 4.7 have shown that the fragment $[\text{Rh}(\text{PPh}_3)_3]^+$ has a fast exchange ratio at room temperature with a broad signal at 31 ppm in the ^{31}P NMR,⁸⁻⁹ but has a 'T'-shape structure at 185-250K with a vacant site in a weakly coordinating solvent such as CH_2Cl_2 . This contrasts with **24**, where separate PPh_3 signals are observed at room temperature, showing that exchange is slow.

In the case of **24**, Fig. 4.6, a 'T' shape molecule in solution has two possibilities for $[\text{RhCl}(\text{PPh}_3)_2]$ that are depicted in Fig. 4.8. Only one has two non-equivalent PPh_3 ligands (**11-T₂**) and could have two kinds of phosphorus in the ^{31}P NMR spectrum.

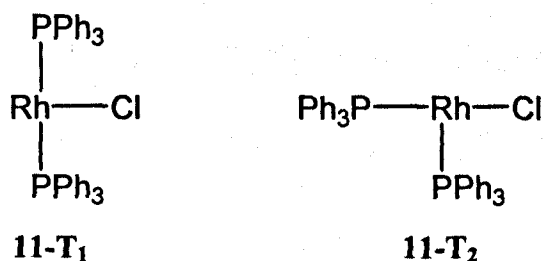


Fig. 4.8. Elimination of PR_3 from Wilkinson's catalyst to produce a 'T' shaped complex.

However, the coupling constant for the PPh_3 *trans* to the vacant site in **11-T₂** is not as big as 244 Hz and is closer to the range of 200 Hz. The coupling constant of P^2Ph_3 in Wilkinson's catalyst, **10**, is 196 Hz. It is *trans* to a chlorine and the last value is more in the average for PPh_3 *trans* to a weak ligand. This result implies once again that the group *trans* to one of the PPh_3 ligands must be a similar ligand to chlorine.

4.1.2. The coordination of nitrogen or the formation of a carbene

The second option, having N_2 on the metallic centre, was avoided by using Ar in every synthesis. The possibility of a carbene derived from $[1-Et-3-Me-imidazolium]^+$ can be discarded because such ligands have as large a *trans*-influence as a tertiary PPh_3 , and it would produce a smaller coupling $^1J(^{103}Rh-^{31}P)$.¹¹ Also, $di(PR_3)$ carbenes have a *trans* structure with coupling $^1J(^{103}Rh-^{31}P)$ of about 136-119 Hz.¹² In addition it is known that carbenes such as $M-CR_2$, where M can be Ir or Rh, are observed under basic conditions, in the presence of alkoxo ligands on the metal,¹³ but not in acidic conditions as exist in $[emim][Al_2Cl_7]$. The formation of a carbene would give new signals in 1H NMR and ^{13}C NMR spectroscopy, but no new signals were observed, essentially due to the large concentration of the organic cation in the ionic solvent.

4.1.3. $[AlCl_4]^-$ as ligand

Finally, the possibility of $[AlCl_4]^-$ as ligand was considered. There are reports where this anion can act as a ligand in transition metals such as Ti (a, Fig. 4.9),¹⁴ Zr (b, Fig. 4.9),¹⁵ W¹⁶ and more recently in Hg.¹⁷ In addition, $[AlCl_4]^-$ as a bridge has been reported by electrochemical studies.¹⁸ In contrast, there is only one example of a crystal structure where $[Al_2Cl_7]^-$ is coordinated to a transition metal in $[(\eta^6-C_6H_6)_2Pd_2\{(\mu-Cl)AlCl_2(\mu-Cl)AlCl_3\}]$,¹⁹ and the structure of $[Al_2Cl_7]^-$ has been observed as an anion in metallic complexes but without interaction with the metallic centre (b, Fig. 4.9).²⁰

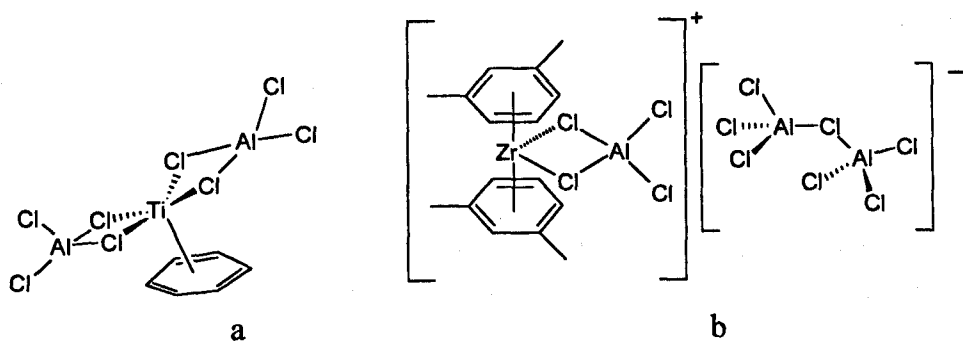


Fig. 4.9. a) Structure for $[Ti\{(\mu-Cl)_2AlCl_2\}_2(\eta^6\text{-benzene})]$; ^{10a} b) Structure of $[Al_2Cl_7]^-$ determined by x-ray diffraction in the complex $[\{\eta^6(\text{Me}_2\text{C}_6\text{H}_4)\text{Zr}\{(\mu-Cl)_2AlCl_2\}\}[Al_2Cl_7]^-$.¹⁹

If that is the case, considering that there is a high concentration of the anion, X can be $[(\mu-Cl)AlCl_3]^-$ in Fig. 4.6 and it can be assumed that P² is *trans* to chloride and P¹ is *trans* to $[(\mu-Cl)AlCl_3]^-$, because of the lower *trans* influence of bridging chlorides. For these reasons, the most likely species in solution, with $[AlCl_4]^-$ as a ligand, is that shown in Fig. 4.10.

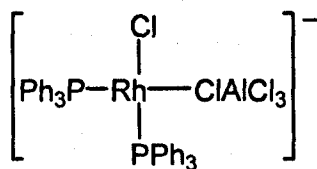


Fig. 4.10. Proposed structure for $[Rh(Cl)\{(\mu-Cl)AlCl_3\}(PPh_3)_2]^-$, 24, in $[emim][Al_2Cl_7]$.

This example is one of a few structures where two bulky PPh₃ are in the *cis* position with weak *trans*-effect ligands in solution. It is clear that the highly acidic medium in $[emim][Al_2Cl_7]$ can pull out a PPh₃ from the metallic centre. The most labile PPh₃ is the one that is *trans* to other PPh₃ due to the higher *trans*-effect of PPh₃, instead of the PPh₃ *trans* to chlorine. Then the *cis*-bis(PPh₃)₂ isomer is trapped due to the coordination of $[(\mu-Cl)AlCl_3]^-$ in the vacant site. No indication of the formation of the *trans*-isomer has been found.

The mechanistic details, proposed by Halpern and Brown for the hydrogenation cycle of $[RhCl(PPh_3)_3]$ in organic solvents, suggest the initial liberation of a PPh₃ and the formation of *trans*- $[Rh(Cl)(PPh_3)_2]$ (section 2.6). The last intermediate has been proposed but never observed. Theoretical calculations of the fragment $[Rh(Cl)(PPh_3)_2]$ suggest the higher stabilization of the *cis*-isomer in a 'T-shaped' arrangement.²¹ Theoretical studies with bulkier PR₃ groups have not been reported for the last intermediate, but would probably suggest the isomerisation to the *trans* isomer due to the higher steric demand in PPh₃. It has been

calculated that the initial formation of 'T'-*trans*- $[Rh(Cl)(PPh_3)_2]$ in the cycle, reacts with H_2 10^4 times faster than $[Rh(Cl)(PPh_3)_3]$.²²

The present section has given evidence of a *cis*-di(PPh_3) rhodium complex that has not been observed before in any organic solvent. This clearly suggests two things:

- The ionic liquid $[emim][Al_2Cl_7]$ is stabilizing a species *cis*- $[Rh(Cl)\{(\mu-Cl)AlCl_3\}(PPh_3)_2]^-$ that may be nonexistent in the organic solvent, which suggests the existence of another mechanistic pathway in the ionic liquid, or
- If $[Rh(Cl)(PPh_3)_2]$ in organic solvents has a *cis* configuration and not the *trans* as has been proposed, then the ionic liquid $[emim][Al_2Cl_7]$ has been able to trap the intermediate due to the coordination of a $[AlCl_4]^-$ anion in the medium.

Whichever of the last two options is true, both show the new chemistry of Wilkinson's catalyst in acidic chloroaluminate (III) ionic liquids. The existence of *cis*- $[Rh(Cl)\{(\mu-Cl)AlCl_3\}(PPh_3)_2]^-$ in $[emim][Al_2Cl_7]$ has certainly given an alternative for a new mechanistic pathway for the hydrogenation in ionic liquids and it may help to support certain intermediates in the already proposed mechanism in organic solvents.

4.1.4. Attempts to record ^{27}Al NMR of $[Rh\{(\mu-Cl)AlCl_3\}(Cl)(PPh_3)_2]^-$ **24**, in $[emim][Al_2Cl_7]$

It is known that ^{27}Al NMR has been used to study the chemical shift of chloroaluminate (III) anions in ionic solutions.²³ Also, ^{13}C NMR signals of the organic cation shift according to the $AlCl_3$ molar fraction (x_{AlCl_3} , eq. 4.1) in the ionic mixture.²³ In an attempt to observe any shift of the ^{27}Al NMR resonance of the solution with **24** or any extra signal for the coordination of $[(\mu-Cl)AlCl_3]^-$ with the rhodium complexes in the ionic solution, the ^{27}Al NMR was recorded. It did not show any new signal due to the coordination of the anion, while the signal due to the ionic liquid that is the solvent shows a broad signal at 104 ppm corresponding to the equilibrium of $[AlCl_4]^-$ and $[Al_2Cl_7]^-$ as was pointed out by Wilkes.²³

It is worth noting that the concentration of the ionic solvent was 9.9 M while the rhodium complex is 0.061 M, at most (with 40 mg of initial $[Rh(Cl)(PPh_3)_3]$) and it is 145 times less than the concentration of the solvent. The diminutive concentration of the new

complex 24 makes it very hard to see in the ionic liquid and attempts to see any change in the ^{27}Al NMR spectrum were unsuccessful.

4.2. Solution of $[Rh(Cl)(PPh_3)_3]$ in $[emim][Al_2Cl_7]/Al^0$

The last section has shown results from using a highly pure batch of $[emim][Al_2Cl_7]$. However, when $[Rh(Cl)(PPh_3)_3]$ is dissolved in $[emim][Al_2Cl_7]$ that has been prepared by Schlenk techniques, the formation of a hydride is observed. The ^{31}P NMR spectrum of the solution of Wilkinson's catalyst in impure $[emim][Al_2Cl_7]$ is shown in Fig. 4.11: 1P, singlet, 6.4 ppm, $^1J(^{31}P-^1H)$ 504 Hz; 2P, doublet, 57.2 ppm, $^1J(^{103}Rh-^{31}P)$ 144 Hz. 1H NMR signal at δ -17.4 ppm as a quartet, $^1J(^{103}Rh-^1H)$ 15 Hz, $^2J(^{31}P-^1H)$ 15 Hz.

The quartet that is observed in the 1H NMR spectrum results from the coupling to ^{103}Rh , (doublet: $^1J(^{103}Rh-^1H)$), and from the coupling to two equivalent PPh_3 (triplet $^2J(^{31}P-^1H)$). Both couplings are similar so the multiplet is seen as a pseudo-quartet that comes from two overlapping triplets. Selective decoupling of the ^{31}P NMR signal at 57.2 resulted in the hydride signal collapsing to a doublet. This shows that there is a triplet structure for the ^{31}P coupling to the hydride signal. Two PPh_3 ligands are coordinated to rhodium and they are equivalent. In addition the magnitude of $^2J(^{31}P-^1H)$ demonstrates that both PPh_3 ligands are *cis* to the hydride.

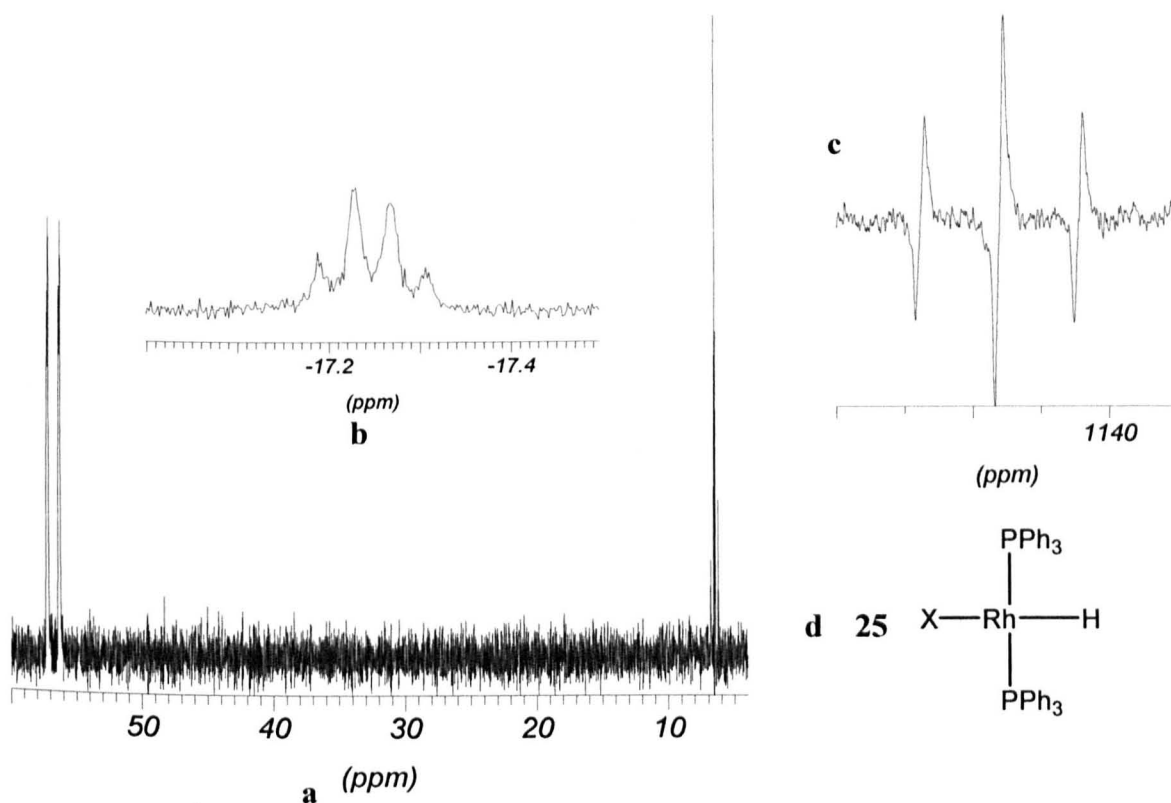
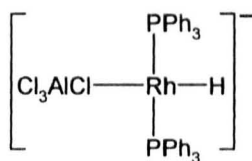


Fig. 4. 11. NMR spectra for $[Rh\{(\mu-Cl)AlCl_3\}H(PPh_3)_2]^-$ a) 162 MHz ^{31}P NMR spectrum of $[RhCl(PPh_3)_3]$ in impure $[emim][Al_2Cl_7]$. The solution shows two equivalent phosphorus attached to rhodium with $^1J(^{103}Rh-^{31}P)$ 144 Hz and $[HPPh_3]^+$. b) Hydride region of 400 MHz 1H NMR spectrum of $[RhCl(PPh_3)_3]$ in impure $[emim][Al_2Cl_7]$. c) 12.6 MHz, ^{103}Rh INEPT NMR spectrum; d) proposed structure for the product in impure $[emim][Al_2Cl_7]$.

The formation of one symmetric hydride with two PPh_3 groups attached to rhodium is deduced from these results and one possibility for the formed species in solution is **25**.



25

Here, $[(\mu-Cl)AlCl_3]^-$ may be interacting with the rhodium centre once again. Configuration **25** is proposed because the value $^1J(^{103}Rh-^{31}P)$ 144 Hz in this compound is similar to phosphorus-rhodium coupling of P^2 in $[RhCl(PPh_3)_3]$ where $^1J(^{103}Rh-^{31}P^2)$ 146 Hz (Fig. 4.5) for the phosphorus atoms that are *trans* to each other. This spectrum corroborates the presence of two equivalent PPh_3 groups attached to a rhodium centre with one hydride in

the *cis*-position and this agrees with structure **25**. In addition, a similar hydride complex, $[Rh(H)(CO)(PCy_3)_2]$, has been reported which shows a ^{31}P NMR doublet at 59.3 ppm ($^1J(^{103}Rh-^{31}P)$ 146.5 and a hydride signal at -5.9 ppm.²⁴

The $^{103}Rh\{INEPT\}$ NMR spectrum was collected and is shown in Fig. 4.11, c, δ 1155 ppm. The ^{103}Rh NMR spectrum shows a triplet ($^1J(^{103}Rh-^{31}P)$ 144 Hz) of doublets ($^1J(^{103}Rh-^1H)$ 15 Hz). Normally, doublets have a +1:+1 splitting, but the INEPT pulse sequence does not follow usual intensity patterns and a doublet due to the hydride is -1:+1 with the separation given by $^1J(^{103}Rh-^1H)$. Other kinds of splitting in the Rh spectrum are: a) -1:0:+1 for dihydrides with $2^1J(^{103}Rh-^{31}P)$ as the separation between -1:+1 signals; b) -1:-1:+1:+1 for trihydrides with separation of $^1J(^{103}Rh-^{31}P)$ among each signal. In $[emim][Al_2Cl_7]$, the doublet -1:+1 in the ^{103}Rh NMR signal suggests the presence of only one hydride and the triplet shows the presence of two PPh_3 ligands. The possible structure for the hydride in impure $[emim][Al_2Cl_7]$ is shown in Fig. 4.11d, and the complex **25** with a square planar structure is considered in the first instance due to the large coupling ($^1J(^{103}Rh-^{31}P)$ 144 Hz).

In addition, the δ (^{103}Rh) of the hydride **25** is quite large in comparison with the known Rh(I) complexes already reported. Unfortunately, there are few examples of ^{103}Rh NMR of Rh(I) hydrides and the known Rh(I) complexes that present a similar chemical shift to **25** present weak ligands such as acac and nitrogen in $[Rh(acac)(\eta^4-MeNBtEtCtCMeSiMe_2)]$ at 2344 ppm.²⁵ All other known Rh(I) compounds contain strong ligands such as CO or dppb and the (^{103}Rh) NMR signal appears between -100 to -1000 ppm,²⁶ which are quite far from the (^{103}Rh) shift in **25**. Hence, the ^{103}Rh chemical shift for **25** may be consistent with Rh(I) hydride with a weak ligand such as Cl^- and interactions with a high concentration of Cl^- in the environment make the δ (^{103}Rh) appear at higher frequency.

The formation of a hydride in the impure $[emim][Al_2Cl_7]$ may be the result of the presence of HCl (section 4.2.2). Traces of H_2O react with chloroaluminates (III) producing HCl and oxochloroaluminate (III) species.³ It is known that Rh(III) complexes such as $[Rh(Cl)_3(PPh_3)_3]$ in CH_2Cl_2 present a small coupling (44 Hz, section 6.2.2).²⁷ However, in the case of impure $[emim][Al_2Cl_7]$, the large coupling ($^1J(^{103}Rh-^{31}P)$ 144 Hz) indicates a Rh(I) centre instead of a Rh(III). Then, it is worth noting that a Rh(I) complex is being formed in a highly acidic environment with $[emim][Al_2Cl_7]/HCl$. The mechanism pathway is not clear but a possible reductant of the rhodium complex can be: *i*) interaction with the hydrides in the organic ring or *ii*) the presence of metallic Al^0 obtained during the sublimation of $AlCl_3$. Both

alternatives are explained below but the evidence suggests that the presence of aluminium metal may be the most likely reason for the reduction of the rhodium centre.

4.2.1. Interaction with the imidazolium ring to give Rh(I) hydride

An alternative to explain the formation of the hydride may be the interaction with the imidazolium ring where there are two sources of hydrogen: the aromatic protons and the alkyl protons.

In the first case, it was considered that H_1 on the ring could easily be lost in the presence of any base. In fact, the solution of 1-ethyl-3-methyl imidazolium chloride in MeOD experiences total exchange of the H^1 for D from the solvent after 3 months, Fig. 4.12. The same process has also been studied by electrochemistry in MeOH.²⁸

If these processes can occur in the solution of $[emim][Al_2Cl_7]$, then the insertion of the rhodium complex would have given the observation of the carbene, Fig. 4.13. Attempts to observe the presence of any carbene by ^{13}C NMR were unsuccessful due to the high concentration of the organic ion from the solvent.

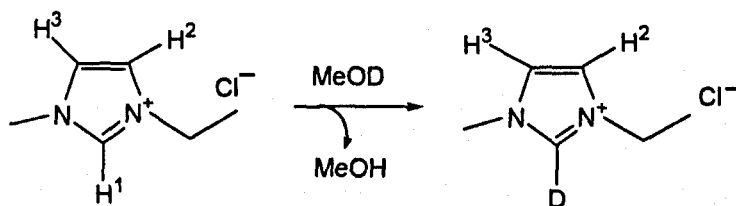


Fig. 4.12. Exchange of H_1 from the ring in the presence of MeOH is observed by losing the NMR signal of H^1 . This process is observed after 3 months in dissolution and by electrochemistry.²⁵

Also, as was mentioned, this kind of reaction has been observed only in a basic medium, and the coupling $^1J(^{103}Rh-^{31}P)$ with dialkylimidazoliumrhodium carbenes is smaller (119-135Hz).¹¹ The mass spectrometry FAB^+ and EI^+ of the reaction mixture does not show any fragment corresponding to $[Rh(H)(emim)(PPh_3)_2]$. It has been known that carbenes with Pd(0) and Ni(0) are highly stable in $[emim][Al_2Cl_7]$ ($x_{AlCl_3} = 0.55$) and they are used as catalysts for the dimerization of olefins with high stability while they do not last long in toluene.²⁹

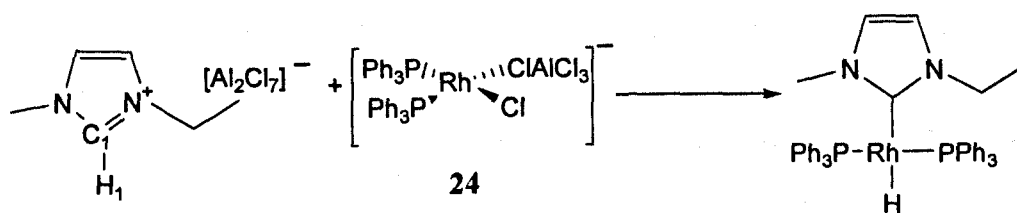


Fig. 4.13. Formation of a carbene rhodium hydride in $[emim][Al_2Cl_7]$. This compound is unlikely due to the absence of a basic agent to produce the stabilization of the negative charge in C_1 and the production of a carbene.

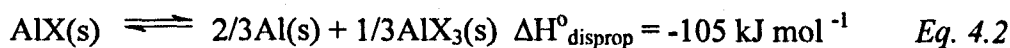
The other source of hydrogen in the imidazolium ring is the ethyl group. It is known that ethyl groups may interact with the metal and produce the corresponding C-C double bond, but the efforts to look for representative signals in the vinyl region, around 4.0-6.0 ppm in the 1H NMR spectrum, were unfruitful.³⁰ It is worth noting that the ethyl group is bound to the ring and the insertion of metal in the N(ring)- sp^3C^1 , to produce a N(ring)-Rh- CH_2CH_3 may be unlikely although this process has been proposed by Dupont's group with Pd.³¹ Then, the hydrogen migration from the β -C to produce (Nring)-Rh-H and ethene was not observed by mass spectrometry FAB⁺ or EI⁺. The interaction of the metal with the organic ring was finally discarded when the same hydride **25** was formed in the solution of $[RhCl(PPh_3)_3]$ in toluene with an excess of $AlCl_3$ without the presence of any imidazolium salt, section 5.2. For this reason, the possibility of the formation of the hydride **25**, due to the interaction of *cis*- $[Rh(Cl)\{(\mu-Cl)AlCl_3\}(PPh_3)_2]^-$, **24**, with the ethyl group or any part of the imidazolium ring was no longer considered.

It is worth noting that the same hydride **25** is formed when hydrogen is passed through the solution and section 4.3 explains the whole reaction. Also, **25** is formed when $[emim][Al_2Cl_7]$ is old or impure. It means that the formation of **25** is dependent on the batch of $[emim][Al_2Cl_7]$ used, where $[emim]^+$ concentration is constant. Hence the formation of **25** must be impurity driven. The next section shows that another possibility to produce the Rh(I) hydride may be the presence of Al^0 impurities in the ionic liquid.

4.2.2. Al^0 as a reductive agent

An alternative explanation for the formation of **25** is the presence of metallic Al^0 . It is worth noting that a rhodium (I) centre is being formed in a highly acidic environment with $[emim][Al_2Cl_7]/HCl$. The mechanistic pathway is not clear, but the sublimation of $AlCl_3$ at

140°C was considered as a possible source of impurities. This purification of $AlCl_3$ may produce small quantities of $AlCl$ and Cl_2 . It is known that $AlCl$ is highly unstable and can disproportionate to form the more stable $AlCl_3$ and Al^0 according to eq. 4.2.³² The reverse reaction to give gaseous $AlCl$ accounts for the ready volatilisation of Al^0 in the presence of $AlCl_3$, hence the presence of Al^0 in the sublimed needles of $AlCl_3$. Then, when the ionic liquid $[emim][Al_2Cl_7]$ is produced by mixing $[emim]Cl$ and freshly sublimed $AlCl_3$, the final product has a considerable concentration of Al^0 . This produces a darker coloration in $[emim][Al_2Cl_7]$. These traces may react with $[Rh(Cl)\{(\mu-Cl)AlCl_3\}(PPh_3)_2]^-$, **24**, to produce $[Rh\{(\mu-Cl)AlCl_3\}(H)(PPh_3)_2]^-$, **25**, while Al^0 produces $Al(III)$.



A possible mechanism to form the hydride **25** observed in $[emim][Al_2Cl_7]$ from **24** is the interaction of Al^0 with Cl^+ from the rhodium complex and the formation of $Al-Cl$ as an intermediate that can consequently trap Cl^+ and produce $AlCl_3$ that can be incorporated into the ionic solution. Fig. 4.14 shows the summary of two reactions occurring in clean $[emim][Al_2Cl_7]$ and impure $[emim][Al_2Cl_7]/HCl$.

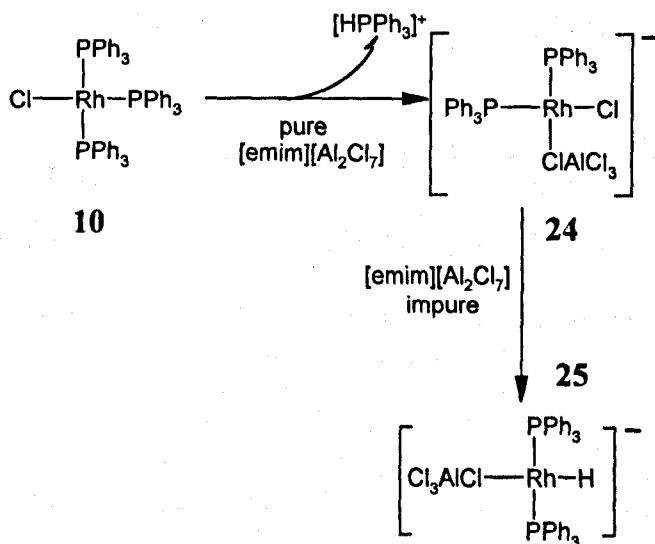
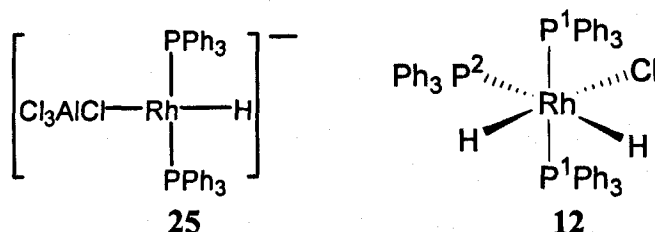


Fig. 4.14. The highly pure $[emim][Al_2Cl_7]$ gives the formation of $[Rh(Cl)\{(\mu-Cl)AlCl_3\}(PPh_3)_2]^-$. The impurities of Al^0 in $[emim][Al_2Cl_7]$ reduce **24** to **25**.

4.2.3. Hydrogenation of $[Rh(Cl)\{\mu-Cl\}AlCl_3\}(PPh_3)_2]^-$ in $[emim][Al_2Cl_7]$, $x_{AlCl_3} = 0.67$

In order to understand the formation of the hydride **25** in $[emim][Al_2Cl_7]$, the hydrogenation of a solution of **24** was studied. Hydrogen was bubbled through the solution of **24** in pure $[emim][Al_2Cl_7]$. The mixture was allowed to stand and the $^{31}P\{^1H\}$ NMR was recorded. This shows the formation of a signal at 6.2 ppm, $[Ph_3PH]^+$. A new signal appears at high frequency δ 57.2 ppm, $^1J(^{103}Rh-^{31}P)$ 144 Hz, as does a 1H NMR signal at δ -17.4 ppm as a quartet, $^1J(^{103}Rh-^1H)$ 15 Hz, $^2J(^{31}P-^1H)$ 15 Hz. This hydride corresponds to the same hydride as **25**, Fig. 4.11. Surprisingly, the hydrogenation of **24** in $[emim][Al_2Cl_7]$ shows the formation of a Rh(I) hydride, while the hydrogenation of $[Rh(Cl)(PPh_3)_3]$ in common organic solvents gives the well known Rh(III) *cis*-hydride **12** with two signals in ^{31}P NMR, assigned to P^1 and P^2 .³³ Fig. 4.15 illustrates the species that have been observed in $[emim][Al_2Cl_7]$.



The hydride **25** is formed when the initial compound $[Rh(Cl)\{\mu-Cl\}AlCl_3\}(PPh_3)_2]^-$, **24**, in pure $[emim][Al_2Cl_7]$ is allowed to stand under argon for two weeks. This certainly allowed the presence of a large amount of moisture that produced HCl in the ionic mixture. Hence, the production of any Rh(III) centre is due to the oxidative addition of HCl and is reduced by the Al^0 traces to produce Rh(I) hydride, **25**.

The addition of 1-methylcyclohexene to the solution of **25** in impure $[emim][Al_2Cl_7]$ (a, Fig. 4.17) produces *cis*- $[Rh(Cl)\{\mu-Cl\}AlCl_3\}(PPh_3)_2]^-$, **24**, two double doublets at lower frequency δ 45.8 and δ 43.6 ppm with similar coupling constants $^1J(^{103}Rh-^{31}P)$ 216.5 and 200.7 Hz respectively. *Cis*- $[Rh(Cl)\{\mu-Cl\}AlCl_3\}(PPh_3)_2]^-$ in Fig. 4.1, Table 4.1 has δ 45.5 and δ 43.5 ppm with coupling constant $^1J(^{103}Rh-^{31}P)$ 216 and 201 Hz respectively which are within the experimental error when these are compared with values in Fig. 4.17, b.

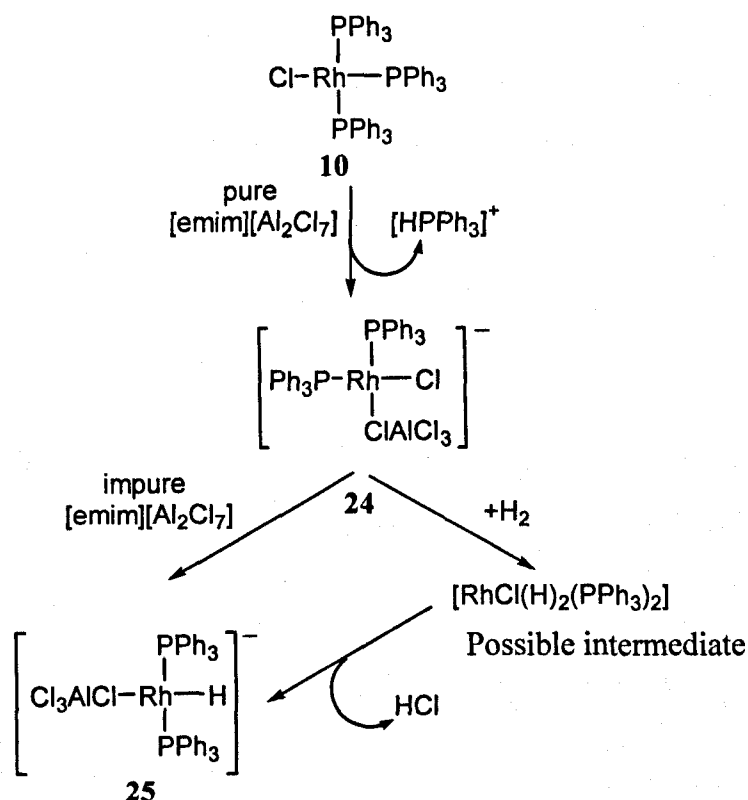


Fig. 4.15. Proposed mechanism to explain the existence of a symmetrical hydride in $[emim][Al_2Cl_7]$. The possible intermediate Rh(III) has not been observed by ^{31}P NMR but explains the formation of **25**.

When the solution of $trans-[Rh(Cl)\{\mu-Cl\}AlCl_3\}(PPh_3)_2]^-$ is allowed to stand for an hour, the starting material reappears and three new species at δ 48.5, singlet, 44.7 doublet and 32.3 ppm doublet are observed (d, Fig. 4.16). The singlet at 48.5 ppm corresponds to the decomposition of the free PPh_3 in the presence of impure $[emim][Al_2Cl_7]$.

The signals at low frequency 32.3 ppm correspond to an organic interaction between the PPh_3 and the olefin. This compound is formed when PPh_3 is added to a mixture of $[emim][Al_2Cl_7]$ with olefin only, without any rhodium complex. The doublet at 44.7 ppm is a new hydride species with $^1J(^{103}Rh-^{31}P)$ 134.8 Hz and 1H δ -11.4 ppm, $^1J(^{103}Rh-^1H) \sim ^2J(^{31}P-^1H)$ 19.9 Hz. The hydride signal appears as a pseudo-quartet that corresponds to two overlapping triplets. The triplets come from the coupling to two similar PPh_3 ligands. The coupling constant $^1J(^{103}Rh-^{31}P)$ and chemical shift for this Rh hydride are smaller than the initial hydride **25** and may correspond to a Rh(III) centre interacting with the $[AlCl_4]^-$ in solution (Fig. 4.17). This compound has not been isolated. The presence of $[AlCl_4]^-$ produces the polymerisation of the olefin and not the Rh complex because the polymerisation occurs even without rhodium. It has been proved that hydrogenation of the olefin occurs in basic and

neutral $[emim][AlCl_4]^{26}$ but also it is believed that the hydrogenation can occur in acidic $[emim][Al_2Cl_7]$ if it is carried out under the right conditions (section 4.3.1).³⁴ In the conditions used in this experiment, instant polymerisation occurs without any signal corresponding to the respective alkane.

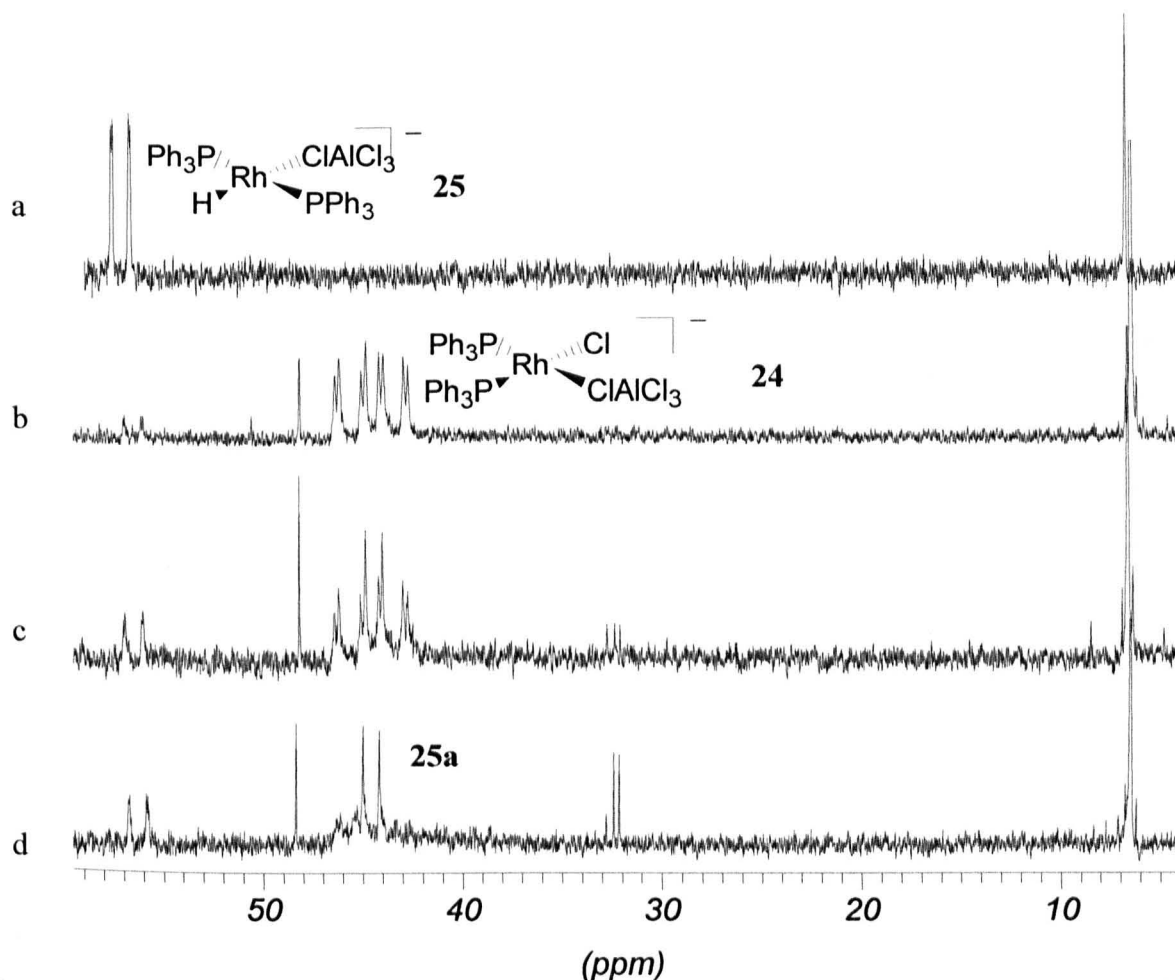


Fig. 4.16. Addition of olefins to the hydride $trans-[Rh\{\mu-Cl\}AlCl_3\}(H)(PPh_3)_2]^-$ gives $trans-[Rh(Cl)\{\mu-Cl\}AlCl_3\}(PPh_3)_2]^-$. ³¹P NMR of a) $[Rh\{\mu-Cl\}AlCl_3\}(H)(PPh_3)_2]^-$; b) addition of 10 equivalent of 1-methylcyclohexene to a, the formation of $[Rh(Cl)\{\mu-Cl\}AlCl_3\}(PPh_3)_2]^-$; c) the same sample as b after 30 min; d) the same as b after 1 hr.

The alkene, 1-methylcyclohexene, is insoluble in $[emim][Al_2Cl_7]$, as are others such as cyclohexene or 4-methylcyclohexene. Each olefin polymerises instantly with the ionic solvent. The presence of chloroaluminate (III) permits the interaction with the double bond in the olefin. The olefin can be inserted into the Al-Cl or Al-H bond producing a σ -bond Al-C (Fig. 4.18), and then the olefin can be consecutively inserted into the Al-C bond and this can produce the polymerisation of the olefin. This reaction is known as ‘Aufbaureaktion’ (growth

reaction) and was discovered by K. Ziegler.³⁵ Alkylchloroaluminate (III) ionic liquids have been used to polymerise ethene in the presence of a nickel catalyst with very good results.³⁶⁻³⁷

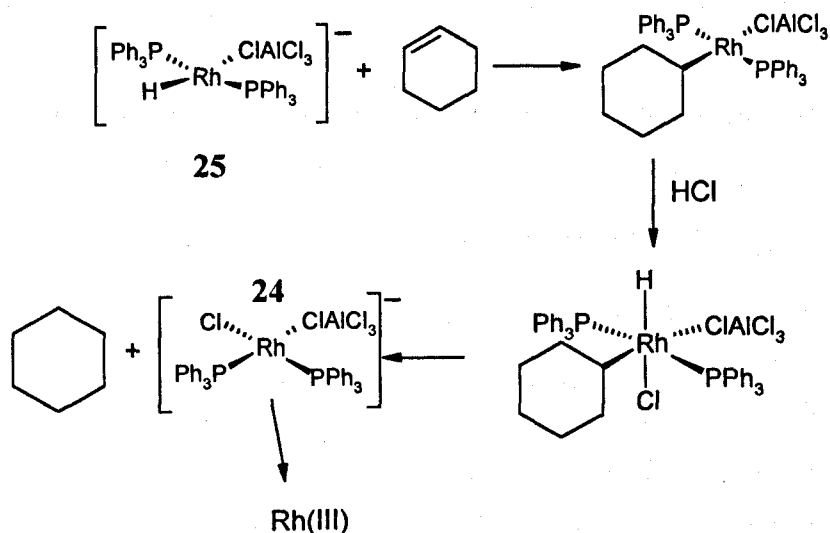


Fig. 4.17. Proposed mechanism for the formation of 24 in the presence of olefin.

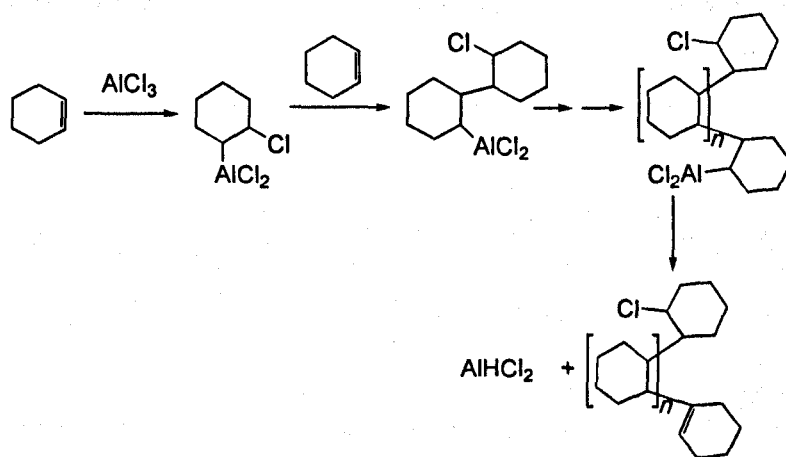


Fig. 4.18. Polymerization of cyclohexene in the presence of $AlCl_3$. Ziegler-Natta polymerisation.

4.2.4. Hydrogenation of cyclohexene in $[emim][Al_2Cl_7]$

It has been noted that the addition of cyclohexenes to the solution of 25 in $[emim][Al_2Cl_7]$ produces the polymerisation of the olefins and a rhodium complex that was unidentified due to the difficulties of isolation (25a, signal at 44.7 ppm). However, the addition of hydrogen to the solution *d* in Fig. 4.16, produces the formation of 25 again and the signal at 44.7 ppm disappears. Then the extra addition of cyclohexene, dissolved in

hexane, to **25** in $[emim][Al_2Cl_7]$ that had been enriched with hydrogen, produced the hydrogenation of the olefin in 99% yield at 40°C, after 24 hours, with a TOF 3.24 h⁻¹. Changes or degradation of **25** were not observed. The concentration of the cyclohexene in hexane is 1.31M and the concentration of initial $[Rh(Cl)(PPh_3)_3]$ to produce **25** in $[emim][Al_2Cl_7]$ is 0.0127M. This produces a ratio of 103:1 for cyclohexene:Rh (details in Table 3.3).

This could be contradictory: the excess of hydrogen in the ionic liquid produces the hydrogenation of cyclohexene when it is diluted, while the absence of hydrogen in a large concentration of cyclohexene produced just the polymerisation product. However, it is known that reactions such as the Heck reaction is a highly condition sensitive reaction that only works at certain conditions and can be stopped by a slight change in temperature or concentration.³⁸ Then, conditions dependence can be applied to the hydrogenation of cyclohexene, especially the concentration. The hydrogenation can be carried out when cyclohexene is diluted and there are more chances to interact with a rhodium centre than with another cyclohexene, while in pure cyclohexene, the polymerisation occurs faster due to the large interaction with aluminium and other cyclohexenes and a poor concentration of the rhodium complex, in comparison with cyclohexene.

The hydrogenation of cyclohexene with **25** in $[emim][Al_2Cl_7]$ represents a good option to develop a hydrogenation system and shows the versatility of the present ionic liquid to develop certain conditions where hydrogenation can be carried out and occurs faster than the polymerisation.

In addition, the polymerisation of cyclohexene agrees with the results of Dupont³⁹ et.al. but the hydrogenation of cyclohexene in acidic ionic liquids has not been reported before and this may show that acidic chloroaluminate (III) ionic liquids are a versatile solvent to produce important hydrogenation conditions although it is a highly air sensitive material.

4.3. Attempts to isolate rhodium (I) from $[emim][Al_2Cl_7]$

Finally, it should be mentioned that the isolation of **24** and **25** from the ionic solvents has proved impossible due to the high solubility of such compounds in $[emim][Al_2Cl_7]$. Extractions with organic solvents like petroleum ether; toluene or hexane were unsuccessful. The production of ionic rhodium species makes the separation and the extraction from an

ionic media into a molecular solvent difficult. Solvents such as dichloromethane or chloroform are completely miscible with the ionic part and any attempt to crystallize any product results in the formation of brown-red oily solutions at room temperature that become more viscous at 4°C or below due to the phase change of $[emim][Al_2Cl_7]$. Isolation by chromatography cannot be considered because of the high air and moisture sensitivity of the ionic liquid.

The product **25** disappeared gradually from the ionic solution until it vanished after 1 month as was observed from the ^{31}P NMR spectrum. Such disappearance was assigned to the degradation of the ionic liquid. Old solutions of $[Rh\{(\mu-Cl)AlCl_3\}(H)(PPh_3)_2]^-$ produce new signals in the ^{31}P NMR spectrum corresponding to phosphorus without rhodium interaction. The explanation of the decomposition of $[HPPH_3]^+$ are explained by the reaction of PPh_3 with Cl_2 . The degradation products of the PPh_3 were also identified as $[ClPPh_3][AlCl_4]$ at 65 ppm⁴⁰ and Ph_2POCl at 42 ppm.⁴¹ The oxidative addition of Cl_2 to the metal produces the elimination of PPh_3 that reacts with the highly acidic medium producing more $[HPPH_3]^+$ and PPh_3Cl_2 . The metal centre, on the other hand, may produce rhodium chloride anionic species that are completely soluble in $[emim][Al_2Cl_7]$ and cannot be extracted into organic solvents. During one of the attempts of separation, slow crystallization with a mixture 1:1:1 of CH_2Cl_2 :ether: $[emim][Al_2Cl_7]$ gave the precipitation of an anionic decomposition product: *trans*- $[RhCl_4(PPh_3)_2]^- [emim]^+$ **26**, Fig. 4.19.

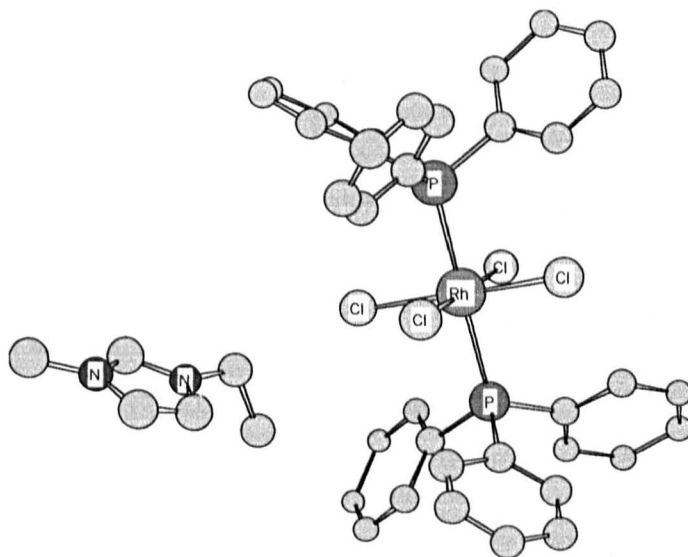


Fig. 4.19. Complex **26** isolated from the solution of $[RhCl(PPh_3)_3]$ in $[emim][Al_2Cl_7]/CH_2Cl_2$. Hydrogen atoms have been omitted due to clarity.

This product has not been reported, though the anion has been known since the 1960's and crystallized with $[\text{PPh}_3(\text{CH}_2\text{CH}=\text{CH}_2)]^+$ as cations.⁴² It is clear that the presence of moisture and oxygen avoid the proper crystallization of $[\text{AlCl}_4]^-$ species around the metallic centre because they decompose to oxochloroaluminate (III). The presence of such impurities around the crystal, that were impossible to remove with any solvent, did not make the diffraction clear. Table 4.3 shows the parameters of the X-ray diffraction of **26**, and the complete diffraction Tables appears in appendix 1.

Table 4.3. Crystal data and structure refinement for *trans*- $[\text{RhCl}_4(\text{PPh}_3)_2][\text{emim}]$, **26**.

Empirical formula	$\text{C}_{42}\text{H}_{41}\text{Cl}_4\text{N}_2\text{P}_2\text{Rh}$	Reflections collected	12295
Formula weight	880.42	Independent reflections	8840 [R(int) = 0.1294]
Temperature	150(2) K	Completeness to theta = 28.33°	90.1 %
Wavelength	0.71073 Å	Absorption correction	Semi-empirical
Crystal system	Triclinic	Max. and min. transmission	0.9524 and 0.8029
Space group	P-1	Refinement method	Full-matrix least-squares on F^2
Unit cell dimensions	a = 9.7840(12) Å; α = 94.293(2)°; b = 11.7699(14) Å; β = 104.517(2)°; c = 18.438(2) Å; γ = 104.563(2)°.	Index ranges	-13 ≤ h ≤ 11, -11 ≤ k ≤ 15, -20 ≤ l ≤ 23
Volume	1967.7(4) Å ³	Data / restraints / parameters	8840 / 0 / 464
Z	2	Goodness-of-fit on F^2	0.960
Density (calculated)	1.486 Mg/m ³	Final R indices [$I > 2\sigma(I)$]	R1 = 0.0739, wR2 = 0.2143
Absorption coefficient	0.820 mm ⁻¹	R indices (all data)	R1 = 0.1015, wR2 = 0.2367
F(000)	900	Largest diff. peak and hole	4.242 and -1.840 e.Å ⁻³
Crystal size	0.28 x 0.14 x 0.06 mm ³	Theta range for data collection	1.15 to 28.33°.

Another attempt to isolate **24** or **25** by extraction with $[\text{AsPh}_4]^+$ was unsuccessful and the addition of $[\text{AsPh}_4]\text{Cl}$ to the ionic solution of each compound gave a complex mixture, which made the identification quite difficult due to the formation of new ionic species that obviously are still soluble in the ionic liquid and stay there instead of the organic solvent.

4.4. Summary

It is worth noting that the coordination of the ion $[AlCl_4]^-$ made the identification of new species that have been unknown in organic solvents possible and the efforts to isolate **24** and **25** from $[emim][Al_2Cl_7]$ agreed with the proposal of the ionic nature of these rhodium species in the ionic liquid. The high solubility of **24** and **25** does not permit their isolation from $[emim][Al_2Cl_7]$, which is considered a highly polar medium.

The next section shows that the formation of ionic species will depend basically of the addition of $AlCl_3$, but later sections will show that the presence of the cation in the ionic liquid may be important to the stability of the substances.

4.5. References

- ¹ P. Haska, W. B. Miller and W. A. Tyssoo, *J. Am. Chem. Soc.*, 1964, **86**, 3577.
- ² C. McFarland and G. J. Olah, *J. Org. Chem.*, 1969, **34**, 1832.
- ³ P. C. Trulove, R. T. Carlin, R. A. Osteryoung, *J. Am. Chem. Soc.*, 1990, **112**, 4567.
- ⁴ A. Abdul-Sada, A. Avent, M. Parkington, A. Ryan, K. R. Seddon and T. Welton, *J. Chem. Soc., Dalton Trans.*, 1993, 3283; R. Osteryoung and T. Zawodzinski, *Inorg. Chem.*, 1987, **26**, 2920.
- ⁵ Y. Chauvin and H. Olivier-Bourbigou, *CHEMTECH*, 1995, **25**, 26.
- ⁶ H. L. M. Van Gaal and F. L. A. Van Den Bekerom, *J. Organomet. Chem.*, 1977, **134**, 237.
- ⁷ R. Romeo and G. Alibrandi, *Inorg. Chem.*, 1997, **36**, 4822; R. Romeo, L. Scolaro, N. Nastasi, B. E. Mann, G. Bruno and F. Nicolo, *Inorg. Chem.*, 1996, **35**, 7691.
- ⁸ R. Bau, S. Miles, C. Reed and Y. Yared, *J. Am. Chem. Soc.*, 1977, **99**, 7076.
- ⁹ F. Barriere and W. E. Geiger, *Organometallics.*, 2001, **20**, 2133.
- ¹⁰ J. A. Long, M. F. Hawthorne, P.E. Behnken and T. B. Marder, *J. Am. Chem. Soc.*, 1984, **106**, 10.
- ¹¹ C. D. David, G. Pimblett and W. Clegg, *J. Chem. Soc., Dalton Trans.*, 1985, 1977.
- ¹² M. J. Doyle, M. F. Lappert, P. L. Pye and P. Terreros, *J. Chem. Soc., Dalton Trans.*, 1984, 2355.
- ¹³ T. Weskamp, V. P. W. Böhm and W. A. Herrman, *J. Organomet. Chem.*, 2000, **600**, 12.
- ¹⁴ M. Horacek, V. Kupfer, B. Muller, U. Thewal and K. Mach, *J. Organomet. Chem.*, 1998, **552**, 75; U. Thewal and F. Oserle, *J. Organomet. Chem.*, 1979, **172**, 317; L. A. Aslano, A. N. Grigorev, I. E. Mochalkin, V. B. Rybakov, S. I. Troyanov and M. A. Zakharov, *Koord. Khim.*, 1996, **22**, 723; K. Mach and S. I. Troyanov, *J. Organomet. Chem.*, 1990, **389**, 41; H. Anropiusova, K. Mach, J. Polacek and S. I. Troyanov, *J. Organomet. Chem.*, 1992, **430**, 317; K. Mach, G. Schmid, U. Thewal and S. I. Troyanov, *J. Organomet. Chem.*, 1993, **453**, 185; E. I. Bzowej, B. Gauheron, J. Hiller, K.

- Mach, P. Meunier, L. E. Paquee, M. R. Sivik, U. Thewal and F. Zaegel, *Organometallics*, 1995, **14**, 2609.
- ¹⁵ T. S. Cameron, M. V. Gaude, A. L. Linden and M. J. Zaworoko, *J. Organomet. Chem.*, 1989, **367**, 267; G. Erker, C. Krueger, R. Noe and S. Werner, *Organometallics*, 1992, **11**, 4174; F. Calderazzo, P. Pallavicini, G. Pampaloni, J. S. Rahle and K. Wurs, *Organometallics*, 1991, **10**, 396.
- ¹⁶ P. R. Sharp, *Organometallics*, 1984, **3**, 1217.
- ¹⁷ A. R. Barron, A. S. Borovik and S. G. Bott, *J. Am. Chem. Soc.*, 2001, **123**, 11219.
- ¹⁸ C. L. Hussey, K. R. Seddon and R. Quigley, *Inorg. Chem.*, 1995, **34**, 370.
- ¹⁹ G. Allegra, P. Delise and G. Nardin, *Gazz. Chim. Ital.*, 1975, **105**, 1047.
- ²⁰ S. Troyanov, A. Pisarevsky and Y. T. Struchkov, *J. Organomet. Chem.*, 1995, **494**, C4.
- ²¹ P. Margl, T. Ziegler and P. E. Blochl, *J. Am. Chem. Soc.*, 1995, **117**, 12625.
- ²² M. Torrent, M. Sola and G. Frenking, *Chem Rev.*, 2000, **100**, 439.
- ²³ J. S. Wilkes, J. S. Frye and G. F. Reynolds, *Inorg. Chem.*, 1983, **22**, 3870.
- ²⁴ M. A. Freeman and D. A. Young, *Inorg. Chem.*, 1986, **25**, 1556.
- ²⁵ R. Köster, G. Seidel, B. Wrackmeyer and D. Schlosser, *Chem. Ber.*, 1989, **122**, 2055.
- ²⁶ F. R. Bregman, J. M. Ernsting, F. Müller, M. D. K. Boele, L. A. Van der Veen and C. J. Elsevier, *J. Organomet. Chem.*, 1999, **592**, 306.
- ²⁷ G. Wilkinson, J. A. Osborn, J. T. Mague and M. C. Baird, *J. Chem Soc. A*, 1967, 1347.
- ²⁸ T. Yoshinori and S. Hideki. *Denkai Chikudenki Hyoron*, 2000, **51**, 133. Reference taken from Chem. Abst. 133:368319m
- ²⁹ D. S. McGuinness, W. Mueller, P. Wassercheid, K. J. Cavell, B. W. Skelton, A. H. White and U. Englert, *Organometallics*, 2002, **21**, 175.
- ³⁰ D. H. Williams and I. Fleming, *Spectroscopic methods in organic chemistry*, McGraw Hill, London, 4th edn., 1989, pp 137.
- ³¹ P. A. Z. Suarez, J. E. L. Dullius, S. Einloft, R. F. De Souza and J. Dupont, *Polyhedron*, 1996, **15**, 1217.
- ³² N. N. Greenwood and A. Earnshaw, *Chemistry of the elements*, 2nd edn., Butterworth, UK, 1997.
- ³³ J. M. Brown, P. Evans and A. Lucy, *J. Chem. Soc., Perkin Trans. 2*, 1987, 1589.
- ³⁴ K. R. Seddon, personal communication; K. Cavell, personal communication.
- ³⁵ A. Salzer and C. Elschenbroich, *Organometallics*, VCH, Weinheim, 2nd edn., 1992, pp 77.
- ³⁶ B. Ellis, W. Keim and P. Wassercheid, *J. Chem. Soc., Chem. Commun.*, 1999, 337.
- ³⁷ Y. Chauvin, B. Gilbert and I. Guibard, *J. Chem. Soc., Chem. Commun.*, 1990, 1715.
- ³⁸ Y. Donde, L. E. Overman, *Asymmetric intramolecular Heck reactions. Catalytic Asymmetric Synthesis*, 2nd edn., 2000, 675-697.
- ³⁹ S. Einloft, F. K. Dietrich, R. F. De Souza and J. Dupont, *Polyhedron*, 1996, **15**, 3257.
- ⁴⁰ J. Mason, *Multinuclear NMR.*, Plenum Press, New York, 1987.
- ⁴¹ M. L. Nielsen, R. R. Ferguson and W. S. Coakley, *J. Am. Chem. Soc.*, 1961, **83**, 99.

4. Results and discussion: $[RhCl(PPh_3)_3]$ in $[emim][Al_2Cl_7]$

- ⁴² T. E. Concolino, P. A. Evans and A. L. Rheingold, 1999, reference taken from Crystallographic database, Daresbury, Laboratory, code: BEDSUY; similar structure with PEt_3 : F. A. Cotton and S. J. Kang, *Inorg. Chem.*, 1993, **32**, 2336.

5. Results and discussion:

Solution of [RhCl(PPh₃)₃] in CH₂Cl₂ with AlCl₃

5.1. [RhCl(PPh₃)₃] in CH₂Cl₂/AlCl₃/HCl

In order to elucidate whether the ready formation of Rh(I) rather than Rh(III) complexes in reactions of [RhCl(PPh₃)₃] in acidic [emimCl]/AlCl₃ were as a result of the ionic liquid or were due to the presence of AlCl₃, [RhCl(PPh₃)₃] was dissolved in CH₂Cl₂ containing AlCl₃ and HCl. The ³¹P-NMR spectrum at room temperature of a solution of Wilkinson's catalyst in CH₂Cl₂/AlCl₃/HCl is shown in Fig. 5.1: sharp signal at δ 6 ppm, broad signal at 45 ppm and an impurity that does not show an interaction with Rh at δ 47.5 ppm. The sharp signal at low frequency is assigned to [HPPh₃]⁺. This signal shows a large coupling ¹J(³¹P-¹H).

Decreasing the temperature for this sample to 241K showed a different spectrum, Fig. 5.2. The broad signal (~45 ppm) at room temperature was split in well-resolved signals at low temperature as two doublets of triplets at δ 46.6, ²J(³¹P-¹H) 18Hz, ²J(³¹P-³¹P) 18Hz, ¹J(¹⁰³Rh-³¹P) 136Hz; δ 46.0, ²J(³¹P-¹H) 18 Hz, ²J(³¹P-³¹P) 18 Hz, ¹J(¹⁰³Rh-³¹P) 139 Hz and a doublet of doublets at δ 43.6, ²J(³¹P-¹H) 16 Hz, ¹J(¹⁰³Rh-³¹P) 136 Hz. Each ³¹P signal is approximately of equal intensity. The coupling ²J(³¹P-¹H) arises from the failure to decouple the hydride signals at δ -16.49 and -16.68 ppm. The ¹H NMR spectrum shows two hydrides at δ -16.49, as doublets, ¹J(¹⁰³Rh-¹H) 14 Hz, of triplets, ²J(³¹P-¹H) 21 Hz, and δ -16.68, as doublets, ²J(¹⁰³Rh-¹H) 14 Hz of triplets, ²J(³¹P-¹H) 21, with intensities of 2:1, Fig. 5.3a. These correspond to two different hydrides. Table 5.1 shows the spectral data. Selective irradiation of ³¹P NMR signals permitted the elucidation of which phosphorus signal corresponds to which hydride signal. Tickling the ³¹P NMR signal at δ 46.6 and 46.0 produced a change in the hydride signal at δ -16.49 while tickling the phosphorus signal at δ 43.7 produced a change in the hydride at δ -16.78 (Fig. 5.3.b). A ³¹P{¹H} COSY NMR spectrum at this temperature established: i) signals at δ 46.6 and 46.1 ppm are coupling each other; ii) the signal at δ 47.0 couples to the one at δ 46.5 and the signal at δ 46.5 couples to the signal at δ

45.6. This permits the determination of $^1J(^{103}Rh-^{31}P)$ 136 and 139 and not 84 and 86; iii) the lack of coupling between the signals at δ 46.1 and 46.6 and that at δ 43.7. Possible structures are discussed below (Fig. 5.6).

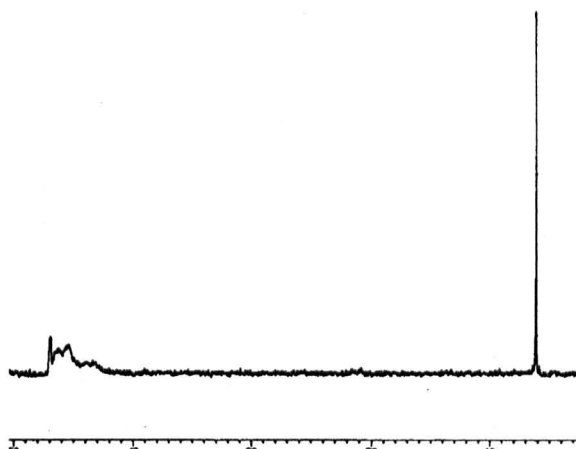


Fig. 5.1 162 MHz $^{31}P\{^1H\}$ -NMR spectrum of $[RhCl(PPh_3)_3]$ in $CH_2Cl_2/AlCl_3/HCl$, room temperature.

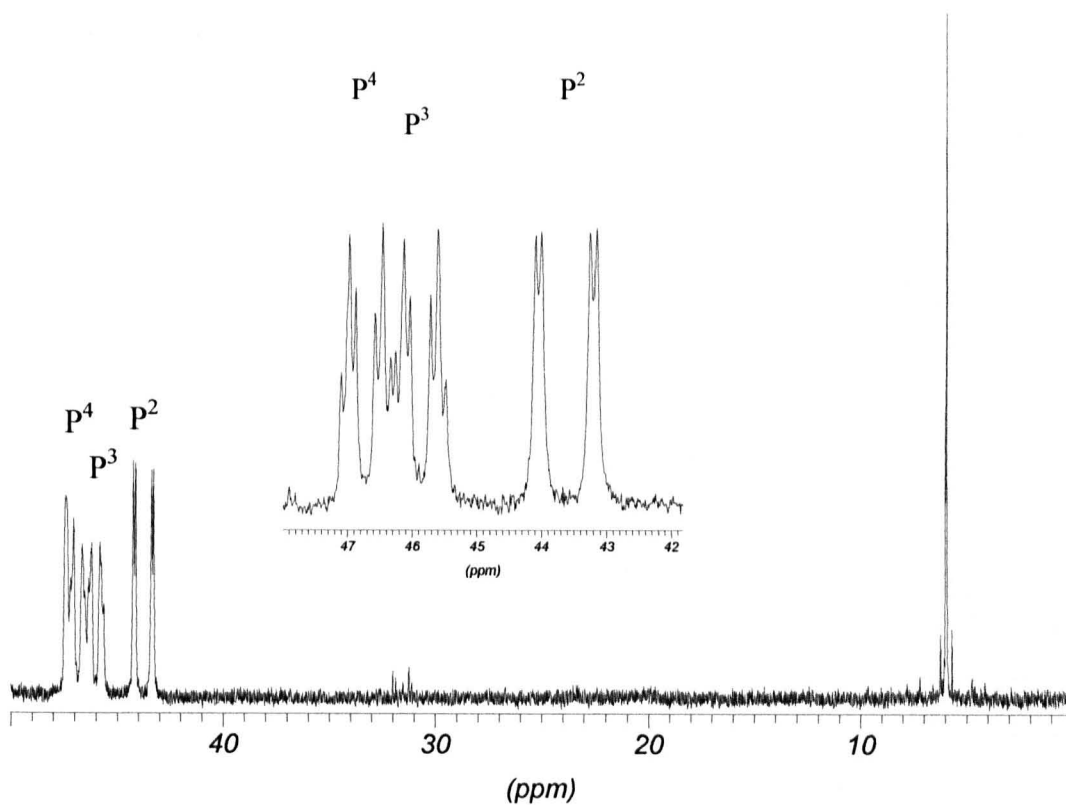


Fig. 5.2. 162 $^{31}P\{^1H\}$ -NMR spectrum of $[RhCl(PPh_3)_3]$ in $CH_2Cl_2/AlCl_3/HCl$, 241K.

Table 5.1. $162\ ^{31}P$ NMR data for Fig. 5.1.

Nuclei	Chemical shift (ppm)	Multiplicity	$^1J(^{103}Rh-^{31}P)$	$^2J(^{31}P_1-^{31}P_2)$	$^2J(^{31}P-^{31}P)$
P ⁴	46.6	td	136	18	21
P ³	46.0	td	139	18	21
P ²	43.6	dd ^a	136	16	21
^b P ¹	6	s	--	--	$^1J(^{31}P-^1H)$ 504

a) Residual $^1H-^{31}P$ coupling; b) assigned to $[Ph_3PH]^+$ cation as in ionic solvent.

From this result we could deduce there are two different species in solution, each one contains a hydride.

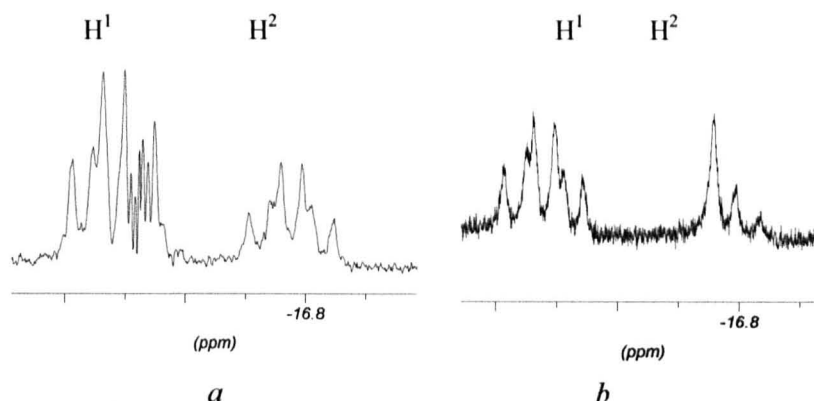


Fig. 5.3. 400 MHz 1H NMR spectrum of $[RhCl(PPh_3)_3]$ in $CH_2Cl_2/AlCl_3/HCl$, 241 K. a) hydride region without perturbation; b) perturbation of signal in ^{31}P NMR frequency at low chemical shift (δ 43.6 ppm, P²).

Firstly, $^1J(^{103}Rh-^{31}P)$ values in Table 5.1 are smaller than $^1J(^{103}Rh-^{31}P)$ for $[RhCl(PPh_3)_3]$ in $[emim][Al_2Cl_7]$, suggesting a Rh(III) centre. The broadness of $^{31}P\{^1H\}$ NMR at room temperature raises the possibility of exchange and hence a $^{31}P\{^1H\}$ EXSY spectrum was recorded at 254 K. This shows exchange between the two inequivalent ^{31}P nuclei of one compound at δ 46.6 and 46.0 and with the second compound at 43.7, Fig. 5.4. This spectrum shows only cross peaks associated with the retention of the ^{103}Rh spin state. The signal at 47.0 correlates with 46.1 and the signal at 46.4 correlates with the signal at 45.6. These exchanges do not involve Rh spin exchange. This condition reveals an intramolecular mechanism. Exchange between δ 46.6 and 46.0 signals gave a rate of $2.2 \pm 0.2 s^{-1}$ (P¹-P² and P₂-P₁ exchange between the ^{31}P NMR signal at 43.7 with both signals at 46.0 and 46.6 with a rate of $5.3 \pm 0.4 s^{-1}$ (P₁-P₃ exchange rate). These rates correspond to $\Delta G^\ddagger_{254} = 60$ and 58 kJ

mol^{-1} respectively. These values were recorded by using $[\text{D8}] = 70 \text{ ms}$ in the NOESY pulse sequence for the solution $[\text{RhCl}(\text{PPh}_3)_3]/\text{CH}_2\text{Cl}_2/\text{AlCl}_3/\text{HCl}$ (Fig. 5.4), 254K.

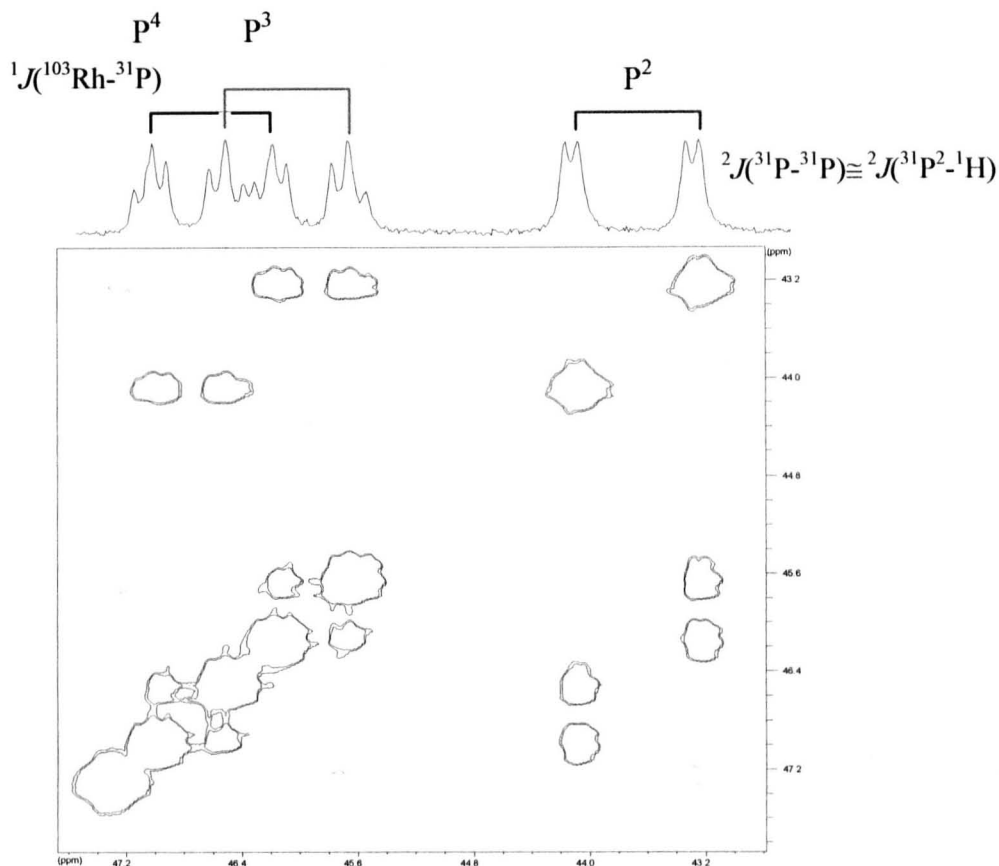


Fig. 5.4. ^{31}P phase sensitive NOESY spectrum of $[\text{RhCl}(\text{PPh}_3)_3]$ in $\text{CH}_2\text{Cl}_2/\text{AlCl}_3/\text{HCl}$, 254K. The signal at 46.78 correlates with 46.5 and the signal at 46.1 correlates with the signal at 45.7. This exchange does not break Rh-P bonds.

The ^{27}Al NMR of this solution showed two sharp signals at 98.3 and 89.9 ppm, Fig. 5.5. The solution of $[\text{AlCl}_3]$ in $\text{CH}_2\text{Cl}_2/\text{CD}_2\text{Cl}_2$ shows a broad signal at 102.5 ppm with line width around 300 Hz, corresponding to free $[\text{AlCl}_4]^-$.¹ This suggests that signals at 98.3 and 89.9 ppm correspond to a species where aluminium trichloride is interacting with rhodium via a chloride bridge. Chloride bridges between Rh and Al reduce the σ donation from Al to Cl because now the Cl is drawing density from the Rh centre. This must increase the electronic density at the aluminium centre, producing a more shielded aluminium nucleus.

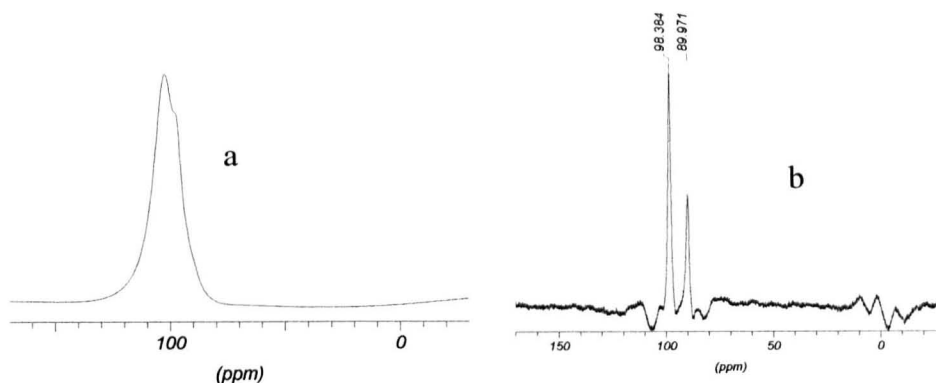
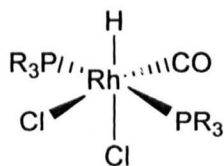


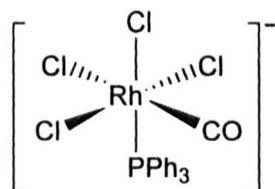
Fig. 5.5. ^{27}Al NMR of dissolution of: a) $[AlCl_3]$ in CD_2Cl_2 ; b) $[RhCl(PPh_3)_3]$ with $AlCl_3$ (1:5 fold excess).

The broadness of the signal at 102.5 ppm in Fig. 5.5 *a* may be related to the concentration of the $AlCl_3$ added to the solution in comparison with *b*, where the concentration of $AlCl_3$ is not as large as the solution of spectrum *a* in the same figure.

The structure of the product presents a problem. The isomer with inequivalent PPh_3 groups is first considered. The $^{31}P\{^1H\}$ NMR clearly shows the presence of *fac*- $RhH(PPh_3)_2$ as $^2J(^{31}P-^{31}P)$ 18 Hz and $^2J(^{31}P-^1H)$ 18 Hz shows a mutual *cis*-relationship between the PPh_3 ligands and between the PPh_3 and the hydride ligand. This rules out the possibility of a square planar structure. Five coordinate structures were also considered. Based on the geometry of crystal structures of complexes of the type $[RhHCl_2(PR_3)_2]$, the compounds have a square pyramidal structure with an axial hydride *trans* to a solvent molecule, with chemical shifts around -31 ppm. The other possibility, a PPh_3 in the axial position, is unknown for rhodium centres but this kind of complex occurs in $[RuCl_2(PPh_3)_3]$ with a very substantial high frequency shift for the axial PPh_3 . Hexacoordinated rhodium (III) centres have small $^1J(^{103}Rh-^{31}P)$ as is the case for $[Rh(Cl)_2(H)(CO)(PR_3)_2]$, (**27**), (section 3.3, synthesis 20-27) and anions such as $[Rh(Cl)_4(CO)(PPh_3)]^-$ (**28**), $^1J(^{103}Rh-^{31}P)$ 70-80 Hz.²



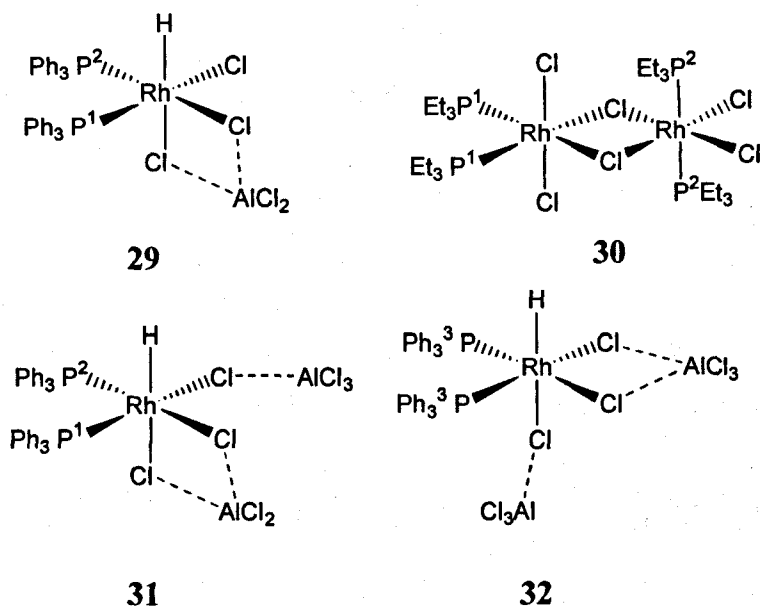
27



28

A possible six-coordinate structure is **29**. However, the value of 136-139 Hz for $^1J(^{103}Rh-^{31}P)$ presents some problems. $[Rh_2Cl_6(PEt_3)_4]$, (**30**), has been reported, with $^1J(^{103}Rh-$

^{31}P) 115 Hz for P^1Et_3 and 81 Hz for P^2Et_3 . In **30**, the P^1Et_3 is *trans* to a bridging chloride. The terminal chloride in **29** should exert a stronger *trans* influence than the Rh-(μ -Cl) and result in a reduction in $^1J(^{103}Rh-^{31}P)$ below 115 Hz rather than the observed 135 Hz. It is generally found that $^1J(^{103}Rh-^{31}P)$ is a little larger when the tertiary phosphine is PPh_3 , rather than PEt_3 , but this difference is normally only a few percent, not 17%. It is possible that aluminium weakens the Rh(μ -Cl) bond more than a second rhodium, as in **31**, with the consequential reduction in *trans*-influence. Hence a possible alternative structure to **29** is **31**.



On this basis, the structure of the isomer with equivalent PPh_3 ligands is **32**. The observed interchange between PPh_3 ligands in **31** and between **31** and **32** can be achieved by either breaking Rh(μ -Cl) or Al(μ -Cl) bonds (Fig. 5.6).

It means that P^1 and P^2 are in equilibrium in the same species because they have the same spin flipping rate, and both of them are exchanging with P^3 because they have the same equilibrium rate.

So, analysing these results, the addition of $AlCl_3/HCl$ to a solution of $[RhCl(PPh_3)_3]$ in common organic solvents, CD_2Cl_2 in this case, gave the expected oxidative addition in the Rh(I) centre. Surprisingly, the addition of $AlCl_3$ produced a mixture of isomers because of its interaction with the chlorides attached to rhodium. A larger $^1J(^{103}Rh-^{31}P)$ coupling constant is clear evidence of the decrease in the *trans*-effect of the chloride as a ligand when it is attached to the chloroaluminium species. The formation of these kinds of Rh(III) species is not observed in the chloroaluminate (III), $x_{AlCl_3} = 0.67$ ionic liquid.

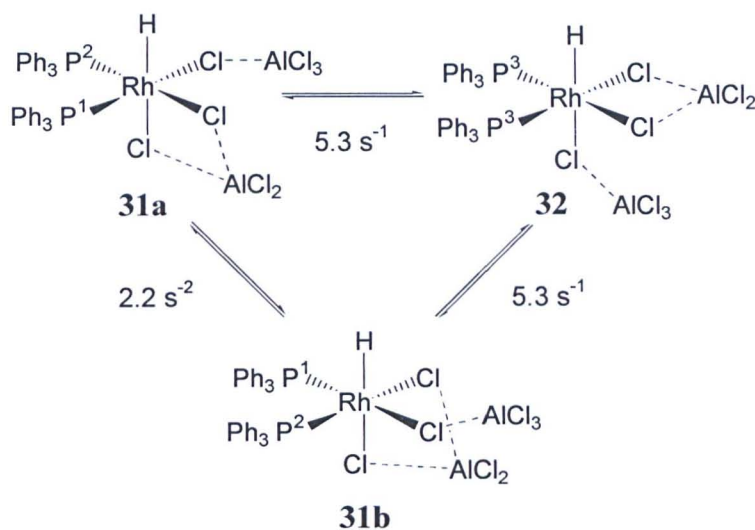


Fig. 5.6. Equilibrium of isomeric $[Rh\{(m-Cl)AlCl_3\}\{(\mu-Cl)_2AlCl_2\}(H)(PPh_3)_2]$ in $CD_2Cl_2/AlCl_3/HCl$. $[(\mu-Cl)AlCl_3]^-$ anion can interact with the metallic centre by one or two bridging chlorides.

This solution was allowed to stand for more than one month under nitrogen and the precipitation of a white powder and a cloudy solution was observed. The precipitation of the oxoaluminate cannot be avoided even in sealed tubes. Impurities such as moisture and air get into the solution within a few days and react with the highly sensitive aluminium trichloride. This permits the elimination of the chloroaluminate (III) from the complex but the chloride remains in the solution. After this period a dimeric face sharing species *trans,cis*- $[(PPh_3)_2ClRh(\mu Cl)_3RhCl_2PPh_3]$, **33**, is crystallized. The structure of this species is shown in Fig. 5.7 and 5.8, the crystallographic data is given in Table 5.2 and the complete parameters are found in appendix 1.

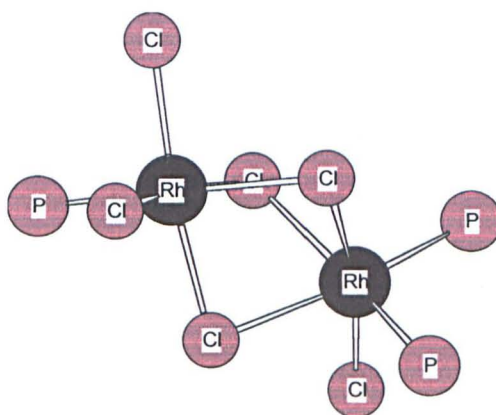


Fig. 5.7. Metallic core of **33**.

This kind of structure was widely studied in the 1980's³ and presented two kinds of conformation, depending on the concentration of free PR_3 and chloride anions. In this case the unexpected complex presented three PR_3 ligands in the dimeric species and two Rh(III) centres.

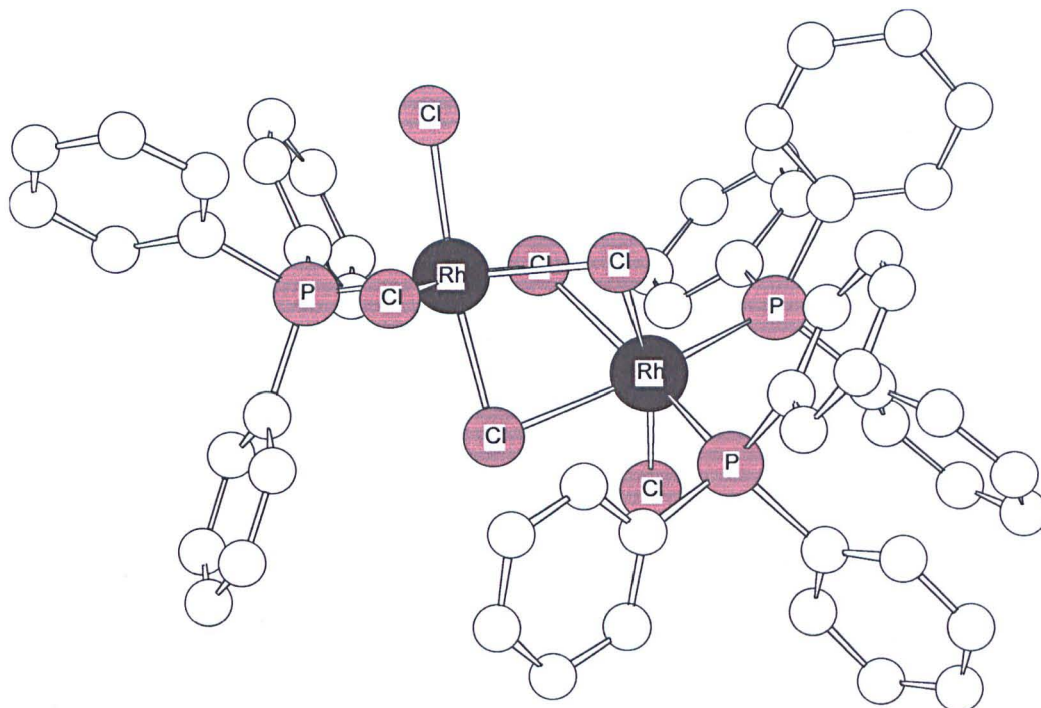


Fig. 5.8. Crystal structure for *trans,cis*- $[(PPh_3)_2(Cl)Rh(\mu^2Cl)_3Rh(Cl)_2(PPh_3)]$, **33**.

Unfortunately, the highly water sensitive $[ClAlCl_3]^-$ was eliminated from the rhodium centre resulting in the formation of the dimer **33**. A simple mechanism for the formation of **33** can be proposed as follows. Chloroaluminate (III) can produce HCl, oxo and hydroxochloroaluminate (III) in the presence of moisture and oxygen (section 2.5). Oxygen can interact with the rhodium complexes and then be transferred to the aluminium to produce hydroxochloroaluminate anions. Then, Cl^- that is abundant in the solution, can occupy the vacant place left by the oxygen on the rhodium complex. Finally, this could produce an oxidation of the rhodium complex and the addition of more chlorides. Also, the high concentration of the initial $[RhCl(PPh_3)_3]$, 50mg dissolved in 1 mL of CD_2Cl_2 which gives a concentration $[Rh(I)] = 0.05$ mM, may be the reason for the dimerization.

Table 5.1. Crystal data and structure refinement for *trans,cis*- $[(\text{PPh}_3)_2(\text{Cl})\text{Rh}(\mu^2\text{Cl})_3\text{Rh}(\text{Cl})_2(\text{PPh}_3)]$, **33**.

Empirical formula	$\text{C}_{68} \text{H}_{61} \text{Cl}_6 \text{P}_3 \text{Rh}_2$	Theta range for data collection	1.38 to 28.36°
Formula weight	1389.60	R indices (all data)	R1 = 0.2543, wR2 = 0.1567
Temperature	150(2) K	Reflections collected	38401
Wavelength	0.71073 Å	Independent reflections	14575 [R(int) = 0.2217]
Crystal system	Monoclinic	Completeness to theta= 28.36°	96.4 %
Space group	$P2_1/n$	Absorption correction	Semi-empirical
Unit cell dimensions	$a = 13.430(4) \text{ \AA};$ $\alpha = 90^\circ$	Index ranges	$16 \leq h \leq 16,$ $17 \leq k \leq 24,$ $32 \leq l \leq 25$
	$b = 18.758(6) \text{ \AA};$ $\beta = 96.554(7)^\circ$		
	$c = 24.185(7) \text{ \AA};$ $\gamma = 90^\circ$		
Volume	$6053(3) \text{ \AA}^3$	Max. and min. transmission	0.9637 and 0.8964
Z	4	Refinement method	Full-matrix least-squares on F^2
Density (calculated)	1.525 Mg/m^3	Data / restraints / parameters	14575 / 126 / 688
Absorption coefficient	0.932 mm^{-1}	Goodness-of-fit on F^2	0.798
F(000)	2824	Final R indices [$ I > 2\sigma(I)$]	R1 = 0.0762, wR2 = 0.1129
Crystal size	$0.12 \times 0.08 \times 0.04 \text{ mm}^3$	Largest diff. peak and hole	0.993 and $-0.668 \text{ e. \AA}^{-3}$

The complexes of interest **31** and **32** could not be crystallized. The observation of a Rh(III) species in common organic solvents, even with AlCl_3 , suggested the idea of studying the chemistry of the same rhodium complex with a higher excess of AlCl_3 . The next section shows the results when $[\text{RhCl}(\text{PPh}_3)_3]$ is dissolved in CD_2Cl_2 and toluene with a 10-fold excess of AlCl_3 .

The presence of oxygen in impure $[\text{emim}][\text{Al}_2\text{Cl}_7]$ was corroborated by adding pure Cl_2PPh_3 to an impure batch of $[\text{emim}][\text{Al}_2\text{Cl}_7]$. The formation of signals at δ 65 ppm assigned to $[\text{ClPPh}_3]^+\text{Cl}^-$ and OPPhCl_2 at 42 ppm were observed.

5.2. Reaction of $[RhCl(PPh_3)_3]$ in CH_2Cl_2 and toluene with 10-fold excess of $AlCl_3$

When looking for more evidence of the interaction of $AlCl_3$ in CH_2Cl_2 , the reaction of Wilkinson's catalyst in this organic medium was performed in an excess of $AlCl_3$. 70 mg of $AlCl_3$ was dissolved in 1 mL of CD_2Cl_2 and 40 mg of $[RhCl(PPh_3)_3]$ was added. The species observed by ^{31}P NMR spectra was the same species as that of the hydride complex **25**, in the ionic liquid (see section 4.2). The chemical shift and $^1J(^{103}Rh-^{31}P)$ coupling constant was exactly the same. Surprisingly, the species $[HPPH_3]^+$ was observed in this solution as can be seen in Fig. 5.9.

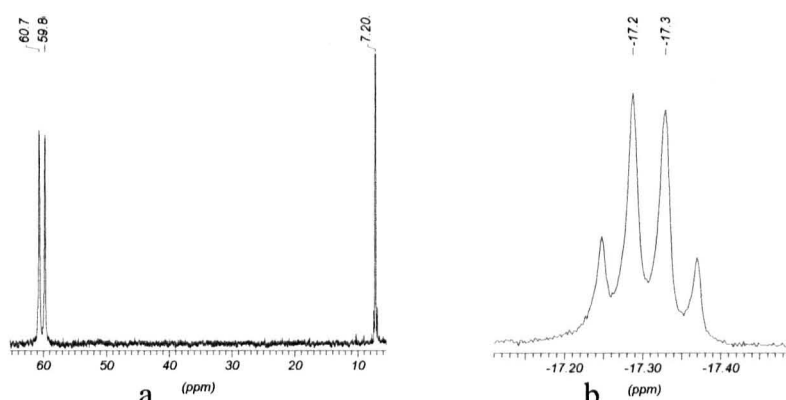


Fig. 5.9. a) $^{31}P\{^1H\}$ NMR of solution of $[Rh(Cl)(PPh_3)_3]$ in CH_2Cl_2 with 10 fold excess of $AlCl_3$; b) 1H NMR, hydride region of the same solution; b) 1H NMR, hydride region of the same solution.

These results were unexpected, because $[RhCl(PPh_3)_3]$ in $CH_2Cl_2/AlCl_3/HCl$ made a mixture of isomers, where HCl was oxidatively added and $AlCl_3$ may interact with the species. However in the absence of HCl and excess of $AlCl_3$, the species showed the presence of a Rh(I) hydride. The origin of this hydride may be the remaining moisture in the mixture that reacted with $AlCl_3$ and produced HCl, (the same explanation as for the ionic liquid, see section 4.2). This produces Rh(I) with the elimination of $[HPPH_3]^+$. The proposed mechanism is explained in section 4.2.2. The $AlCl_3$ formed can be incorporated into the ionic dissolution once again producing $[Al_2Cl_7]^-$.

On the basis of this result, the stabilization of the Rh(I) centre can be attributed to the existence of $[Al_mCl_n]^-$ species. Chloroaluminate (III) may extract chlorine species from the metallic centre due to the availability of many anions in equilibrium.^{4,5} The other source of hydride may be the presence of a $[HA_l_mX_n]^-$ species. The hydride would have come from the

reaction of $[Al_mX_n]$ with CH_2Cl_2 , which forms $[HAl_mX_n]^-$ and $CHCl_2^+$. However, the reaction was performed in toluene and gave the same results.

The interaction of the chloroaluminate (III) with the metallic centre may be seen in the ^{27}Al NMR spectrum. Here, the broad signal at 94.6 ppm with a linewidth of 1950 Hz may be attributed to the presence of the $[(\mu-Cl)AlCl_3]^-$ anion interacting with the rhodium centre by a chlorine bridge (Fig. 5.10b).

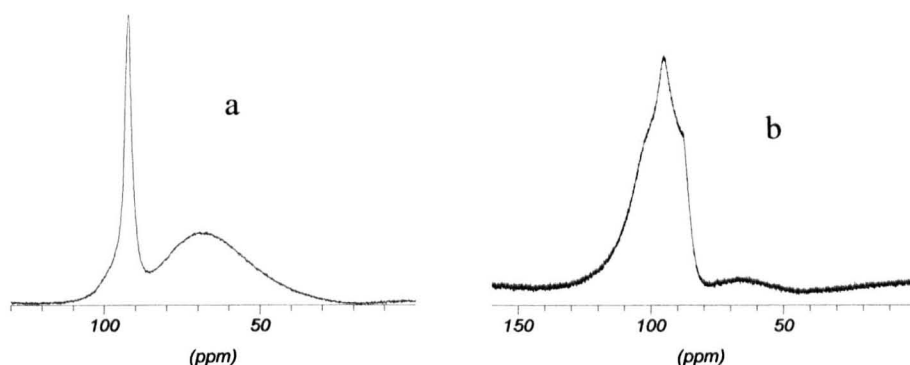
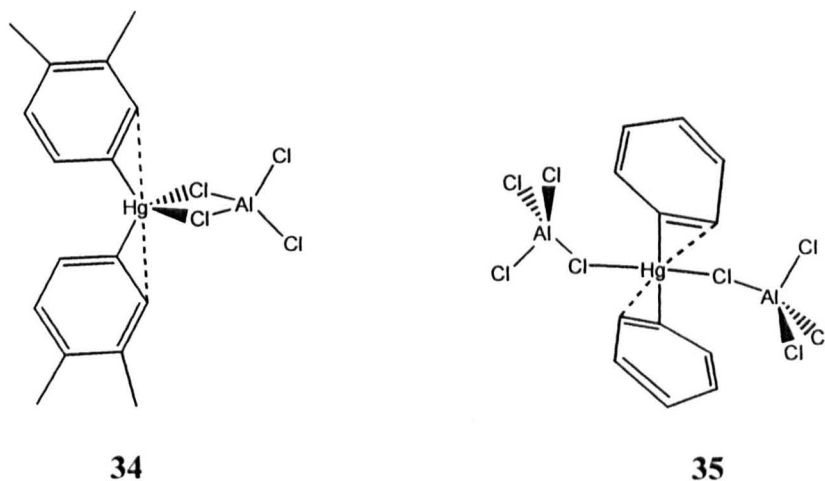


Fig. 5.10. ^{27}Al NMR of a) $AlCl_3$ in CD_2Cl_2 ; b) $[RhCl(PPh_3)_3]$ dissolved in a). Evidence of interaction of chloroaluminate (III) in the metallic centre.

This kind of proposal is known. Compounds based on Hg centres have recently been characterized by X-ray diffraction (**34**, **35**) with ^{27}Al NMR δ 104-105 ppm and linewidth 1870 Hz was reported for the dissolution of both species.⁶ Essentially, the chemical shift towards lower frequency in the case of the rhodium complex may be attributed to the higher electronic density at the rhodium (I) centre, surrounded by a hydride and phosphines, which are known as being σ -basic, increasing the shielding in the aluminium centre.



When the reaction was repeated in toluene, a different solution was observed.⁷ In this case, the addition of $AlCl_3$ to toluene gave a yellow-green solution. ^{27}Al NMR of this complex shows a broad singlet at 91 ppm with a linewidth of 300 Hz, as in Fig. 5.11a.⁶ The broad signal at 71 ppm came from the alumina in the probe of the NMR equipment and the glass from the NMR tube. The consecutive addition of the rhodium complex gave red-brown oil. When the mixture was allowed to stand, a deep brown oil separated from the organic phase. ^{31}P NMR of the oily product shows the same pattern as $[Rh\{\mu\text{-}Cl\}AlCl_3\}(H)(PPh_3)_2]^-$ and $[HPPPh_3]^+$ in the ionic liquid and in CD_2Cl_2 with an excess of $AlCl_3$. However, the ^{27}Al NMR spectrum (Fig. 5.12b) shows a broader signal than Fig. 5.11b at 102.6 ppm.

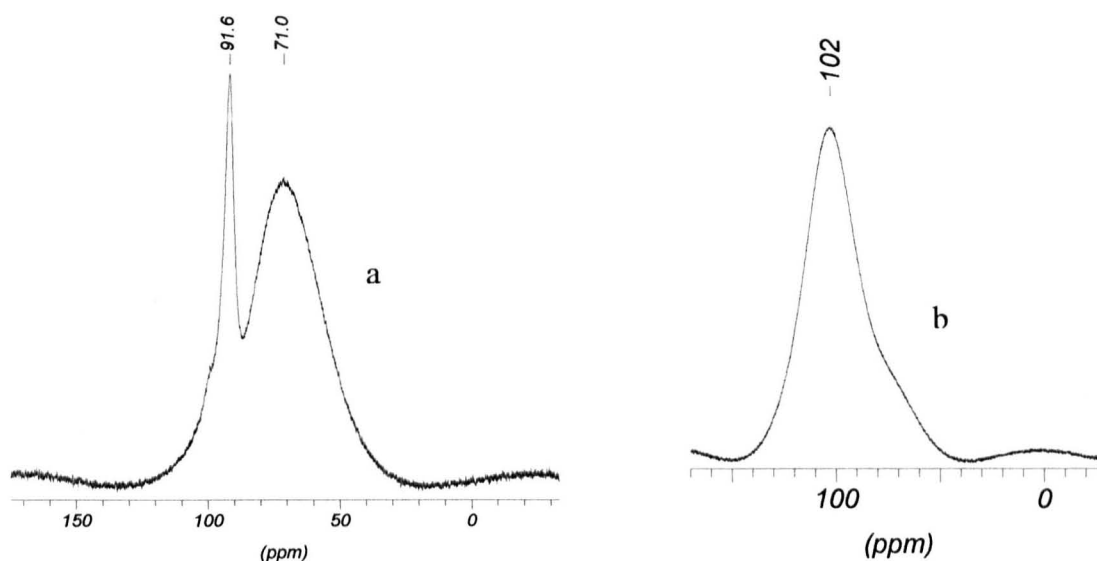


Fig. 5.11. a) ^{27}Al NMR of $AlCl_3$ in toluene- d_8 . Signal at 91 ppm $[Al_2Cl_6]$, signal at 71 ppm due to the Al in glass and ceramics; b) Addition product, $[Rh(Cl)\{\mu\text{-}Cl\}AlCl_3\}(H)(PPh_3)_2]^-$, **24**, in toluene.

This result agrees with the proposal that $[(\mu\text{-}Cl)AlCl_3]^-$ is interacting with the metallic centre, giving a Rh(I) species. Clearly, the presence of chloroaluminate (III) is the reason for the stabilization of the Rh(I) centre. Unfortunately, the crystallization of this complex was not possible. This could be a result of the high concentration of hydrogen bonds that chlorines can have around the phosphines in the complex. The higher concentration of chlorines the stronger the bonding of $[(\mu\text{-}Cl)AlCl_3]^-$ to the complex. This avoids the separation from the organic solvent. The other reason is the highly viscous dissolution that increases in viscosity when it is cool and does not permit the proper crystallization of the compound.

A conclusion from these results can be that the stabilization of species that do not exist in organic solvents has occurred. The dissolution of $[RhCl(PPh_3)_3]$ gives new compounds that have been characterized. This example marks a new beginning in the chemistry of Wilkinson's catalyst. It is necessary to know more about the differences that can occur when using chloroaluminate (III) ionic liquids and organic solvents. Hence, the next section explains the results of carbonylation of $[Rh(Cl)\{(\mu-Cl)AlCl_3\}(PPh_3)_2]^-$ **24**, and $[Rh\{(\mu-Cl)AlCl_3\}(H)(PPh_3)_2]^-$, **25** in $[emim][Al_2Cl_7]$. The results are compared with the corresponding chemistry of Wilkinson's catalyst in organic solvents. After that, the chemistry of Vaska type complexes in such ionic media is discussed. The results once again are quite surprising. The solution of such complexes gave different species from the one already known in organic solvents. The carbonylation of such compounds was carried out and some important intermediates have been observed and partially characterized by ^{31}P and ^{13}C NMR spectroscopy.

5.3. References

- ¹ B. E. Mann and R. K. Harris, *NMR and the Periodic Table*, Academic Press, London, 1978, ch. 9.
- ² A. M. Lebuis, M. G. L. Petrucci and A. K. Kakkar, *Organometallics*, 1998, **17**, 4966.
- ³ M. Pasquale, *J. Coord. Chem.*, 1999, **48**, 503; F. A. Cotton and S. J. Kang, *Inorg. Chem.*, 1993, **32**, 2336; J. A. S. Duncan, T. A. Stephenson, M. D. Walkinshaw, D. R. Hedden and D. Max, *J. Chem. Soc., Dalton Trans.*, 1984, **5**, 801; J. A. S. Duncan, T. A. Stephenson, M. D. Walkinshaw, D. R. Hedden and D. Max, *Angew. Chem.* 1982, **94**, 463.
- ⁴ V. Frey and W. Hieber, *Chem. Ber.*, 1966, **99**, 2614.
- ⁵ A. Salzer and C. Elschenbroich, *Organometallics: A concise introduction*, VCH, Germany, 2nd edn, 1992, pp 75.
- ⁶ A. S. Borovik, S. G. Bott and A. R. Barron, *J. Am. Chem. Soc.*, 2001, **123**, 11219.
- ⁷ B. Chevier and R. Weiss, *Ang. Chem. Int. Ed. Eng.*, 1974, **13**, 1; P. Tarakeshwar, J. Y. Lee and K. S. Kim, *J. Phys. Chem. A*, 1998, **102**, 2253.

6. Results and discussion: Carbonylation of rhodium complexes in [emim][Al₂Cl₇]

The last chapter has examined solutions of [RhCl(PPh₃)₃] in organic solvents with the addition of AlCl₃. It has been proved that the presence of [AlCl₄]⁻ changes the chemistry of [Rh(Cl)(PPh₃)₃] due to an interaction of the metallic centre, possibly through chlorine bridges and the elimination of a PPh₃ group. The difficulties of separation of the Rh(I) species formed in [emim][Al₂Cl₇] and the difficulties of crystallization of Rh(III) from the CH₂Cl₂/AlCl₃ systems have been discussed. However, in order to know more about the chemistry of the [Rh(Cl)(PPh₃)₃] in [emim][Al₂Cl₇], carbonylation of [RhCl{(μ-Cl)AlCl₃}(PPh₃)₂]⁻, **24**, was carried out in [emim][Al₂Cl₇]. This chapter shows the results of this study from ³¹P NMR spectroscopy and the carbonylation of [RhCl(CO)(PR₃)₂] compounds in this ionic liquid.

6.1. Carbonylation of [RhCl{(μ-Cl)AlCl₃}(PPh₃)₂]⁻ in [emim][Al₂Cl₇]

CO was bubbled through the solution of [RhCl{(μ-Cl)AlCl₃}(PPh₃)₂]⁻, **24**, in pure [emim][Al₂Cl₇]. The colour of the solution changed from dark to light brown. The ³¹P{¹H} NMR spectrum of this solution is shown in Fig. 6.1.

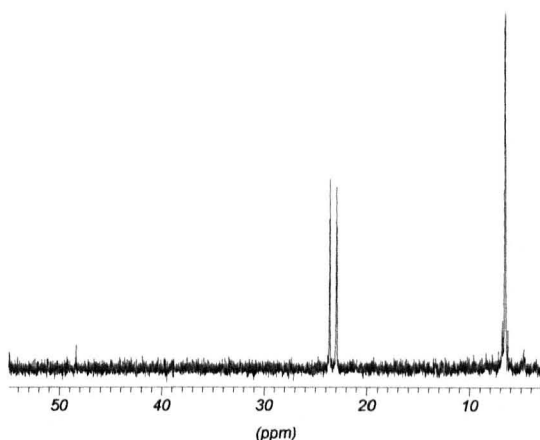


Fig. 6.1. 162 MHz ³¹P{¹H} NMR of [RhCl{(μ-Cl)AlCl₃}(PPh₃)₂]⁻ in [emimCl][Al₂Cl₇] with CO. ¹J(¹⁰³Rh-³¹P) 107.5 Hz.

The same compound was formed when CO was bubbled through the solution of [Rh{(μ-Cl)AlCl₃}(H)(PPh₃)₂]⁻ **25**, in impure [emim][Al₂Cl₇]. The final complex does not show any hydride signal in the ¹H NMR spectrum. The ³¹P{¹H} NMR spectrum corresponds to: singlet, 6.5 ppm (2P); doublet, 23.3 ppm, (1P), ¹J(¹⁰³Rh-³¹P) 107.5 Hz. The singlet at low frequency corresponds to [HPPH₃]⁺ and integrates as two PPh₃ ligands while the doublet at high frequency is due to one PPh₃ attached to the rhodium centre. The elimination of a PPh₃ from the initial [RhCl{(μ-Cl)AlCl₃}(PPh₃)₂]⁻, complex **24**, gives the possibility of the coordination of CO to the metallic centre (complex **37** in Fig. 6.2). It is known that carbonylation of [Rh(Cl)(PPh₃)₃] in CH₂Cl₂ yields the Vaska's type complex [Rh(Cl)(CO)(PPh₃)₂], **36**, as a yellow powder with δ 29, ¹J(¹⁰³Rh-³¹P) 127 Hz.¹ In the [emim][Al₂Cl₇] solution, complex **36** is not observed.

It was clear that the reaction with CO involved the removal of a PPh₃ from **24**. The reaction of [Rh{(μ-Cl)AlCl₃}(H)(PPh₃)₂]⁻, **25**, with CO gave the same results and the formation of the same species. The nature of the compound found in the carbonylation of **24** and **25** are discussed in section 6.3. A summary of reactions appears in Fig. 6.2.

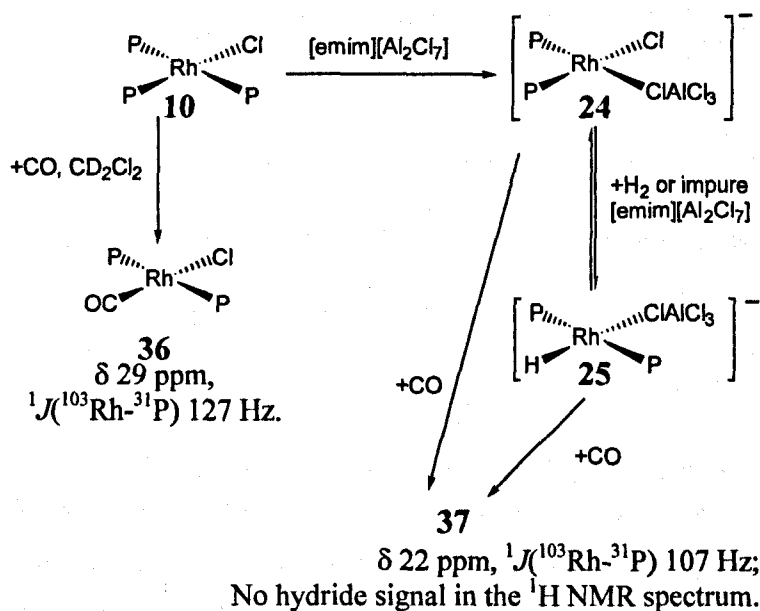


Fig. 6.2. Summary of reactions until now. The carbonylation of **24** and **25** gives an unexpected signal **37** that does not show any hydride signal in the ¹H NMR spectrum. The carbonylation of [Rh(Cl)(PPh₃)₃] in organic solvents gives [Rh(Cl)(CO)(PPh₃)₂].

The coupling constant of the carbonyl complex observed in the ionic liquid, **37**, is compared with known complexes in section 6.3, where the reaction with enriched ¹³CO is followed. A partial explanation of the structure of **37** is given with a clearer scenario for its

formation. It is clear that *cis*-[Rh(Cl){(μ-Cl)AlCl₃}(PPh₃)₂]⁻, **24**, in [emim][Al₂Cl₇] releases a phosphine, and coordinates CO but no [RhCl(CO)(PPh₃)₂] is formed. In order to know more about the formation of the new carbonyl, the monocarbonyldiphosphine, [RhCl(CO)(PPh₃)₂] was added to a fresh sample of [emim][Al₂Cl₇]. The next section describes the study of this solution, giving details about the carbonyls observed as intermediates in [emim][Al₂Cl₇], and compares the ³¹P NMR parameters with known Rh complexes in organic solvents.

6.2. Reaction of [Rh(Cl)(CO)(PPh₃)₂] in [emim][Al₂Cl₇] x_{AlCl₃} = 0.67

As with the previous results with [RhCl(PPh₃)₃] in impure [emim][Al₂Cl₇] (section 4.2), ³¹P{¹H} NMR of a solution of [Rh(Cl)(CO)(PPh₃)₂] in the ionic liquid showed the liberation of one phosphine which was protonated forming [HPPH₃]⁺ (singlet at 6 ppm, ¹J(³¹P-¹H) 504 Hz, 1P). A doublet at high frequency 52 ppm, ¹J(¹⁰³Rh-³¹P) 105 Hz, 1P, appears and the ¹H NMR spectrum shows the presence of a hydride with δ -12.5 and ¹J(¹⁰³Rh-¹H) ~ ²J(³¹P-¹H) 15 Hz, with the multiplicity of a pseudotriplet, Fig. 6.3b.

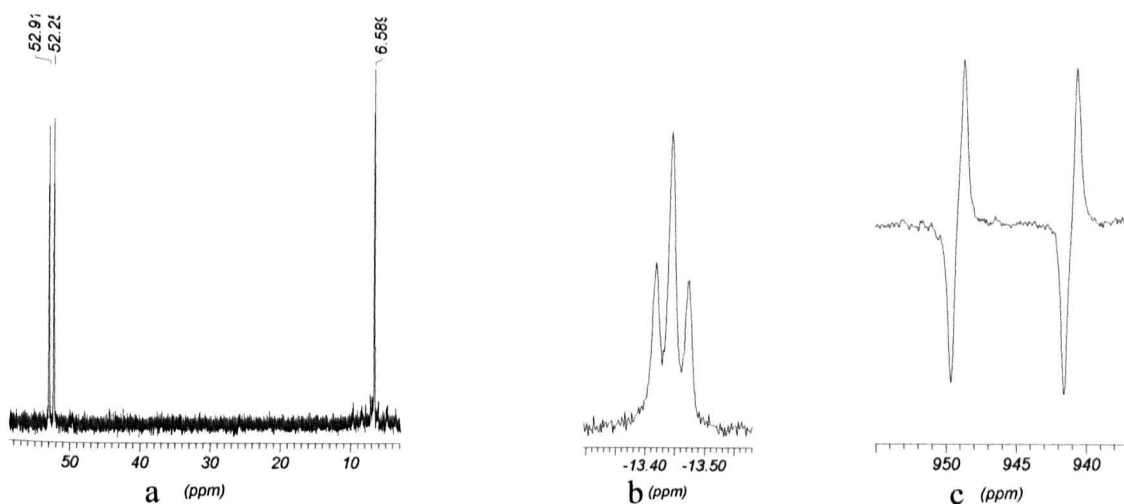


Fig. 6.3. NMR spectra for solution of [Rh(Cl)(CO)(PPh₃)₂] in [emim][Al₂Cl₇]; a) ³¹P{¹H} NMR, b) Hydride region in ¹H NMR ; c) ¹⁰³Rh {INEPT} NMR spectrum.

¹³C{¹H} NMR of the complex shows a signal at 172.8 ppm, as a doublet, ¹J(¹⁰³Rh-¹³C) 76.5 Hz, of doublets ²J(³¹P-¹³C) 10.3 Hz. The ν_{CO} in the FT-IR spectrum is at 2117 cm⁻¹. The presence of the hydride enables the application of the ¹⁰³Rh{¹H} INEPT NMR pulse sequence to get the rhodium signal. The ¹⁰³Rh {INEPT} spectrum is shown in c, Fig.

6.3, δ 945, where two couplings are evident: $^1J(^{103}\text{Rh}-^1\text{H})$ 15 Hz; $^1J(^{103}\text{Rh}-^{31}\text{P})$ 105 Hz. The coupling constant $^1J(^{103}\text{Rh}-^{31}\text{P})$ 105 Hz can indicate Rh(I) or Rh(III), the ν_{CO} at 2117 cm^{-1} for this compound could indicate Rh(III). From the integration of the ^{31}P NMR spectrum (Fig. 6.3a) and from the multiplicity in the ^{13}C and ^{103}Rh NMR spectra, it can be seen that the complex has only one PPh_3 attached to the rhodium, which is *cis* to CO, due to the small coupling $^2J(^{31}\text{P}-^{13}\text{C})$. In the ^{13}C NMR spectrum with ^1H coupling, $^2J(^{13}\text{C}-^1\text{H})$ is not observed at all, which is consistent with a *cis*-arrangement C-Rh-H, otherwise the coupling would be in the range of 15-60 Hz.^{2,3} The ^{103}Rh {INEPT} NMR spectrum shows the presence of only one hydride and one PPh_3 . The isolation of this compound was unsuccessful, but an additional experiment was performed. The synthesis of $[\text{Rh}(\text{Cl})_2(\text{H})(\text{CO})(\text{PPh}_3)_2]$, **39**, from **36** and HCl gives: ^{31}P δ 38 ppm, $^1J(^{103}\text{Rh}-^{31}\text{P})$ 85.9 Hz. This compound was dissolved in [emim][Al₂Cl₇] and the same complex with the spectra in the Fig. 6.3, was observed. Fig. 6.4 shows a summary of reactions.

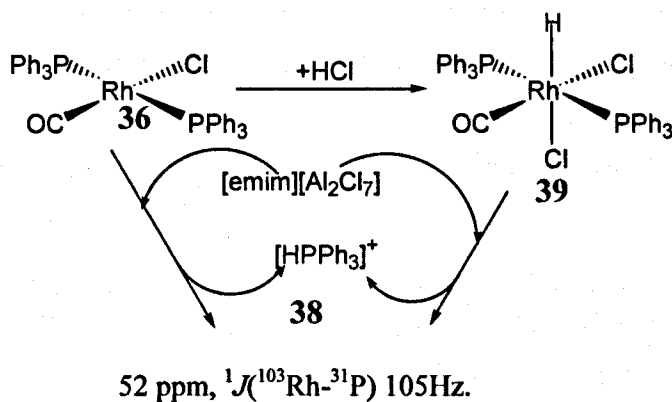


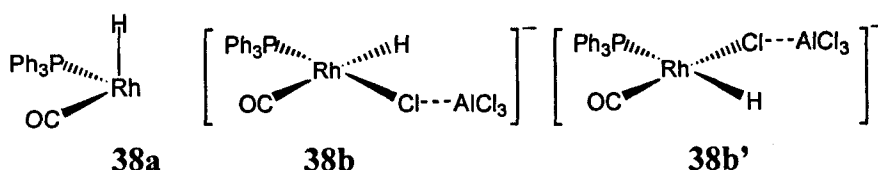
Fig. 6.4. Formation of **38**, a new monocarbonyl rhodium species in [emim][Al₂Cl₇] whose structure is proposed in the following sections.

From the NMR evidence, the initial proposal of structure **38** must have a hydride, a PPh_3 and a CO, all *cis* to each other. Possible structures are: *i*) Rh(I) pentacoordinated trigonal bipyramidal structure or *ii*) hexacoordinated rhodium (III) complex; the next two sections discuss both oxidation states as alternatives.

6.2.1. The alternative of a rhodium (I) complex for **38**

It has been discussed that the NMR evidence agrees with a structure based on **38a**, where the PPh_3 group, the hydride and CO are mutually *cis*. Hence, a square planar Rh(I) complex such as **38b** or **38b'** can be discarded completely.

6. Results and discussion: Carbonylation of rhodium complexes in [emim][Al₂Cl₇]



In addition, structure **38b** does not agree with a small $^1J(^{103}\text{Rh}-^{31}\text{P})$ 105 Hz as is observed in **38**. Square planar (sp) Rh(I) complexes usually have couplings around 120-130 Hz (see Table 6.5 and appendix 2, Table A2.2). On the other hand, **38b'** would agree with a decrease in the $^1J(^{103}\text{Rh}-^{31}\text{P})$ coupling from a common value of 120-130 Hz to 105 Hz as is observed, but a *trans* coupling $^1J(^{31}\text{P}-^1\text{H})$ is usually very large and visible in the ^1H NMR spectra. Such coupling is not observed in the ^1H NMR spectrum of **38**.

Another common structure for Rh(I) is a trigonal bipyramidal geometry (tbp). Firstly, the alternative with the hydride in the apical position and the PPh₃ and CO in the equatorial position is a suitable structure, **38c**. The optional isomer with a hydride in the equatorial position in a trigonal bipyramidal structure is unknown for rhodium compounds due to the preference of hydrides to being in apical positions.⁴ The optional isomers with PPh₃ *trans* to hydride or with the CO *trans* to hydride do not agree with the NMR evidence of PPh₃, hydride and CO mutually *cis*. The *trans* coupling $^1J(^{31}\text{P}-^1\text{H})$ is usually very large as has been mentioned above, but also a *trans* coupling $^1J(^{13}\text{C}-^1\text{H})$ is large enough to be visible (15-65 Hz).^{2,3} Then, the alternative **38c** agrees with the NMR evidence with a hydride, a CO group and a PPh₃ group mutually *cis*. Also, the possibility of a bidentate $[(\mu\text{-Cl})_2\text{AlCl}_2]$, **38c**, may produce its alternative stereoisomer **38c'** but the monodentate $[(\mu\text{-Cl})\text{AlCl}_3]$ **38c''** cannot be discarded.

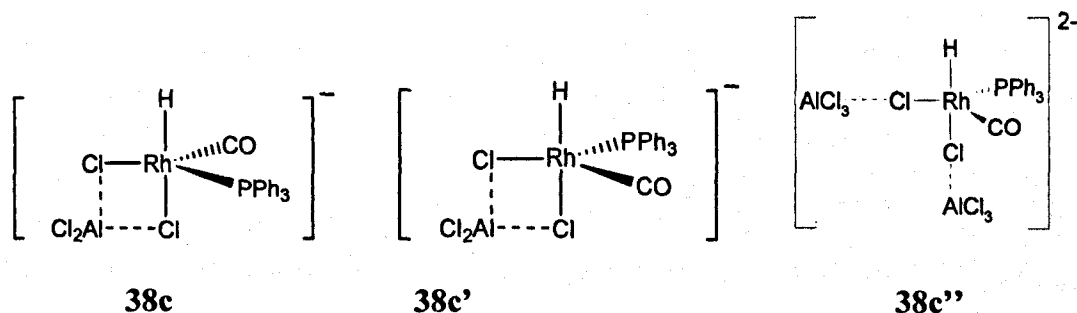


Table 6.1 shows some tbp-Rh(I) complexes similar to **38c**, as a point of comparison. Rotondo's group has reported the formation of **40** from the dimer $[\text{RhCl}(\text{CO})_2]_2$ with PPh₃ at δ 31.0, $^1J(^{103}\text{Rh}-^{31}\text{P})$ 116 Hz at -50°C ,⁵ while at lower temperature **41** has been proposed with δ 35.4, $^1J(^{103}\text{Rh}-^{31}\text{P})$ 92.7 at -70°C by Sanger.⁶

Table 6.1. Known *tbp*-Rh(I) complexes.

	40 ⁵	41 ⁵	42a ²	42b ²
¹ H	--	--	δ H -9.3 ¹ J(¹⁰³ Rh- ¹ H) 3 ¹ J(³¹ P- ¹ H) 99, -13 ¹ J(¹³ C- ¹ H) 13.5	δ H -9.3 ¹ J(¹⁰³ Rh- ¹ H) 6.5 ¹ J(³¹ P- ¹ H) -14 ¹ J(¹³ C- ¹ H) 13.5
³¹ P	δ 31.0 ¹ J(¹⁰³ Rh- ³¹ P) 116	δ 35.4 ¹ J(¹⁰³ Rh- ³¹ P) 92	δ 39.9 ¹ J(¹⁰³ Rh- ³¹ P) 138	δ 39.9 ¹ J(¹⁰³ Rh- ³¹ P) 138
¹³ C	Not reported	Not reported	δ 200.3 ¹ J(¹⁰³ Rh- ¹³ C) 63 ¹ J(³¹ P- ¹³ C) 11	δ 200.3 ¹ J(¹⁰³ Rh- ¹³ C) 63 ¹ J(³¹ P- ¹³ C) 11

Compounds such as [Rh(H)(CO)₂(PPh₃)₂], **42a** and **42b**, are in equilibrium when [Rh(H)(CO)(PPh₃)₃] is in solution under a CO atmosphere. They have been observed with trigonal bipyramidal geometry. **42a** has ²J(³¹P-¹H) 99 Hz, while an average coupling of both isomers ²J(¹³C-¹H) in **42a** and **42b** is 13.5 Hz.² With these examples, it is worth pointing out that:

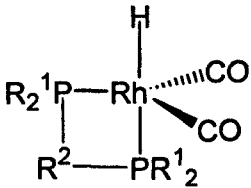
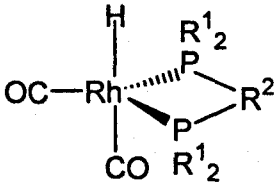
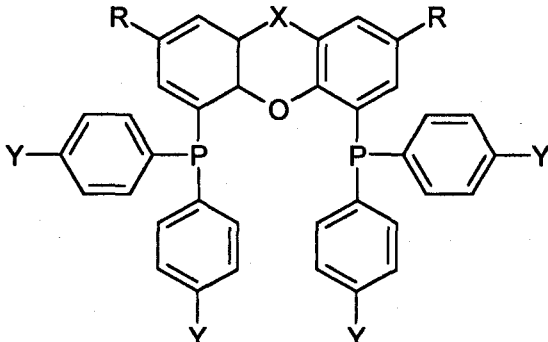
- A hydride in the axial position with a PPh₃ and CO in the equatorial position, as in **38c**, is a good structural alternative, it agrees with the NMR evidence, considering a Rh(I) centre. Other possibilities with a hydride in the axial position *trans* to PPh₃ or CO do not agree with the NMR evidence because no ²J(¹³C-¹H), ²J(³¹P-¹H), couplings are observed.

It is known that Rh(I) complexes present ν_{CO} values below free CO 2132 cm⁻¹ due to the higher π back donation from the metal to the antibonding π^* LUMO orbital in CO. That weakens the CO stretch and shifts the ν_{CO} energy in the IR spectra towards lower frequency, and a ν_{CO} of 2117 cm⁻¹ for **38c** is quite high.

6. Results and discussion: Carbonylation of rhodium complexes in [emim][Al₂Cl₇]

An important observation is the ¹⁰³Rh chemical shift for **38**. Some examples of δ ¹⁰³Rh for pentacoordinate biphosphines Rh(I) complexes have been recently reported. Table 6.2 shows the ¹⁰³Rh NMR frequencies for some tbp complexes observed in solution. Such values show that tbp Rh(I) species are between -500 to -1200 ppm, depending on the attached diphosphine.⁷ There is equilibrium between two possible arrangements **43a** and **43b**. The chelating phosphines are shown below.

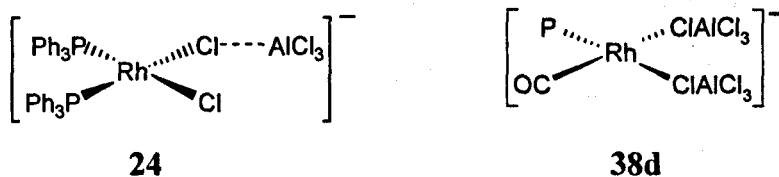
Table 6.2. ¹⁰³Rh δ for complexes **43a**-**43b** that are in equilibrium in solution.

 <p style="text-align: center;">43a</p>		 <p style="text-align: center;">43b</p>		
				
P-P ligand	R	X	Y	¹⁰³ Rh δ
Phenyl-P-xantphos	H	P-Ph	H	-828.2
Sixantphos	H	Si-Me ₂	H	-817.1
Thixantphos	Me	S	H	-840.0
Xantphos	H	C-Me ₂	H	-800.0

Such ¹⁰³Rh chemical shifts for **43a-b** are quite far from the chemical shift observed in **38** at 945 ppm. If the replacement of a CO and a PR₂ with a [(μ-Cl)₂AlCl₂]⁻ group in **43a** were possible, then the ¹⁰³Rh δ would not be as large as the observed value for **38**. That

replacement is unlikely to produce a shift from -500 ppm to 945 ppm as is observed in **38**. This evidence weakens the proposal of a Rh(I) structure such as **38c** in [emim][Al₂Cl₇]. Also the coupling $^1J(^{103}\text{Rh}-^{31}\text{P})$ observed in **40-42a,b** may not agree with the one for **38** having the oxidation state of (I).

Finally, it is worth noting that the presence of the Rh(I) hydride **38** would require the reduction of the initial rhodium centre, which is a Rh(I) chloride **36**. Such an explanation may be similar to the explanation given in chapter 4 where the Rh(I) chloride **24**, produces the Rh(I) hydride, **25**. The formation of the hydride, **25**, depends on the batch of [emim][Al₂Cl₇] used due to the presence of aluminium impurities in [emim][Al₂Cl₇]. Also, **25** is formed from **24** and H₂. However, in the case of the hydride **38**, the same product was always observed and no alteration of the results was observed for different batches of [emim][Al₂Cl₇]. This result produces a big difference in the chemistry of the monocarbonylphosphine rhodium **38** in comparison with the diphosphine rhodium **24**. In the case of **38** no Rh(I) carbonyl chloride intermediate, **38d**, analogue to **24**, was observed.



6.2.2. Alternative of Rh(III) for **38**

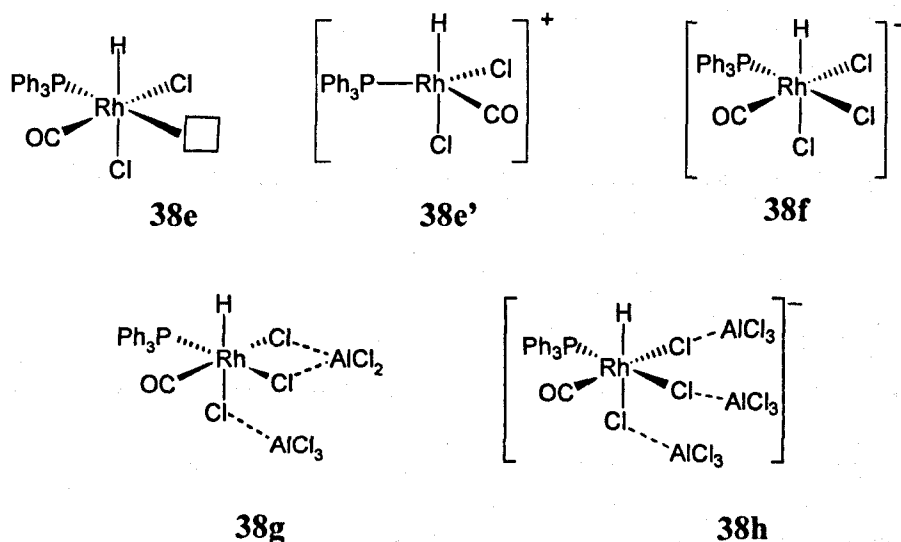
The proposal that **38** is a Rh(III) complex is based on the coupling constant $^1J(^{103}\text{Rh}-^{31}\text{P})$, the ^{103}Rh chemical shift and ν_{CO} in the FT-IR.

It has been noted that the oxidative addition of HCl to [Rh(Cl)(CO)(PPh₃)₂] gives the complex [RhCl₂(H)(CO)(PPh₃)₂], **39**, whose coupling $^1J(^{103}\text{Rh}-^{31}\text{P})$ in CDCl₃ is 85.9 Hz. **39** gives the same ^{31}P NMR signal as does [Rh(Cl)(CO)(PPh₃)₂] in Fig. 6.1, when **39** is dissolved in [emim][Al₂Cl₇]. One PPh₃ is released from **39** and protonated, while the other PPh₃ is still attached to the rhodium. Also, the formation of the hydride **38** in [emim][Al₂Cl₇] from [Rh(Cl)(CO)(PPh₃)₂], **36**, may suggest that HCl has been oxidatively added to **36**. Accordingly, this result is consistent with the formation of a Rh(III) species in [emim][Al₂Cl₇]. The addition of HCl has been discussed earlier (section 4.2). The presence

of moisture that reacts with chloroaluminate (III) species $[emim][Al_2Cl_7]$ and produces HCl, has also been mentioned.⁸ HCl can react with the Rh(I) centre producing Rh(III).

Any possible Rh(II) complex for **38** was completely discarded because this oxidation state in rhodium is paramagnetic and would give broad and shifted signals in the NMR spectrum.

Note that the elimination of a phosphine from the original bis-PPh₃ complex **39** produces a species with a vacant site where the phosphine originally was. The option **38e** has an empty site. If this occurs, the structure in solution may be that of a trigonal bipyramidal species such as **38e'**. However, in a coordinating environment where Cl^- , $[AlCl_4]^-$ and $[Al_2Cl_7]^-$ are present, such a vacant site in **38e'** may be filled. The first possibility is the addition of a Cl^- from the ionic media, interacting with the Rh centre, producing a Rh(III) anion, such as **38f**.



Interaction of a chloride in **38f** with $AlCl_3$ may produce other possibilities such as **38g** and **38h**. It has been mentioned that $[Al_2Cl_7]^-$ has a lower coordinating ability than the monomer $[AlCl_4]^-$. Then, $[AlCl_4]^-$ may be the most likely ligand in such an environment. The existence of **38g** and **38h** gives a situation already discussed in chapter 5 where the vacant site was filled by $[AlCl_4]^-$ ligands *via* $(\mu-Cl)$ and $(\mu-Cl)_2$ and produces the equilibrium shown in Fig. 6.5 which has already been described.

6. Results and discussion: Carbonylation of rhodium complexes in $[emim][Al_2Cl_7]$

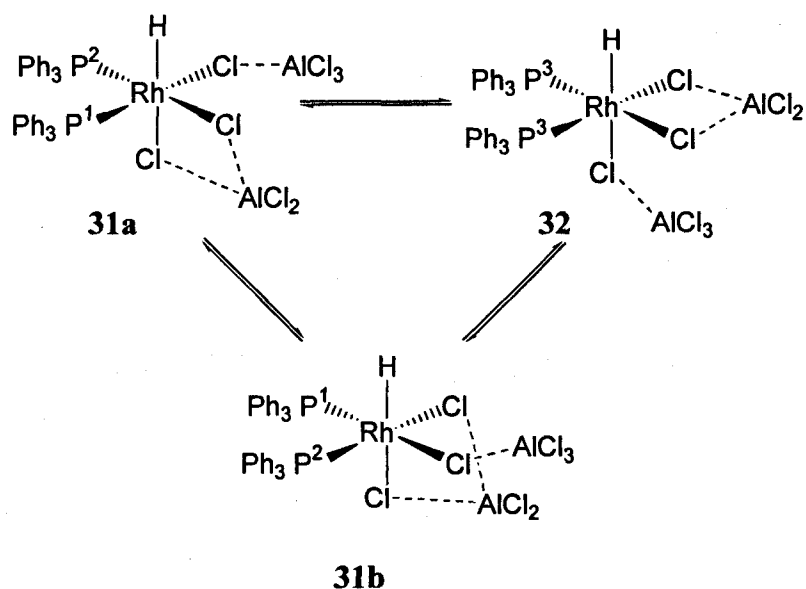


Fig. 6.5. Equilibrium deduced by NMR in solution when $[RhCl(PPh_3)_3]$ is dissolved in $CD_2Cl_2/AlCl_3/HCl$, chapter 5.

Following the same argument as in chapter 5, the possibility of the interaction of $[AlCl_4]^-$ with **38d** also gives three alternative isomers, Fig. 6.6. However, the NMR evidence has shown the presence of only one isomer and this may suggest the instability of the other two. The actual results cannot discard any of the isomers **38g,i-j**.

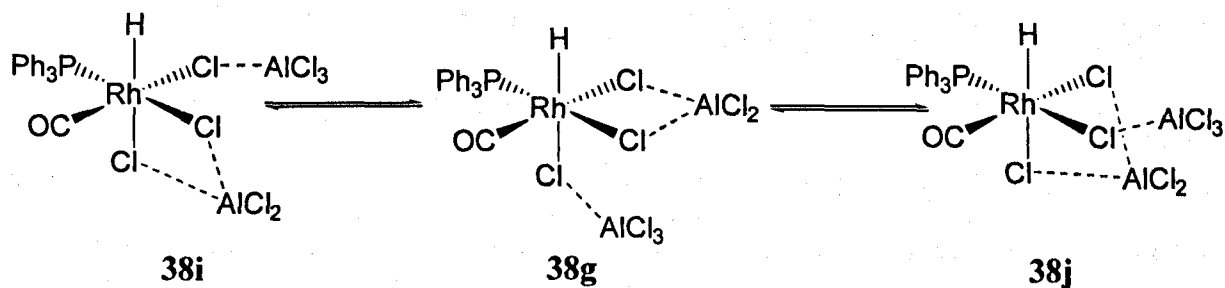
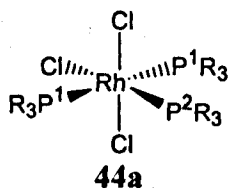


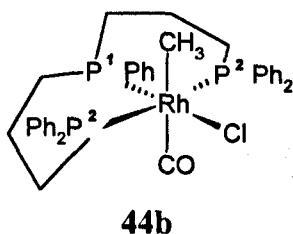
Fig. 6.6. Isomers of **38g** that may exist in accordance with the position of the $[(\mu-Cl)AlCl_3]^-$ and $[(\mu-Cl)_2AlCl_2]^-$ ligand in $[emim][Al_2Cl_7]$.

Some examples of Rh(III) complexes such as *mer*- $[RhCl_3(PR_3)_3]$, **44a**, where $R_3 = Ph_3, Me_3, Et_3, Pr^n_3, Bu^n_3, Me_2Ph, Et_2Ph, Pr^n_2Ph$, have values of coupling $^1J(^{103}Rh-^{31}P^1)$ around 83-84 Hz and $^1J(^{103}Rh-^{31}P^2)$ around 110-115.⁹

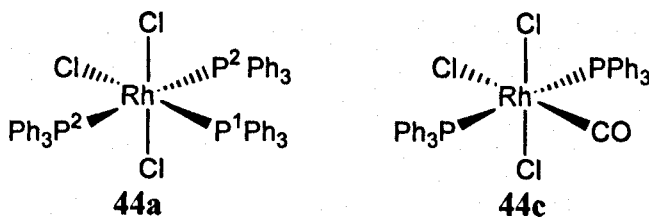


6. Results and discussion: Carbonylation of rhodium complexes in [emim][Al₂Cl₇]

In the case of **38** in [emim][Al₂Cl₇] the $^1J(^{103}\text{Rh}-^{31}\text{P})$ coupling of 105 Hz is large to be an octahedral Rh(III) centre, but the FT-IR spectrum of the solution of **38** in [emim][Al₂Cl₇] shows a band at 2117 cm⁻¹ which is also characteristic of the Rh(III) centre. Also, a coupling $^1J(^{103}\text{Rh}-^{31}\text{P})$ 105 Hz for **38** in [emim][Al₂Cl₇], agrees with known anionic or cationic Rh(III) compounds. For example, the anionic species such as *cis*-[Rh(Cl)₄(CO)(PPh₃)] [NH₂(CH₂CH₃)₂], **28**, has a coupling $^1J(^{103}\text{Rh}-^{31}\text{P})$ 102.3 Hz,¹⁰ and the octahedral cationic species, [Rh(CH₃)(Cl)(ttp)(CO)] [FSO₃], **44b**, has $^1J(^{103}\text{Rh}-^{31}\text{P}^1)$ 108.1 Hz, and $^1J(^{103}\text{Rh}-^{31}\text{P}^2)$ 83.2 Hz.¹¹ This is due to the low *trans*-influence of chlorine which is *trans* to P¹ in **44b**, producing a larger coupling than P².



It is worth noting that in **31-32** the coupling $^1J(^{103}\text{Rh}-^{31}\text{P})$ 136-137 Hz is larger than in **38** in [emim][Al₂Cl₇]. The origin of this difference may be the replacement of a PPh₃ group with a CO. In other words, the reduction of the coupling constant $^1J(^{103}\text{Rh}-^{31}\text{P})$ from 136 Hz in **31-32** to 105 Hz in **38f** or **38g** may be due to the larger electron withdrawing properties of CO. The CO creates a less effective π back donation from rhodium to PPh₃ and hence a reduction of the coupling $^1J(^{103}\text{Rh}-^{31}\text{P})$. This kind of reduction has been observed before in complexes such as **44a** and **44c**. The replacement of a PPh₃ with a CO in **44a** to give **44c** reduces the coupling $^1J(^{103}\text{Rh}-^{31}\text{P})$ from 86 Hz (P²) to 70 Hz,¹² which represents a reduction of 18%; while the reduction from **31-32** to **38** is around 21%. Hence, this reduction in the coupling is consistent with a Rh(III) centre for a hexacoordinated **38**.



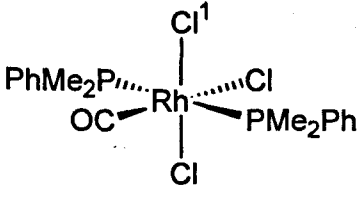
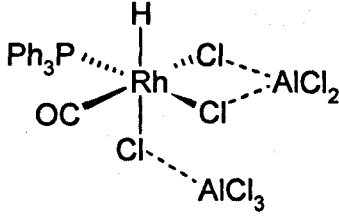
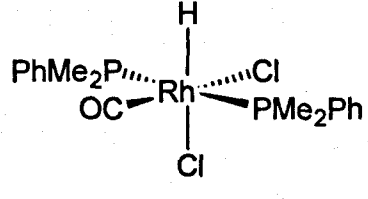
In addition the ³¹P chemical shift for **38** of 52 ppm is more characteristic of Rh(III) complexes as can be seen in Appendix 2. Also, no less important, a Rh(III) complex could

explain the shift ν_{CO} in the FT-IR which is more characteristic for centres with less electron density.⁹

¹⁰³Rh chemical shift can help to support the proposal of a Rh(III) centre. Table 6.3 shows the ¹⁰³Rh chemical shifts for known complexes **45a** and **45b**, with PMe₂Ph as ligand and can be considered as an analogue to PPh₃ ligand, due to the lack of ¹⁰³Rh NMR parameters with PPh₃. It is known that PMe₂Ph can have similar effects in the metal as PPh₃, and the replacement of PMe₂Ph or another group in **38** may not produce a dramatic change in the ¹⁰³Rh δ , then the comparison is valid.

In the first instance, note that the ¹⁰³Rh δ at 945 ppm of **38** in [emim][Al₂Cl₇] is in the range for rhodium compounds in the +3 oxidation state.

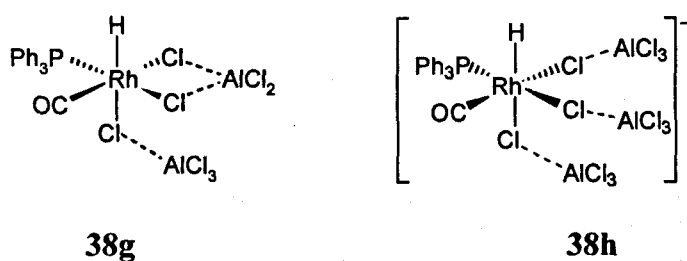
Table 6.3. Comparison in ¹⁰³Rh chemical shifts for Rh(III) known complexes **45a**, **45b** with the proposed structure **38**.

45a	38g	45b
		
1588 ppm	945 ppm	240 ppm

In Table 6.3 it can be seen that the replacement of Cl¹ in **45a** with a hydride that is a strong σ -donor and a strong ligand in the crystal field produces **45b**. The hydride in the last compound produces a large ΔE and a small $(\Delta E_{av})^{-1}$, which directly affects the ¹⁰³Rh δ (see section 6.2.4). Then the signal ¹⁰³Rh δ of **45b** with two chlorides and a hydride appears at lower frequency in comparison with **45a** with three chlorides that produce smaller ΔE_{av} in the last case and then a shift to higher frequency. Now, the replacement of a PMe₂Ph in **45b** for another chlorine, and the interaction with the [emim][Al₂Cl₇], produces **38g** that has a ¹⁰³Rh δ towards high frequency. Such a shift is not as large as for **45a** due to the presence of the hydride and the bridging chlorides in **38g**. Nevertheless the ¹⁰³Rh δ of **38g** is closer to **45a** than to **45b**. Then the addition of $[(\mu\text{-Cl})\text{AlCl}_3]^-$ as ligands in **45b** and the Cl¹ for a hydride to give **38g** does not produce a larger shift towards higher frequencies and it is not

as strong as in **45a** with terminal chlorides. This agrees with a weaker interaction of bridging chlorides in the Rh centre.

Finally, an alternative that was discussed in chapter 5 was the interaction of a monodentate $[(\mu\text{-Cl})\text{AlCl}_3]^-$ and a bidentate $[(\mu\text{-Cl})_2\text{AlCl}_2]^-$ form, **38g**, vs only monodentate, **38h**. The latter case produces only one isomer with terminal $[(\mu\text{-Cl})\text{AlCl}_3]^-$ groups and is consistent with the NMR evidence of only one isomer present in solution, however this cannot be proved with these results.



Further discussions of **38** will imply the structures **38f** or **38g**, although the other alternatives have not been completely rejected. Also, a Rh(III) complex may be a good alternative to elucidate further mechanisms in the next sections. Finally, in order to understand the new chemistry in the ionic liquid similar compounds to **36** with other tertiary phosphines were studied and the next section explains these results.

6.2.3. Solution of $[\text{Rh}(\text{Cl})(\text{CO})(\text{PR}_3)_2]$ in $[\text{emim}][\text{Al}_2\text{Cl}_7]$

In order to compare the reactivity of other systems, the phosphine PPh_3 , was changed in $[\text{RhCl}(\text{CO})(\text{PR}_3)_2]$ for $\text{R}_3 = \text{Me}_2\text{Ph}$, (**45**), Et_3 , (**46**), MePh_2 , (**47**), EtPh_2 , (**48**), Cy_3 , (**49**), Bu^tEt_2 , (**50**), Bu^tBu^n_2 , (**51**), Bu^tPr^i_2 , (**52**), Bu^t_2Ph , (**53**), and each complex was dissolved in the ionic liquid (**54-62**). All of them show a similar result to that for $[\text{RhCl}(\text{CO})(\text{PPh}_3)]$, **36**. All liberate a phosphine from the original compound and show the formation of a hydride, Table 6.5. The liberated phosphine is protonated and the formation of $[\text{HPR}_3]^+$ is observed in every case. $[\text{emim}][\text{Al}_2\text{Cl}_7]$ can extract a phosphine due to the highly acidic medium. Eq. 6.1 shows the possible reaction and all the ^{31}P , ^1H and ^{103}Rh NMR spectra of every solution appear in Appendix 4.

6. Results and discussion: Carbonylation of rhodium complexes in [emim][Al₂Cl₇]

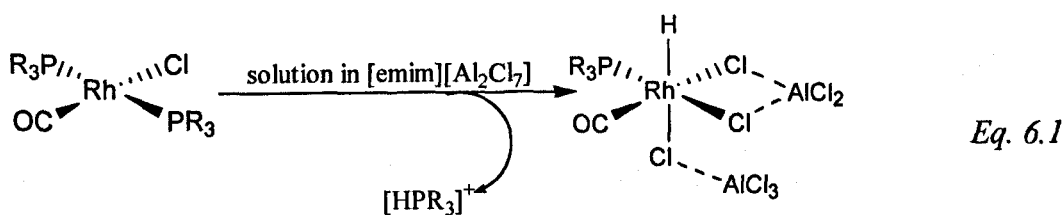


Table 6.4 shows the ³¹P NMR parameters of the complexes observed in [emim][Al₂Cl₇] according to Eq. 6.1. In order to understand the electronic and steric effects involved in [emim][Al₂Cl₇], the values of Δ of the chemical shift of [HPR₃]⁺ in [emim][Al₂Cl₇] and the chemical shift of free PR₃ in organic solvents were plotted, Eq. 6.2. Mann and co-workers,¹³ in an attempt to determine the relationship of the chemical shift of free PR₃ and the chemical shift of the same PR₃ when it is coordinated, firstly proposed a value of Δ in 1971. This value showed clearly a linear relationship of δ free (PR₃) vs Δ in [RhCl(CO)(PR₃)₂] complexes, hence, the same procedure was followed with the solutions in [emim][Al₂Cl₇], to compare the different linearity with the known one in CDCl₃.¹⁰ Mann and co-workers¹³ procedure fits the changes in chemical shifts with Δ in square planar rhodium complexes in the series: i) PEt_nPh_{3-n} and ii) PBuⁿ₂Ph, PBuⁿ₃. There is a change in the magnitude of the coupling. In the first case the magnitude of the coupling increases as the number of n decreases and in the second case the coupling of PBuⁿ₂Ph is larger than PBuⁿ₃. But their work could not explain completely the relationship in the type of bonding of the PR₃ to the metal and the changes in coupling and chemical shift.

The values of δ in [HPR₃]⁺ are determined by both electronic and steric factors, and the values of Δ appear in Table 6.5. The same procedure was followed with the other Rh(III) species observed in [emim][Al₂Cl₇] with different phosphines. All the graphs are shown in Appendix 3. The case of [Rh{(μ-Cl)AlCl₃}{(μ-Cl)₂AlCl₂}(H)(CO)(PR₃)], A, in Fig. 6.8, shows a similar behaviour to the graph in Fig. 6.7.

$$\Delta = \delta[\text{HPR}_3]^+ \text{ ppm in } [\text{emim}][\text{Al}_2\text{Cl}_7] - \delta[\text{PR}_3] \text{ free ppm in organic solvent} \quad \text{Eq. 6.2}$$

Table 6.4. ³¹P{¹H} spectrum parameters for the solution of [Rh(Cl)(CO)(PR₃)₂] in [emim][Al₂Cl₇] according to Eq. 6.1. The letter A corresponds to [Rh{(μ-Cl)AlCl₃}{(μ-Cl)₂AlCl₂}(H)(CO)(PR₃)].

Phosphine	δ ³¹ P of [HPR ₃] ⁺	¹ J(³¹ P- ¹ H) [HPR ₃] ⁺ , Hz	δ ³¹ P of A	¹ J(³¹ P- ¹⁰³ Rh) A	δ ¹⁰³ Rh of A
45b. PMe ₂ Ph	-1.4	497	37.1	98.8	839
54. PEt ₃	22	467	78.0	99	724
55. PMePh ₂	1.9	503	44.0	104.1	874
56. PEtPh ₂	12.3	493	58.5	104.2	868
38. PPh ₃	6.5	505	52.5	108.2	945
57. PBu ^t Et ₂	38.6	456	99.1	101.1	743
58. PBu ^t Bu ⁿ ₂	32.4	459	94.5	101.08	752
59. PBu ⁿ Pr ⁱ ₂	30.9	n.d.	92.9	101.1	750
60. PCy ₃	32.5	443	97.8	102.3	779
61. PBu ^t ₂ Ph	50.8	452	100.0	Broad signal	n.d.

Table 6.5. Delta values for [HPR₃]⁺ in [emim][Al₂Cl₇] and free [PR₃] in organic solvents.

PR ₃	Cone angle	Free PR ₃	δ [HPPH ₃] ⁺ ppm	Δ
45b. PMe ₂ Ph	122°	-47.5	-1.4	46.1
54. PEt ₃	132°	-20.1	22	42.1
55. PMePh ₂	136	-27.6	1.9	29.5
56. PEtPh ₂	140°	-12.3	12.3	24.6
38. PPh ₃	145°	-7.0	6.5	13.5
57. PBu ^t Et ₂	148°	6.8	38.6	31.8
58. PBu ^t Bu ⁿ ₂	147°	-4.3	32.4	36.7
59. PBu ⁿ Pr ⁱ ₂	147°	-8.7	30.9	39.6
60. PCy ₃	170°	37.2	32.5	-4.7
61. PBu ^t ₂ Ph	170°	37.9	50.8	12.9

Bulky phosphines with t-butyl groups follow one linearity while less constrained phosphines with small Me and Et groups follow another linearity. The higher the cone angles the higher the frequency for free PR₃ group and the more positive value for δ in [HPR₃]⁺ and for Δ. Note that ¹J(³¹P-¹H) coupling is observed in every case, for every [HPR₃]⁺ species, Table 6.4. This shows that the chemical shift for each protonated group is a real shift for the protonated species and not equilibrium acid/base between the two species [HPR₃]⁺/PR₃.

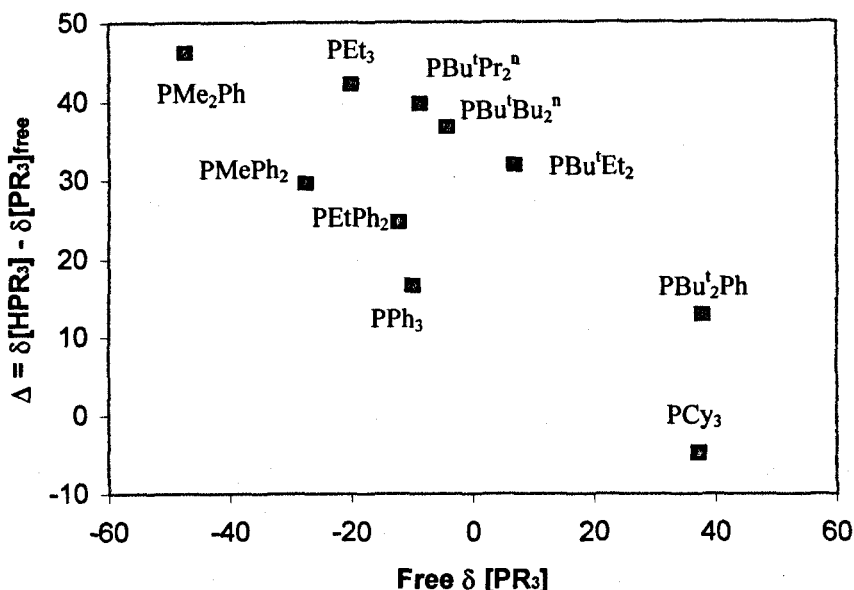


Fig. 6.7. The graph shows the correlation of Δ of $[\text{HPR}_3]^+$ (Eq. 6.2.) vs the ^{31}P δ of free PR_3 in organic solvents (Table 6.5).

Table 6.4 shows the ^{31}P NMR values for the observed rhodium complexes $[\text{Rh}\{(\mu\text{-Cl})\text{AlCl}_3\}\{(\mu\text{-Cl})_2\text{AlCl}_2\}(\text{H})(\text{CO})(\text{PR}_3)]$, A in $[\text{emim}][\text{Al}_2\text{Cl}_7]$. The structure in solution for these complexes may be considered as analogues to structure 38g. A similar procedure, using Δ values of A vs free PR_3 , appears in Fig. 6.8. In the last case, Δ corresponds to ^{31}P δ of A minus the value of ^{31}P δ of free PR_3 in organic solvents. The plot in Fig. 6.8 shows a similar behaviour to that in Fig. 6.7. Bulky phosphines are in a certain region, while less constrained alkyl groups in the phosphine produce a smaller value of Δ . The Δ for PEt_3 in the complex $[\text{Rh}\{(\mu\text{-Cl})\text{AlCl}_3\}\{(\mu\text{-Cl})_2\text{AlCl}_2\}(\text{H})(\text{CO})(\text{PEt}_3)]$ is similar to that in Fig. 6.7. This can be a result of basicity. However, a more detailed study with other kinds of PR_3 groups would produce a conclusive result.

Also, in order to have further evidence of the oxidation state of the complexes the synthesis of $[\text{Rh}(\text{Cl})_2(\text{H})(\text{CO})(\text{PR}_3)_2]$ was carried out. It is known that the simple oxidative addition of HCl to the metallic centre in $[\text{RhCl}(\text{CO})(\text{PR}_3)_2]$ generates compounds already characterized by elemental analysis and IR.¹⁴ In the absence of NMR parameters, Table 6.6 shows $^{31}\text{P}\{^1\text{H}\}$ NMR parameters of $[\text{Rh}(\text{Cl})_2(\text{H})(\text{CO})(\text{PR}_3)_2]$ complexes in solution (38, 45c, 62-67). The complete ^{31}P NMR and ^1H NMR parameters are shown in Appendix 3.



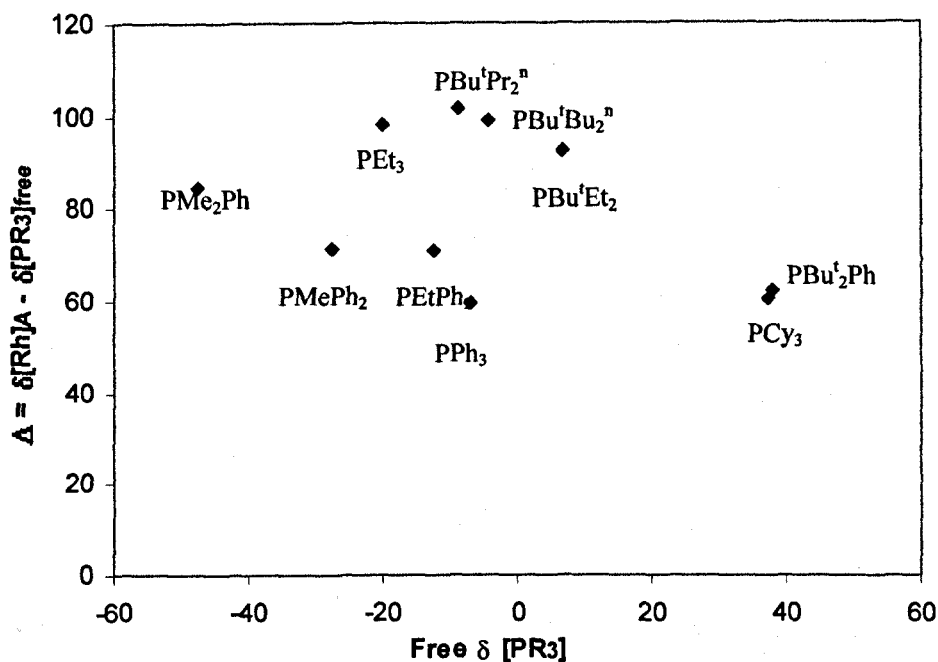


Fig. 6.8. This graph shows the correlation of Δ of Rh complexes vs the frequency of free PR_3 in organic solvents: Complex $[\text{Rh}\{(\mu\text{-Cl})\text{AlCl}_3\}\{(\mu\text{-Cl})_2\text{AlCl}_2\}(\text{H})(\text{CO})(\text{PR}_3)]$ in $[\text{emim}][\text{Al}_2\text{Cl}_7]$.

Table 6.6. $^{31}\text{P}\{^1\text{H}\}$ parameters for $[\text{RhCl}_2(\text{H})(\text{CO})(\text{PR}_3)_2]$ in CDCl_3 . The compounds **58** and **59** with $\text{PR}_3 = \text{PBu}'_2\text{Ph}$ and $\text{PBu}'_2\text{Pr}^i$ respectively do not react with HCl.

Phosphine	$\delta^{31}\text{P}\{^1\text{H}\}$, ppm ^a	$^1J(^{103}\text{Rh}-^{31}\text{P})\text{Hz}$
45c PMe ₂ Ph	3.5	80.2
62 PEt ₃	26.5	80.1
63 PMePh ₂	18.7	83.9
64 PEtPh ₂	25.1	82.9
38 PPh ₃	25.3	85.9
65 PBu ¹ Et ₂	44.6	80.0
66 PBu ¹ Bu ₂ ⁿ	40.6	79.9
67 PCy ₃	35	79.3

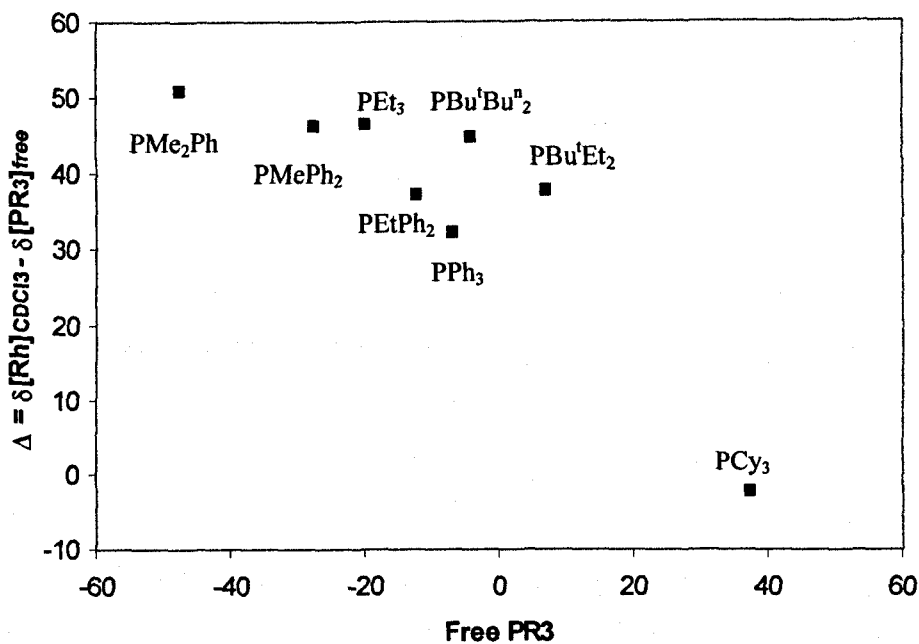


Fig. 6.9. This graph shows the correlation of Δ for the complexes $[\text{Rh}(\text{Cl})_2\text{H}(\text{CO})(\text{PR}_3)_2]$ in CDCl_3 vs free PR_3 in organic solvents.

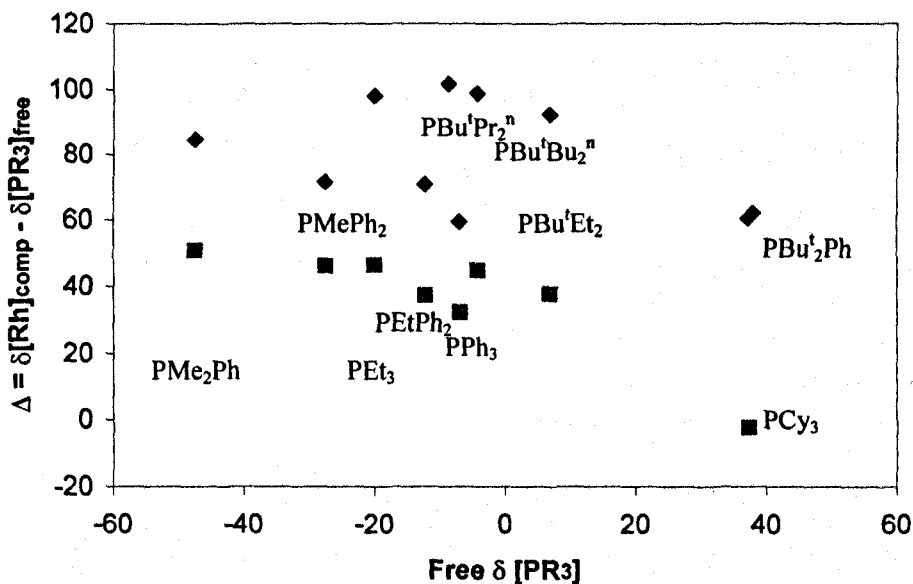


Fig. 6.10. This graph shows a direct comparison of the correlations of Δ of: \blacklozenge Complex A $[\text{Rh}\{(\mu\text{-Cl})\text{AlCl}_3\}\{(\mu\text{-Cl})_2\text{AlCl}_2\}(\text{H})(\text{CO})(\text{PR}_3)]$ in [emim][Al₂Cl₇] Fig. 6.8. and \blacksquare complexes $[\text{Rh}(\text{Cl})_2\text{H}(\text{CO})(\text{PR}_3)_2]$ in CDCl_3 Fig. 6.9.

Note that the ³¹P chemical shifts of complexes A in [emim][Al₂Cl₇] are larger than the complexes in CDCl₃. This can be the result of a weaker *trans*-influence of bridging Cl⁻ in [(μ-Cl)AlCl₃]⁻. They produce a stronger interaction of Rh-P, increasing the ¹J(¹⁰³Rh-³¹P) that has been discussed and increasing the chemical shift of the phosphorus in PR₃.

Note that Rh(III) compounds such as [RhH(Cl)₂(CO)(PR₃)₂] in Table 6.6 have smaller ¹J(¹⁰³Rh-³¹P) values than their respective complex A, [Rh{(μ-Cl)AlCl₃}{(μ-Cl)₂AlCl₂}(H)(CO)(PR₃)], in [emim][Al₂Cl₇]. The values of ¹J(¹⁰³Rh-³¹P) couplings in Table 6.6 are more characteristic for Rh(III) complexes, while the values in Table 6.4 are not. Complexes [Rh(Cl)₂H(CO)(PR₃)₂] with PR₃ = PMe₂Ph, PEtPh₂, PPh₃ and PCy₃, **45b**, **64**, **38**, **67** shown in Table 6.6 were dissolved in [emim][Al₂Cl₇]. They gave the compound [Rh{(μ-Cl)AlCl₃}{(μ-Cl)₂AlCl₂}(H)(CO)(PR₃)] with the respective phosphine, the same complex as [Rh(Cl)(CO)(PR₃)₂] with the respective phosphine, **45d**, **55**, **39**, **60** in [emim][Al₂Cl₇]. This reaction is depicted in Fig. 6.4 but Fig. 6.11 explains with more clarity. These results show that the ionic liquid may initially produce Rh(III) centres and the interaction with coordinating chloroaluminate (III) anions gives the formation of different structures that have not been observed before. The formation of complexes A from a Rh(III) species may be further evidence that the compounds observed in [emim][Al₂Cl₇] are Rh(III).

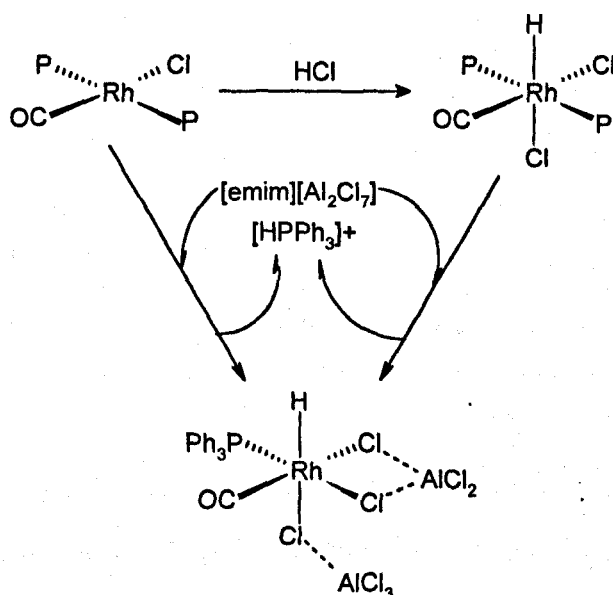


Fig. 6.11. Formation of $[\text{Rh}\{(\mu\text{-Cl})\text{AlCl}_3\}\{(\mu\text{-Cl})_2\text{AlCl}_2\}(\text{H})(\text{CO})(\text{PR}_3)]$ in $[\text{emim}][\text{Al}_2\text{Cl}_7]$ from two sources, Rh(I) and Rh(III). This reaction was found with $\text{P} = \text{PMe}_2\text{Ph}$, **45d**, PEtPh_2 , **55**, PPh_3 , **39** and PCy_3 , **60**.

Complexes **39**, **45c** and **54-61** are impossible to isolate from [emim][Al₂Cl₇] but the presence of a hydride in the complexes enables the application of the ¹⁰³Rh{INEPT} NMR pulse sequence and the analysis of the ¹⁰³Rh frequencies allows the study to determine the oxidation state in the metal and the results are shown in the next section.

6.2.4. ¹⁰³Rh {INEPT} NMR data

Sections 4.2 and 6.1 have shown the results of ¹⁰³Rh NMR chemical shift for [Rh(H){(μ-Cl)AlCl₃}(PPh₃)₂]⁻, **24**, and [Rh{(μ-Cl)AlCl₃}{(μ-Cl)₂AlCl₂}(H)(CO)(PPh₃)₂], **38**, respectively. The chemical shift of samples are referenced to Ξ = 3.16 MHz.¹⁵ Table 6.1 shows the results for all solutions of [Rh(Cl)(CO)(PR₃)₂] in [emim][Al₂Cl₇]. The addition of a hydride and the reduction of the coupling constant from 125-130 Hz in the original material to 100-115 Hz in [emim][Al₂Cl₇] suggests the formation of a Rh(III) centre and here the ¹⁰³Rh NMR results suggest the same oxidation state of the Rh complexes. All the ¹⁰³Rh spectra are shown in Appendix 4 and Table 6.2 shows the ¹⁰³Rh chemical shift of each solution.

The INEPT pulse sequence allows enhancement of the ¹⁰³Rh signal due to polarization transfer from ¹H. The pulse sequence is:¹⁶

$$\begin{array}{cccccccc}
 {}^1\text{H} & D_1 & 90_x & \tau & 180_x & \tau & 90_y & \\
 {}^{103}\text{Rh} & & & & 180_x & \tau & 90_x & \text{aq}
 \end{array}$$

Where $D_1 = 2T_1$ and $\tau = [4J]^{-1}$.

The variation in nuclear shielding of transition metal nuclei such as ¹⁰³Rh is mainly determined by the paramagnetic contribution σ^p to the overall shielding, which may, according to the Ramsey equation, Eq. 6.4, be described by changes in the average excitation energy, ΔE_{av} , the *d*-orbital radius, $\langle r_d^{-3} \rangle$, and the angular imbalance of charge, ΣQ_N .⁶ ΔE_{av} is the average energy difference between filled and empty '*d*' orbital, and '*r_d*' is the average radius of a valence level *d*-orbital. ΔE_{av} is influenced by weak/strong properties of ligands and increases according to the spectrochemical series; '*r_d*' is influenced by hard/soft properties and increases according to the nephelauxetic series.¹⁷ Weak hard ligands cause a shift in ¹⁰³Rh δ to high δ , and strong soft ligands cause a shift to low δ . For weak soft

ligands, where the two effects oppose each other, and for ligands that occupy a position towards the middle of each scale, such as pyridine, the influence on ¹⁰³Rh δ may be difficult to predict. In general, for π-coordinating ligands, the $\langle r_d^{-3} \rangle$ term is dominant and for strong-field ligands the ΔE_{av}^{-1} term is dominant.

$$\sigma = \sigma^d - \sigma^p = A - c(\Delta E_{av})^{-1} \langle r_d^{-3} \rangle \Sigma Q_N \quad \text{Eq. 6.4}$$

The ligand field splitting term, ΔE_{av} , becomes larger as the number of phenyl groups in a PR₃ increases. Small changes in their structure will be reflected in the ¹⁰³Rh chemical shift. The terms ΔE_{av} and $\langle r_d^{-3} \rangle$ are closely related in the present series of **38**, **45b**, **54-61** and govern the magnitude of σ^p and hence it may for qualitative purposes be referred for comparison within this series.

Table 6.7 shows the ¹⁰³Rh δ for some known Rh(I) carbonyl complexes and it is clear that the chemical shift range for this rhodium oxidation state is below 0 ppm. In addition, the introduction of a hydride into the coordination sphere decreases the chemical shift toward lower frequency.

Table 6.7. NMR chemical shifts for known Rh(I) complexes.

Complex	δ (¹⁰³ Rh) ppm	Ref.
10 [RhCl(PPh ₃) ₃]	-81	18
10a [RhBr(PPh ₃) ₃]	-142	17
36 [RhCl(CO)(PPh ₃) ₂]	-368	17
36a [RhCl(CO)(PMe ₂ Ph) ₂]	-405	10
36b [Rh(H)(CO) ₂ (dppe)]	-1073	5

Table 6.8 shows ¹⁰³Rh δ of some monocarbonyl Rh(III) compounds. The region of the chemical shift of these complexes is in the region of the chemical shift of **45b**, **54-61**, as is expected for Rh(III) compounds containing ligands of intermediate to weak ligand field for the octahedral geometry.

Table 6.8. Chemical shifts of monocarbonylrhodium (III) complexes.⁹

Complex	δ (^{103}Rh) ppm
45d $[\text{Rh}(\text{Cl})(\text{I})(\text{CF}_3)(\text{CO})(\text{PMe}_2\text{Ph})_2]$	706
45e $[\text{Rh}(\text{Br})(\text{I})(\text{CF}_3)(\text{CO})(\text{PMe}_2\text{Ph})_2]$	625
45f $[\text{Rh}(\text{I})_2(\text{CF}_3)(\text{CO})(\text{PMe}_2\text{Ph})_2]$	453
45a <i>mer-trans</i> - $[\text{Rh}(\text{Cl})_3(\text{CO})(\text{PMe}_2\text{Ph})_2]$	1588
45c <i>trans</i> - $[\text{Rh}(\text{Cl})_2(\text{H})(\text{CO})(\text{PMe}_2\text{Ph})_2]$	240

It is worth noting in Table 6.8 that increasing the atomic number of the halides decreases the chemical shift from $\text{I} > \text{Br} > \text{Cl}$ (towards low frequency) due to a larger ΔE in heavier halides, then for **45d** > **45e** > **45f**. A replacement of chloride by a hydride from **45a** to **45c** produces a dramatic decrease in the chemical shift. The hydride produces a high ΔE_{av} , hence $(\Delta E_{av})^{-1}$ is smaller and the chemical shift goes to lower frequency. This explains the large change from **45a** (1588 ppm) \gg **45c** (204 ppm) due to a decrease of $(\Delta E_{av})^{-1}$.

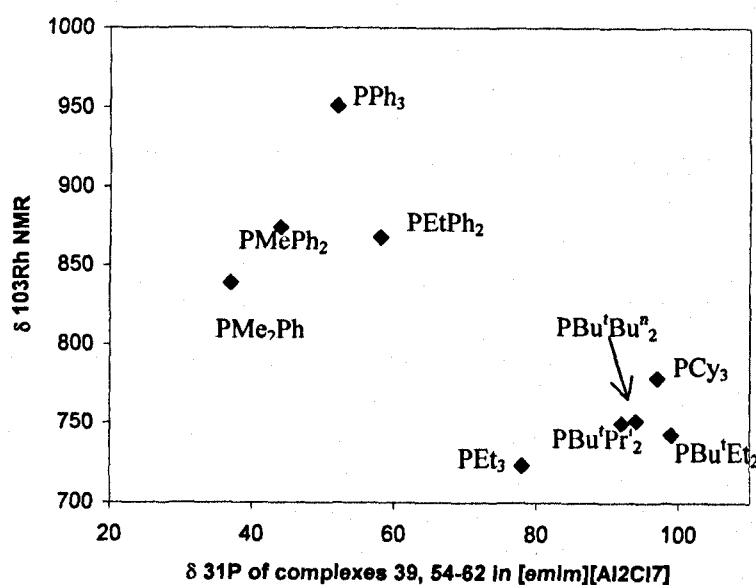


Fig. 6.12. ^{103}Rh chemical shift vs $\delta^{31}\text{P}$ of $[\text{Rh}\{(\mu\text{-Cl})\text{AlCl}_3\}\{(\mu\text{-Cl})_2\text{AlCl}_2\}(\text{H})(\text{CO})(\text{PPh}_3)_2]$ in $[emim][Al_2Cl_7]$.

From Fig. 6.12, it is clear that the linearity of the complex with small PR_3 is different to the linearity with bulky PR_3 . The same behaviour was observed in the graph of Fig. 6.7, and here the position of the complex with PEt_3 is unusual and would be expected to be closer to the smaller phosphines such as PEtPh_2 , PMe_2Ph and PMePh_2 . The result of PEt_3 may be a combination of cone angle and basicity. Analysing the line with small phosphines

in Fig. 6.8 it is clearly observed that the ¹⁰³Rh shift decreases in the order PMe₂Ph > PMePh₂ > PPh₃ due to stronger π acidity of Ph groups in phosphines.

The phenyl groups increase the back donation from the metal to the phosphines and make the separation ΔE_{av} larger, hence (ΔE_{av})⁻¹ smaller and the ¹⁰³Rh shift appears at lower frequency. Also, a simple argument would be with a simple approximation of shielding and screening: the π back donation from the rhodium to the phosphine due to the presence of phenyls groups in the PR₃ decreases the shielding in the metallic centre and produces a higher chemical shift of the metal. Contrarily, PR₃ with bulky alkyl substituents, Fig. 6.8, present smaller chemical shifts than phenylphosphines due to higher σ donation to the Rh centre. This allows shielded rhodium centres, hence these appear at lower ¹⁰³Rh δ. It means that there is a direct relation between the shielding in ¹⁰³Rh nuclei and the coupling constant ¹J(¹⁰³Rh-³¹P) in the complexes and Fig. 6.13 shows the graph of ¹⁰³Rh chemical shifts of complexes [Rh{(μ-Cl)AlCl₃}{(μ-Cl)₂AlCl₂}(H)(CO)(PR₃)₂] in [emim][Al₂Cl₇] vs their coupling Rh-P, where the linear relationship is clearly observed.

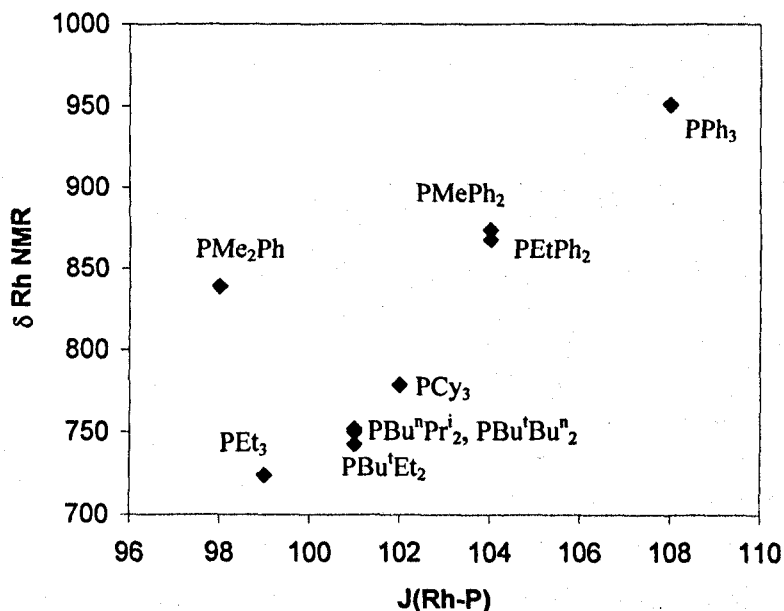


Fig. 6.13. Determination of linearity ¹⁰³Rh chemical shift vs coupling constant ¹J(¹⁰³Rh-³¹P) in Hz of [Rh{(μ-Cl)AlCl₃}{(μ-Cl)₂AlCl₂}(H)(CO)(PR₃)₂] in [emim][Al₂Cl₇].

Finally, it can be seen that the ¹⁰³Rh NMR data are further evidence in determining the oxidation state in Rh and support the proposal of Rh(III) in [emim][Al₂Cl₇] for complexes [Rh{(μ-Cl)AlCl₃}{(μ-Cl)₂AlCl₂}(H)(CO)(PR₃)₂].

Subsequent reactions were carried out and carbonylation of such compounds did give an idea of the reactivity of these complexes. The next section shows the results when **38f** reacts with CO and the partial identification of the formed complex by ³¹P, ¹³C and 2D NMR spectroscopy. This gives a clear understanding of the product in the carbonylation of *trans*-[Rh(H){(μ-Cl)AlCl₃}(PPh₃)₂]⁻, **25**, and the structure in solution of the complex **37**, in Fig. 6.1.

6.3. Carbonylation of [Rh(Cl){(μ-Cl)₂AlCl₂}(CO)(H)(PPh₃)], **38**, in [emim][Al₂Cl₇], *x*_{AlCl₃} = 0.67

When CO is passed through the solution of **38** in [emim][Al₂Cl₇], the ³¹P NMR spectrum changes completely to two doublets: at 22.5 ppm, ¹J(¹⁰³Rh-³¹P) 107.5 Hz, **37**, and 38.5 ppm, ¹J(¹⁰³Rh-³¹P) 123.2 Hz., **68**, Fig. 6.14a. Compound **37** was observed earlier, when [Rh(Cl){(μ-Cl)AlCl₃}(PPh₃)₂]⁻, **24**, was treated with CO (section 6.1). The FT-IR spectrum in the region of ν_{CO} gives the initial signal at 2117 cm⁻¹ for **38g** and two broad signals at 2089 and 2091 cm⁻¹. The reaction of **38** with ¹³CO enhanced the ¹³C NMR signals in the carbonyl area and this experiment can show the number of carbonyls attached to the metallic centre. The phosphorus NMR spectra was recorded when ¹³CO was passed through the solution, Fig. 6.14b. The signal for **37** with ¹³CO is clearly broader in 6.14b than in 6.14a when ¹²CO is used. This suggests the presence of a dynamic process in the solution. The high viscosity of [emim][Al₂Cl₇] does not permit clear resolution of the signals when the temperature is decreased. The addition of CD₂Cl₂ to the solution decreases the viscosity and permits decreasing the temperature to -40°C. ³¹P{¹H} and ¹³C{¹H} NMR of the region of compound **37** at this temperature is shown in Fig. 6.15.

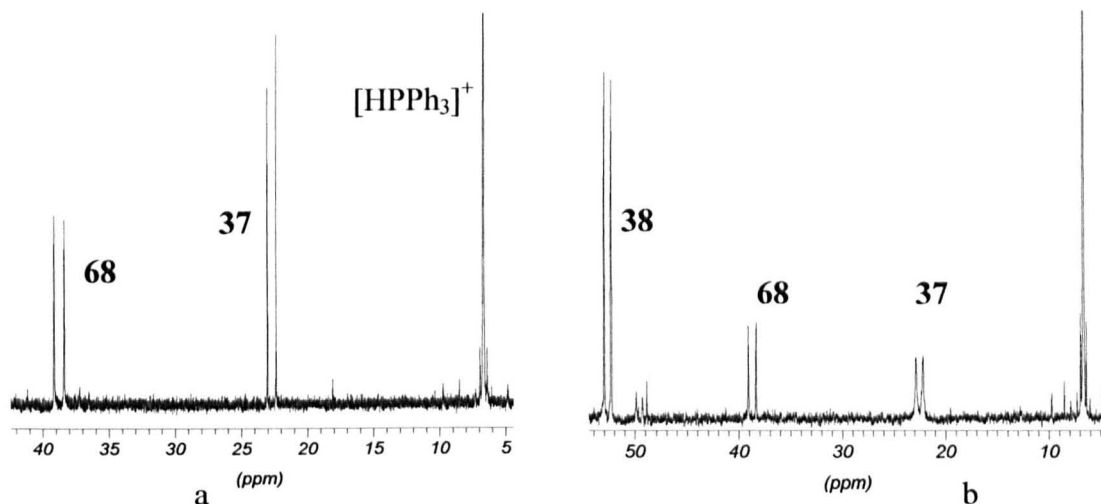


Fig. 6.14. 162 MHz $^{31}\text{P}\{^1\text{H}\}$ NMR of the reaction of $[\text{Rh}\{\mu\text{-Cl}\text{AlCl}_3\}\{\mu\text{-Cl}\}_2\text{AlCl}_2\}\text{(H)(CO)(PPh}_3)]$ in $[emim][\text{Al}_2\text{Cl}_7] \cdot x\text{AlCl}_3 = 0.67$ with a) ^{12}CO and b) ^{13}CO .

The ^{31}P NMR spectrum shows a large coupling at 22.7 ppm $^1J(^{103}\text{Rh}\text{-}^{31}\text{P})$ 107.5 Hz, as well as two smaller couplings to two different carbonyls: $^2J(^{31}\text{P}\text{-}^{13}\text{C}_{\text{trans}})$ 87.7 Hz, $^2J(^{31}\text{P}\text{-}^{13}\text{C}_{\text{cis}})$ 15 Hz, Fig. 6.15a. ^{13}C NMR spectrum shows C^1 which is *trans* to PPh_3 , δ 178.1 ppm, $^1J(^{103}\text{Rh}\text{-}^{13}\text{C}_{\text{trans}})$ 54.9 Hz, $^2J(^{31}\text{P}\text{-}^{13}\text{C}_{\text{trans}})$ 88.5 Hz; C^2 *cis* to PPh_3 , δ 180.2 ppm, $^1J(^{103}\text{Rh}\text{-}^{13}\text{C}_{\text{cis}})$ 64.9 Hz, $^2J(^{31}\text{P}\text{-}^{13}\text{C}_{\text{cis}})$ 15.1 Hz, Fig. 6.15b.

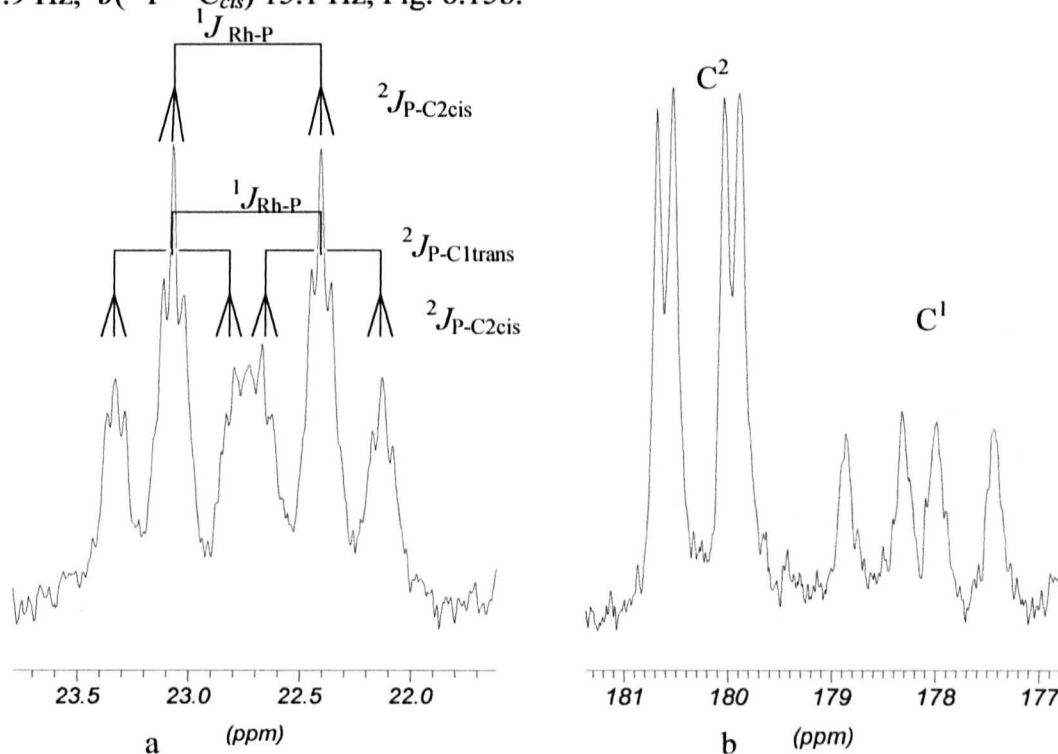
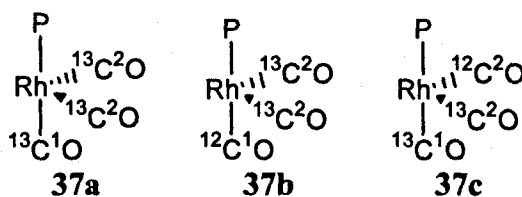


Fig. 6.15. NMR spectra for the expansion of key signals of compound 37 at -40°C , 233K: a) 162MHz $^{31}\text{P}\{^1\text{H}\}$ NMR, all the couplings are explained, see text for values; b) 100 MHz $^{13}\text{C}\{^1\text{H}\}$ NMR.

The integration of C¹ and C² correspond to 1:2 respectively in the ¹³C NMR signals. The spectrum shows a carbonyl *trans* to PPh₃ and two carbonyls *cis* to phosphine. The starting material contains ¹²CO and the reaction with ¹³CO produces the isotopic isomers **37a-c**. The signals with lower intensity correspond to the fully enriched product with ¹³CO *trans* to P, **37a**, while the signals with higher intensity correspond to the partially enriched product **37b**. The signal for **37a** is quite broad suggesting the presence of the partially enriched product with ¹²CO in an equatorial position, **37c**. In addition, this broadness is a result of high viscosity in the ionic solution even with the addition of CD₂Cl₂.



In order to get more conclusive results, the carbonylation of the 60% enriched [Rh(Cl)(¹³CO)(PPh₃)₂] in the ionic liquid was carried out. In such a case the addition of 0.4 mL of CD₂Cl₂ to 0.3 mL of [emim][Al₂Cl₇] with enriched **37a-c** was studied. The addition of a larger quantity of organic solvent to the ionic solution decomposes **37**. The importance of a high concentration of chloroaluminate (III) and the low stability of such compounds in common organic solvents can be concluded with the addition of more organic solvent. ³¹P NMR and ¹³C NMR of such a solution is shown in Fig. 6.16. The splitting of the signals in both spectra is much clearer and better resolved than in Fig. 6.15. The first thing to note is the higher intensity of the fully enriched product with respect to the partially enriched complex.

The ³¹P{¹H} NMR at -43°C showed well resolved coupling of the signals for **37a-c**. This spectrum clearly showed the coupling of only one phosphine to three carbonyls (Fig. 6.15); δ = 22.5 ppm, **37a**, ¹J(¹⁰³Rh-³¹P) 107.5 Hz, ²J(³¹P-¹³C_{*trans*}) 86.8 Hz, ²J(³¹P-¹³C_{*cis*}) 15.0 Hz. The enrichment is not 100% and all the isotopic isomers, where ¹²CO is in the *trans* (**37b**) and one of the *cis* positions (**37c**) to the phosphine, are clearly observed.

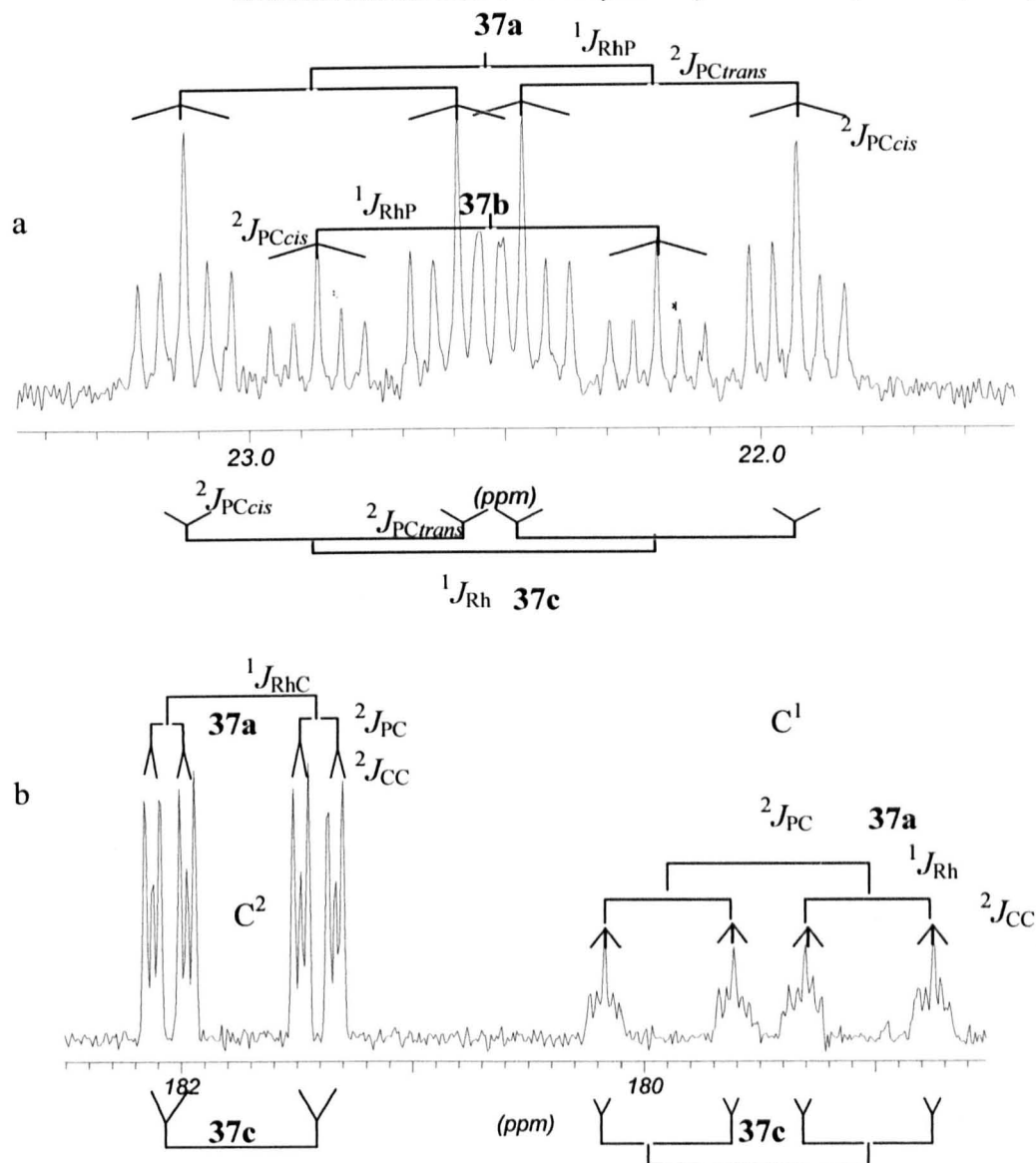


Fig. 6.16. NMR spectra at -43°C (230K) of the solution of carbonylation of **37** in [emim][Al₂Cl₇]/CD₂Cl₂, 0.3:0.4 mL respectively. a) 162MHz $^{31}\text{P}\{^1\text{H}\}$ NMR; b) 100 MHz $^{13}\text{C}\{^1\text{H}\}$ NMR.

$^{13}\text{C}\{^1\text{H}\}$ NMR shows the presence of three carbonyls (**37**), two *cis*-equatorial to phosphine and one axial which is *trans* to phosphine: δC^1 *trans* 179.4 ppm; $^2J(^{31}\text{P}-^{13}\text{C}^1)$ 86.8 Hz, $^1J(^{103}\text{Rh}-^{13}\text{C}^1)$ 55.9 Hz, $^2J(^{13}\text{C}^1-^{13}\text{C}^2)$ 6.5 Hz; δC^2 *cis* 181.7 ppm, $^1J(^{103}\text{Rh}-^{13}\text{C}^2)$ 54.4 Hz; $^2J(^{31}\text{P}-^{13}\text{C}^2)$ 15.0 Hz; $^2J(^{13}\text{C}-^{13}\text{C})$ 6.5 Hz. The isotopic isomers **37a** (dd at 181.5ppm, and ddd, at 179.4 ppm) are observed. The ^{13}C NMR shows *cis* C-C coupling clearly in Fig. 6.16b, while this coupling was not well resolved when the raw material was not enriched as in Fig. 6.15b, where only broad signals were observed. There are some reasons that may produce such broadness in Fig. 6.15b: i) the low concentration of CD₂Cl₂ added in Fig. 6.14 is not

enough to decrease the large viscosity of the ionic liquid at that temperature and produce broad signals; ii) the temperature in Fig. 6.15 may not be as low as the spectrum in Fig. 6.16 due to errors in the measurement of temperature in the NMR equipment. One or a combination of these causes can be the reason of broadness and poorly resolved signals in Fig. 6.15.

The presence of broad signals at room temperature suggests fluxionality. 2D ¹³C-¹³C EXSY NMR spectrum was recorded at -48°C and it showed the ¹³C-¹³C exchange rate for this compound and gave an idea about the exchange mechanism, Fig. 6.17. Such an experiment uses a 2D phase sensitive NOESY sequence and it is useful to predict the rearrangements in molecules.¹⁹ In the spectrum in Fig. 6.17 it is shown that the signal at δ 182.1 (1) correlates with δ 179.3 (7); the signal at δ 181.9 (2) correlates with the signal at δ 180.1 (5); the signal at δ 181.4 (3) correlates with δ 178.7 (8); the signal at δ 181.3 (4) correlates with δ 179.6 (6). Exchange from C¹ to C² gave a rate of 5.64 ± 0.2 s⁻¹ that corresponds to ΔG[‡]₂₅₄ = 58 kJ mol⁻¹.

Note that the *trans* coupling ²J(³¹P-¹³C) has been given as absolute value |²J(³¹P-¹³C)|. Absolute signs for coupling constants are often based on the well-founded assumption that all values of ¹J(¹³C-¹H) are positive, and in general that any ¹J(X-Y) is positive and ²J(X-Y) is negative.²⁰ Relative signs of coupling constants can be measured by double resonance methods²¹ but absolute signs are more difficult to obtain experimentally. It is known that homonuclear and heteronuclear coupling constants are sensitive to the electronic structure of bonded atoms and molecular geometry in terms of dihedral angles,²² the magnitude of coupling constants can provide information about the stereochemistry of metal complexes, oxidation state and coordination geometry of the central metal atom, as all this work has shown.²³ Field and co-workers have established that in six coordinate iron(II) phosphine complexes the relative magnitude of ³¹P-³¹P coupling constants are as follows: *trans*-²J(³¹P-³¹P) > *cis*-²J(³¹P-³¹P) and *trans*-²J(³¹P-³¹P) with opposite sign to *cis*-²J(³¹P-³¹P).²⁴ Similar trends were apparent in heteronuclear coupling constants *cis/trans*-²J(³¹P-¹H) in a series of octahedral Fe and Ru hydrido phosphine complexes.²⁵ The use of a 2D NMR experiment was used to measure magnitude and relative signs of the ³¹P-¹H, ³¹P-³¹P and ¹³C-¹H coupling constants in the mentioned series of iron and ruthenium hydrides.

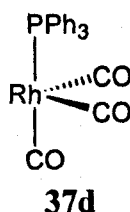
The relative signs of homonuclear and heteronuclear coupling constants have been established only for a limited number of organometallic complexes.²⁶ The relative

magnitudes of ${}^2J(^{13}\text{C}-^1\text{H})$ in octahedral Rh compounds have been measured in few reports²⁷ and more recently the relative signs of the coupling $\text{cis-}{}^2J(^{31}\text{P}-^{13}\text{C})$ has been assigned as positive,³ using PMe_3 as reference, in which ${}^1J(^{13}\text{C}-^1\text{H}) > 0$ and ${}^1J(^{13}\text{C}-^{31}\text{P}) < 0$ have been established.²⁸ Then, a rough assignment can be done by assuming that $\text{cis-}{}^2J(^{31}\text{P}-^{13}\text{C})$ in **37** has opposite signs than $\text{trans-}{}^2J(^{31}\text{P}-^{13}\text{C})$ and this is consistent with the literature.

By definition a positive sign implies that the coupling interaction stabilises anti-parallel rather than parallel spins, i.e. the term $J_{AB}m_A m_B$ in the equation $E_{\text{h}}^{-1} = -\sum \nu_A m_A + \sum J_{AB} m_A m_B$ is negative when m_A and m_B have opposite signs. In the present case, the relative sign of the value of trans coupling ${}^2J(^{31}\text{P}-^{13}\text{C})$ was not carried on and the relative value was considered for qualitative analysis. Signs are very important for theoretical interpretation of coupling constants, and conversely theory can give signs with confidence in favourable cases.

The spectrum in Fig. 6.17 shows only cross peaks associated with the retention of the ${}^{31}\text{P}$ and ${}^{103}\text{Rh}$ spin state, which suggests an intramolecular mechanism. Similar to section 6.2, the structure of **37** in [emim][Al₂Cl₇] was deduced by comparison with known Rh complexes and a suitable mechanism for hexacoordinated Rh(III) and Rh(I) trigonal bipyramidal is discussed below.

NMR resonance agrees with a structure that has been mentioned as a tricarbonylmonophosphine rhodium with a CO *trans* to PPh_3 and the other two CO groups, *cis* to PPh_3 as structure **37d** shows. According to the last structure, two geometries can be discussed: i) hexacoordinated Rh(III) or ii) Rh(I) structure where pentacoordinated or square planar. The next section discusses these alternatives.



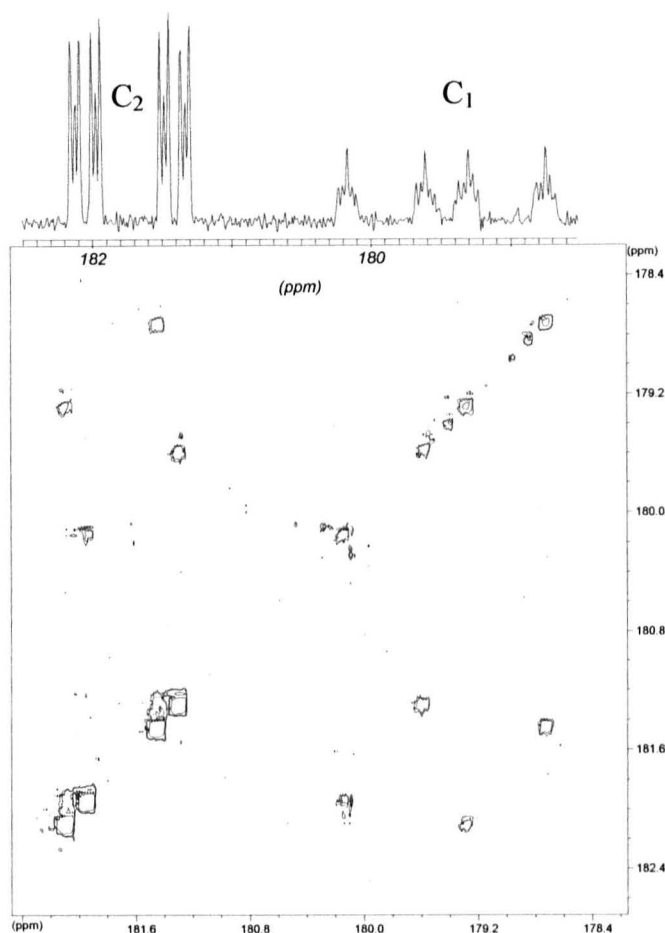


Fig. 6.17. ^{13}C EXSY spectrum for $[Rh_1(\mu-Cl)AlCl_3\{CO\}_3(PPh_3)]^+$ **37**, in $[emim][Al_2Cl_7]/CD_2Cl_2$ 1:1 at $-48^\circ C$.

6.3.1. Hexacoordinated Rh(III) complex, an alternative for **37**

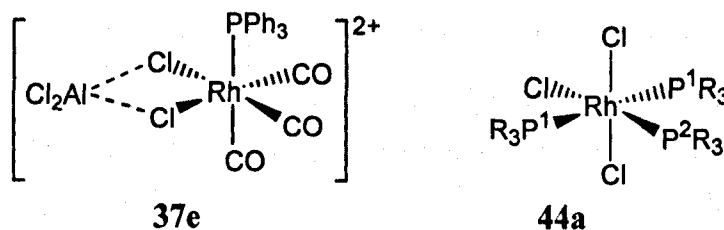
The presence of a PPh_3 and three carbonyls may suggest an octahedral structure interacting with the chloroaluminate (III) anions. Coupling constants $^1J(^{103}Rh-^{31}P)$ of 102.5 Hz were reported before for $cis-[Rh(Cl)_4(CO)(PPh_3)]^- [NH_2(CH_2CH_3)_2]^+$ and 104 Hz for $[Rh(Cl)_3(\text{triphos})]$, triphos = $CH_3C\{CH_2P(C_6H_5)_2\}_3$,²⁹ and is similar to the starting material **38**, which is consistent with a Rh(III) complex. In addition, chemical shifts for Rh(III) carbonyls are in the range of 168-180 ppm and the chemical shift for **37** is in this range, Table 6.9. Appendix 2 shows a larger list for Rh(III) carbonyls, for a better comparison.

Axial C¹ *trans* to PPh₃ presents a smaller $^1J(^{103}\text{Rh}-^{13}\text{C})$ than C² in **37**. This is a result of the higher *trans*-influence of the phosphine. A clear example of this influence is the different $^1J(^{103}\text{Rh}-^{13}\text{C}^1)$ in **36a**: for C¹ *trans* to P $^1J(^{103}\text{Rh}-^{13}\text{C})$ 60.3 while for C² *trans* to Cl $^1J(^{103}\text{Rh}-^{13}\text{C})$ is 71.4 Hz.

Table 6.9. ¹³C NMR parameters of some other known Rh(I) and Rh(III) carbonyl compounds.³⁰

Complex	¹³ C NMR		Ref
	δ	¹ J _{RhC}	
69 [Rh(μ-Cl)(CO) ₂] ₂	177.5	75	31
70a [RhCl ₂ (CO) ₂] ⁻	180.6	72.2	31
70b [Pr ₄ N] ⁺ [Rh(CO) ₂ (Cl) ₂] ⁻	183.1	72	31
44c <i>mer,trans</i> -[Rh(Cl) ₃ (CO)(PPh ₃) ₂]	175.5	58	31
71 <i>cis</i> -[Rh(Cl) ₄ (CO) ₂] ⁻	168.5	52.7	25
72 [Rh ₂ (Cl) ₈ (CO) ₂] ₂ ²⁺	170.0	61.3	25

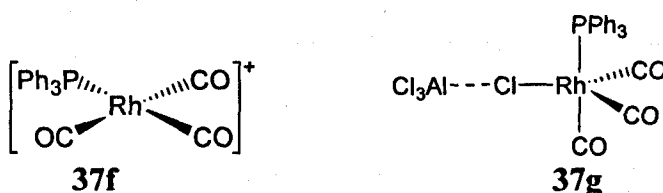
It is important to point out that **71**, which is a Rh(III) complex, has CO *trans* to Cl with a coupling constant $^1J(^{103}\text{Rh}-^{13}\text{C})$ 52.7 Hz. Then, assuming a Rh(III) complex in **37**, the CO *trans* to PPh₃ would reduce the coupling $^1J(^{103}\text{Rh}-^{13}\text{C})$ to smaller values due to larger *trans*-influence of PR₃ groups than chlorides. The coupling $^1J(^{103}\text{Rh}-^{13}\text{C})$ observed in **37** is 55.9 Hz that is larger than expected for Rh(III) centres with CO *trans* to PR₃. Hence, this evidence weakens the proposal of a Rh(III) centre with an octahedral geometry in **37e**, although it cannot be proved.



Also, it has been mentioned in section 6.2.2 that Rh(III) complexes such as **44a**, with P *trans* to each other, have $^1J(^{103}\text{Rh}-^{31}\text{P}^1)$ around 83-84 Hz.²⁵ Then, if complex **37** were a Rh(III) centre, the P *trans* to CO would be smaller than 83-84 Hz, but it is 107.5 Hz and such large coupling may not be consistent with a Rh(III) complex. The next section explains the other two possibilities for Rh(I) for **37**.

6.3.2. Rhodium (I) centre, a second alternative for 37

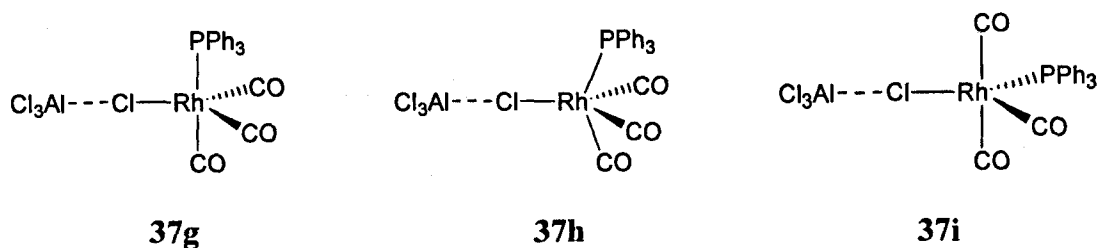
The first alternative for this oxidation state may be the square planar structure such as **37f**. Such a structure may be unlikely because the coupling $^1J(^{103}\text{Rh}-^{31}\text{P})$ characteristic for this kind of structure is between 120-130 Hz, as can be seen from **36** and **48**, Table 6.10. Also, the high concentration of $[\text{AlCl}_4]^-$ anions makes it improbable that such an anion is not coordinated to rhodium complex **37f**. Note that the *trans* coupling $^2J(^{31}\text{P}-^{13}\text{C})$ in **37** is 86.8 Hz that is smaller than the same coupling in **36a**. This makes a square planar structure improbable.



Hence, another alternative in this oxidation state is a trigonal bipyramidal structure **37g**. Compounds with *tbp* arrangement are known with coupling constants $^1J(^{103}\text{Rh}-^{31}\text{P})$ similar to **37** and Table 6.10 shows examples such as **41** and **73**, where the coupling $^1J(^{103}\text{Rh}-^{31}\text{P})$ and chemical shift ^{31}P are similar to those observed in **37**. However, note that the NMR parameters for **37** in Table 6.10 do not fit completely with known Rh(I) *tbp* NMR parameters such as **40**, **41** and **73** or *sp* such as **36a**, **36** and **48**. For example, note that:

- ^{13}C chemical shift of **73** is toward higher frequency than **37**, and may not be comparable to **37**. Also, the coupling $^1J(^{103}\text{Rh}-^{13}\text{C})$ in **73** is larger than the coupling $^1J(^{103}\text{Rh}-^{13}\text{C}^2)$ in the same complex.
- $\delta^{13}\text{C}$ NMR of complex **37** in the solution [emim][Al₂Cl₇]/CD₂Cl₂ is comparable with the chemical shift of C¹O and C²O in **36a**, Table 6.10, but **37** shows slightly smaller couplings $^1J(^{103}\text{Rh}-^{13}\text{C})$ than **36a** and in general it is smaller than any square planar compound such as **36** or **48**.
- Finally, $\delta^{13}\text{CO}$ for Rh(III) complexes such as **44c**, **71** and **72** in Table 6.9 are observed at lower frequency than **37**. That may suggest that **37** do not agree with a Rh(III) option.

Then, it is important to note that the *trans* coupling $^2J(^{31}\text{P}-^{13}\text{C})$ is still smaller for a strictly 180° angle. There is another possibility for the origin of such a difference.



A proper tbp, **37g**, with a 180° P-Rh-C angle would produce a large $^2J(^{31}\text{P}-^{13}\text{C})$. A smaller distortion toward a square based pyramid, **37h**, would decrease the P-Rh-C angle to 150° , giving a decrease of the coupling $^2J(^{31}\text{P}-^{13}\text{C})$. Last distortion may be a result of an interaction of the complex with the ionic environment producing a deformation in the original 180° of P-Rh-C in a trigonal bipyramidal structure, hence the couplings for $^1J(^{103}\text{Rh}-^{13}\text{C}^1)$ and $^2J(^{31}\text{P}-^{13}\text{C}^1)$ in **37** are not as large as in **36a**.

Another possibility is a fast rearrangement to **37i** that would reduce the angle P-Rh-C to 120° producing the same reducing effect of $^2J(^{31}\text{P}-^{13}\text{C})$. For example, a very large coupling $^2J(^{31}\text{P}-^{13}\text{C}^1)$ in **36a**, agrees with a 180° P-Rh-C angle. However, the coupling constant $^2J(^{31}\text{P}-^{13}\text{C}^1)$ in **37** is smaller and does not give as large a coupling as in **36a** with an 180° angle, and this is consistent with a smaller angle P-Rh-C¹ and may come from the exchange P-C¹ 180° to P-C¹ 120° , giving an average coupling, depending on the relative quantities of **37g** and **37i**.

A rapid interconversion from **37g** to **37i** is produced by Berry-pseudo rotation. This kind of interconversion has been studied in the 1970's for metal phosphites and it is depicted in Fig. 6.18. This rotation produces an exchange from axial ligands to equatorial positions.³¹ This rotation in **37h** may be the origin of the exchange of CO as the ¹³C correlation NMR shows in Fig. 6.19.

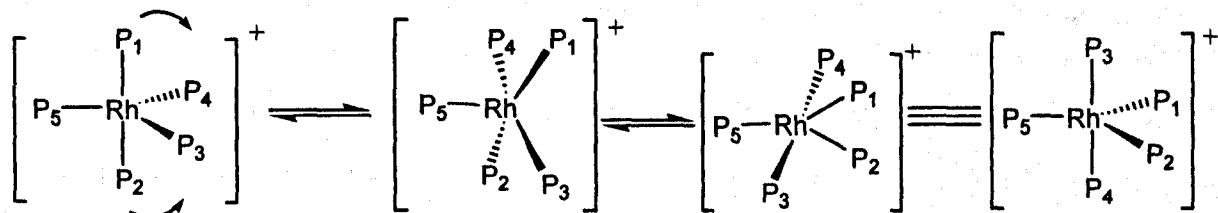


Fig. 6.18. Berry pseudo-rotation for a trigonal bipyramidal structure in five coordinated rhodium phosphites; $\text{P} = \text{P}(\text{OMe})_3$.

Then a rapid interconversion by Berry-pseudo-rotation in **37g** would produce the isomers depicted in Fig. 6.19. The first rotation in **37g**, noted by *l* would give **37i** with a

reduction in the P-Rh-C¹ angle. Then, the existence of a rapid interconversion of **37g** and **37i** would produce a smaller coupling $^2J(^{31}\text{P}-^{13}\text{C})$ as is observed in the NMR evidence.

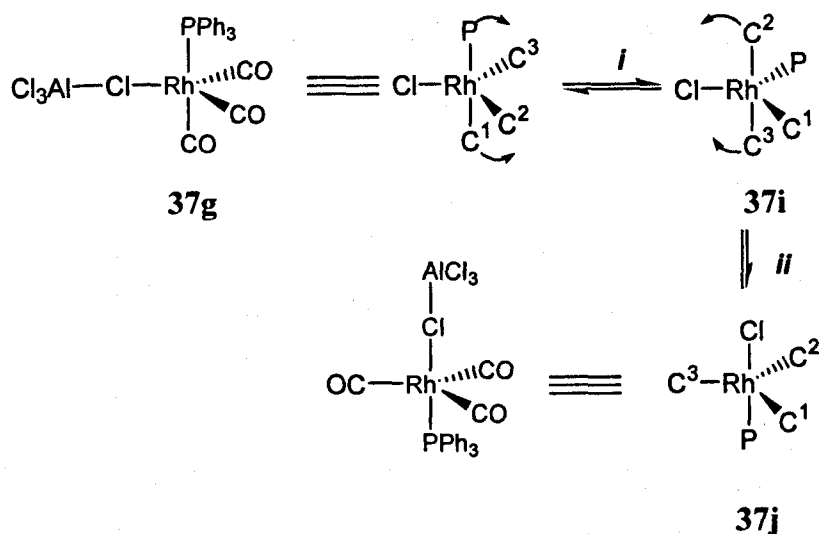


Fig. 6.19. Proposed mechanism to exchange the carbonyls: *i* produce an exchange of the axial to equatorial position of PPh₃ in **37**.

Note that the first Berry-pseudo-rotation, *i* Fig. 6.19 does not interconvert C¹ and C². However, a second rearrangement marked as *ii* in the same figure would produce an interconversion due to the equivalence of all CO ligands. The second rotation has a chlorine bridge in axial position. This arrangement is presumably a higher energy state and may be the origin of a large ΔG^\ddagger . A common value of 30-40 kJ mol⁻¹ for the activation state is generally found for [RhP₃]⁺, Table 6.11, at low temperature. Such a value is considered a low activation energy. In the case of **37**, the activation state obtained by the EXSY NMR in Fig. 6.15 is 58 kJ mol⁻¹. Then, the second arrangement, having a bridging chlorine in the apical position, may be the origin for the high ΔG^\ddagger . It is considered that a chloride in the apical position is a high-energy stage due to the low apicophilicity of chlorides and the large π -acidity of carbonyls in the same plane that draws electron density. Such a large energy state agrees with the larger energy to exchange the carbonyls calculated by NMR.

Table 6.10. NMR parameters of 37 and some other known Rh(I) carbonyl compounds.

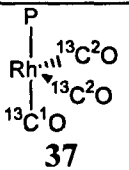
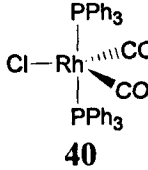
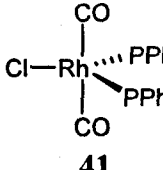
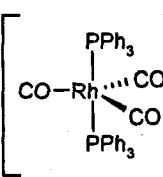
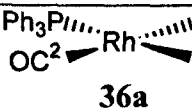
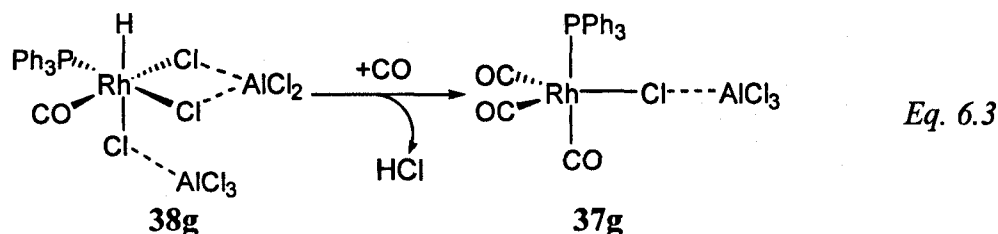
Complex	³¹ P{ ¹ H} NMR _ρ			¹³ C{ ¹ H} NMR		Ref.
	δ ppm	¹ J _{Rh P}	² J _{P C}	δ ppm	¹ J _{Rh C}	
 37	22	107.5	86.8 C ¹ 15.1 C ²	179.4 C ¹ 181.7 C ²	55.9 64.4	
 40	31	116	n.o.	185.9	n.o.	6
 41	25	96				5
 73	21.8	102.7	14.4	188.8	80.6	32
 36a	25.3	127.3	123.4 C ¹ 16.3 C ²	182.0 183.3	60.3 C ¹ 71.4 C ²	6
<i>trans</i> - [Rh(Cl)(CO)(PPh ₃) ₂] 36	28.5	126.6	16	187.4	73	6
<i>trans</i> - [Rh(Cl)(CO)(PEt ₂ Ph) ₂] 48	27.4	123.1	9.6	179.8	64.9	33

Table 6.11. Values of ΔG^{*} for known Rh(I) complexes with trigonal bipyramidal structure that exchange by pseudo-Berry rotation.

Complex	ΔG [*] kJ mol ⁻¹	Temp K	Ref.
[Fe{P(OCH ₃) ₃ } ₅]	36.5	200	34
[Ru{P(OCH ₃) ₃ } ₅]	30.1	200	"
[Os{P(OCH ₃) ₃ } ₅]	31.8	200	"
[Co{P(OCH ₃) ₃ } ₅]	41.8		"
[Rh{P(OCH ₃) ₃ } ₅]	31.4		"
[Ir{P(OCH ₃) ₃ } ₅]	33.5		"
[Ni{P(OCH ₃) ₃ } ₅]	33.5		"
[Pd{P(OCH ₃) ₃ } ₅]	25.9		"
[Pt{P(OCH ₃) ₃ } ₅]	27.2		"
[Rh{P(OBu ⁿ) ₃ } ₅]	46.4	228	35

An important observation is the agreement of the oxidation state of Rh(I) in **37**. The addition of CO to a Rh(III) complex **38f** or **38g** can replace HCl and add CO, hence the reaction in Eq. 6.3 is consistent with a Rh(III) in **38** in [emim][Al₂Cl₇].



The structure of **37** fits with the coordination of [AlCl₄]⁻ with the interaction of a (μ-Cl) to the metal. However, the species **37** is also formed from a Rh(I) centre, when [Rh{(μ-Cl)AlCl₃}(H)(PPh₃)₂]⁻ **24**, reacts with CO. This kind of reaction is the result of the replacement of a PPh₃ group and chlorine in **24** with CO that is bubbled through the mixture reaction, *ii*, Fig. 6.20.

It is worth noting that the addition of CO to **25** eliminates a PPh₃ that is trapped by the acidic environment and this permits the addition of CO. Then a possible alternative to the production of **37** from **25** is the formation of **38** as intermediate, but this pathway cannot be proved.

Fig. 6.20 gives a summary of the reactions, where **37** is formed by two routes. The formation of **37** from **38** has already been mentioned in Eq. 6.3. The other pathway (*i*) that has been observed is the formation of **37** from **25**. The replacement of the hydride and the PPh₃ in **25** with CO to form **37** may include a Rh(III) intermediate due to the addition of HCl. Then the elimination of H₂ may produce **37** and Fig. 6.21 shows a possible route to produce **37**.

6. Results and discussion: Carbonylation of rhodium complexes in [emim][Al₂Cl₇]

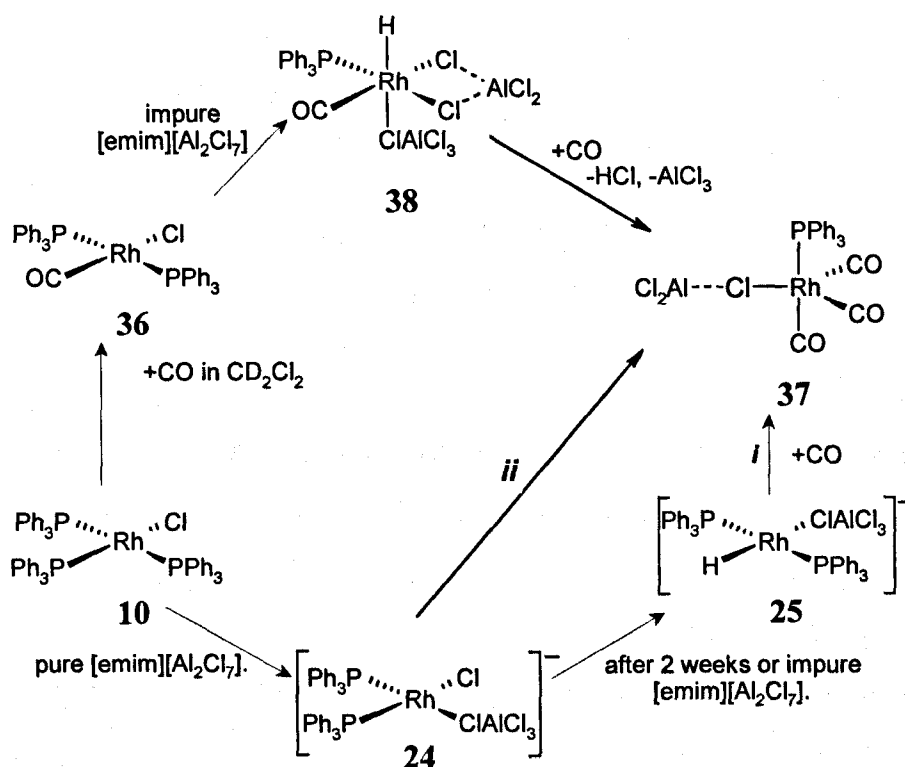


Fig. 6.20. Oxidation of $[\text{Rh}\{\mu\text{-Cl}\}\text{AlCl}_3\{\text{H}\}(\text{PPh}_3)_2]^-$ with the addition of CO in $[\text{emim}][\text{Al}_2\text{Cl}_7]$.

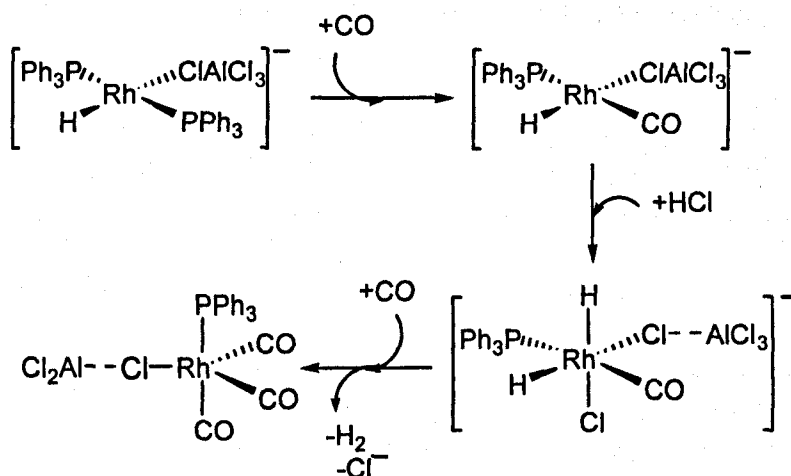


Fig. 6.21. Possible route for the formation of 37 from 25.

The next section explains the possible structure of 68, which is the second product from the consecutive addition of ^{13}CO to 37. Also, it mentions the presence of more rhodium carbonyls in solution and discusses possible structures in solution based on known rhodium complexes. Finally, it gives a complete summary of reactions that are possible in $[\text{emim}][\text{Al}_2\text{Cl}_7]$.

6.4. Characterization of [Rh(Cl){(μ-Cl)AlCl₃}(CO)₂(PPh₃)]⁻, **68; the second product of carbonylation of [Rh{(μ-Cl)AlCl₃}(H)(PPh₃)₂]⁻, **25** and [Rh{(μ-Cl)AlCl₃}{(μ-Cl)₂AlCl₂}(H)(CO)(PPh₃)], **38****

Firstly, the addition of ¹³CO to the reaction mixture that contains **38** [Rh{(μ-Cl)AlCl₃}{(μ-Cl)₂AlCl₂}(H)(¹³CO)(PPh₃)] produces the enriched **37** [Rh{(μ-Cl)AlCl₃}(¹³CO)₃(PPh₃)], that has been partially identified in section 6.4. It has been mentioned that **37** does not last very long in mixtures of [emim][Al₂Cl₇]/CD₂Cl₂ 1:1 and the consecutive addition of ¹³CO to the reaction mixture of **38** and **37** produces other compounds that are going to be discussed in following sections.

After **37** has appeared, a second product is observed at room temperature with a doublet signal in the ³¹P NMR at δ 38.5 ppm, ¹J(¹⁰³Rh-³¹P) 123 Hz and it has been assigned to complex **68** in Fig. 6.14b. ¹³C NMR spectrum shows a broad doublet at room temperature at δ 172 ppm, ¹J(¹⁰³Rh-¹³C) 73 Hz. The ³¹P NMR spectrum of the signal of **68** is a doublet at the same frequency at -40°C as room temperature. While the ¹³C NMR signal of the complex looks as a doublet ²J(³¹P-¹³C) 10.8 Hz doublet ¹J(¹⁰³Rh-¹³C) 76.2 Hz at δ 174.9 ppm at -40°C. Fig. 6.22 shows spectra at room temperature of ³¹P NMR and low temperature of ¹³C NMR. Note that the signal of **68** in ¹³C NMR spectrum is broad in the base due to the presence of a small amount of **38** that has the same chemical shift and similar coupling ¹J(¹⁰³Rh-¹³C) as **68**. A summary of the products in the reactions appears in Fig. 6.23 due to clarity. The signal of **68** appears after **37** has appeared and the former increases in intensity with the decrease of the latter.

When the signal of complex **68** is the only signal detected in the ³¹P NMR spectrum there is no hydride signal in the ¹H NMR spectrum of such a solution. The multiplicity in the ¹³C NMR spectrum for **68** implies the presence of only one PPh₃ group in the complex. The proposed structure for **68** is going to be based on the comparison of coupling constants of known Rh complexes.

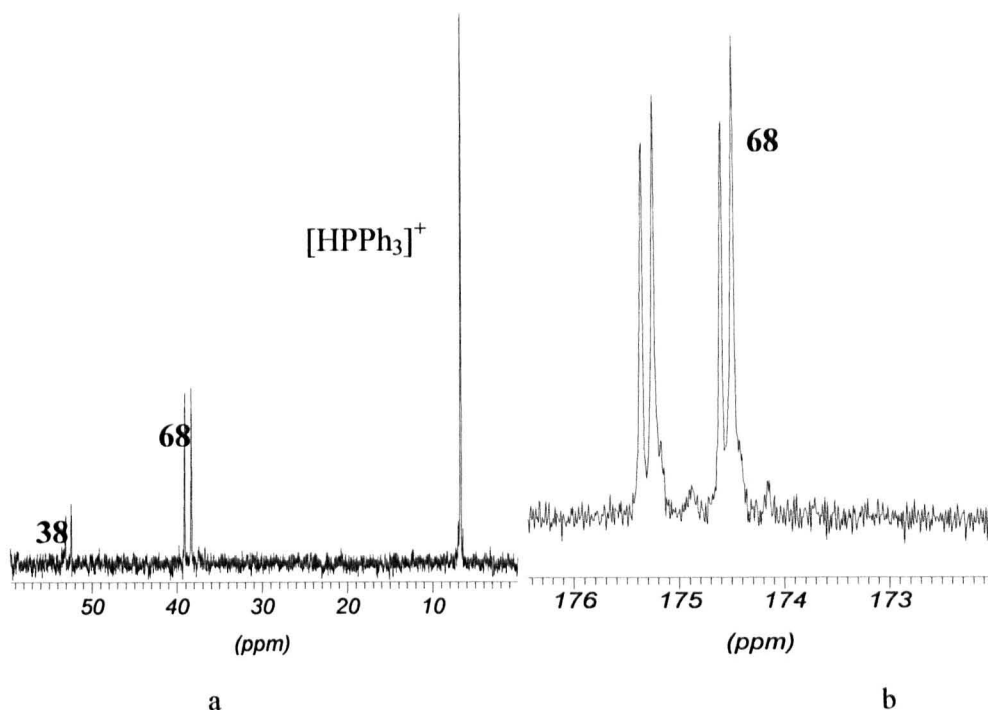


Fig. 6.22. Solution of **68** after the addition of CO to $[Rh\{\mu\text{-Cl}\}AlCl_3\}(H)(PPh_3)_2]^-$, **25** and $[Rh\{\mu\text{-Cl}\}AlCl_3\}\{\mu\text{-Cl}\}_2AlCl_2\}(H)(CO)(PPh_3)]$, **38** in $[emim][Al_2Cl_7]/CD_2Cl_2$ 1:1. a) $^{31}P\{^1H\}$ NMR at room temperature and b) $^{13}C\{^1H\}$ NMR spectra at $-40^\circ C$.

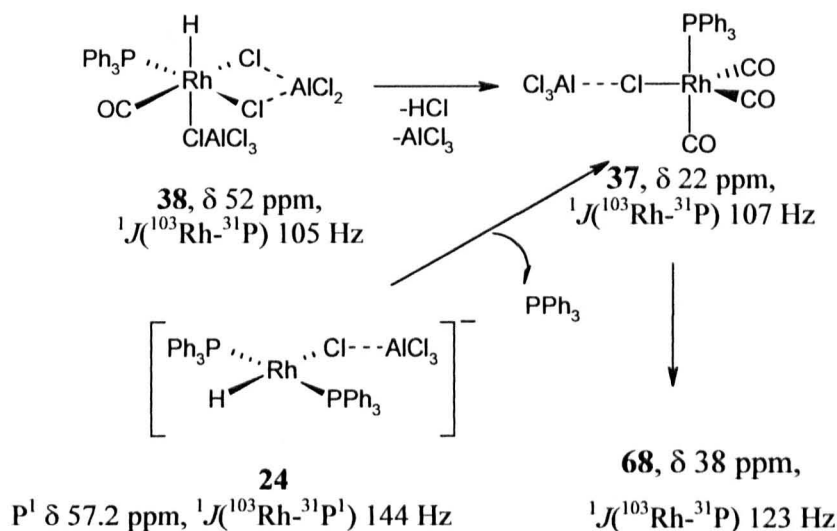
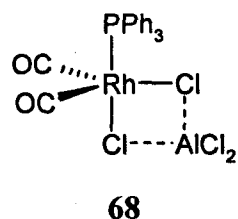


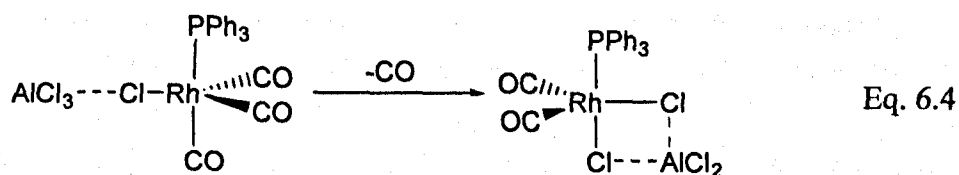
Fig. 6.23. Summary of reactions with NMR parameters of every complex observed until now.

Note that $^{103}\text{Rh}-^{31}\text{P}$ coupling is more in the range for Rh(I) complexes, see Table 6.10 and compare values with Table 6.9 for Rh(III). It is known that the dicarbonyl-diphosphine complexes such as **40** and **41** have been detected after bubbling CO through solutions of $[RhCl(CO)(PPh_3)_2]$ at low temperature under CO atmospheres, Table 6.1.⁵ These complexes

have been proposed using IR and ³¹P NMR techniques but they lose the CO at room temperature even under CO atmospheres. The reaction of **38**, [Rh{(μ-Cl)AlCl₃}{(μ-Cl)₂AlCl₂}(H)(CO)(PPh₃)], with CO may follow a similar route. The initial formation of a tricarbonyl **37**, which is unstable, even at low temperature, may release a CO molecule to form the dicarbonyl **68**. Also, the ¹³C NMR evidence suggests the presence of only one PPh₃ group. A possible structure of **68** in [emim][Al₂Cl₇] is a Rh(I) monophosphine such as [Rh{(μ-Cl)₂AlCl₂}(CO)₂(PPh₃)] being a *tbp* structure. Note that **68** may be a consequent product of **37**, from the elimination of a CO from **37** to produce a dicarbonylphosphine complex, Eq. 6.4.



While, ¹³C NMR evidence agrees with the presence of only one PPh₃ group, the ³¹P NMR signal shows the coupling to only one CO at room temperature. However, when the reaction is carried out with enriched ¹³CO, the signal of **68** in the ³¹P NMR spectrum became broad at -40°C, Fig. 6.24, and although the splitting is not well defined, the broadness of each peak is 11 Hz, which is due to unresolved *cis*-coupling ²J(³¹P-¹³C).² Note that the coupling ²J(³¹P-¹³C) in the ¹³C NMR corresponding to **68** is 10.8 Hz, Fig. 6.23. This result may be due to a fast exchange of CO.



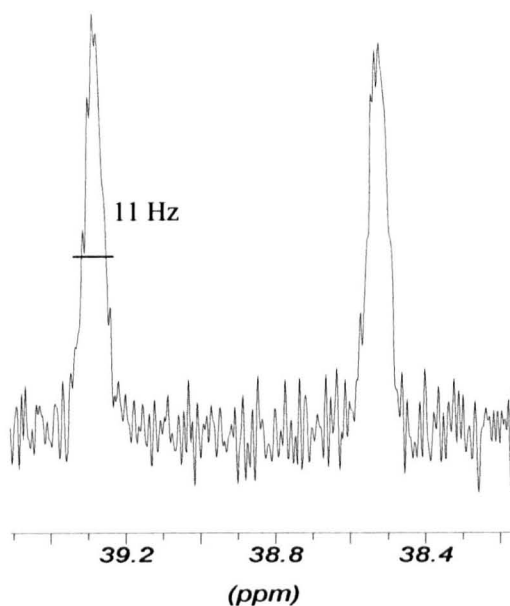


Fig. 6.24. Signal of **68** in the ³¹P NMR spectra at low temperature, -40°C. The broadness of each peak is 11 Hz approximately and it is in the average of the *cis*-coupling ²J(³¹P-¹³C).

A fast exchange may be the reason that the ³¹P signal does not detect the two similar CO in **68** even at -40°C. Also, the *cis*-coupling ²J(³¹P-¹³C) in similar complexes is in the average of 10-15 Hz.³⁶

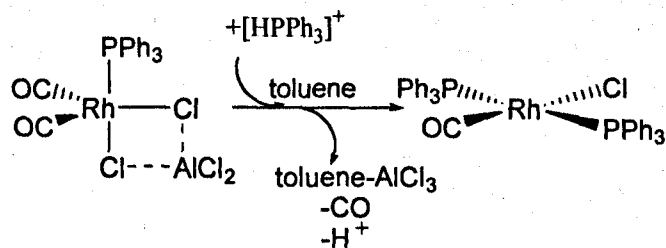
Complex **68** is very stable in [emim][Al₂Cl₇]. It remains in the reaction mixture for many days, contrary to **37** that has a short lifetime in solution of 4 hours. Complex **68** is the final carbonyl rhodium product with a PPh₃ group in the reaction of **38** with CO and **25** with CO. The final solution of [emim][Al₂Cl₇] containing **68** was treated with toluene. The extracted complex from [emim][Al₂Cl₇] in toluene shows ³¹P NMR δ 29.9 ppm and ¹J(¹⁰³Rh-³¹P) 128.3 Hz and ¹³C NMR gives a broad doublet at 181.3 ppm, ¹J(¹⁰³Rh-¹³C) 65.2 Hz. The toluene solution, after 2 hours, shows the precipitation of a yellow powder that corresponds to the initial compound **36**, [RhCl(CO)(PPh₃)₂], and the FAB⁺ mass spectrum of this powder corresponded to 626 which suggests the presence of the fragment [Rh(PPh₃)₂]⁺. Also, a white powder that corresponds to the oxoaluminates and hydroxoaluminate (III) species appears. This result suggests two possibilities: i) the observation of **68** in the ionic liquid but it cannot survive in organic solvents or ii) the presence of moisture in toluene destroyed the complex **68** that has been extracted in the toluene and produced its decomposition. The latter possibility was avoided by using dried and freshly distilled toluene. Then, the initial possibility of the instability of **68** in toluene was considered. It is known that AlCl₃ may interact with the aromatic ring of toluene, producing yellow complexes.

Then, the elimination of $[\{\mu\text{-Cl}\}_2\text{AlCl}_2]^-$ from **68** produced its decomposition. Also, the elimination of super acid conditions that originally existed in the [emim][Al₂Cl₇] and were able to eliminate a PPh₃ group from [RhCl(CO)(PPh₃)₂] and produce **38** are not present in toluene. Then, the coordination of PPh₃ that was forming [HPPh₃]⁺ in [emim][Al₂Cl₇], can come back to **68**. Also, the liberation of another CO molecule from **68** may produce **36** again, Eq. 6.5.

An additional test was performed. The addition of water to a solution of **68** in [emim][Al₂Cl₇] produced the decomposition of the ionic liquids due to the formation of oxochloroaluminates and hydroxochloroaluminate (III) and the formation of compound **36**, [RhCl(CO)(PPh₃)₂], FAB⁺ 626 [Rh(PPh₃)₂]⁺. This suggests that the destruction of the ionic liquid produces the decomposition of the complex that is stable only in the ionic liquid due to the interaction of [AlCl₄]⁻ with the metallic centre.

Table 6.11. ³¹P and ¹³C NMR parameters for the complex **36** and **68**: a) **36** in CDCl₃; b) **68** in [emim][Al₂Cl₇]; c) yellow powder recovered from the addition of water to the solution of **68** in [emim][Al₂Cl₇]; d) yellow powder extracted with toluene from **68** in [emim][Al₂Cl₇].

Complex	$\delta^{31}\text{P}$	$^1J(^{103}\text{Rh}-^{31}\text{P})$	$\delta^{13}\text{C NMR}$	$^1J(^{103}\text{Rh}-^{13}\text{C})$
a) 36 [Rh(Cl)(CO)(PPh ₃) ₂] in CDCl ₃	29.3	126.7	187.0	74.4
b) 68 [Rh{($\mu\text{-Cl}$)AlCl ₃ }(CO) ₂ (PPh ₃)] in [emim][Al ₂ Cl ₇]	38.5	123.2	172	73
c) 36 recovered from the destruction of [emim][Al ₂ Cl ₇]	29.9	127.3	188.1	75.2
d) 36 recovered from toluene	29.9	128.3	181.3	65.2



Eq. 6.5

After 30 minutes of reaction with ¹³CO, the only product in the mixture is **68** in the ³¹P NMR spectra. The ¹³C NMR spectrum shows a broad doublet at room temperature, corresponding to **68** and a triplet at 171.9 ppm. This signal is going to be discussed in next section.

6.5. The observation of a possible carbonyl rhodium complex in the carbonylation of [Rh{(μ-Cl)AlCl₃}(H)(PPh₃)₂]⁻, **25 and [Rh{(μ-Cl)AlCl₃}{(μ-Cl)₂AlCl₂}(H)(CO)(PPh₃)], **38** in [emim][Al₂Cl₇]**

The spectrum in Fig. 6.25 shows the formation of a rhodium carbonyl in the ¹³C NMR with δ 171.9 ppm, ¹J(¹⁰³Rh-¹³C) 36.7 Hz, that does not correlate with a ³¹P NMR signal, the ³¹P NMR spectrum of last solution shows the signal for **68** only. Also, no hydride associated with this complex has been identified. This suggests the species giving the triplet in the ¹³C NMR spectrum does not contain any PPh₃ or hydride group. This complex is observed after 30 minutes of reaction with ¹³CO. The absence of a hydride or a PPh₃ correlated to this species suggests the presence of a new rhodium carbonyl that has not been reported before. Complex **74** is stable for a few hours after the reaction with ¹³CO is finished.

The coupling ¹J(¹⁰³Rh-¹³C) 36.7 Hz is small for a single Rh-C interaction and combined with the triplet structure in Fig. 6.25, suggests that the ¹³C is scrambling over two rhodium atoms. The ¹³C NMR spectrum does not provide enough evidence to suggest a unique structure for this complex that has not been isolated from the ionic solution, but there are a few important issues to point out as base to propose structures.

Firstly, it is worth noting that the chemical shift 171.9 ppm for **74** is typical for terminal CO. Some examples have been given in Table 6.10 where terminal CO appears at 175-173 ppm. Also, Table 6.12 shows examples of chemical shift for bridging CO in rhodium complexes, where the common frequency for this kind of CO is higher than 200 ppm. This suggests that the signal of **74** may correspond to terminal CO.

Secondly, note that the multiplicity for the signal of **74**, that is a triplet, is uncommon for terminal CO. This kind of splitting may be the result of two coupling ¹J(¹⁰³Rh-¹³C) and

$^2J(^{31}\text{P}-^{13}\text{C})$. However, there is no signal in the ^{31}P NMR spectrum that correlates to the signal of **74** in the ^{13}C NMR spectrum. This clearly suggests that the triplet corresponds to the coupling $^1J(^{103}\text{Rh}-^{13}\text{C})$ only. Knowing that the frequency for ^{13}CO for **74** corresponds to terminal CO, the triplet may suggest the scrambling of terminal CO between two rhodium. However, the magnitude of coupling $^1J(^{103}\text{Rh}-^{13}\text{C})$ of terminal CO is around 70 Hz (see Table 6.10) and the magnitude observed for **74** is far smaller. A possible explanation is that the exchange of CO between two rhodium would produce an average of $^1J(^{103}\text{Rh}-^{13}\text{C})$ 35 Hz, which is in the observed magnitude.

Table 6.12. ^{13}C NMR parameters for bridging CO of Rh(0) complexes.

complex	δ CO ppm	$^1J(^{103}\text{Rh}-^{13}\text{C})$ Hz	Ref.
75a [Rh ₄ (CO) ₉ (triphos)]	244	34.5	37
75b [Rh ₄ (CO) ₁₂]	228	25	38

A first alternative for the exchange in **74** may be [(CO)₃Rh(μ -CO)₂Rh(CO)₃] where the chemical shift may be weighted between three terminal CO and one bridging CO. Then, the chemical shift may be more in the average of terminal CO but with the multiplicity of bridging CO.

Also note that the triplet can be the result of a AA'X spectrum being AA' the rhodium atoms. This would require that $^1J(^{103}\text{Rh}-^{103}\text{Rh})$ were larger than $^1J(^{103}\text{Rh}-^{13}\text{C})$ that is normally 70 Hz. This is virtually an order of magnitude larger than any coupling $^1J(^{103}\text{Rh}-^{103}\text{Rh})$ so far observed. Table 6.13 shows some examples of coupling $^1J(^{103}\text{Rh}-^{103}\text{Rh})$ where it is seen that is far smaller than 70 Hz.

Table 6.13. Coupling in rhodium dimers.

Complex	$^1J(^{103}\text{Rh}-^{103}\text{Rh})$ Hz	Ref
[Rh ₂ (C ₂ H ₃)(C ₂ Me ₃)(η^5 -indenyl) ₂]	17	39
[Cp ₂ Rh ₂ (CO) ₃]	4.2	40
[Cp ₂ Rh ₂ (CO) ₂ (CH ₂)]	4.4	6
[Cp ₂ Rh ₂ (NO) ₂]	4.4	6

The next sections discuss possible structural alternatives based on Rh(III), Rh(I) and Rh(0) dimers where CO may be scrambling between two rhodium at room temperature.

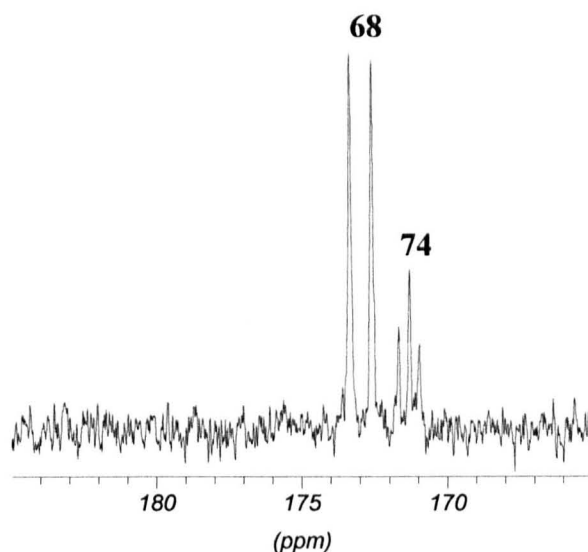


Fig. 6.25. ¹³C NMR spectrum of solution of **68** after two hours under ¹³CO atmosphere. The triplet at 171.9 ppm may correspond to a rhodium carbonyl dimer with scrambling CO. Possible structural alternatives for the triplet are discussed in following sections.

6.5.1. Possibilities of Rh(III) for **74**

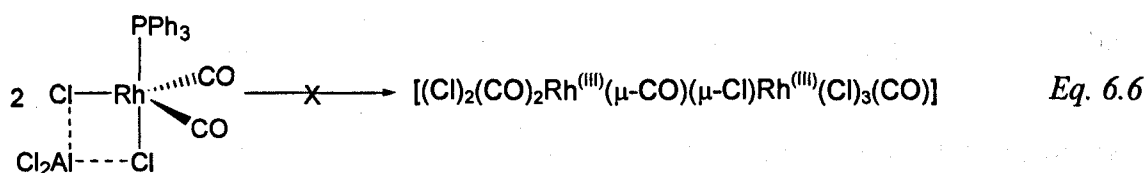
Table 6.14 shows the chemical shift for Rh(III) carbonyl dimers and its coupling constants. The chemical shift observed for the complex **74** is in the range of Rh(III) complexes reported by Heaton.³⁰ These dimeric species of Rh(III) carbonyls do not have any CO bridge, Table 6.14. In the case of complex **74**, the coupling constant ¹⁰³Rh-¹³C in complex **74** suggests the vicinity of two rhodium centres for the same CO.

Table 6.14. ¹³C NMR parameters for known Rh(III) dimers observed by Heaton and coworkers.²

	Complex	$\delta^{13}\text{C}$ ppm	$^1J(^{103}\text{Rh}-^{31}\text{P})$ Hz
72a	$[\text{Rh}_2(\text{Cl})_8(\text{CO})_2]^{2-}$	170.0	61.3
72b	$[\text{Rh}_2(\text{Cl})_9(\text{CO})_2]^{3-}$	172.7	61.5

Considering this information, it may be suggested that the triplet at 171.5 ppm in Fig. 6.25 is not consistent with a Rh(III) dimeric species having CO bridges.

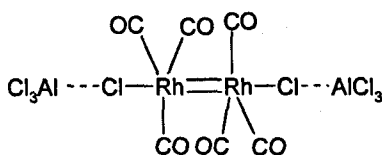
Note that complex **68** has been proposed as a Rh(I) tbp complex, then a Rh(III) dimer from a Rh(I) tbp carbonyl may not match with a consecutive reaction of **68** in the presence of CO, which may be a reductive agent but not an oxidant agent.⁴¹ If this is the case, it would be necessary that Rh(I) **68** converts to Rh(III) on reaction with CO which is an unlikely reaction. It is known that Rh(I) carbonyls are stable under high acidic conditions in the presence of CO.⁴² This could be evidence of a Rh(III) carbonyl with a scrambling CO between two rhodium for **74a** is unlikely.



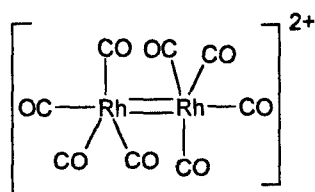
6.5.2. Possibilities for Rh(I) for **74**

Rh(I) dimers with bridging CO are unknown. The crystal structure of the dimer [(CO)₂Rh(μ-Cl)₂Rh(CO)₂] is known and shows the presence of bridging chlorines without the possibility of bridging CO. Also, terminal CO could be favoured by a weak interaction with [AlCl₄]⁻ in the media. Some examples have been reported with other metals such as Mo⁴³ and Mn.⁴⁴ A possible alternative for a Rh(I) dimer is **74a** where each rhodium centre has a terminal [ClAlCl₃]⁻ ligand and each centre obeys the 18 electron rule.⁴⁵

Note that the triplet **74** is formed when **68** is abundant in the solution. It has been discussed that **68** maybe a dicarbonyl Rh(I) species. The release of CO from **37** to form **68** produces an excess of CO in the ionic solution that can react with the remaining **68** and produce the elimination of the remaining PPh₃ in **68**. This can produce a new species with only CO ligands. Then, if **74** is formed from **68** with CO, the possible oxidation state of **74** suggests a Rh(I).



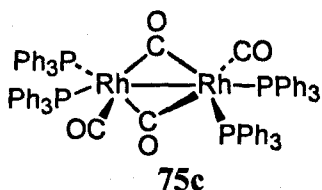
74a



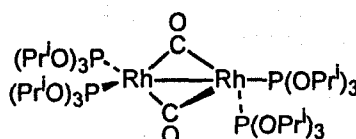
74b

6.5.3. Possibilities for Rh(0) for 74

Some Rh(0) carbonyl complexes have been characterized by x-ray diffraction, their ¹³C NMR parameters have not been reported due to a lack of solubility in organic solvents. Such is the case of the dimer [Rh(CO)(μ-CO)(PPh₃)₂]₂, **75c**, that has been observed by IR⁴⁶ and the X-ray diffraction of [Rh(μ-CO){P(OPrⁱ)₃]₂, **75d**,⁴⁷ but no ³¹P NMR data have been reported for **75b** due to the insolubility of the dimer. Brown⁴⁸ and coworkers have calculated a coupling ¹J(¹⁰³Rh-³¹P) of 138 Hz for the dimer [Rh(μ-CO)(PPh₃)₂]₂ that has been isolated and diffracted without any ³¹P NMR data.⁴⁹ However, the analogous dimer with PCy₃ such as [Rh₂(μ-CO)₂(CO)(PCy₃)₃], **75c**, was reported with two different phosphorus signals but no ¹³C NMR information.⁵⁰

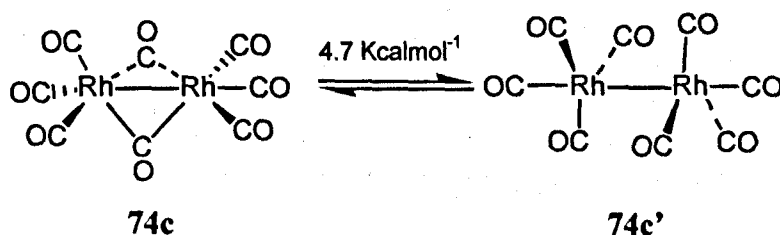


75c



75d

The dimer [Rh₂(CO)₈] has been postulated at high pressure and low temperature by IR.⁵¹ Theoretical calculations suggest the existence of **74c** with CO bridges with very low difference in energy between the bridged and non-bridged structure; while its analogues [Co₂(CO)₈] and [Ir₂(CO)₈] may exist without CO bridges.⁵²



74c

74c'

In addition, the interaction with the chloroaluminates (III) in the ionic environment may be the reason for an uncommon chemical shift.

It has been discussed that the existence of species that may have never been observed in organic solvents but they have been stabilized in [emim][Al₂Cl₇] due to an interaction of the chloroaluminate (III) anion. This is the case for the diphosphine **24**, [RhCl(ClAlCl₃)(PPh₃)₂]⁻ and the tricarbonyl **37**, [Rh{(μ-Cl)AlCl₃}(CO)₃(PPh₃)]. The possible existence of the dimer **74c** in the ionic liquid supports the proposal of the existence of unknown complexes in organic solvents.

The chemical shift for the complex (triplet) **74** appears for terminal CO frequency, but the Rh-C coupling shows that it is in the vicinity of two rhodium centres.

A few years ago, the reaction of [Rh₄(CO)₁₂] with P(OPh)₃ was followed by ³¹P and ¹³C NMR and the results suggest the formation of [Rh₂(CO)_{8-x}{P(OPh)₃}_x], **76**, at 400 bar of CO pressure.⁵³ The chemical shift in ¹³C NMR spectrum is around 200 ppm which is characteristic for bridging carbonyls and it is quite high when it is compared to the ¹³C δ in **74** in the ionic liquid.

The formation of a Rh(0) centre may be explained by the presence of Al⁰ impurities that were responsible for the reduction of Rh chloride to rhodium hydride in section 4.2. The attempts to extract the compound with the triplet in the ¹³C NMR spectrum with toluene were unsuccessful. Finally, it is also worth noting that complex **74** does not last more than 48 hours in solution and this makes it too difficult to isolate.

Although it is difficult to assign the compound giving the triplet in ¹³C NMR of the complex **74**, the possibility of a dimer such as **74c** and **74c'** is a good alternative and possibly fits with the type of reaction expected in the carbonylation of the rhodium complex.

In a further attempt to understand the chemistry of the rhodium carbonyl dimer the complex [Rh(CO)₂Cl]₂ was dissolved in [emim][Al₂Cl₇] and the addition of PPh₃ to the solution was followed. Rotondo¹ has studied this reaction previously in CD₂Cl₂ at low temperature. The results of the same reaction in the ionic liquid and the comparison within the organic solvent are shown in the next section and may give a clearer understanding of the chemistry in the chloroaluminate ionic liquids. Fig. 6.27 shows a summary of the reactions that have been observed in [emim][Al₂Cl₇] in chapters 4 and 6.

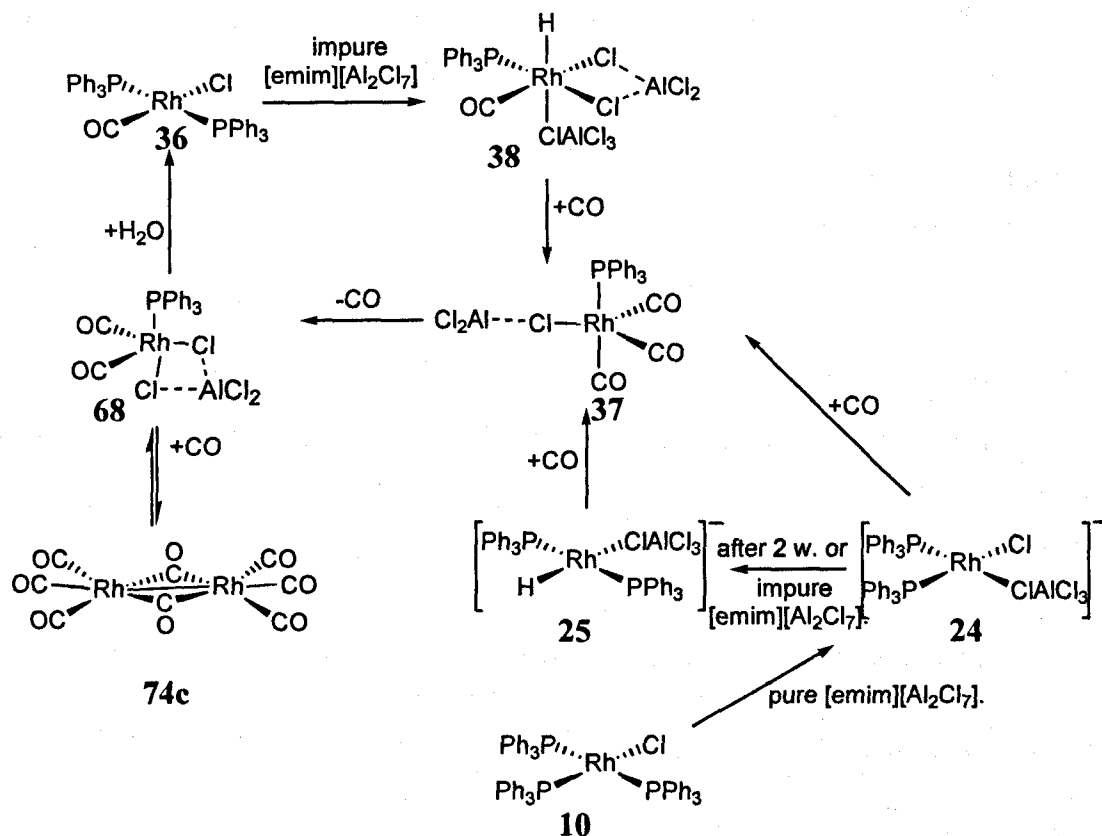


Fig. 6.27. Summary of reactions reviewed in chapters 4 and 6. The possible structure of 74 cannot be proposed with certainty.

6.6. Solution of $[\text{Rh}(\mu\text{-Cl})(\text{CO})_2]_2$ in $[\text{emim}][\text{Al}_2\text{Cl}_7]$ with the addition of PPh_3

The initial dimer $[\text{Rh}(\mu\text{-Cl})(\text{CO})_2]_2$ is well known with a ^{13}C signal at δ 177.5 and $^1J(^{103}\text{Rh}\text{-}^{13}\text{C})$ 75 Hz. When it is dissolved in $[\text{emim}][\text{Al}_2\text{Cl}_7]$, the ^{13}C NMR spectrum shows a signal at ^{13}C δ 175.4, $^1J(^{103}\text{Rh}\text{-}^{13}\text{C})$ 80.1 Hz, which suggests a different complex in the ionic solution. The coupling constant of the complex in the ionic liquid is larger than the original material in organic solvents. This suggests the formation of a new complex and the possibilities for the structure are going to be discussed as follows.

Firstly, note that the dimer can be dissociated in a coordinating environment. It has been mentioned that [AlCl₄]⁻ can act as a ligand and the possible interaction of this ligand with the rhodium centre can produce **77a** or **77b**, depending on the type of coordination of the chloroaluminate (III) ligand. Table 6.15 shows that the anion [RhCl₂(CO)₂]⁻, **70a**, has a chemical shift at 180.6 ppm, ¹J(¹⁰³Rh-¹³C) 72.2 Hz. It is worth noting that the monomer in the organic solvents [RhCl₂(CO)₂]⁻ has a coupling constant ¹J(¹⁰³Rh-¹³C) smaller than the monomer **77a-b** in [emim][Al₂Cl₇].

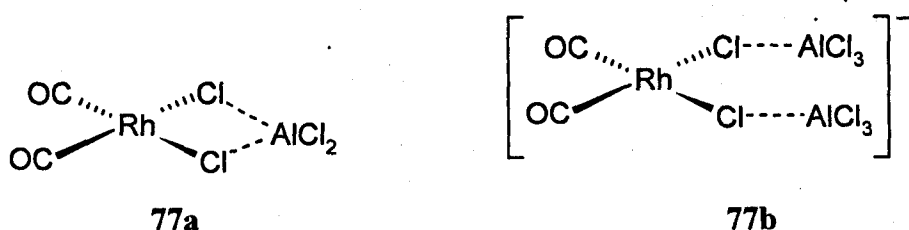


Table 6.15. ¹³C NMR parameters of some Rh(I) carbonyl compounds.³⁰

Complex	¹³ C NMR		Ref
	δ	¹ J _{RhC}	
69 [Rh ₂ (μ-Cl) ₂ (CO) ₂]	177.5	75	³¹
70a [RhCl ₂ (CO) ₂] ⁻	180.6	72.2	³¹
77b [Rh{(μ-Cl)AlCl ₃ } ₂ (CO) ₂] ⁻	175.4	80.1	

This clearly suggests the formation of another species and the chemical shift of the dimer in the ionic solution is lower frequency and with a larger coupling. The increase in the coupling from the starting material to its solution in [emim][Al₂Cl₇] may be as a result of the interaction of the ionic environment. This agrees with the weaker *trans* influence of chlorine bridges in **77a-b** than terminal chlorines in the monomer **70a**.

In order to understand the carbonylation reaction explained in previous sections the addition of PPh₃ to the solution of **77** in [emim][Al₂Cl₇], was studied. The addition of phosphine to the solution was followed by ¹³C NMR, but the small concentration of every intermediate did not allow further characterization with this nucleus, Fig. 6.28. Then, the ³¹P NMR gives more information of specific intermediates, Fig. 6.29.

The initial addition of PPh₃ produces [HPPH₃]⁺ at δ ³¹P 6 ppm, Fig. 6.29. This is due to the high affinity of the free phosphine for the protons available in the medium. The

presence of protons arises when traces of moisture reacts with AlCl₃ in the media, producing HCl that produce superacidity conditions in the ionic liquid.⁵

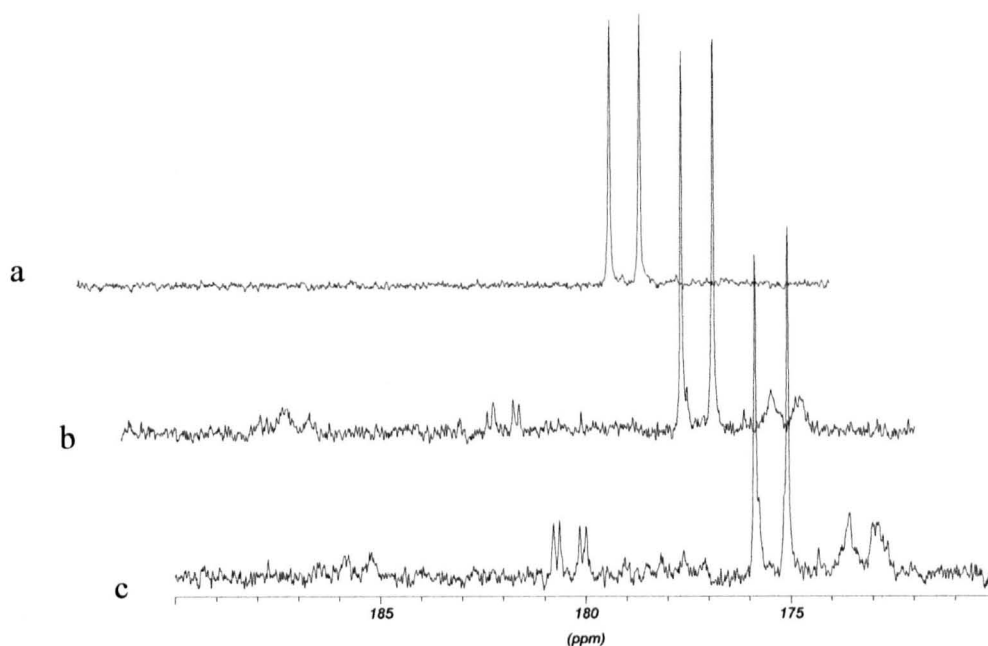


Fig. 6.28. ¹³C NMR for the addition of PPh₃ to the solution of [Rh(μ-Cl)(CO)₂]₂ in [emim][Al₂Cl₇]: a) an equivalent, b) three equivalents; c) ten equivalents. Table 6.16 shows the ¹³C NMR details for each signal.

The consecutive addition of more equivalents of PPh₃ introduces moisture in the solution in the NMR tube, increasing the intensity of the signal of [HPPH₃]⁺. Also, the addition produces more complexes and Fig. 6.28 shows three representative ³¹P NMR spectra during the addition of PPh₃ to the initial solution of [Rh{(μ-Cl)AlCl₃}₂(CO)₂], **77**. For example, the addition of three equivalents of PPh₃ produces the formation of the hydride [Rh{(μ-Cl)AlCl₃}{(μ-Cl)₂AlCl₂}H(CO)(PPh₃)], **38**, at 53.4 ppm. Also, due to the introduction of moisture during each addition, the formation of a complex that has been assigned as **78a**, was observed at 26.1 ppm, ¹J(¹⁰³Rh-³¹P) 67 Hz, b Fig. 6.29. The structure of this complex is proposed as a Rh(III) due to the small Rh-P coupling. The ¹³C NMR spectrum of this solution shows 4 new signals at 175.1, 175.3, 173, and 172 ppm corresponding to complexes **77**, **38**, **68** and **78a** respectively. All those signals are broad and not clearly split due to a possible fast exchange of CO between them.

Table 6. 16. ^{13}C NMR parameter of the addition of PPh_3 to the solution of $[Rh(\mu-Cl)(CO)_2]_2$ in $[emim][Al_2Cl_7]$.

^{13}C NMR data	77, 68	38	78a, 78b	78c	37
$\delta^{13}C$	175.1	175.3	173.1, 173.8	185.5	180.3
$^1J(^{103}Rh-^{13}C)$	80.5	60.4	60.13, 58.9	Broad signal	64.6
$^1J(^{31}P-^{13}C)$ Hz					15.03

The addition of ten equivalents of PPh_3 produces the formation of another three complexes, the tricarbonyl $[Rh\{(\mu-Cl)_2AlCl_2\}(CO)_3(PPh_3)]$, **37**, and **78b**, at 26.4 ppm, $^1J(^{103}Rh-^{31}P)$ 106 Hz and **78c** at 32.9 ppm, $^1J(^{103}Rh-^{31}P)$ 71 Hz. Table 6.17 shows the ^{31}P NMR parameters of every complex observed during the three additions. The formation of **68** and the tricarbonyl **37** is not surprising considering that the elimination of CO from **68** may produce **38** in the presence of HCl impurities and the free CO can be attached to other rhodium dicarbonyl and produce **37**. Fig. 6.30 shows this reaction clearly.

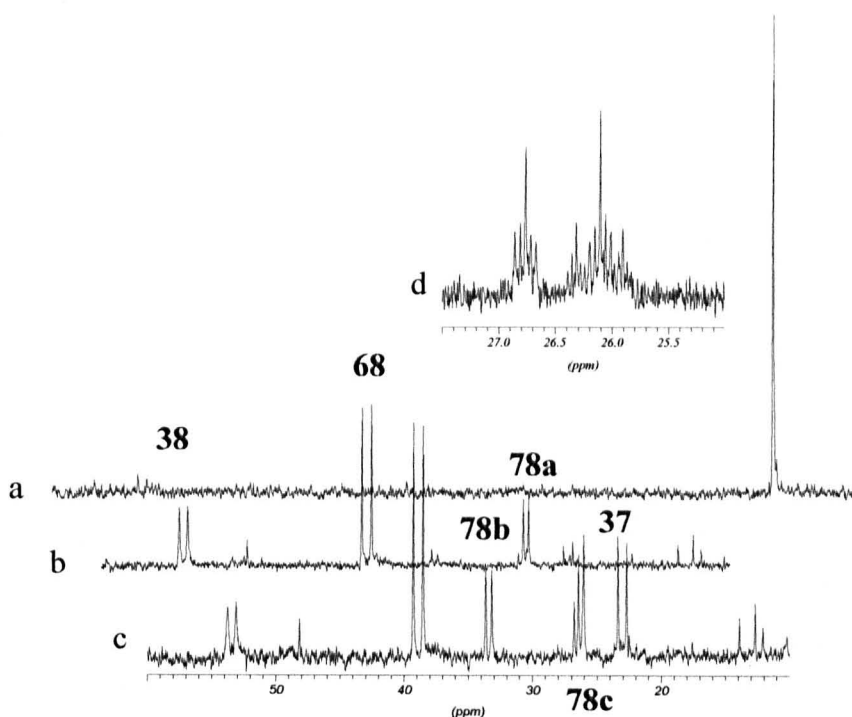


Fig. 6.29. Addition of PPh_3 to a solution of $[Rh(\mu-Cl)(CO)_2]_2$ in $[emim][Al_2Cl_7]$: a) an equivalent; b) three equivalents; c) ten equivalents. Table 6.17 shows the ^{31}P NMR parameters; d) Expansion of signal of **78a** and **78c** at $-40^\circ C$ when ^{13}CO is used.

Table 6.17. ³¹P NMR parameters for every species observed in the addition of PPh₃ to the solution of [Rh(μ-Cl)(CO)₂]₂ in [emim][Al₂Cl₇].

³¹ P NMR	38	68	78a	78b	78c	37
δ ³¹ P	53.4	38.8	26.1	32.9	26.4	22.9
¹ J(¹⁰³ Rh- ³¹ P)	107.4	123.1	67.2	71.5	106.2	106.9

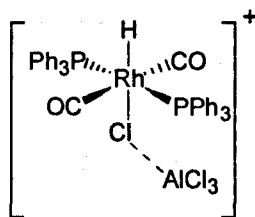
The observation of new signals, assigned as **78a**, **78b** and **78c** should be explained in terms of the quantity of PPh₃ in solution. The magnitude of the Rh-P coupling in **78a** and **78b** suggests Rh(III) species. The multiplicity of the signals in Fig. 6.29d of complexes **78a** and **78c** due to the enrichment of the starting material and their spectrum at low temperature gives possible alternatives for their structures, Fig. 6.30.

The ¹³C NMR spectra of this solution show signals at 185, 180.3, 175.1 and 173.0 ppm. It is known that complexes **37**, **68/38/77** correspond to 180.3 and 175.1 ppm signals respectively. The signal at 175.1 ppm corresponds to a doublet with a broad base that suggests that **68** and **38** are hidden by the large amount of **77**. The addition of 8 equivalents and then 10 equivalents of PPh₃ to the solution make the signals at 26.1 ppm in the ³¹P NMR spectra increase and the signal at 26.4 ppm decrease in the same spectrum. In the same way, the signal at 173.1 ppm increases while the signal at 185.5 ppm decreases in the ¹³C NMR spectrum. This gives the conclusion that the signal at 26.1 ppm corresponds to the one at 173.1 ppm (complex **78a**) in the ¹³C NMR spectrum and the signal at 26.4 ppm corresponds to 185.5 ppm at room temperature, (complex **78c**). In addition, the signal of **78c** was observed before, during the characterization of **37** in very low concentration at -40°C. The multiplicity of the signal in the ³¹P NMR spectrum by using ¹³C enriched material corresponds to a doublet of triplets for the fully enriched complex and a double of doublets for the partially enriched compound. This multiplicity corresponds to two *cis*-CO coupling to the PPh₃. Also, this signal correlates to a signal in the ¹³C NMR spectrum at 187.7 ppm, as a doublet ¹J(¹⁰³Rh-¹³C) 65.5 Hz of triplet ¹J(³¹P-¹³C) 15.0 Hz. The coupling P-C suggests the presence of two phosphines.

The signal at 171 shows a broad doublet without clear multiplicity. Table 6.16 shows the ¹³C NMR parameters of the signals observed during the addition and the Fig. 6.28 shows the ¹³C NMR spectra. The ¹H NMR spectrum of the last solution does not show any clear

hydride signal and the only visible signal is the one at -12.5 ppm that corresponds to complex **38**.

Note that the signal due to **78a** is observed during the formation of **38** which suggests the presence of HCl in the medium to get Rh(III) complexes. The multiplicity of **78a** at low temperature with the enrichment of ¹³CO suggests the presence of two ¹³CO *cis* to a phosphine. The ¹H NMR spectrum during the observation of **38** and **78a** in 6.28b shows two small signals that are not very clear at -12.9 ppm and -13.5 ppm. The signal at -12.5 corresponds to **38** hydride (section 6.1). The signal at -13.5 is very small, and it is unknown how many PPh₃ groups are attached to **78a**. The possibility of the addition of HCl to **38** without losing the PPh₃, before the formation of **38** may be considered, although it cannot be proved.



78a

The signal of **78b** is a new signal that has not been observed before and may correspond to a Rh(III) due to the small Rh-P coupling. A Rh(III) species such as **78b** may be easily reduced to **68** by losing HCl. Also, this complex does not show any correlation with any ¹³CO signal in the ¹³C NMR spectrum. A possible elimination of the CO in the initial complex can give this result. There is not a hydride signal observed in the ¹H NMR associated to signal of **78c**, but the coupling suggests an oxidation state of (III) for rhodium.

It has been reported that AlCl₃ reacts with [Rh(CO)₂(Cl)(PR₃)₃], PR₃ = PPh₃, PCy₃, to give [Rh(CO)₂(PR₃)₂][AlCl₄] and the IR corresponds to ν_{CO} 2017 and 1997 cm⁻¹ respectively.⁵⁴ This band does not match with the product **77** that shows a strong band at 2119 and 2071 cm⁻¹ in the ν_{CO} region. The last experiment has shown that the presence of CO and the introduction of moisture may produce other species that have not been observed by Rotondo's study. The observation of new species in [emim][Al₂Cl₇] is producing a new area to study in more detail. A possibility to elucidate the structures of complexes **78a-c** may be a ³¹P - ¹³C correlation NMR spectrum to ensure which signal of the ³¹P spectrum in Fig. 6.29 correlates with the ones in Fig. 6.28 for ¹³C NMR. Until now it is not conclusive.

The next section shows the carbonylation of [Rh{(μ-Cl)AlCl₃}{(μ-Cl)₂AlCl₂}(H)(PR₃)₂] in [emim][Al₂Cl₇] and their comparison with the results observed with PPh₃.

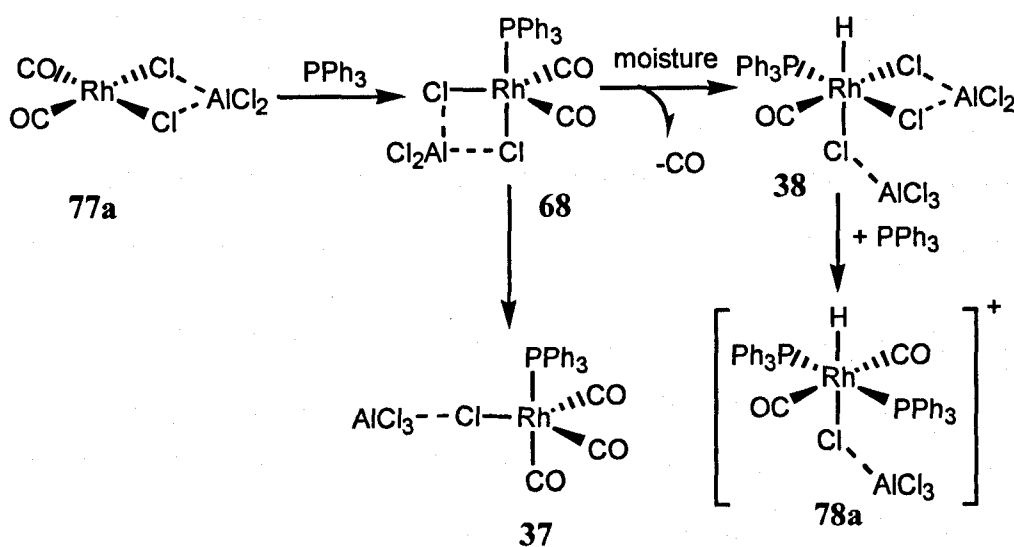


Fig. 6.30. Formation of the complexes observed during the addition of [PPh₃] to [Rh{(μ-Cl)₂AlCl₂}(CO)₂], 77 in [emim][Al₂Cl₇].

6.7. Carbonylation of [Rh{(μ-Cl)AlCl₃}{(μ-Cl)₂AlCl₂}(H)(CO)(PR₃)] in [emim][Al₂Cl₇]

The comparison of PPh₃ and other PR₃ gives further information on behaviour observed in the chloroaluminate ionic liquid. This comparison gives more detail about the origin of the interaction with the medium but also gives a background to compare with the known complexes and corroborates that the species observed in [emim][Al₂Cl₇] has not been observed before in any organic solvent.

The addition of CO to the NMR tubes containing a solution of [Rh{(μ-Cl)AlCl₂}{(μ-Cl)AlCl₃}H(CO)(PR₃)] where R₃ = Me₂Ph, (45b), Et₃, (54), MePh₂, (55), EtPh₂, (56), Bu^tEt₂, (57), Bu^tBuⁿ₂, (58), Bu^tPrⁱ₂, (59), Cy₃, (60), Bu₂Ph, (61), gives the observation of two products in all cases. The first observed product corresponds to an analogue of 37 and has been assigned as carbonyl B in Fig. 6.31. The second product, which is the most stable in every case, is the product corresponding to an analogue of 68, and has been assigned as

carbonyl **C** in the same figure. Table 6.18 shows the values of the ³¹P NMR parameters for the observed products for each phosphine.

Note that the coupling constant of the carbonyl **B** complexes in Table 6.18 shows smaller coupling in all cases than the second carbonyl **C**. The coupling constant Rh-P for the case of PEt₃, complex **80a**, is smaller for the rest of the phosphines. Once again PEt₃ shows a combination of basicity and size. The complex with PPh₃ shows the larger coupling for the first and second carbonyl complex. Note that for the case of the second carbonyl, the coupling ¹J(¹⁰³Rh-³¹P) of the complex with PPh₃ is larger than all the rest. The complexes of Rh(III) in Table 6.6 that come from the addition of HCl to the Vaska's type complexes show that the complex with PPh₃ has also the larger coupling constant. This is the result of the larger ability of the phenyl groups to make the phosphine able to accept electron density from the metal and increase the interaction Rh-P. Then, the coupling is larger than the rest of the phosphine that are less acceptor but more basic such as PCy₃.

Surprisingly, the expected second carbonyl **86b** was not observed in the case of PCy₃ under the same conditions as the other complexes. This result is not well understood. Possible explanations may be the larger stability of the complex **86a** with the last phosphorus group due to the basicity of PCy₃.

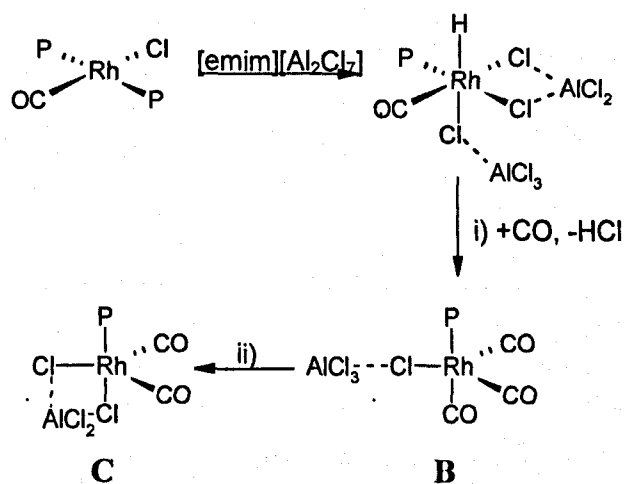


Fig. 6.31. Summary of reactions that generalize the formation of analogues species to **37**, (**B**) and **68**, (**C**) but with different PR₃. The initial formation of carbonyl **A** has been explained in section 6.2.3. Condition for the conversion of **B** to **C** is the continuous addition of CO in [emim][Al₂Cl₇].

Fig. 6.32 shows the graphs of Δ vs δ for carbonyl **B**. The value of Δ is defined by the difference between the chemical shift of the carbonyl complex and the free phosphine in

organic solvents. This definition has been explained in section 6.2.3 and Eq. 6.7 clearly explains the definition for Δ for the case of carbonyl B.⁵⁵

$$\Delta = \delta[\text{Rh}\{(\mu\text{-Cl})\text{AlCl}_3\}(\text{CO})_3(\text{PR}_3)] \text{ ppm in } [\text{emim}][\text{Al}_2\text{Cl}_7] - \delta[\text{PR}_3] \text{ free ppm organic solvent Eq. 6.7}$$

Table 6.18. ³¹P NMR parameters for products after the carbonylation of [Rh{(μ-Cl)AlCl₃}{(μ-Cl)₂AlCl₂}(H)(CO)(PR₃)] in [emim][Al₂Cl₇]. Carbonyl B correspond to [Rh{(μ-Cl)AlCl₃}{(CO)₃(PR₃)}], analogue of 37, while carbonyl C correspond to [Rh{(μ-Cl)₂AlCl₂}{(CO)₂(PR₃)}]. See Fig. 6.31.

Phosphine	First carbonyl Carbonyl B		Phosphine	Second carbonyl Carbonyl C	
	$\delta^{31\text{P}}$	$^1J(^{103}\text{Rh}-^{31}\text{P})$		$\delta^{31\text{P}}$	$^1J(^{103}\text{Rh}-^{31}\text{P})$
79a PMe ₂ Ph	25.3	105.9	79b PMe ₂ Ph	31.7	112.6
80a PEt ₃	29.7	96.7	80b PEt ₃	66.7	112.1
81a PMePh ₂	8.6	104.4	81b PMePh ₂	30.4	117.4
82a PEtPh ₂	22.3	105.7	82b PEtPh ₂	45.5	117.4
37 PPh ₃	22.7	108.1	68 PPh ₃	38.8	123.4
83a PBu ^t Et ₂	50.1	101.9	83a PBu ^t Et ₂	88.9	114.6
84a PBu ^t Bu ₂ ⁿ	45.5	103.1	84b PBu ^t Bu ₂ ⁿ	84.9	114.4
85a PBu ^t Pr ₂ ⁿ	44.7	101.0	85b PBu ^t Pr ₂ ⁿ	84.2	114.2
86a PCy ₃	49.7	103.2	86b PCy ₃	Not observed	
87a Bu ^t ₂ Ph	68.3	104.4	87b Bu ^t ₂ Ph	70.2	110.5

Table 6.19 shows the values of Δ that are plotted in Fig. 6.32 for the carbonyls [Rh{(μ-Cl)AlCl₃}{(CO)₃(PR₃)}], B, in the reaction of carbonylation of [Rh{(μ-Cl)AlCl₃}{(μ-Cl)₂AlCl₂}(H)(CO)(PR₃)], A, with different PR₃ groups. It is clear that PR₃ with bulky groups such as *ter*-butyls shows a different linearity to PR₃ with less steric demanding groups. In the same way, when Δ for carbonyls [Rh{(μ-Cl)₂AlCl₂}{(CO)₂(PR₃)}], C, that are shown in Table 6.20, are plotted in Fig. 6.33, the larger steric demanding groups show a different Δ to the values of less steric demanding groups.

Table 6.19. Values of Δ for carbonyl $[Rh\{(\mu\text{-Cl})AlCl_3\}(CO)_3(PR_3)]$, **B** and carbonyl $[Rh\{(\mu\text{-Cl})_2AlCl_2\}(CO)_2(PR_3)]$, **C**. The value of Δ has been defined in Eq. 6.7. The plot for Δ **B** is shown in Fig. 6.32 and for Δ **C** is shown in Fig. 6.33.

Phosphine	Free PR ₃ org. solv.	Δ carbonyl B	Complex	Δ carbonyl C
79a PMe ₂ Ph	-47	72	79b	78
81a PMePh ₂	-27	35	81b	57
80a PEt ₃	-20	49	80b	
84a P ^t Bu ⁿ Bu ₂	-4	49	84b	88
37 PPh ₃	-10	32	68	48
83a P ^t BuEt ₂	6	44	83b	82
82a PEtPh ₂	14	8	82b	31
86a PCy ₃	37	44	86b	
87a P ^t Bu ₂ Ph	37	31	87b	33

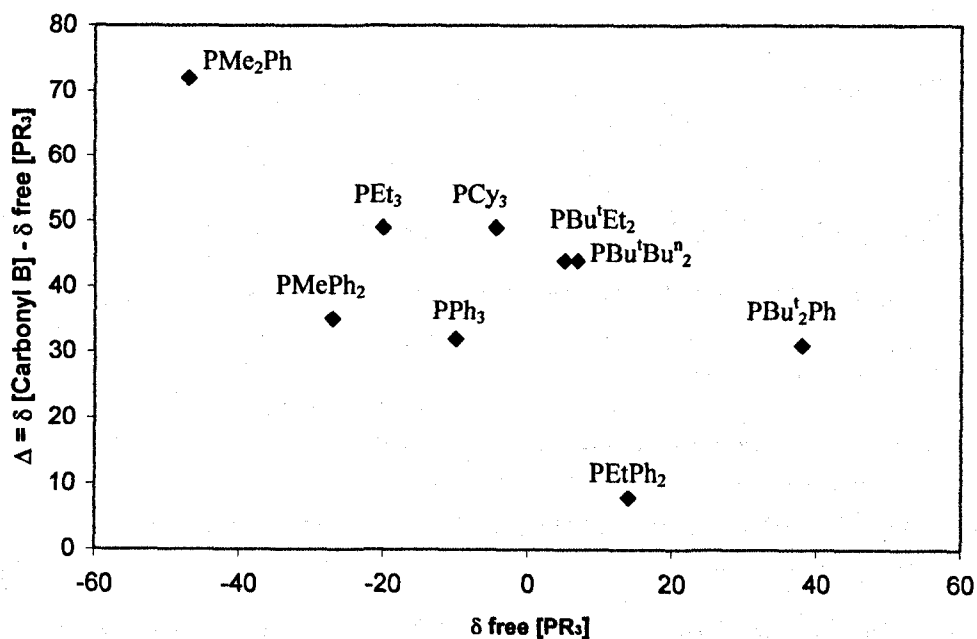


Fig. 6.32. This graph shows the correlation of Δ of Rh complexes vs the frequency of free PR₃ in organic solvents: Complex **B** corresponds to $[Rh\{(\mu\text{-Cl})AlCl_3\}(CO)_3(PR_3)]$ in [emim][Al₂Cl₇].

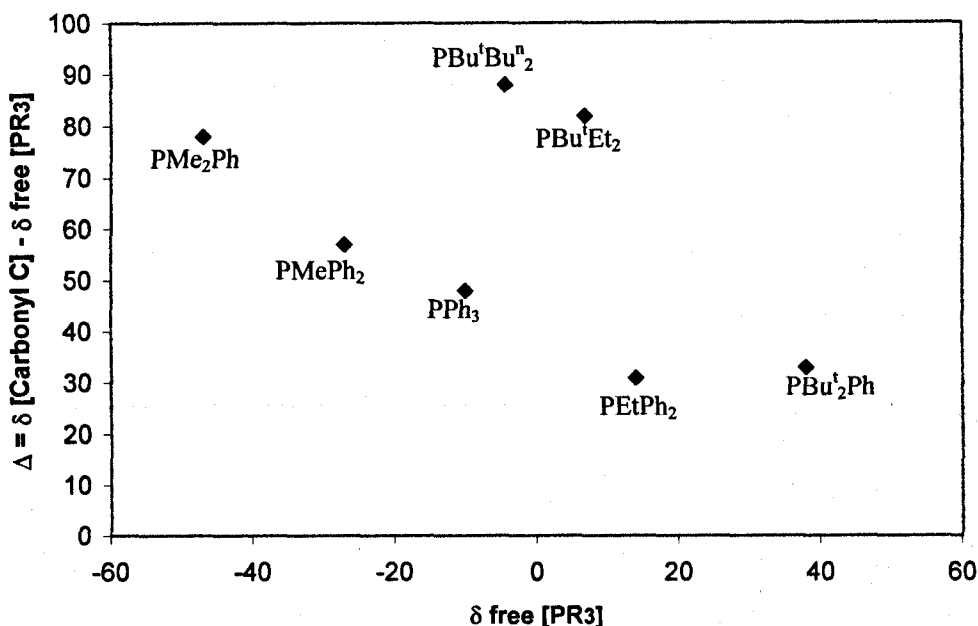


Fig. 6.33. This graph shows the correlation of Δ of Rh complexes vs the frequency of free PR_3 in organic solvents: Complex C corresponds to $[\text{Rh}\{(\mu\text{-Cl})_2\text{AlCl}_2\}(\text{CO})_2(\text{PR}_3)]$ in $[\text{emim}][\text{Al}_2\text{Cl}_7]$.

6.8. Solution of $[\text{Rh}(\text{H})(\text{CO})(\text{PPh}_3)_3]$ in $[\text{emim}][\text{Al}_2\text{Cl}_7]$

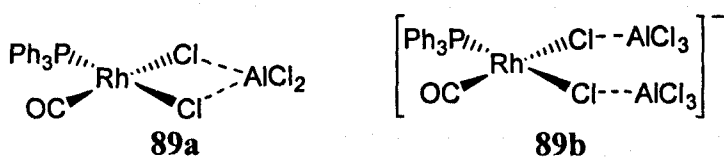
Finally, this section explains the results by using the last rhodium complex in this chapter. The importance of this reaction is the observation of many of the complexes already observed with $[\text{RhCl}(\text{PPh}_3)_3]$ and $[\text{RhCl}(\text{CO})(\text{PPh}_3)_2]$. It is known that $[\text{Rh}(\text{H})(\text{CO})(\text{PPh}_3)_3]$ is an important precursor in the catalytic hydroformylation of olefins, hence it is important to know the differences in chemistry that occurs in $[\text{emim}][\text{Al}_2\text{Cl}_7]$.⁵⁶

When the ³¹P NMR spectrum of the solution of $[\text{Rh}(\text{H})(\text{CO})(\text{PPh}_3)_3]$ in $[\text{emim}][\text{Al}_2\text{Cl}_7]$ is observed, three main species are observed: $[\text{HPPh}_3]^+$, 6.5 ppm, $[\text{Rh}\{(\mu\text{-Cl})\text{AlCl}_3\}(\text{H})(\text{PPh}_3)_2]$, **24**, at 58 ppm, $^1J(^{103}\text{Rh}\text{-}^{31}\text{P})$ 144 Hz, and a new signal at 44.7 ppm, $^1J(^{103}\text{Rh}\text{-}^{31}\text{P})$ 182.9 Hz. The last signal had not been observed before but the first alternative to chose was a dimer that Rotondo's group has proposed but with the interaction of the anion $[\text{AlCl}_4]^-$. Rotondo's work⁵ has postulated the formation of the dimer **88a** with a large coupling of around 174 Hz and with the ³¹P chemical shift similar to the one observed in $[\text{emim}][\text{Al}_2\text{Cl}_7]$; **88a** has also an isomer **88b** with similar NMR data, Table 6.21.

Table 6.21. ³¹P NMR parameters for known complexes **88a-b** proposed by Rotondo and the dimer observed in [emim][Al₂Cl₇] in the solution of [Rh(H)(CO)(PPh₃)₃].

δ ppm	45.9 ppm	44.7	44.7
J_{RhP} Hz	175.8	176.9	182

Based on the complexes **88a-b**, the structure **89** is proposed for the species present in [emim][Al₂Cl₇]. The position of the phosphine in **89** cannot be known and it can be either in *cis* or *trans* position. This dimer was not observed before in solution of [Rh(Cl)(PPh₃)₃] or [Rh(Cl)(CO)(PPh₃)₂] in [emim][Al₂Cl₇] with CO. It does not survive solution more than one day with the formation of [Rh{(μ-Cl)AlCl₃}{(μ-Cl₂)AlCl₂}(H)(CO)(PPh₃)₃], **38**. It is worth noting that the existence of terminal [(μ-Cl)AlCl₃]⁻ or [(μ-Cl)₂AlCl₂]⁻ in **89** produces two alternatives in the structure in solution and they cannot be eliminated.



The addition of cyclohexene to the solution of **25** or **89** in [emim][Al₂Cl₇] produces the destruction of the signal of **25**, which was an expected reaction and section 4.3, Fig. 4.17 has explained this reaction. The signal of the dimer **89** does not disappear in the presence of cyclohexene and this agrees with the assumption that rhodium dimers are not the direct catalyst in the hydrogenation or hydroformylation cycles.⁵⁷ The signal of **89** disappears after some hours and produces a separate complex that was assumed to be an analogue to **37** but with two phosphines at 26.6 ppm, 107 Hz or it may be the interaction with oxygen or oxochloroaluminate (III) species in the ionic solution, **78c**.

This also produces a different chemistry of the hydride *trans*-[Rh{(μ-Cl)AlCl₃}(H)(PPh₃)₂]⁻, **24**, and the monocarbonylphosphine **89**. It's not well understood why the Vaska's type complex gives only Rh(III) complex hydride and the triphosphine hydride produces a different complex. The presence of an excess of PPh₃ in the media may

be a source of such a difference. This complex is not observed during the addition of PPh₃ to [Rh{(μ-Cl)AlCl₃}₂(CO)₂][□], 77, section 6.7.

6.9. Summary of the solutions of [Rh(Cl)(PPh₃)₃], [RhCl(CO)(PR₃)₂], [Rh(μ-Cl)(CO)₂]₂ and [Rh(H)(CO)(PPh₃)₂] in [emim][Al₂Cl₇]

The present chapter has shown the ability of chloroaluminate (III) anions to stabilize new rhodium species that had not been observed before in common organic solvents. The formation of ionic species in the ionic liquid may be the reason for the unsuccessful isolation of any of these species and increase the difficulty of complete characterization. However, by comparison with known rhodium complexes, the proposal of the formed species in the ionic liquid can be backed up although they cannot be proved completely. Fig. 6.34 shows a complete review of the complexes that have been proposed in chapters 4 and 6.

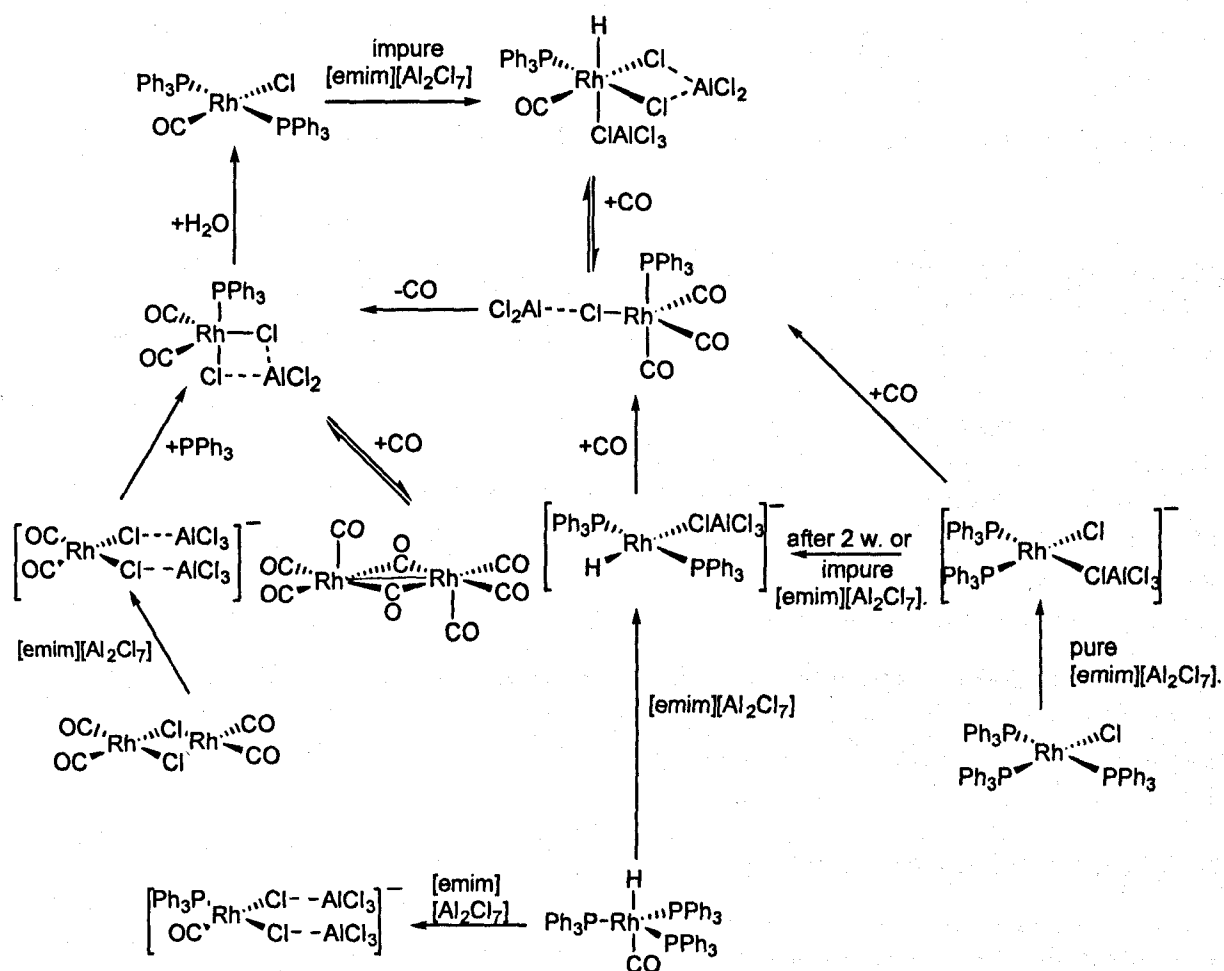


Fig. 6.34. General review of the complexes proposed in chapters 4 and 6.

In addition, the formation of ionic species may be the clue to explain why these species remain the ionic liquids, not only chloroaluminate but also in [Sn₂Cl₅]⁻ and the next section will show the interaction of some rhodium complexes with the last kind of ionic liquids.

If this is true, the use of ionic liquids can produce new mechanistic pathways to the one already established in organic solvents. This produces, indeed, a new area to research.

6.10. References

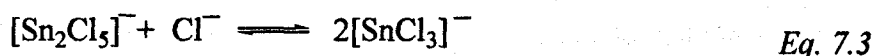
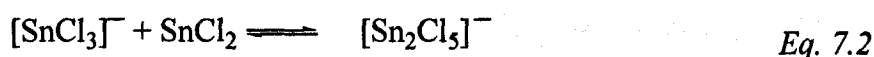
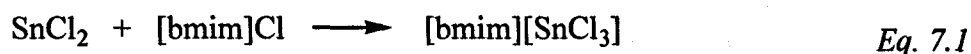
- ¹ G. Wilkinson, *J. Chem. Soc. A*, 1967, 1357.
- ² J. M. Brown, L. R. Canning, A.G. Kent and P. J. Sidebottom, *J. Chem. Soc., Chem. Commun.*, 1982, 721.
- ³ M. G. Partridge, B. A. Mersserle and L. D. Field, *Organometallics*, 1995, **14**, 3527.
- ⁴ J. E. Huheey, *Inorganic Chemistry: principles of structure and reactivity*, Harper Collins College Publishers, New York, 1993, 4th edn.
- ⁵ G. Battaglia, F. P. Cusmano, G. Giordano and E. Rotondo, *J. Organomet. Chem.*, 1993, **450**, 245.
- ⁶ A. R. Sanger, *Can. J. Chem.*, 1985, **63**, 571.
- ⁷ F. R. Bregman, J. M. Ernsting, F. Muller, M. D. K. Bolee, L. A. Van der Veen and C. J. Elsevier, *J. Organomet. Chem.*, 1999, **592**, 306.
- ⁸ T. A. Zawodzinski and R. A. Osteryoung, *Inorg. Chem.*, 1987, **26**, 2920; T. Zawodzinski and R. Osteryoung, *Inorg. Chem.*, 1990, **26**, 2842; A. Absul-Sada, A. Greenway, K. R. Seddon and T. Welton, *Org. Mass Spectrom.*, 1993, **28**, 759.
- ⁹ B. E. Mann, C. Masters and B. L. Shaw, *J. Chem. Soc., Dalton Trans.*, 1971, 704.
- ¹⁰ A. M. Lebuis, A. K. Kakkar and M. G. L. Petrucci, *Organometallics*, 1998, **17**, 4966.
- ¹¹ J. A. Tiethof, J. L. Peterson and D. W. Meek, *Inorg. Chem.*, 1976, **15**, 1365.
- ¹² E. M. Hyde, J. D. Kennedy, B. L. Shaw and W. McFarlene, *J. Chem. Soc., Dalton Trans.*, 1977, 1571.
- ¹³ B. E. Mann, C. Masters and B. L. Shaw, *J. Chem. Soc.*, 1971, 1104.
- ¹⁴ G. Deganello, P. Uguagliati, B. Crociani and U. Belluco, *J. Chem. Soc. A*, 1969, **18**, 2726; G. M. Intille, *Inorg. Chem.*, 1972, **11**, 695; J. Gallay, D. De Montauzon and R. Poilblanc, *J. Organomet. Chem.*, 1972, **38**, 179.
- ¹⁵ R. K. Harris, E. D. Becker, S. M. Cabral, R. Goodfellow and P. Granger, *Pure Appl. Chem.*, 2001, **73**, 1795.
- ¹⁶ G. A. Morris and R. Freeman, *J. Am. Chem. Soc.*, 1979, **101**, 760; B. E. Mann, *Ann. Rep. NMR*, 1991, **23**, 141.
- ¹⁷ J. Mason, *Chem. Rev.*, 1987, **87**, 1299; B. E. Mann, *Transition Metal NMR*, P. S. Pregosin, Elsevier, Amsterdam, 1991, pp 177.
- ¹⁸ T. H. Brown and P. J. Green, *J. Am. Chem. Soc.*, **92**, 2359, 1970.

- 19 I. S. Butler, A. A. Ismail, F. Sauriol and J. Sedman, *Organometallics*, 1985, **4**, 1914.
- 20 R. K. Harris and B. E. Mann., *NMR and the Periodic Table*, Academic Press, London, 1978.
- 21 R. A. Hoffman and S. Forsén, *Prog. Nucl. Magn. Reson. Spectrosc.*, 1966, **1**, 15.
- 22 P. Güntert, W. Braun, M. Billeter and K. Wüthrich, *J. Am. Chem. Soc.*, 1989, **111**, 3997.
- 23 D. S. Moore and S. D. Robinson, *Chem. Soc. Rev.*, 1983, **12**, 415.
- 24 L. D. Field and M. V. Baker, *Inorg. Chem.* 1987, **26**, 2011.
- 25 L.D. Field, N. Bampos and B. A. Messerle, *Organometallics*, 1993, **12**, 2529.
- 26 P. S. Pregosin and R. W. Kunz, *NMR Basic Princ. Prog.*, 1979, **15**, 28; M. Pankowski, W. Chodkiewicz and M. P. Simonnin, *Inorg. Chem.*, 1985, **24**, 533.
- 27 J. M. Brown and A. G. Kent, *J. Chem. Soc., Perkin Trans. 2*, 1987, 1597.
- 28 C. J. Jameson, *J. Am. Chem. Soc.*, 1969, **91**, 6232.
- 29 E. G. Thaler, K. Folting and K. G. Caulton, *J. Am. Chem. Soc.*, 1990, **112**, 2664.
- 30 B. T. Heaton, C. Jacob and S. Moffet, *J. Organomet. Chem.*, 1993, **462**, 353.
- 31 J. P. Jesson and E. L. Muetterties, in *Dynamic Nuclear Magnetic Resonance Spectroscopy*, by L.M. Jackman and F.A. Cotton, Academic Press, New York, 1975, ch. 8.
- 32 H. Lee, J. Bae, J. Ko, Y. S. Kang, H. S. Kim, S. Kim, J. H. Chung and S. O. Kang, *J. Organomet. Chem.* 2000, **614**, 83.
- 33 A. Bresler, N. A. Buzina, Y. S. Varshavsky, N. V. Kiseleva and A. G. Cherkasova, *J. Organomet. Chem.*, 1979, **171**, 229.
- 34 A. D. English, S. D. Ittel, P. Jesson, P. Meakin and C. A. Tolman, *J. Am. Chem. Soc.*, 1977, **99**, 117.
- 35 A. D. English, P. Meakin and P. Jesson, *J. Am. Chem. Soc.*, 1976, **98**, 7590.
- 36 L.D. Field, N. Bampos and B. A. Messerle, *Organometallics*, 1993, **12**, 2529.
- 37 C. Allevi, M. Golding, B. T. Heaton, C. A. Ghilardi, S. Midollini and A. Orlandini, *J. Organomet. Chem.*, 1987, **326**, C19.
- 38 F. A. Cotton, L. Kruczynski, B. L. Shapiro, and L. F. Jonson, *J. Am. Chem. Soc.*, 1972, **94**, 6191.
- 39 P. Caddy, M. Green, L. E. Smart and N. White, *J. Chem. Soc., Chem. Commun.* 1978, 839.
- 40 R. J. Lawson and J. R. Shapley, *Inorg. Chem.*, 1978, **17**, 2963.
- 41 R. T. Carlin and J. Fuller, *Inorg. Chim. Acta*, 1997, **255**, 189.
- 42 Q. Xu, S. Inoue, Y. Souma and H. Nakatani, H., *J. Organomet. Chem.*, 2000, **606**, 147.
- 43 T. G. Richmond, F. Basolo and D. F. Shriver, *Inorg. Chem.*, 1982, **21**, 1272.
- 44 S. B. Butts, S. H. Strauss, E. M. Holt, R. E. Stimson, N. W. Alcock and D. F. Shriver, *J. Am. Chem. Soc.*, 1980, **102**, 5093.
- 45 J. E. Huheey, *Inorganic chemistry: principles of structure and reactivity*, 2nd edn, New York 1978.
- 46 C. O'Connor, G. Yagupski, D. Evans and G. Wilkinson, *J. Chem. Soc., Chem. Commun.* 1968, 421.

- ⁴⁷ R. R. Burch, E. L. Muetterties, A. J. Schultz, E. G. Gebert and J. M. Williams, *J. Am. Chem. Soc.*, 1981, **103**, 5517; A. S. C. Chan, H. S. Shieh and J. R. Hill, *J. Chem. Soc., Chem. Commun.*, 1983, 688.
- ⁴⁸ J. M. Brown and A. G. Kent, *J. Chem. Soc., Perkin Trans. 2*, 1987, 1597.
- ⁴⁹ P. Singh, C. B. Dammann and D. J. Hodgson, *Inorg. Chem.*, 1973, **12**, 1335.
- ⁵⁰ M. A. Freeman and D. A. Young, *Inorg. Chem.*, 1986, **25**, 1556.
- ⁵¹ R. Whyman, *J. Chem. Soc., Chem. Commun.* 1970, 230; R. Whyman, *J. Chem. Soc., Chem. Commun.* 1970, 1194; R. Whyman, *J. Chem. Soc., Chem. Commun.* 1972, 1375; L. A. Halan and G. A. Ozin, *J. Am. Chem. Soc.*, 1974, **96**, 6324.
- ⁵² G. Aullon and S. Alvarez, *Eur. J. Inorg. Chem.*, 2001, 3031.
- ⁵³ D. T. Brown, T. Eguchi, B. T. Heaton, J. A. Iggo and R. Whyman, *J. Chem. Soc., Dalton. Trans.*, 1991, 677.
- ⁵⁴ W. Heiber and V. Frey, *Chem. Ber.* 1966, **99**, 2614.
- ⁵⁵ B. E. Mann, C. Masters and B. L. Shaw, *J. Chem. Soc.*, 1971, 1104.
- ⁵⁶ A. M. Trzeciak and J. J. Ziolkowski, *Coord. Chem. Rev.*, 1999, **190-192**, 883.
- ⁵⁷ C. A. Tolman, P. Z. Meakin, D. L. Lindner and J. P. Jesson, *J. Am. Chem. Soc.*, 1971, **96**, 1571; M. Torrent, M. Sola and G. Frenking, *Chem. Rev.*, 2000, **100**, 439.

7. Results and discussion: Solutions in [bmim][Sn₂Cl₅]

This chapter shows the study of [bmim][Sn₂Cl₅], $x_{\text{SnCl}_2} = 0.6$, which is an acidic ionic liquid but not as strong as the chloroaluminate (III). The addition of an excess of SnCl₂ into the mixture allows the existence of equilibrium in Eq. 7.2, and the presence of chlorides from the organic salt allows the dissociation of the dimeric tin anion to give the [SnCl₃]⁻ again as is shown in Eq. 7.3. Similar to chloroaluminate (III), the excess of SnCl₂ in the mixture $x_{\text{SnCl}_2} > 0.5$ produces acid mixtures while a molar fraction $x_{\text{SnCl}_2} < 0.5$ in the mixture produces basic mixtures.¹



The results in the present chapter show the use of acidic mixtures where the rhodium complexes are completely soluble and as an analogue to compare with chloroaluminate (III) ionic liquids in chapters 4 and 6. Also, the presence of [SnCl₃]⁻ in the media can act as ligands and interact with metals (section 2.7). The insertion of SnCl₂ in Rh-Cl bonds in the used complexes produces new Rh-SnCl₃ species that have not been observed before in organic solvents. The existence of similar complexes has been reported without any detail and that is the case for [Rh(Cl)(CO)(PR₃)₂], PR₃ = PEt₃, PPh₃ and PEtPh₂ with SnCl₂.²

Tin has three NMR active nuclei ¹¹⁹Sn, ¹¹⁷Sn and ¹¹⁵Sn in 8.6, 7.6 and 0.35% abundance respectively. ¹¹⁹Sn is the one usually studied due to higher abundance and sensitivity while ¹¹⁵Sn is very seldom used. The concentration of [Sn₂Cl₅]⁻ in the ionic solvent is very high and this prevents the observation of ¹¹⁷Sn or ¹¹⁹Sn signals from the rhodium complexes. However, ³¹P NMR was very helpful in clarifying the structure in solution due to the ^{119/117}Sn satellites and the partial identification of each new complex. It is known that the main signal resonance of molecules with several tin atoms is flanked by satellites arising from coupling between ¹¹⁹Sn, ¹¹⁷Sn and ^{117/119}Sn that cannot be resolved in

many cases, especially when the Sn-P coupling is small.³ The integration of the main signal and the satellites gives an estimate of how many tins are coupled to the phosphorus, hence how many tins are attached to the rhodium centre.

7.1. Solution of [RhCl(PPh₃)₃] in [bmim][Sn₂Cl₅].

The study of the Wilkinson catalysts with SnCl₂ has been reported before but no details about structure and NMR spectroscopy have been given.⁴ Fig. 6.1 shows the ³¹P NMR spectra of the solution of the Wilkinson catalyst in [bmim][Sn₂Cl₅] at room temperature: δ – 5.9 ppm free PPh₃; and a doublet 43.4 ppm ¹J(¹⁰³Rh-³¹P) 124 Hz. The integration of the signals corresponds to one and two phosphorus nuclei respectively.

The signal that corresponds to the free PPh₃ is particularly broad. The interaction of PPh₃ with tin(IV) halides has been recently reported,⁵ suggesting that a Sn-P bond can be formed in the presence of an excess of tin halides. This may be a similar case in [bmim][Sn₂Cl₇] that has a large concentration of tin(II) halide anions. Note that an important characteristic of tin is its availability to increase the coordination number, this characteristic makes possible the interaction of PPh₃ with the ionic medium.

The doublet at 43.4 ppm shows tin satellites, giving a coupling ²J(^{117/119}Sn-³¹P) 153.0 Hz and has been assigned as 90. It is consistent with the formation of a rhodium species with the interaction of chlorostannates and the liberation of a phosphine from the original material (similar to chloroaluminate (III), chapter 4). It has been mentioned that the integration of the satellites gives information about how many tins are coupled to the phosphorus. This information is a result of the splitting of the main signal. The presence of only one tin gives a pattern with intensity in the satellites 8.3%:83.4%:8.3%. The coupling of the phosphorus to two similar tins changes the intensity of the main signal and the satellites to 14.3%:71.4%:14.3%. The intensity of the tin satellite 1 in Fig. 7.1 is 7.8%, the same as satellite signal 4. The main signal at 43.4 ppm in the spectrum in Fig. 7.1 (signal 2-3) is broad in the base because it is hiding half of the tin satellites and it integrates to 84.4%. This suggests that each complete tin satellite is 15.6% and the main signal is 68.8% once the tin satellites have been subtracted from the observed value. Having an integration of 15.6%:68.8%:15.6%, suggests the presence of two tins in the metallic centre.

The coupling constant $^1J(^{103}\text{Rh}-^{31}\text{P})$ 124 Hz for complex **90** is common for Rh(I) complexes. A clear example is the Vaska's type complex **36** [Rh(Cl)(CO)(PPh₃)₃] whose coupling is 127 Hz and Table 6.10 shows more examples of these kinds of complexes. Note that the species observed in [bmim][Sn₂Cl₇] has two tins, two phosphorus and the coupling is consistent with a Rh(I) centre. Hence, two good possibilities for the structure in solution are **90a** and **90b**. The *cis*-arrangement is unlikely because the large *trans*-influence of tin would produce a smaller constant $^1J(^{103}\text{Rh}-^{31}\text{P})$ and it is known that the magnitude of *trans*-coupling Sn-P is usually very large, about 2000 Hz for Rh(III) complexes⁶ and it is even larger for complexes with Pt(II) 3044-4848 Hz, which is a *d*⁸ centre, the same as Rh(I) in **90**.⁷

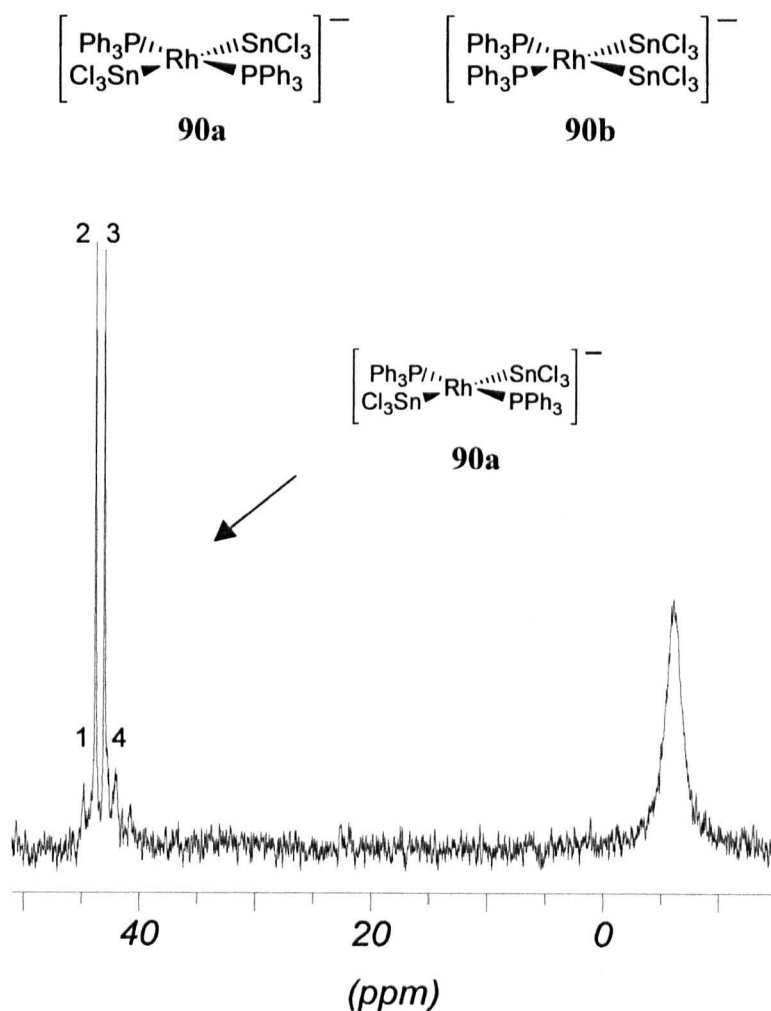


Fig. 7.1. $^{31}\text{P}\{^1\text{H}\}$ -NMR of [RhCl(PPh₃)₃] in [bmim][Sn₂Cl₅] at room temperature, complex **90**. The cation in this case may be the [bmim]⁺ present in the ionic liquid.

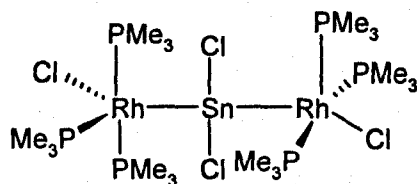
The *trans*-arrangement **90a** is a better possibility. Also, the value of coupling in **95a** is in the average of the Vaska's type complex where coupling constant $^1J(^{103}\text{Rh}-^{31}\text{P})$ is 126 Hz.

It is known that complexes with d^8 centres such as [Pt(SnCl₃)₂(P(OR)₃)₂], where R = Et, Prⁱ, Ph, have shown the preference of *trans* arrangements over the *cis*.⁸ The complex *trans*-[Pt(SnCl₃)₂(P(OPh)₃)₂] has been fully characterized by x-ray diffraction.⁸

The relative intensities of the two signals at 43.5 and -5.9 ppm in the spectrum in Fig. 7.1 are 2:1. The addition of CD₂Cl₂ to the ionic liquid in the NMR tube makes the signals sharper and the broad singlet at -5.9 ppm is moved to -9.7 ppm. This result may be consistent with the elimination of any P-Sn interaction of the free phosphine in [bmim][Sn₂Cl₅] when it is diluted.

The appearance of the ionic solution with [Rh(SnCl₃)₂(PPh₃)₂]⁻, **90a**, shows the suspension of small red-purple powder and the addition of CH₂Cl₂ allows the precipitation of an oil that is insoluble in any common organic solvent, including toluene, hexane, THF, methanol and ether. Attempts to analyze the oil were unsuccessful due to the oily particles that remained in the glass container and prevented its characterization by other techniques. The attempts to investigate the product in CD₂Cl₂ or any deuterated solvent by running the ¹¹⁹Sn NMR spectrum were unsuccessful due to the insolubility of the isolated compound. The ³¹P NMR spectrum was also quite poor but the last spectrum was clear enough to see the separated complex **90** as the only product in the reaction.

The NMR data on complex **90a** are consistent with the presence of two *trans* PPh₃ and two *trans* [SnCl₃]⁻ ligands. The presence of PPh₃ in a solution of [Rh(SnCl₂)₃] has been reported before and increases the rate of hydrogenation of alkenes and the selective hydrogenation of alkynes but the formation of any new complex was not discussed.⁹ Chan and Marder have discussed the unreactivity of [RhCl(PPh₃)₃] with SnCl₂,¹⁰ but [RhCl(PMe₃)₃] gives a dimer, **23**, that was characterized by x-ray diffraction.



23

They proposed that high electron density and lack of steric hindrance round the metallic centre are essential for a successful complexation of [SnCl₃]⁻ with the metal,⁴ but the reaction of [RhH(SnCl₃)₄][NBu₄] with PBu^t₃ has been described and produces the

complexation of two PBu^t₃ to form [RhClH(SnCl₃)₂(PBu^t₃)₂]⁻.¹¹ Then the formation of **90a** in [bmim][Sn₂Cl₅] may be the result of the high concentration of [SnCl₃]⁻ in solution.

The addition of cyclohexene to the solution of **90** with [bmim][Sn₂Cl₅] does not produce any alteration in the ³¹P NMR spectra. This result may be due to insolubility of the complex in the [bmim][Sn₂Cl₅] and the immiscibility of the olefin with the ionic phase. There is no direct interaction of the rhodium complex with the olefin. It is known that [SnCl₃]⁻ has a stronger *trans*-effect and produces faster catalytic cycles and that is the case for [Pt(PEt₃)₃] in [bmim][Sn₂Cl₅] with hydrogen.¹²

7.2. Solution of [Rh(Cl)(CO)(PPh₃)₂] in [bmim][Sn₂Cl₅]

The solution of [RhCl(CO)(PPh₃)₂] in [bmim][Sn₂Cl₅] shows broad signals at 34.9 ppm in the ³¹P NMR spectrum at room temperature. The signal is not clear and does not show any clear interaction with tin by showing clear ^{119/117}Sn satellites as in the case of [Rh(SnCl₃)₂(PPh₃)₂]⁻, **90a** (Fig. 7.1). The addition of CH₂Cl₂ does not change the pattern of the spectrum at room temperature but decreases the viscosity of the ionic mixture and enables the temperature to be decreased to 240 K. At this temperature the ³¹P signal is split to a doublet with Sn satellites, at 35.5 ppm, ¹J(¹⁰³Rh-³¹P) 93.3 Hz, ²J(Sn-³¹P) 341 Hz and has been assigned to complex **91**. The small coupling ²J(Sn-³¹P) is consistent with a *cis* configuration P-Rh-Sn. The intensities of the tin satellites in the signal at δ 35.5 ppm with respect to the main signal are 13%:74%:13% and are close to the expected intensities for the presence of two tins coupling to phosphorus. In this case, there is no free PPh₃ signal observed. This result suggests the direct addition of two [SnCl₃]⁻ groups to the starting material and the formation of [Rh(SnCl₃)₂(CO)(PPh₃)₂]⁻. The oxidation state of the product may be consistent with Rh(I) due to the similar coupling ¹J(¹⁰³Rh-³¹P) as the pentacoordinated species proposed for **41**, Table 6.10.

Surprisingly, when [Rh(H)(CO)(PPh₃)₃], **42c**, is dissolved in [bmim][Sn₂Cl₅], it shows two broad signals at δ 35.5 and 2.5 ppm, Fig. 7.2a. The solution does not show the presence of any hydride in the ¹H NMR spectrum. It showed the formation of the same signal of **91** at 240 K in [bmim][Sn₂Cl₅]/CD₂Cl₂, in the ³¹P NMR spectrum, Fig. 7.2,b, 35.5 ppm, ¹J(¹⁰³Rh-

³¹P) 93.3 Hz, ²J(Sn-³¹P) 341 Hz. This suggests the formation of the same species as **91** that comes from the interaction of [SnCl₃]⁻ into the Rh centre and the elimination of PPh₃. Also the insertion of a [SnCl₃]⁻ group into the Rh-H bond.

Intensities of the signals at δ 35.5 and 2.5 ppm, in Fig. 7.2, are 2:1 respectively by suppressing nOe in the ³¹P NMR. The signal at 2.5 ppm at low temperature may correspond to the free PPh₃ that has been released from the original complex. Note that the broadness of this signal may correspond to the interaction with the tin chlorides in the environment as has been mentioned before (section 7.1).

The formation of species **91** from the hydride **42c** suggests the elimination of a phosphine from [RhH(CO)(PPh₃)₃] and the replacement of the hydride by [SnCl₃]⁻. It is known that SnCl₂ can weaken the hydride by an agostic interaction. This interaction has been well characterized and may be the explanation of the elimination of the hydride from [Rh(H)(CO)(PPh₃)₃].¹³ The reaction may be accelerated by the addition of the species [SnCl₃]⁻, which has as strong a *trans* influence as the hydride.¹⁴⁻¹⁵

Table 7.1 shows some examples of ³¹P NMR parameters of phosphine Rh(I) complexes with one and two [SnCl₃]⁻ groups. The coupling ²J(Sn-³¹P) of **91** is in the average of the anionic complexes of Rh(I) with two tins, **92f**, **92h-i**. Note that **92a-92e**, that are Rh(I) complexes with one [SnCl₃]⁻, listed in the same table, have a larger coupling ¹J(¹⁰³Rh-³¹P) than complex **91**. Also, the coupling ²J(Sn-³¹P) in the solution of **91** is far larger than the coupling for the Rh(I) complexes with one [SnCl₃]⁻ as ligand, **92a-92e**. This suggests that Rh(I) for **91** with a tin is not a good alternative. However, it has been stated that **91** has two [SnCl₃]⁻ groups and the observed coupling ²J(Sn-³¹P) of **91** is in the average of **92h-i** which are complexes with the same number of tintrichlorides.

Pentacoordinated species with two [SnCl₃]⁻ in *trans* configuration have been observed for Co(I) in the complex [Et₄N][*trans*-(Cl₃Sn)₂Co(CO)₃] which is a *d*⁸ configuration, similar to **91**.¹⁶

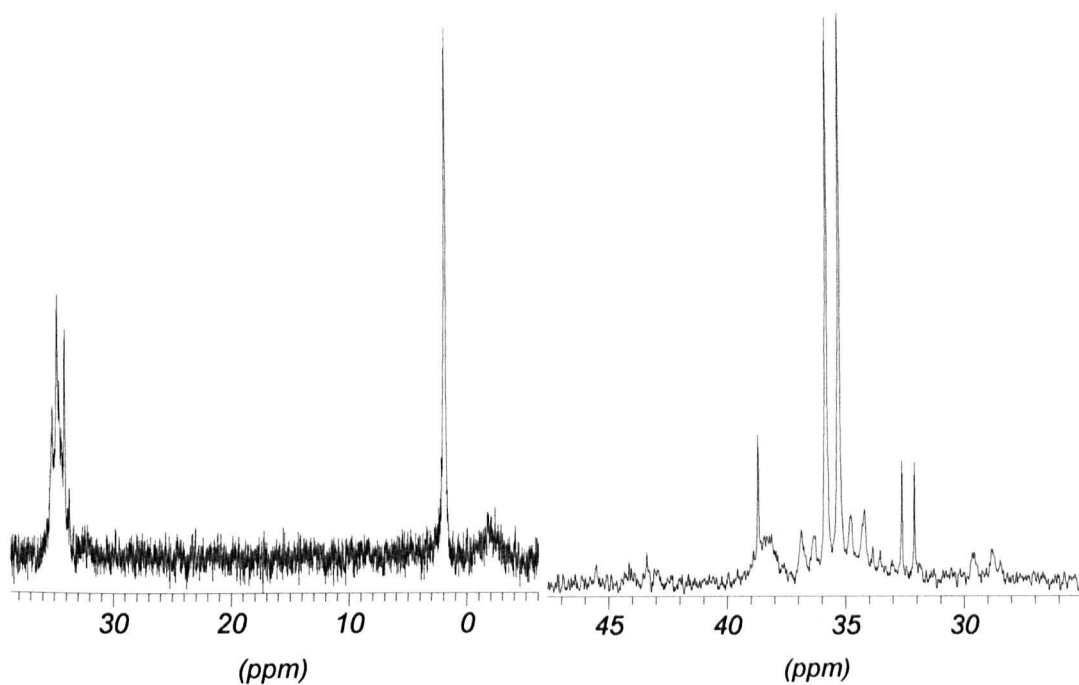


Fig. 7.2. ³¹P NMR of [RhH(CO)(PPh₃)₃] in [emim][Sn₂Cl₅] at: a) room temperature; b) the same as 'a', after adding 0.3 mL of CD₂Cl₂, 240K (-33°C).

The ¹H NMR spectrum does not show any H-Sn interaction, and then the final place of the H⁻ cannot be known with certainty. However, the possibility of the formation of a Sn-H cannot be excluded but the chemical shift for this species is around 1 ppm¹⁷ and it is in the organic part where the strong signals of the ionic liquid do not allow the observation of this weak signal. Fig. 7.3 shows the two pathways for the formation of **91a** and the possible structure of the product as a trigonal bipyramidal anion.

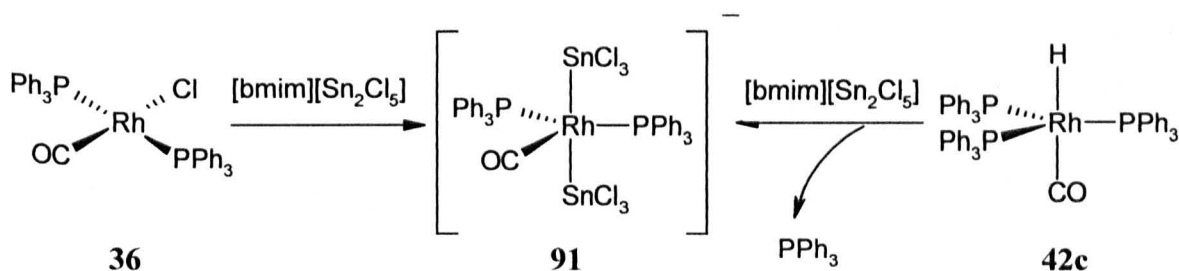


Fig. 7.3. Possible formation of **91a** in [bmim][Sn₂Cl₅] from two different complexes.

Table 7.1. ³¹P NMR parameters of some known Rh-SnCl₃ complexes.

Complex	$\delta^{31}\text{P}$ ppm	$^1J(^{103}\text{Rh}-^{31}\text{P})$ Hz	$^2J(\text{Sn}-^{31}\text{P})$ Hz	Ref.
92a [Rh(SnCl ₃)(NBD)(PEtPh ₂) ₂]	28.9	131	149	18
92b [Rh(SnCl ₃)(NBD)(PPh ₃) ₂]	34.8	132	184	21
92c [Rh(SnCl ₃)(NBD)(dppb)]	30.9	131	129,122	18
92d [Rh(SnCl ₃)(COD)(dppp)]	16.1	117	88	14
92e [Rh(SnCl ₃)(COD)(dppb)]	29.1	122	104	12
92f [Et ₄ N][Rh(SnCl ₃) ₂ (C ₂ H ₄) ₂ (P(p-tol) ₃) ₃]	43	127	336	19
92g [Rh(SnCl ₃)(CO)(C ₂ H ₄) ₂ {P(p-tol) ₃ } ₃]	42.4	115	287	21
92h [PPN] [Rh(SnCl ₃) ₂ (COD)(PPh ₃) ₂]	40.6	117	350	20
92i [PPN] [Rh(SnCl ₃) ₂ (NBD)(PPh ₃) ₂]	45.5	129	349	23

In an attempt to prepare a complex such as **91** in organic solvents, the reaction of [RhCl(CO)(PPh₃)₂] with a 6 fold excess of SnCl₂ was carried out in CD₂Cl₂. An initial change in colour from yellow to orange suggests the formation of the product. The addition of methanol gave the precipitation of the starting material without any interaction of tin, as was suggested by ³¹P NMR spectroscopy. In a second attempt, a 10 fold excess of SnCl₂ was used without success. Finally, the reaction was carried out by adding some drops of [bmim][Sn₂Cl₅] into a solution of [RhCl(CO)(PPh₃)₂] in CH₂Cl₂ and the complex **91** was observed again. These results may suggest the importance of the presence of [SnCl₃]⁻ to stabilize the species.

Attempts to record the rhodium NMR spectra of the last complexes failed, due to the low concentration of compounds and due to the absence of a polarization transfer from any neighbour nuclei such as ³¹P or ¹³C to increase the signal. The ¹¹⁹Sn NMR spectrum was unsuccessful due to the low concentration of the complexes in solution.

The next section shows the results when other PR₃ groups are used in the original complex [RhCl(CO)(PR₃)₂].

7.3. Solution of [Rh(Cl)(CO)(PR₃)₂], R₃ = Et₃, MePh₂ in [bmim]-[Sn₂Cl₅]

In order to understand the interaction with other systems, the complexes [Rh(Cl)(CO)(PR₃)] where R₃ = Me₂Ph, (45), Et₃, (46), MePh₂, (47), EtPh₂ (48), Cy₃, (49), Bu^tEt₂, (50), Bu^tBuⁿ₂, (51), Bu^tPrⁱ₂, (52), Bu^t₂Ph, (53), were dissolved in [bmim][Sn₂Cl₅]. Complexes 45-48 gave a new series of complexes, which suggest the direct interaction with chlorostannates, but in this case with no liberation of PR₃ for R₃ = Me₂Ph, (45), Et₃, (46), MePh₂, (47), EtPh₂ (48). The case where R₃ = Cy₃, (49), Bu^tEt₂, (50), Bu^tBuⁿ₂, (51), Bu^tPrⁱ₂, (52), Bu^t₂Ph, (53) did not give any signal in the ³¹P NMR spectrum due to insolubility of these complexes in [bmim][Sn₂Cl₅]. It is known that [Rh(dppb)(diene)][BF₄], where diene = NBD or COD, reacts with SnCl₂ to give pentacoordinated species that have been reported. To be sure if this kind of interaction exists in [bmim][Sn₂Cl₅], a standard test was carried out. The addition of some drops of [bmim][Sn₂Cl₅] to a solution with [Rh(dppb)(NBD)][BF₄] was studied by ³¹P NMR and it gave the known complex [Rh(SnCl₃)(dppb)(NBD)],²¹ Table 7.1.

Table 7.2 ³¹P{¹H}-NMR data of solutions of complexes in [bmim][Sn₂Cl₅].

Starting material	No	Chemical shift (ppm)	¹ J(¹⁰³ Rh- ³¹ P) Hz	² J(Sn- ³¹ P) Hz
10 [Rh(Cl)(PPh ₃) ₃]	90	43.4	124	327.4
46 [Rh(Cl)(CO)(PEt ₃) ₂]	93	27.0	80.5	345.5
47 [Rh(Cl)(CO)(PMePh ₂) ₂]	94	17.4	86.4	300.0
36 [Rh(Cl)(CO)(PPh ₃) ₂] ^a	91	35.5	93.3	341.1
18c [Rh(Cl)(COD)(dppb)]	21	27.4	122.3	104.0 ²²

^a 240K

The solution of 46-47 in [bmim][Sn₂Cl₅] gave the addition of SnCl₂ into the Rh-Cl bond and the consequent addition of more species [SnCl₃]⁻. ³¹P NMR spectra of complexes 36, 46 and 47 show the ¹¹⁹Sn satellites, which are produced from the coupling ²J(¹¹⁹Sn-³¹P). In every case the coupling is small and suggests a *cis* configuration P-Rh-Sn, Table 7.2. The integration of the intensity of the tin satellites and the main ³¹P signal is 1:6:1 which is a characteristic pattern for the coupling to two tins.

Similar complexes reported by L. Oro²³ and M. Garralda²⁴ groups show the interaction of SnCl₂ in rhodium and all of them have shown similar couplings to that found in 93-94. Table 7.1 shows some couplings of the known complexes. It was found that complexes of Rh(I) with only one [SnCl₃]⁻ as ligand has a small coupling ²J(Sn-³¹P) while complexes with the same oxidation state but with two [SnCl₃]⁻ ligands present larger couplings around 300

Hz. These last complexes are anionic in every case. In addition, compounds with Sn-Rh-P in *trans* position have very large $^2J(\text{Sn}-^{31}\text{P})$ couplings around 2000 Hz,^{9, 25} and this suggests that the *trans* Sn-P configuration in **91** and **93-94** is not a suitable structure.

In addition, the structure of pentacoordinated neutral Rh(I) complexes with [SnCl₃]⁻ have been characterized by X-ray diffraction and have been described as distorted trigonal bipyramidal or distorted square planar, depending on the steric demand of the ligand. For example, **92c** and **92e** are better described as distorted square pyramidal structures, having the rhodium over the plane of the 4 equatorial ligands (dppb) and the diolefin, and the [SnCl₃]⁻ in the apical position.²⁶ On the other hand, complex **92d** presents two conformations in the solid state, in the same unit cell where one molecule is described as a distorted trigonal bipyramidal while the other is described as distorted square pyramidal.²⁷ It has been noted that **92a-92e** have smaller couplings $^2J(\text{Sn}-^{31}\text{P})$ in comparison with the anionic examples **92f** and **92h-92i**. Hence, the small coupling in the first cases may be consistent with a 90° among P-Rh-Sn in a square pyramidal structure. Other examples with less constrained PR₃ have not been reported with rhodium but they may suggest a trigonal bipyramidal structure as was observed in the iridium analogue [Ir(SnCl₃)(NBD)(PMePh₂)₂].²⁸

Hence, for the cases of **90** and **93-94** complexes in [bmim][Sn₂Cl₅], the structure of the new compounds seems to be closer to trigonally bipyramidal as in Fig. 7.4, **91a**. The counter ion may be any [bmim]⁺ available in the solution. The coupling $^2J(^{119}\text{Sn}-^{31}\text{P})$ for the last cases is more usual for *cis* configuration with two [SnCl₃]⁻ P-Rh-Sn. Fig. 7.5 shows the ³¹P NMR spectrum of [RhCl(CO)(PEt₃)₂] in [bmim][Sn₂Cl₅] at room temperature. In the cases of complexes **45-48** in [bmim][Sn₂Cl₅], similar spectra are obtained.

The broad Sn satellites in each case may suggest the presence of more than one Sn interacting with the rhodium. In addition, the broadness can be due to the coupling to the two active isotopes ¹¹⁹Sn and ¹¹⁷Sn.²⁹ In this case the elimination of any PEt₃ from the starting material is not observed. For the case of PEt₃, the ³¹P NMR spectrum is very clear and shows the ¹¹⁹Sn satellites at room temperature. This suggests the formation of [Rh(SnCl₃)₂(CO)(PEt₃)₂]⁻.

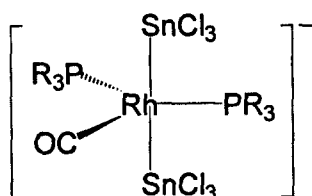


Fig. 7.4. Structure of **91** and **93-94** proposed in $[bmim][Sn_2Cl_5]$. The cation may be $[bmim]^+$.

Note that the coupling constants $^1J(^{103}Rh-^{31}P)$, in complexes **93-94** are very small, similar to Rh(III) anionic complexes, however, cationic $[Rh(COD)(L_2)]^+$ have larger couplings, while the introduction of $[SnCl_3]^-$ reduces the coupling $^1J(^{103}Rh-^{31}P)$ from 143 Hz (for $L_2 = dppb$) to 122 Hz which represents a reduction of 14%. On the other hand, **91** has a reduction of 31% of the same coupling when it is compared to the original starting material **45**. Then a large reduction may be the result of the presence of an extra tin. It is known that tin has a large *trans* influence and must also reflect a *cis* influence, hence a reduction of the coupling of its adjacent ligands.

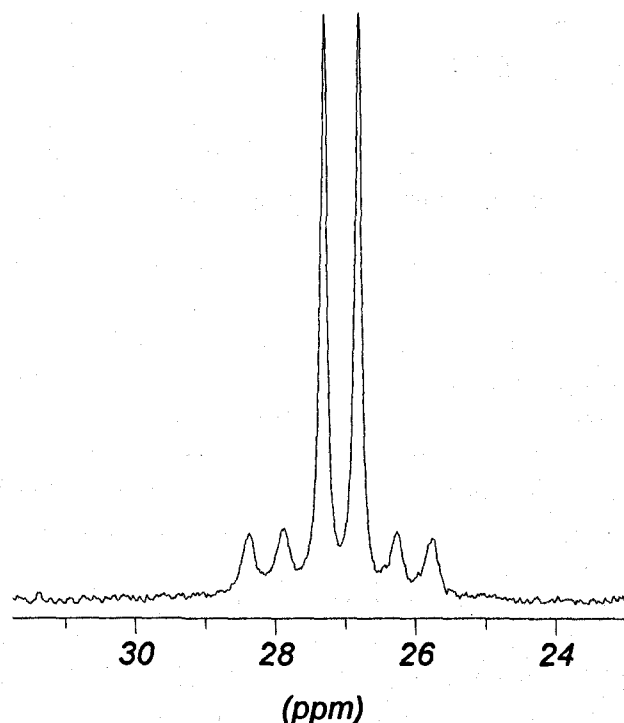


Fig. 7.5. ^{31}P NMR of $[RhCl(CO)(PEt_3)_2]$ in $[emim][Sn_2Cl_5]$ at room temperature.

Finally, complexes with bulky phosphines such as **49-53** were completely insoluble at room temperature and the heating of their suspension in the ionic liquid produces a yellow

solution without any signal in the ³¹P NMR spectrum. The addition of methanol to the last yellow solution gives the precipitation of the starting material 45-48 in each case. This suggests the possible weak interaction of the chlorostannates with the rhodium, which may be reversible. In addition, the absence of the [SnCl₃]⁻ results from the steric hindrance of bulky phosphine toward the addition of a fifth ligand in a square planar complex as Chan and Maden had mentioned before.⁷

7.4. Summary

The solutions of rhodium complexes in [bmim][Sn₂Cl₃] have shown the direct interaction with the [SnCl₃]⁻. The high concentration of the last anion allowed the observation of new complexes which have not been previously observed in common organic solvents. It is known that [SnCl₃]⁻ can form complexes with Rh, e.g. [Rh(SnCl₃)(dppb)-(NBD)]. It is worth noting that the addition of [SnCl₃]⁻ to complexes 36 and 46-47 has shown the coordination of two tins in each case producing Rh(I) for the case of 90a but the possible Rh(I) tbp complexes for the case of 91 and 93-94. The formation of Rh(I) species agrees with the property of [SnCl₃]⁻ to stabilize low valent metals as was described before.

The isolation of the new products did not represent large problems although their texture makes it difficult to handle them and fully characterise them.

7.5. References

- ¹ P. Wasserscheid and H. Waffenschmidt, *J. Mol. Catal. A*, 2000, **164**, 61.
- ² R. Uson, L. A. Oro, M. T. Pinillos, A. Arruebo, K. A. O. Starzewski and P. S. Pregosin, *J. Organomet. Chem.*, 1980, **192**, 227.
- ³ A. R. Sanger, *Inorg. Chim. Acta*, 1992, **191**, 81.
- ⁴ N.V. Borunova, L. K. Freidlin, P. G. Antonov, Y. N. Kukushkin, N. Y. Trink, V. M. Inगतov and A. R. Ganeeva, *Ser. Khim.* 1977, **9**, 2045.
- ⁵ C. H. Yoder, L. A. Margolis, J. M. Horne, *J. Organomet. Chem.*, 2001, **633**, 33.
- ⁶ L. Carlton, *Inorg. Chem.*, 2000, **39**, 4510; Y. Saito, S. Shinoda, T. Yamakawa, P. S. Pregosin and H. Moriyama, *Mag. Res. Chem.*, 1985, **23**, 202.
- ⁷ P. S. Pregosin, S. N. Sze, *Helv. Chim. Acta*, 1978, **61**, 1848; K. A. O. Starzewski, P. S. Pregosin, H. Rügger, *Inorg. Chim. Acta*, 1979, **36**, L445; K. A. O. Starzewski, P. S. Pregosin, H. Rügger, *Angew. Chem. Int. Ed. Engl.*, 1980, **12**, 316; P. S. Pregosin, H. Rügger, *Inorg. Chim. Acta*, 1981, **54**, L59; K. A. O. Starzewski, P. S. Pregosin, H. Rügger, *Helv. Chim. Acta.*, 1982, **65**, 785.

- ⁸ A. Albinati, P. S. Pregosin and H. Rügger, *Inorg. Chem.*, 1984, **23**, 3223.
- ⁹ N. V. Borunova, L. K. Freid, P. G. Antonov, Y. N. Kukushkin, N. Y. Trink, V. M. Ignatov and A. R. Ganeeva, *Ser. Khim.*, 1977, **9**, 2045.
- ¹⁰ D. M. Chan and T. B. Marder, *Angew. Chem. Int. Ed. Engl.*, 1988, **27**, 442.
- ¹¹ D. P. Krut'ko, A. B. Permin, U. S. Petrosyan and O. A. Reutov, *Ser. Khim.* 1985, **4**, 909.
- ¹² P. Wasserscheid and H. Waffenschmidt, *J. Mol. Catal. A*, 2000, **164**, 1-2, 61.
- ¹³ L. Carlton, R. Weber and D. C. Leventis, *Inorg. Chem.*, 1998, **37**, 1264.
- ¹⁴ A. Salzer and C. Elschnebroich, *Organometallic Chemistry. An Introduction*, VCH, 1992.
- ¹⁵ D. S. McGuinness, W. Mueller, P. Wasserscheid, K. J. Cavell, B. W. Skelton, A. H. White and U. Englert, *Organometallics*, 2002, **21**, 175.
- ¹⁶ O. J. Curnow, B. K. Nicholson and M. J. Severinsen, *J. Organomet. Chem.*, 1990, **388**, 379.
- ¹⁷ J. M. Bellama, R.A. Gsell, *Inorg. Nuc. Chem. Lett.*, 1971, **7**, 365; M. L. Maddox, N. Flitcroft, H. D. Kaesz, *J. Organomet. Chem.*, 1965, **4**, 50; P. E. Potter, L. Pratt, G. Wilkinson, *J. Chem. Soc.*, 1964, 524.
- ¹⁸ M. Garralda, M. Ketschmer, H. Ruegger, V. Garcia and S. Pregosin, *Helvet. Chim. Acta*, 1981, **64**, 1150.
- ¹⁹ V. Garcia and M. A. Garralda, *Inorg. Chim. Acta*, 1991, **180**, 177.
- ²⁰ M. Kretschmer, P.S. Pregosin and M. Garralda, *J. Organomet. Chem.*, 1983, **244**, 175.
- ²¹ M. Garralda, E. Pinilla and M. A. Monge, *J. Organomet. Chem.*, 1992, **427**, 193.
- ²² R. Usón, L. A. Oro, M. T. Pinillos, K. A. Ostoja-Starzewski and P. S. Pregosin, *J. Organomet. Chem.*, 1980, **192**, 227.
- ²³ M. A. Esteruelas, F. J. Lahoz, E. Oñate, L. A. Oro and L. Rodriguez, *Organometallics*, 1996, **15**, 3670.
- ²⁴ M. Garralda, E. Pinilla and M. A. Monge, *J. Organomet. Chem.*, 1980, **192**, 227; L. Fidalgo, M. A. Garralda, R. Hernandez and L. Ibarlucea, *Inorg. Chim. Acta*, 1993, **207**, 121.
- ²⁵ L. Carlton, *Inorg. Chem.*, 2000, **39**, 4510.
- ²⁶ V. Garcia, M. A. Garralda and E. Pinillia, *J. Organomet. Chem.*, 1997, **545**, 93.
- ²⁷ V. Garcia, M. A. Garralda, R. Hernandez, M. A. Monge and E. Pinilla, *J. Organomet. Chem.*, 1994, **476**, 41.
- ²⁸ M. R. Churchill and K. G. Lin, *J. Am. Chem. Soc.*, 1974, **96**, 76.
- ²⁹ B. E. Mann and J. W. Akitt, *NMR and chemistry: an introduction to modern NMR spectroscopy*, 1971, Cheltenham, 4th edn., ch. 14.

8. General Conclusions

This work has shown the study of solutions of known rhodium complexes in [emim][Al₂Cl₇] $x_{\text{AlCl}_3} = 0.67$ and [bmim][Sn₂Cl₅] $x_{\text{SnCl}_3} = 0.60$ by multinuclear NMR techniques. Contrary to initial perceptions, the interaction of [AlCl₄]⁻ in chloroaluminates (III) ionic solutions changes the metallic environment dramatically, giving the formation of new species that are unexpected.

The addition of [RhCl(PPh₃)₃] in acidic solutions of [emim][Al₂Cl₇] gives the formation of a bisphosphine rhodium complex with the possible interaction of [ClAlCl₃]⁻ species. The coordination of [ClAlCl₃]⁻ to Rh appears to stabilise Rh(I). The formation of *cis*-[Rh{(μ-Cl)AlCl₃}Cl(PPh₃)₂], **24**, opens up the possibility of new mechanistic pathways of the rhodium chemistry in ionic liquids. Also, the liberation of a PPh₃ from the original material due to a highly acidic medium produces a new reaction that has been unknown in organic solvents. The presence of H⁺ in chloroaluminate (III) ionic liquids removes one PPh₃ as [HPPh₃]⁺. The addition of hydrogen in solutions of **24** gives the formation of a *trans* diphosphine hydride, **25**, in [emim][Al₂Cl₇] with unknown precedent in organic solvents. Also, the presence of impurities in the initial batch of AlCl₃ gives the formation of the same hydride by reduction of Rh(I) chloride due to the action of Al⁰. The insolubility of the latter ionic liquid with non-polar hydrocarbons allows the formation of two-phase systems, giving facilities of quick separation of reactants from the catalytic system and products. Unfortunately, the attempts of hydrogenation of cyclohexene gave the polymerisation of cyclohexene by action of AlCl₃. Further attempts to recrystallize the hydride **25** gave the precipitation of [RhCl₄(PPh₃)₂]⁻ anion as a decomposition product.

Attempts to reproduce the conditions of [emim][Al₂Cl₇] in CD₂Cl₂ by addition of AlCl₃/HCl mixtures gave the formation of Rh(III) complexes with the interaction of [(μ-Cl)AlCl₃] but not the formation of analogues of **24** or **25**. ²⁷Al NMR spectroscopy produced some evidence of the formation of new interactions in the ionic solution with the rhodium centre, although it is not completely conclusive. The isolation of these complexes was unsuccessful due to the high instability of the compounds. The precipitation of a decomposition material [(PPh₃)₂ClRh(μ-Cl)₃Rh(PPh₃)Cl₂] was afforded.

The study of the carbonylation reaction of **25** was followed by ^{31}P , ^{13}C and ^1H NMR. This reaction gave evidence of the formation of intermediates that have not been known before in any organic solvent. The formation of the tricarbonyl monophosphine **37** that is unstable even under CO atmosphere showed high instability in CD_2Cl_2 due to the dilution of the ionic environment. The continued addition of CO to **25** produces a final product that has been proposed as a dicarbonyl phosphine that is a product after the liberation of a CO molecule from **37**. This final product is stable in the ionic environment but showed instability in organic solvents. The reaction with CO, also produces a possible dimeric rhodium species that was impossible to identify but the ^{13}C chemical shift suggests a terminal CO scrambling between two rhodium to produce a triplet in the ^{13}C NMR.

The solution of $[\text{RhCl}(\text{CO})(\text{PPh}_3)_2]$ gave the formation of a Rh(III) hydride in $[\text{emim}][\text{Al}_2\text{Cl}_7]$ and the elimination of a PPh_3 from the starting material due to the high acidity of the ionic environment, forming $[\text{HPPH}_3]^+$. This showed a completely different chemistry between $[\text{RhCl}(\text{PPh}_3)_3]$ and $[\text{RhCl}(\text{CO})(\text{PPh}_3)_2]$ and its reactivity in the same ionic environment due to the presence of a CO in the starting material.

Further studies of a solution of $[\text{Rh}(\mu\text{-Cl})(\text{CO})_2]_2$ in $[\text{emim}][\text{Al}_2\text{Cl}_7]$ showed the interaction with $[\text{AlCl}_4]^-$ to produce a monomeric species that was proposed as $[\text{Rh}\{(\mu\text{-Cl})\text{AlCl}_3\}_2(\text{CO})_2]^-$. The addition of PPh_3 to the last solution produces a mixture of complexes that have been seen before such as **37**, **68** and **25**. This result showed that the formation of such species is reversible and may be in equilibrium among them. Also the formation of other rhodium (III) species was observed without further characterization due to the high instability of such intermediates.

The solution of $[\text{RhCl}(\text{PPh}_3)_3]$ in $[\text{bmim}][\text{Sn}_2\text{Cl}_5]$ produces the *trans*-bisphosphine complex with the elimination of a PPh_3 from the starting material. The free PPh_3 shows an interaction with the ionic environment due to a high concentration of $[\text{SnCl}_3]^-$. The solution of $[\text{RhCl}(\text{CO})(\text{PPh}_3)_2]$ and $[\text{RhH}(\text{CO})(\text{PPh}_3)_3]$ in $[\text{bmim}][\text{Sn}_2\text{Cl}_5]$ gave the same complex that is $[\text{Rh}(\text{SnCl}_3)_2(\text{CO})(\text{PPh}_3)]$ and the elimination of a PPh_3 from the initial complex.

Contrary to bulky PPh_3 's, the solution of complexes with less steric demanding phosphines such as $[\text{RhCl}(\text{CO})(\text{PR}_3)_2]$ where $\text{R}_3 = \text{MePh}_2, \text{Me}_2\text{Ph}, \text{Et}_3$ and EtPh_2 in $[\text{bmim}][\text{Sn}_2\text{Cl}_5]$ gave the products with $[\text{SnCl}_3]^-$ coordinated to the rhodium centre in pentacoordinated Rh(I) complexes without the liberation of a PR_3 from the starting material.

The isolation of those complexes was impossible due to the high solubility of the complexes in the ionic liquid and the instability of the complexes in the organic solvents.

Finally, it is worth noting that the study of hydrogenation of $[\text{Rh}(\text{diolefin})(\text{dppb})][\text{BF}_4]$ where diolefin = COD or NBD in $[\text{bmim}][\text{BF}_4]$ ionic liquids did not offer any clear evidence of different behaviour from the one known in polar organic solvents such as acetone or methanol. The high viscosity of diluted $[\text{bmim}][\text{BF}_4]$ makes impossible the characterization of any formed species even at low temperature by ^{31}P NMR techniques. Also the study of $[\text{Rh}(\text{PPh}_3)_3][\text{PF}_6]$ in $[\text{bmim}][\text{PF}_6]/\text{CD}_2\text{Cl}_2$ systems did not offer any evidence of interaction of $[\text{PF}_6]^-$ anion with the rhodium centre, even though the interaction of M-F- PF_6 is known in other metals such as Ir (I) or W. Further studies with this ionic liquid to prove interactions of the metal with the weak coordinating anions were unsuccessful.

This work has been so far one of few examples of the mechanistic point of view of transition metal complexes in $[\text{emim}][\text{Al}_2\text{Cl}_7]$ and $[\text{bmim}][\text{Sn}_2\text{Cl}_5]$ ionic liquids by NMR techniques.

A further aim of the present work is the study of other metallic systems such as platinum $[\text{Pt}(\text{PEt}_3)_3]$ or ruthenium $[\text{Ru}(\text{H})(\text{CO})(\text{PPh}_3)_3]$ in acidic $[\text{emim}][\text{Al}_2\text{Cl}_7]$ and $[\text{bmim}][\text{Sn}_2\text{Cl}_5]$. Also the study of another ionic liquid based on $[\text{CF}_3\text{SO}_4]^-$ or $[\text{SbF}_6]^-$ would give clear ideas about the different environments that ionic liquids can offer. The possibility of other cationic choices such as phosphonium salts or pyridinium systems can offer other kinds of coordinating abilities that have not been studied yet in ionic liquids and remains as an open field to study in the future.

Appendix 1

Crystallographic data

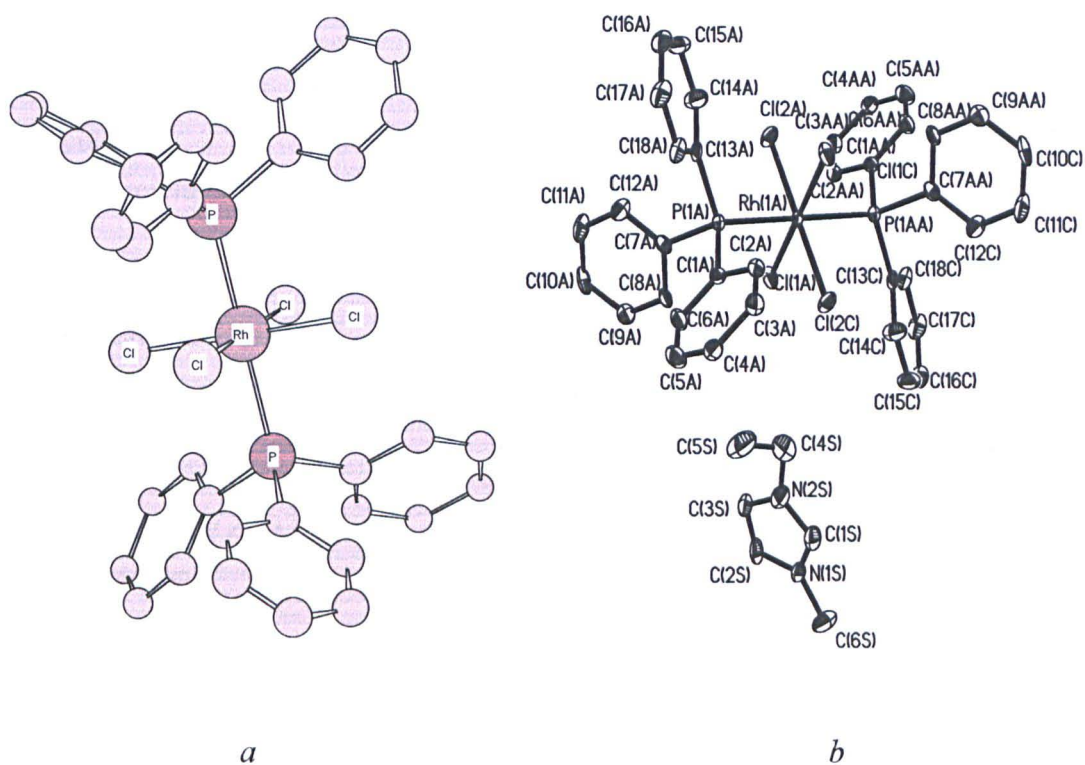


Fig. A1.1. Crystal structure of *trans*-[RhCl₄(PPh₃)₂][emim], **26**: a) structure of the anion only; b) ORTEP structure of the complete compound.

Table A1.1. Crystal data and structure refinement for *trans*-[RhCl₄(PPh₃)₂][emim], 26.

Empirical formula	C ₄₂ H ₄₁ Cl ₄ N ₂ P ₂ Rh	
Formula weight	880.42	
Temperature	150(2) K	
Wavelength	0.71073 Å	
Crystal system	Triclinic	
Space group	P-1	
Unit cell dimensions	a = 9.7840(12) Å	α = 94.293(2)°.
	b = 11.7699(14) Å	β = 104.517(2)°.
	c = 18.438(2) Å	γ = 104.563(2)°.
Volume	1967.7(4) Å ³	
Z	2	
Density (calculated)	1.486 Mg/m ³	
Absorption coefficient	0.820 mm ⁻¹	
F(000)	900	
Crystal size	0.28 x 0.14 x 0.06 mm ³	
Theta range for data collection	1.15 to 28.33°.	
Index ranges	-13 ≤ h ≤ 11, -11 ≤ k ≤ 15, -20 ≤ l ≤ 23	
Reflections collected	12295	
Independent reflections	8840 [R(int) = 0.1294]	
Completeness to theta = 28.33°	90.1 %	
Absorption correction	Semi-empirical	
Max. and min. transmission	0.9524 and 0.8029	
Refinement method	Full-matrix least-squares on F ²	
Data / restraints / parameters	8840 / 0 / 464	
Goodness-of-fit on F ²	0.960	
Final R indices [I > 2σ(I)]	R1 = 0.0739, wR2 = 0.2143	
R indices (all data)	R1 = 0.1015, wR2 = 0.2367	
Largest diff. peak and hole	4.242 and -1.840 e.Å ⁻³	

Table A1.2. Bond lengths [\AA] and angles [$^\circ$] for *trans*-[RhCl₄(PPh₃)₂][emim], 26.

Rh(1)-Cl(1)	2.3476(13)	Rh(1)-Cl(1)#1	2.3476(13)
Rh(1)-Cl(2)#1	2.3562(14)	Rh(1)-Cl(2)	2.3562(14)
Rh(1)-P(1)#1	2.4009(14)	Rh(1)-P(1)	2.4009(14)
P(1)-C(7)	1.826(6)	P(1)-C(13)	1.830(6)
P(1)-C(1)	1.831(6)	C(1)-C(2)	1.399(8)
C(1)-C(6)	1.404(8)	C(2)-C(3)	1.394(8)
C(3)-C(4)	1.374(10)	C(4)-C(5)	1.383(10)
C(5)-C(6)	1.404(8)	C(7)-C(12)	1.397(9)
C(7)-C(8)	1.398(8)	C(8)-C(9)	1.396(9)
C(9)-C(10)	1.378(10)	C(10)-C(11)	1.392(10)
C(11)-C(12)	1.402(9)	C(13)-C(18)	1.402(8)
C(13)-C(14)	1.406(8)	C(14)-C(15)	1.386(9)
C(15)-C(16)	1.390(9)	C(16)-C(17)	1.378(9)
C(17)-C(18)	1.388(9)	Rh(1A)-Cl(2A)	2.3425(14)
Rh(1A)-Cl(2A)#2	2.3425(14)	Rh(1A)-Cl(1A)	2.3529(15)
Rh(1A)-Cl(1A)#2	2.3529(15)	Rh(1A)-P(1A)	2.4099(14)
Rh(1A)-P(1A)#2	2.4099(14)	P(1A)-C(1A)	1.825(6)
P(1A)-C(7A)	1.829(6)	P(1A)-C(13A)	1.841(6)
C(1A)-C(6A)	1.385(8)	C(1A)-C(2A)	1.410(8)
C(2A)-C(3A)	1.375(9)	C(3A)-C(4A)	1.396(9)
C(4A)-C(5A)	1.375(10)	C(5A)-C(6A)	1.399(9)
C(7A)-C(12A)	1.398(8)	C(7A)-C(8A)	1.401(8)
C(8A)-C(9A)	1.388(9)	C(9A)-C(10A)	1.391(9)
C(10A)-C(11A)	1.398(10)	C(11A)-C(12A)	1.395(9)
C(13A)-C(14A)	1.381(9)	C(13A)-C(18A)	1.402(9)
C(14A)-C(15A)	1.394(9)	C(15A)-C(16A)	1.371(11)
C(16A)-C(17A)	1.370(11)	C(17A)-C(18A)	1.395(9)
N(1S)-C(1S)	1.329(9)	N(1S)-C(2S)	1.377(8)
N(1S)-C(6S)	1.460(8)	N(2S)-C(1S)	1.330(9)
N(2S)-C(3S)	1.373(9)	N(2S)-C(4S)	1.493(11)
C(2S)-C(3S)	1.340(10)	C(4S)-C(5S)	1.485(13)
Cl(2A)-Rh(1A)-Cl(2A)#2	180.00(7)	Cl(2A)#2-Rh(1A)-P(1A)#2	291.05(5)
Cl(2A)#2-Rh(1A)-Cl(1A)	90.20(6)	Cl(1A)#2-Rh(1A)-P(1A)#2	295.74(5)

Cl(2A)#2-Rh(1A)-Cl(1A)#289.80(6)	C(1A)-P(1A)-C(7A)	104.0(3)
Cl(2A)-Rh(1A)-P(1A) 91.05(5)	C(7A)-P(1A)-C(13A)	103.4(3)
Cl(1A)-Rh(1A)-P(1A) 95.74(5)	C(7A)-P(1A)-Rh(1A)	115.43(19)
Cl(2A)-Rh(1A)-P(1A)#2 88.95(5)	C(6A)-C(1A)-C(2A)	118.6(6)
Cl(1A)-Rh(1A)-P(1A)#2 84.26(5)	C(2A)-C(1A)-P(1A)	118.1(4)
P(1A)-Rh(1A)-P(1A)#2 180.0	C(2A)-C(3A)-C(4A)	120.1(6)
C(1A)-P(1A)-C(13A) 100.8(3)	C(4A)-C(5A)-C(6A)	120.5(6)
C(1A)-P(1A)-Rh(1A) 114.41(19)	C(8A)-C(7A)-P(1A)	118.8(5)
C(13A)-P(1A)-Rh(1A) 116.87(19)	C(8A)-C(9A)-C(10A)	121.2(6)
C(6A)-C(1A)-P(1A) 122.9(5)	C(12A)-C(11A)-C(10A)	120.5(6)
C(3A)-C(2A)-C(1A) 120.8(6)	C(14A)-C(13A)-C(18A)	118.7(6)
C(5A)-C(4A)-C(3A) 119.7(6)	C(18A)-C(13A)-P(1A)	121.2(5)
C(1A)-C(6A)-C(5A) 120.3(6)	C(3S)-N(2S)-C(4S)	126.6(7)
C(12A)-C(7A)-P(1A) 121.7(5)	C(3S)-C(2S)-N(1S)	107.4(6)
C(9A)-C(8A)-C(7A) 119.8(6)	C(5S)-C(4S)-N(2S)	112.9(8)
C(9A)-C(10A)-C(11A) 118.9(6)	C(16A)-C(15A)-C(14A)	120.8(7)
C(11A)-C(12A)-C(7A) 120.1(6)	C(16A)-C(17A)-C(18A)	119.8(7)
C(14A)-C(13A)-P(1A) 120.1(5)	C(1S)-N(1S)-C(2S)	108.1(6)
Cl(2A)-Rh(1A)-Cl(1A) 89.80(6)	C(2S)-N(1S)-C(6S)	126.9(6)
Cl(2A)-Rh(1A)-Cl(1A)#2 90.20(6)	C(1S)-N(2S)-C(4S)	125.1(7)
Cl(1A)-Rh(1A)-Cl(1A)#2 180.000(16)	N(1S)-C(1S)-N(2S)	108.8(6)
Cl(2A)#2-Rh(1A)-P(1A) 88.95(5)	C(2S)-C(3S)-N(2S)	107.4(6)
Cl(1A)#2-Rh(1A)-P(1A) 84.26(5)		

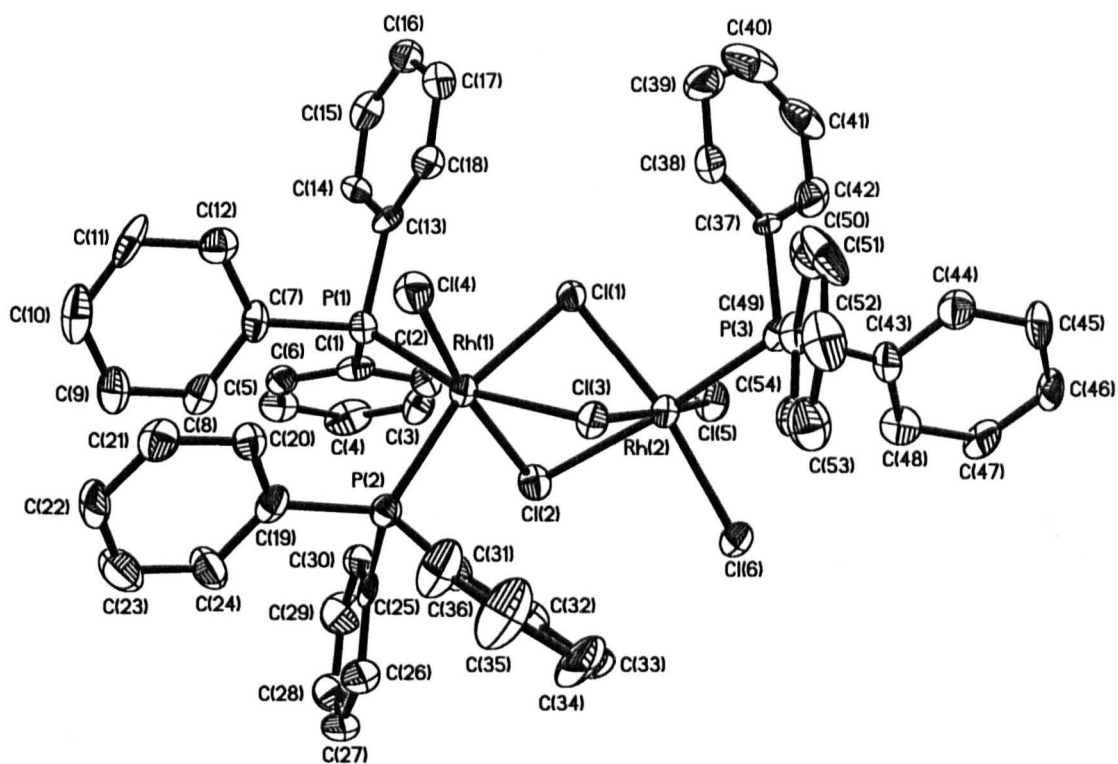


Fig. A1.2. Crystal structure of *trans,cis*-[(PPh₃)₂(Cl)Rh(μ -Cl)₃Rh(Cl)₂(PPh₃)], **33**.

Table A1.3. Crystal data and structure refinement for *trans,cis*-[(PPh₃)₂(Cl)Rh(μ-Cl)₃Rh(Cl)₂(PPh₃)], 33.

Empirical formula	C ₆₈ H ₆₁ Cl ₆ P ₃ Rh ₂
Formula weight	1389.60
Temperature	150(2) K
Wavelength	0.71073 Å
Crystal system	Monoclinic
Space group	P2 ₁ /n
Unit cell dimensions	a = 13.430(4) Å α = 90°. b = 18.758(6) Å β = 96.554(7)°. c = 24.185(7) Å γ = 90°.
Volume	6053(3) Å ³
Z	4
Density (calculated)	1.525 Mg/m ³
Absorption coefficient	0.932 mm ⁻¹
F(000)	2824
Crystal size	0.12 x 0.08 x 0.04 mm ³
Theta range for data collection	1.38 to 28.36°.
Index ranges	-16 ≤ h ≤ 16, -17 ≤ k ≤ 24, -32 ≤ l ≤ 25
Reflections collected	38401
Independent reflections	14575 [R(int) = 0.2217]
Completeness to theta = 28.36°	96.4 %
Absorption correction	Semi-empirical
Max. and min. transmission	0.9637 and 0.8964
Refinement method	Full-matrix least-squares on F ²
Data / restraints / parameters	14575 / 126 / 688
Goodness-of-fit on F ²	0.798
Final R indices [I > 2σ(I)]	R1 = 0.0762, wR2 = 0.1129
R indices (all data)	R1 = 0.2543, wR2 = 0.1567
Largest diff. peak and hole	0.993 and -0.668 e.Å ⁻³

Table A1.4. Bond lengths [\AA] and angles [$^\circ$] for *trans,cis*- $[(\text{PPh}_3)_2(\text{Cl})\text{Rh}(\mu\text{-Cl})_3\text{Rh}(\text{Cl})_2(\text{PPh}_3)]$, 33.

Rh(1)-P(1)	2.315(3)	Rh(1)-Cl(4)	2.333(2)
Rh(1)-P(2)	2.334(3)	Rh(1)-Cl(2)	2.387(2)
Rh(1)-Cl(3)	2.437(3)	Rh(1)-Cl(1)	2.469(2)
Rh(2)-P(3)	2.252(3)	Rh(2)-Cl(5)	2.310(3)
Rh(2)-Cl(6)	2.331(3)	Rh(2)-Cl(3)	2.353(2)
Rh(2)-Cl(1)	2.371(2)	Rh(2)-Cl(2)	2.488(3)
P(1)-C(7)	1.793(10)	P(1)-C(13)	1.832(9)
P(1)-C(1)	1.847(10)	P(2)-C(31)	1.811(10)
P(2)-C(19)	1.845(10)	P(2)-C(25)	1.848(10)
P(3)-C(49)	1.812(9)	P(3)-C(37)	1.816(9)
P(3)-C(43)	1.843(8)	C(1)-C(6)	1.391(13)
C(1)-C(2)	1.399(12)	C(2)-C(3)	1.373(12)
C(3)-C(4)	1.372(14)	C(4)-C(5)	1.408(13)
C(5)-C(6)	1.351(12)	C(7)-C(12)	1.383(12)
C(7)-C(8)	1.429(13)	C(8)-C(9)	1.379(12)
C(9)-C(10)	1.369(13)	C(10)-C(11)	1.383(15)
C(11)-C(12)	1.397(13)	C(13)-C(14)	1.382(12)
C(13)-C(18)	1.396(13)	C(14)-C(15)	1.371(13)
C(15)-C(16)	1.360(13)	C(16)-C(17)	1.374(14)
C(17)-C(18)	1.371(13)	C(19)-C(20)	1.372(12)
C(19)-C(24)	1.383(13)	C(20)-C(21)	1.390(12)
C(21)-C(22)	1.349(13)	C(22)-C(23)	1.396(13)
C(23)-C(24)	1.375(13)	C(25)-C(30)	1.357(12)
C(25)-C(26)	1.381(13)	C(26)-C(27)	1.430(13)
C(27)-C(28)	1.343(14)	C(28)-C(29)	1.341(14)
C(29)-C(30)	1.390(13)	C(31)-C(32)	1.376(12)
C(31)-C(36)	1.383(13)	C(32)-C(33)	1.407(13)
C(33)-C(34)	1.344(13)	C(34)-C(35)	1.382(14)
C(35)-C(36)	1.403(15)	C(37)-C(42)	1.396(13)
C(37)-C(38)	1.400(12)	C(38)-C(39)	1.378(15)
C(39)-C(40)	1.353(16)	C(40)-C(41)	1.357(16)
C(41)-C(42)	1.390(14)	C(43)-C(48)	1.378(11)
C(43)-C(44)	1.397(11)	C(44)-C(45)	1.382(12)

C(45)-C(46)	1.359(12)	C(46)-C(47)	1.388(13)
C(47)-C(48)	1.392(12)	C(49)-C(50)	1.366(12)
C(49)-C(54)	1.390(13)	C(50)-C(51)	1.421(15)
C(51)-C(52)	1.358(16)	C(52)-C(53)	1.373(14)
C(53)-C(54)	1.391(13)	C(1A)-C(2A)	1.3900
C(1A)-C(6A)	1.3900	C(1A)-C(7A)	1.497(12)
C(2A)-C(3A)	1.3900	C(3A)-C(4A)	1.3900
C(4A)-C(5A)	1.3900	C(5A)-C(6A)	1.3900
C(8A)-C(9A)	1.3900	C(8A)-C(13A)	1.3900
C(8A)-C(14A)	1.516(12)	C(9A)-C(10A)	1.3900
C(10A)-C(11A)	1.3900	C(11A)-C(12A)	1.3900
C(12A)-C(13A)	1.3900		
P(1)-Rh(1)-Cl(4)	85.14(9)	P(1)-Rh(1)-P(2)	101.81(9)
Cl(4)-Rh(1)-P(2)	95.29(9)	P(1)-Rh(1)-Cl(2)	104.42(9)
Cl(4)-Rh(1)-Cl(2)	169.28(9)	P(2)-Rh(1)-Cl(2)	87.59(9)
P(1)-Rh(1)-Cl(3)	164.08(10)	Cl(4)-Rh(1)-Cl(3)	86.56(9)
P(2)-Rh(1)-Cl(3)	92.45(10)	Cl(2)-Rh(1)-Cl(3)	83.00(8)
P(1)-Rh(1)-Cl(1)	88.88(9)	Cl(4)-Rh(1)-Cl(1)	96.16(9)
P(2)-Rh(1)-Cl(1)	164.95(9)	Cl(2)-Rh(1)-Cl(1)	79.43(8)
Cl(3)-Rh(1)-Cl(1)	78.53(8)	P(3)-Rh(2)-Cl(5)	90.68(9)
P(3)-Rh(2)-Cl(6)	92.73(9)	Cl(5)-Rh(2)-Cl(6)	92.11(9)
P(3)-Rh(2)-Cl(3)	95.04(9)	Cl(5)-Rh(2)-Cl(3)	172.46(9)
Cl(6)-Rh(2)-Cl(3)	92.50(9)	P(3)-Rh(2)-Cl(1)	95.83(9)
Cl(5)-Rh(2)-Cl(1)	92.38(9)	Cl(6)-Rh(2)-Cl(1)	170.27(9)
Cl(3)-Rh(2)-Cl(1)	82.18(9)	P(3)-Rh(2)-Cl(2)	174.84(9)
Cl(5)-Rh(2)-Cl(2)	91.31(9)	Cl(6)-Rh(2)-Cl(2)	91.95(9)
Cl(3)-Rh(2)-Cl(2)	82.58(8)	Cl(1)-Rh(2)-Cl(2)	79.33(8)
Rh(2)-Cl(1)-Rh(1)	82.90(8)	Rh(1)-Cl(2)-Rh(2)	82.17(7)
Rh(2)-Cl(3)-Rh(1)	83.97(8)	C(7)-P(1)-C(13)	102.8(5)
C(7)-P(1)-C(1)	106.0(5)	C(13)-P(1)-C(1)	99.8(4)
C(7)-P(1)-Rh(1)	116.0(3)	C(13)-P(1)-Rh(1)	113.3(3)
C(1)-P(1)-Rh(1)	116.9(3)	C(31)-P(2)-C(19)	104.9(4)
C(31)-P(2)-C(25)	103.5(5)	C(19)-P(2)-C(25)	101.8(5)
C(31)-P(2)-Rh(1)	108.3(3)	C(19)-P(2)-Rh(1)	122.6(3)
C(25)-P(2)-Rh(1)	113.8(3)	C(49)-P(3)-C(37)	107.5(5)

C(49)-P(3)-C(43)	101.9(4)	C(37)-P(3)-C(43)	102.4(5)
C(49)-P(3)-Rh(2)	113.2(3)	C(37)-P(3)-Rh(2)	110.9(3)
C(43)-P(3)-Rh(2)	119.7(3)	C(6)-C(1)-C(2)	120.4(9)
C(6)-C(1)-P(1)	121.3(8)	C(2)-C(1)-P(1)	118.2(8)
C(3)-C(2)-C(1)	117.9(10)	C(4)-C(3)-C(2)	121.7(9)
C(3)-C(4)-C(5)	120.1(10)	C(6)-C(5)-C(4)	118.7(10)
C(5)-C(6)-C(1)	121.2(9)	C(12)-C(7)-C(8)	116.3(9)
C(12)-C(7)-P(1)	122.1(8)	C(8)-C(7)-P(1)	121.7(8)
C(9)-C(8)-C(7)	121.5(10)	C(10)-C(9)-C(8)	121.1(11)
C(9)-C(10)-C(11)	118.3(10)	C(10)-C(11)-C(12)	121.6(11)
C(7)-C(12)-C(11)	121.1(10)	C(14)-C(13)-C(18)	117.9(9)
C(14)-C(13)-P(1)	118.5(7)	C(18)-C(13)-P(1)	123.0(7)
C(15)-C(14)-C(13)	121.9(10)	C(16)-C(15)-C(14)	119.5(10)
C(15)-C(16)-C(17)	119.7(10)	C(18)-C(17)-C(16)	121.3(11)
C(17)-C(18)-C(13)	119.4(10)	C(20)-C(19)-C(24)	119.4(9)
C(20)-C(19)-P(2)	121.6(8)	C(24)-C(19)-P(2)	118.7(8)
C(19)-C(20)-C(21)	120.4(10)	C(22)-C(21)-C(20)	120.0(9)
C(21)-C(22)-C(23)	120.5(9)	C(24)-C(23)-C(22)	119.4(10)
C(23)-C(24)-C(19)	120.3(10)	C(30)-C(25)-C(26)	120.4(10)
C(30)-C(25)-P(2)	119.3(8)	C(26)-C(25)-P(2)	120.2(8)
C(25)-C(26)-C(27)	116.4(10)	C(28)-C(27)-C(26)	121.7(10)
C(29)-C(28)-C(27)	120.8(11)	C(28)-C(29)-C(30)	119.1(11)
C(25)-C(30)-C(29)	121.5(10)	C(32)-C(31)-C(36)	118.7(10)
C(32)-C(31)-P(2)	119.3(8)	C(36)-C(31)-P(2)	121.8(8)
C(31)-C(32)-C(33)	120.7(10)	C(34)-C(33)-C(32)	119.6(10)
C(33)-C(34)-C(35)	121.4(11)	C(34)-C(35)-C(36)	118.8(11)
C(31)-C(36)-C(35)	120.7(11)	C(42)-C(37)-C(38)	116.4(9)
C(42)-C(37)-P(3)	120.6(8)	C(38)-C(37)-P(3)	122.9(8)
C(39)-C(38)-C(37)	120.5(12)	C(40)-C(39)-C(38)	120.9(12)
C(39)-C(40)-C(41)	121.3(13)	C(40)-C(41)-C(42)	118.4(12)
C(41)-C(42)-C(37)	122.5(10)	C(48)-C(43)-C(44)	120.6(8)
C(48)-C(43)-P(3)	123.7(7)	C(44)-C(43)-P(3)	115.6(7)
C(45)-C(44)-C(43)	119.7(9)	C(46)-C(45)-C(44)	120.4(9)
C(45)-C(46)-C(47)	119.9(8)	C(46)-C(47)-C(48)	121.1(9)
C(43)-C(48)-C(47)	118.3(9)	C(50)-C(49)-C(54)	119.1(9)

C(50)-C(49)-P(3)	122.4(9)	C(54)-C(49)-P(3)	118.5(8)
C(49)-C(50)-C(51)	118.9(11)	C(52)-C(51)-C(50)	121.1(11)
C(51)-C(52)-C(53)	120.4(11)	C(52)-C(53)-C(54)	118.7(11)
C(49)-C(54)-C(53)	121.8(10)	C(2A)-C(1A)-C(6A)	120.0
C(2A)-C(1A)-C(7A)	126.5(9)	C(6A)-C(1A)-C(7A)	113.5(9)
C(1A)-C(2A)-C(3A)	120.0	C(4A)-C(3A)-C(2A)	120.0
C(3A)-C(4A)-C(5A)	120.0	C(6A)-C(5A)-C(4A)	120.0
C(5A)-C(6A)-C(1A)	120.0	C(9A)-C(8A)-C(13A)	120.0
C(9A)-C(8A)-C(14A)	122.4(9)	C(13A)-C(8A)-C(14A)	117.2(9)
C(8A)-C(9A)-C(10A)	120.0	C(11A)-C(10A)-C(9A)	120.0
C(10A)-C(11A)-C(12A)	120.0	C(11A)-C(12A)-C(13A)	120.0
C(12A)-C(13A)-C(8A)	120.0		

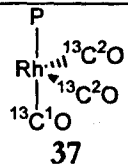
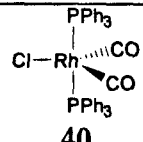
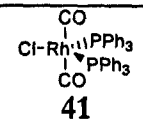
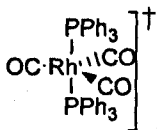
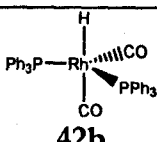
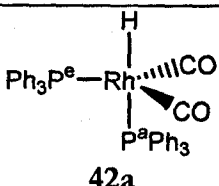
Appendix 2

Table A2.1. FT-IR ν_{CO} stretching bands of characteristic rhodium complexes.

Complex	$\nu_{CO} \text{ cm}^{-1}$	Ref.
[Rh {(μ -Cl) ₂ AlCl ₂ } {(μ -Cl)AlCl ₃ } (H)(CO)(PPh ₃)], 38	2117	
[Rh {(μ -Cl) ₂ AlCl ₂ } {(μ -Cl)AlCl ₃ } (H)(¹³ CO)(PPh ₃)], 38	2138, 2119, 2076	
[Rh {(μ -Cl) ₂ AlCl ₂ } (CO) ₂ (PPh ₃)], 37	2089	
Mixture of 37 and 68	2133, 2089	
[Rh {(μ -Cl) ₂ AlCl ₂ } (CO)(PPh ₃)], 68	2133	
[Rh {(μ -Cl) ₂ AlCl ₂ } (CO)(PPh ₃)], 68	2071	
Final carbonyl, 74	1635, 1815	
Square planar Rh(I) complex		
[(CO)(Cl)(Rh)(PPh ₂ O(p-C ₆ (CH ₃) ₄)OPPh ₂)Rh(CO)(Cl)]	1973	1
[(CO)(Cl)(Rh)(PPh ₂ O(p-C ₆ CH ₄)OPPh ₂)Rh(CO)(Cl)]	1978	1
[Rh(Cl)(CO)(PPh ₃) ₂]	1980	2
[Rh(Cl)(¹³ CO)(PPh ₃) ₂]	1915	
[(Rh(CO) ₄) ⁻]	1895	3
[(Rh(CO)(P(pyrrolyl) ₃) ₂) ⁻]	1970, 1900	3
Pentacoordinated Rh(I) complex		
[Rh(Cl)(CO) ₂ (PPh ₃) ₂]	1982	2
[Rh(Cl)(¹³ CO) ₂ (PPh ₃) ₂]	1922	2
Cis-[Rh(RSCH ₂ CH ₂ PPh ₂) ₂]BF ₄		
R = {Fe(C ₅ H ₅)(C ₅ H ₄)}-	2014, 1966	4
R = Ph	2017, 1972	4
R = p-FC ₆ H ₄	2017, 1972	4
R = p-NO ₂ C ₆ H ₄	2018, 1980	4
[Rh(diphos)(CO)(H)(PPh ₃)] homoxantphos	1982, 1921	5
[Rh(diphos)(CO) ₂ (H)] homoxantphos	2040, 1997 1974, 1951	5
[Rh(dipho)(CO)(H)(PPh ₃)] benzylnixantphos	2000, 1920	5
[Rh(dipho)(CO) ₂ (H)] benzylnixantphos	2038, 1997 1977, 1951	5
[(CO) ₂ (I)(Rh)(PPh ₂ S(p-C ₆ CH ₄)SPPPh ₂) ₂ Rh(CO) ₂ (Cl)]	2017, 1978	6
sp[(Rh(CO)(Cl)(PPh ₃) ₂ (SO ₂)]	2035	6
[(Rh(CO)(dppp) ₂][BF ₄]	1929	
[Rh(CO) ₃ (PPh ₃) ₂][BF ₄]	2076, 2025	7
Rh(III) and Ir(III) carbonyls		
[Ir(CO) ₅ Cl][Sb ₂ F ₁₁] ₂	2246	8

$[\text{Ir}(\text{CO})_6][\text{SbF}_6]_3 \cdot 4\text{HF}$	2268	9
$[\text{RhCl}_3(\text{CO})_2(\text{PPh}_3)]$	2111	10
$[\text{Rh}(\text{Cl})_2(\text{CO})_3(\text{PPh}_3)]\text{Cl}$	2110, 2093, 2012	
$[\text{Rh}(\text{Cl})_2\text{H}(\text{CO})(\text{PPh}_3)_2]$	2122	11
$[\text{Rh}(\text{Cl})_2\text{Ph}(\text{PPh}_3)_2]$	2071	
Non classical carbonyls		
$[\text{Rh}(\text{CO})_4]^+$	2138	12
$[\text{Rh}(\text{CO})_5\text{Cl}]$	2247	12

Table A2.2. NMR parameters of known complexes that illustrate the examples given in section 4.6.

Complex	$^{31}\text{P}\{^1\text{H}\}$ NMR,			$^{13}\text{C}\{^1\text{H}\}$ NMR		Ref.
	δ ppm	$^1J_{\text{RhP}}$	$^2J_{\text{PC}}$	δ ppm	$^1J_{\text{RhC}}$	
 37	22	107.5	86.8 $\text{C}^1_{\text{trans}}$ 15.1 C^2_{cis}	179.4 C^1 181.7 C^2	55.9 64.4	
Rh(I) trigonal bipyramidal						
 40	31 25	116 96	no	185.9	no	2
 41	35.4 36	92.7 89.5	-	-	-	13
 41a	21.8	102.7	14.4	188.8	80.6	13
 42b	39.9	138	10	200.3	63	14
 42a						14
$[\text{Rh}\{\text{P}(\text{OCH}_3)_3\}_5]$	11.0 a -3.7 e	143 206	P-P = 68 -136K			15

$[\text{Rh}(\text{H})\{\text{P}(\text{OCH}_3)_3\}_4]$	-12.8 ^1H		Pa-H 152 Pe-H 5			15
$[(\text{Rh}(\eta^2\text{TMPP})(\text{TMPP})(\text{CO})(\text{Cl}))^+]$	-11.1	128				
$[\text{Rh}(\eta^3\text{TMPP})_2][\text{BF}_4]_3$	37.4	107				
$[(\text{Rh}(\text{CO})(\text{dppp})_2)[\text{BF}_4]$	-14.2 13.2	86 113				
Rh(I) Square planar						
36a	25.3	127.3	123.4 <i>trans</i> 16.3 <i>cis</i>	182.0 183.3	60.3 <i>trans</i> 71.4 <i>cis</i>	13
	20.6	124.9	15.4	186.8	74.0	16
	32.6	117.1	14.6	187.3	67.0	
<i>trans</i> - $[\text{Rh}(\text{Cl})(\text{CO})(\text{PPh}_3)_2]$, 36	28.5	126.6	16	187.4	73	17
<i>trans</i> - $[\text{Rh}(\text{Cl})(\text{CO})(\text{PEt}_2\text{Ph})_2]$, 48	27.4	123.1	9.6	179.8	64.9	18

Table A2.3. ^{13}C NMR parameters of Rh(I) and Rh(III) anionic carbonyls.¹⁸

Complex	^{13}C NMR	
	δ	$^1J_{\text{RhC}}$
70a $[\text{RhCl}_2(\text{CO})_2]^-$	180.6	72.2
71 $[\text{Rh}(\text{Cl})_4(\text{CO})_2]^-$	168.5	52.7
72 ^a $[\text{Rh}_2(\text{Cl})_8(\text{CO})_2]_2^-$	170.0	61.3

^a With all the possible isomers, δ , $^1J(^{103}\text{Rh}-^{13}\text{C})$: 172.1, 53.8; 171.6, 54.3; 171.6; 62.2; 171.1, 56.5; 170.1, 61.3.

Table A2.4. $^{31}\text{P}\{^1\text{H}\}$ and ^1H NMR parameters for solution of $[\text{Rh}(\text{Cl})(\text{CO})(\text{PR}_3)_2]$ in ionic liquids.

Phosphine	$\delta^{31}\text{P}$ of $[\text{HPR}_3]^+$	$^1J(^{31}\text{P}-^1\text{H})$ $[\text{HPR}_3]^+$, Hz	$\delta^{31}\text{P}$ - $[\text{Rh}(\text{PR}_3)_2\text{H}(\text{CO})]$	$^1J(^{31}\text{P}-^{103}\text{Rh})$ $[\text{RhH}(\text{CO})(\text{P}(\text{R}_3)_2)]$	$\delta^1\text{H}$ ppm	$^1J(^{103}\text{Rh}-^1\text{H})=^2J(^{31}\text{P}-^1\text{H})$ Hz
45b. PMe_2Ph	-1.4	497	37.1	98.8	-13.82	13.5
54. PEt_3	22	467	78.0	99	-14.55	12.7
55. PMePh_2	1.9	503	44.0	104.1	-14.01	11.5
56. PEtPh_2	12.3	493	58.5	104.2	-14.48	11.8
38. PPh_3	6.5	505	52.5	108.2	-13.45	10.5
57. PBu^tEt_2	38.6	456	99.1	101.1	-14.75	11.3
58. $\text{PBu}^t\text{Bu}_2^n$	32.4	459	94.5	101.08	-14.52	Broad signal
59. PBu^tPr_2	30.9		92.9	101.1	-14.73	11.3
60. PCy_3	32.5	443	97.8	102.3	-14.84	9.0
61. PBu_2^tPh	50.8	452	100.0	Broad signal	-14.79	10.1

Table A2.5. $^{31}\text{P}\{^1\text{H}\}$ and ^1H NMR parameters for $[\text{Rh}(\text{Cl})_2(\text{H})(\text{CO})(\text{PR}_3)_2]$ in CDCl_3 . $\text{P}^t\text{Bu}_2\text{Ph}$ and $\text{P}^t\text{Bu}_2^i\text{Pr}$ do not react with HCl .

Phosphine	$\delta^{31}\text{P}\{^1\text{H}\}$, ppm ^a	$^1J(^{103}\text{Rh}-^{31}\text{P})$ Hz	$\delta^1\text{H}$	$^1J(^{31}\text{P}-^1\text{H})$	$^2J(^{103}\text{Rh}-^1\text{H})$
45c PMe_2Ph	3.5	80.2	-13.3	Broad signal	Broad signal
62 PEt_3	26.5	80.1	-13.4	9.9	9.9
63 PMePh_2	18.7	83.9	-12.4	Broad signal	Broad signal
64 PEtPh_2	25.1	82.9	-12.6	9.9	15.1
38 PPh_3	25.3	85.9	-12	9.9	13.9
65 PBu^tEt_2	44.6	80.0	-13.49	15.19	8.9
66 $\text{PBu}^t\text{Bu}_2^n$	40.6	79.9	-13.5	15.1	8.29
67 PCy_3	35	79.3	-13	9.9	13.9

Table A2.6. ^{31}P NMR parameters of some known Rh-SnCl₃ complexes.

Complex	$\delta^{31}\text{P}$ ppm	$^1\text{J}(^{103}\text{Rh}-^{31}\text{P})$ Hz	$^2\text{J}(^{119}\text{Sn}-^{31}\text{P})$ Hz	Ref.
[Rh(SnCl ₃)(NBD)(PEtPh ₂) ₂]	28.9	131	149	19a
[Rh(SnCl ₃)(NBD)(PPh ₃) ₂]	34.8	132	184	19a
[Rh(SnCl ₃)(NBD)(dppb)]	30.9	131	129,122	19b
[Rh(SnCl ₃)(COD)(dppp)]	16.1	117	88	20
[Rh(SnCl ₃)(COD)(dppb)]	29.1	122	104	20
[Et ₄ N][Rh(SnCl ₃) ₂ (C ₂ H ₄)(P(p-tol) ₃)]	43	127	336	21
[Et ₄ N][Rh(SnCl ₃) ₂ (C ₂ H ₄)(P(m-tol) ₃)]	44.5	128	327	17
[Et ₄ N][Rh(SnCl ₃) ₂ (C ₂ H ₄)(P(p-F) ₃)]	43.2	128	326	17
[PPN][Rh(SnCl ₃) ₂ (C ₂ H ₄)(P(p-tol) ₃)]	44.0	130	346	17
[Et ₄ N][Rh(SnCl ₃) ₂ (C ₂ H ₄)(P(p-Cl) ₃)]	44.5	126	326	17
[Rh(SnCl ₃) ₂ (C ₂ H ₄){P(p-tol) ₃ } ₂]	32.0	134	178	17
[Rh(SnCl ₃)(CO)(C ₂ H ₄) ₂ {P(p-tol) ₃ }]	42.4	115	295	17
[PPN][Rh(SnCl ₃) ₂ (COD)(PPh ₃)]	40.6	117	350	22
[PPN][Rh(SnCl ₃) ₂ (COD){P(p-OMe) ₃ }]	35.5	115	358	18
[PPN][Rh(SnCl ₃) ₂ (COD){P(p-F) ₃ }]	38.1	118	346	18
[PPN][Rh(SnCl ₃) ₂ (COD){P(p-Cl) ₃ }]	38.7	117	344	18
[PPN][Rh(SnCl ₃) ₂ (NBD)(PPh ₃)]	45.5	129	349	18
[PPN][Rh(SnCl ₃) ₂ (NBD){P(p-OMe) ₃ }]	40.9	128	352	18
[PPN][Rh(SnCl ₃) ₂ (COD){P(p-F) ₃ }]	43.0	129	349	18
[PPN][Rh(SnCl ₃) ₂ (COD){P(p-Cl) ₃ }]	44.3	131	344	18

A2.1. References

- 1 F.M. Dixon, A.H. Eisenberg, J.R. Farrel, L.M. Liable-Sands, C.A. Mirkin and A. L. Rheingold, *Inorg. Chem.*, 1999, **39**, 3432.
- 2 A. Sanger, *Can.J. Chem.*, 1985, **63**, 571.
- 3 K. G. Moloy and J. L. Petersen, *J. Am. Chem. Soc.*, 1995, **117**, 7696.
- 4 I. V. Kourkine, L. M. Liable-Sands, C. A. Mirkin, S. C. Slone and A. L. Rheingold, *Inorg. Chem.*, 1999, **38**, 2758.
- 5 L.A. Van der Veen, P.H. Keeven, G.C. Schoemaker, J. N. H. Reek, P. C. J. Kamer, P. W. N.M. Van Leeuwen, M. Lutz and A. L. Spek, *Organometallics*, 2000, **19**, 872.
- 6 J. Ibers and K. W. Muir, *Inorg. Chem.* 1969, **8**, 1921.
- 7 H. Lee, J. Bae, J. Ko, Y. S. Kang, H. S. Kim, S. Kim, J. H. Chung and S. O. Kang, *J. Organomet. Chem.* 2000, **614**, 83.

- ⁸ F. Aubke, C. Bach, S. J. Rettig, J. Trotter, C. Wang and H. Willner, *Angew. Chem. Int. Ed. Engl.*, 1996, **35**, 1974; F. Aubke, C. Bach, V. Jonas, S. J. Rettig, W. Thiel, J. Trotter, C. Wang, R. Wartchow and H. Willner, *Inorg. Chem.*, 2000, **39**, 1933.
- ⁹ F. Aubke, M. Berkei, G. Henkel, B. Von Ahsen and H. Willner, *J. Am. Chem. Soc.*, 2001, **124**, 8371.
- ¹⁰ G. Deganello, P. Uguagliati, B. Crociani and U. Belluco, *J. Chem. Soc. A*, 1969, 2726.
- ¹¹ M.C. Baird, J.T. Magee, J.A., Osborn and G. Wilkinson, *J. Chem. Soc. A*, 1967, 1347.
- ¹² O.P. Anderson, M. D. Havighurst, A. J. Lupinetti, S. M. Miller and S. H. Strauss, *J. Am. Chem. Soc.*, 1999, **121**, 11920.
- ¹³ G. Battaglia, F. P. Cusmano, G. Giordano and E. Rotondo, *J. Organomet. Chem.*, 1993, **450**, 245.
- ¹⁴ J. M. Brown, L. R. Canning, A. G. Kent and P. J. Sidebottom, *J. Chem. Soc., Chem. Commun.*, 1982, 721.
- ¹⁵ J. P. Jesson and E. L. Muetterties, in *Dynamic Nuclear Magnetic Resonance Spectroscopy*, by L.M. Jackman and F.A. Cotton, Academic Press, New York, 1975, ch. 8.
- ¹⁶ A. DeCian, J. Fischer, J. S. Frye, J. M. Kessler and J. H. Nelson, *Inorg. Chem.*, 1993, **32**, 1048.
- ¹⁷ A. Bresler, N. A. Buzina, Y. S. Varshavsky, N. V. Kiseleva and A. G. Cherkasova, *J. Organomet. Chem.*, 1979, **171**, 229.
- ¹⁸ B. T. Heaton, C. Jacob and S. Moffet, *J. Organomet. Chem.*, 1993, **462**, 353.
- ¹⁹ a) M. Garralda, M. Ketschmer, H. Ruegger, V. Garcia and S. Pregosin, *Helvet. Chim. Acta*, 1981, **64**, 1150; b) M. A. Esteruelas, F. J. Lahoz, E. Oñate, L. A. Oro and L. Rodriguez, *Organometallics*, 1996, **15**, 3670.
- ²⁰ M. Garralda, E. Pinilla and M. A. Monge, *J. Organomet. Chem.*, 1980, **192**, 227; L. Fidalgo, M. A. Garralda, R. Hernandez and L. Ibarlucea, *Inorg. Chim. Acta*, 1993, **207**, 121.
- ²¹ V. Garcia and M. A. Garralda, *Inorg. Chim. Acta*, 1991, **180**, 177.
- ²² M. Kretschmer, P.S. Pregosin and M. Garralda, *J. Organomet. Chem.*, 1983, **244**, 175.

Appendix 3

Graphics

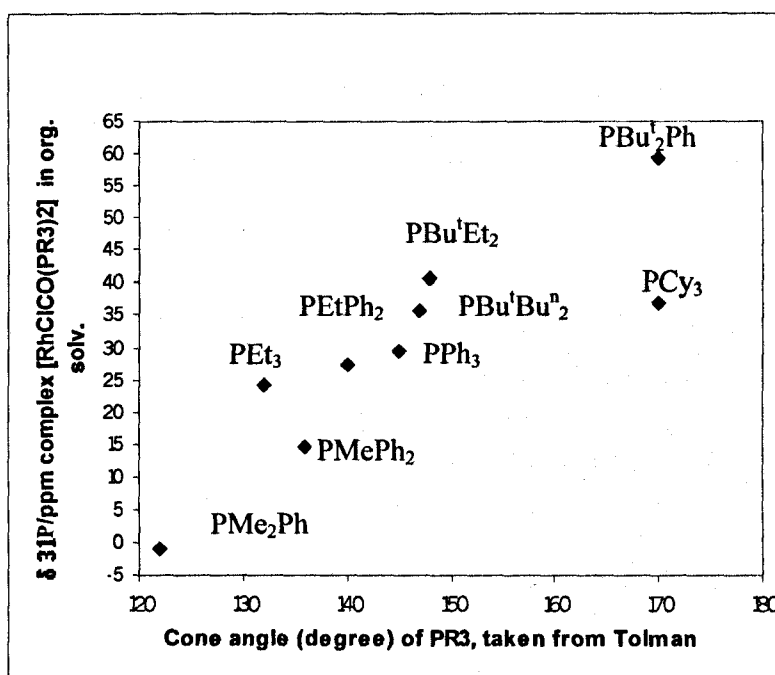


Table A3.1. Cone angle of used phosphines in degree vs chemical shift in ppm of complexes $[RhCl(CO)(PR_3)_2]$ in $CDCl_3$.

PR ₃	Cone angle degree ¹	δ ³¹ P/ppm complex
47 PEt ₃	132	24.1
46 PMe ₂ Ph	122	-0.9
48 PMePh ₂	136	14.5
49 PEtPh ₂	140	27.4
36 PPh ₃	145	29.5
50 PCy ₃	170	37.1
51 PBu ¹ Et ₂	148	40.7
52 PBu ¹ ₂ Ph	170	59.5
53 PBu ¹ Bu ⁿ ₂	147	35.7

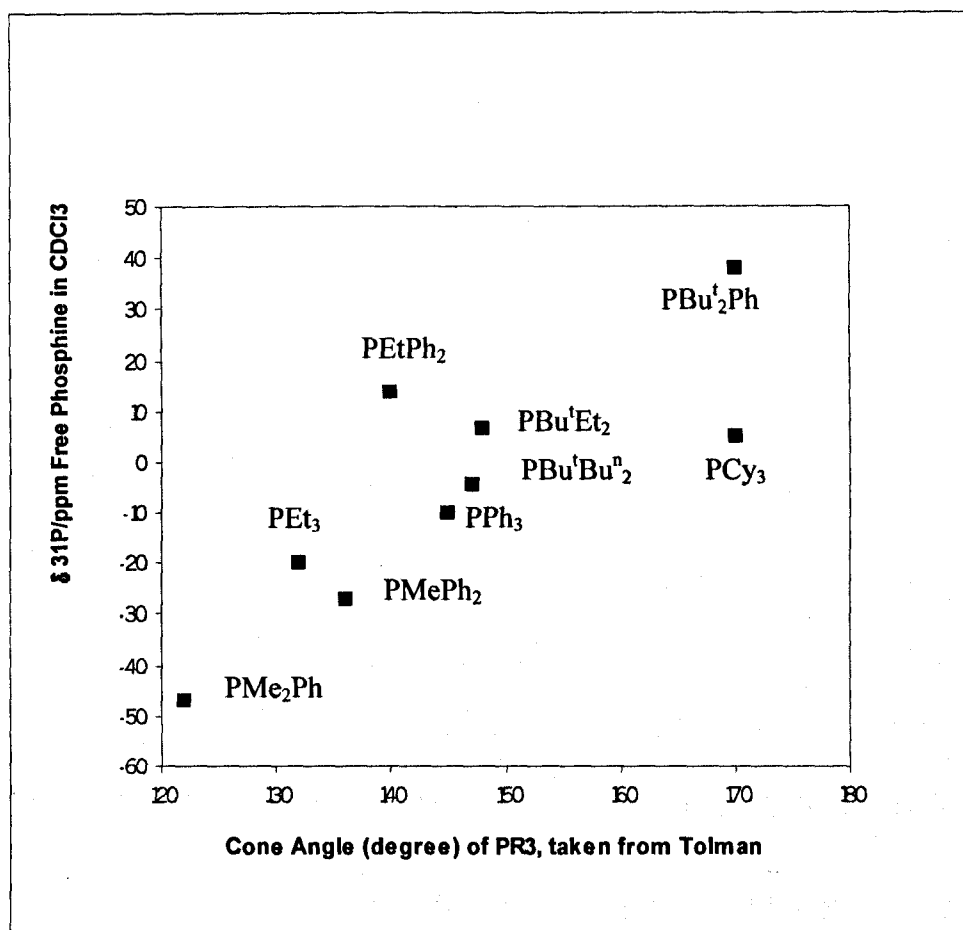


Table A3.2. Cone angle (degree) of used phosphines vs chemical shift in ppm of free phosphine in CDCl₃.

PR ₃	Cone angle ¹	$\delta^{31}\text{P}$ free PR ₃ ppm
47 PEt ₃	132	-20
46 PMe ₂ Ph	122	-47
48 PMePh ₂	136	-27
49 PEtPh ₂	140	14
36 PPh ₃	145	-10
50 PCy ₃	170	5.1
51 PBU ¹ Et ₂	148	6.86
52 PBU ₂ Ph	170	37.99
53 PBU ¹ BU ²	147	-4.38

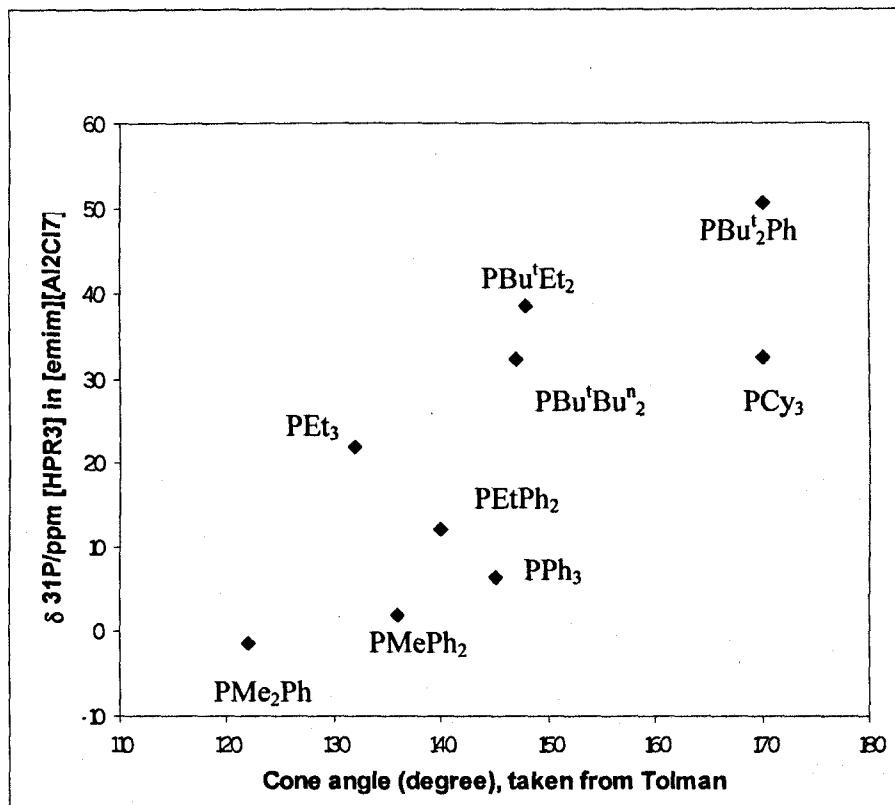


Table A3.3. Cone angle of used phosphines vs chemical shift in ppm of protonated species $[\text{HPR}_3]^+$ in $[\text{emim}][\text{Al}_2\text{Cl}_7]$, $x_{\text{AlCl}_3} = 0.67$.

PR ₃	Cone angle (degree) ¹	$\delta^{31}\text{P}$ [HPR ₃] ⁺
47 PEt ₃	132	22
46 PMe ₂ Ph	122	-1.4
48 PMePh ₂	136	1.9
49 PEtPh ₂	140	12.3
36 PPh ₃	145	6.5
50 PCy ₃	170	32.5
51 PBu ^t Et ₂	148	38.6
52 PBu ^t ₂ Ph	170	50.8
53 PBu ^t Bu ⁿ ₂	147	32.4

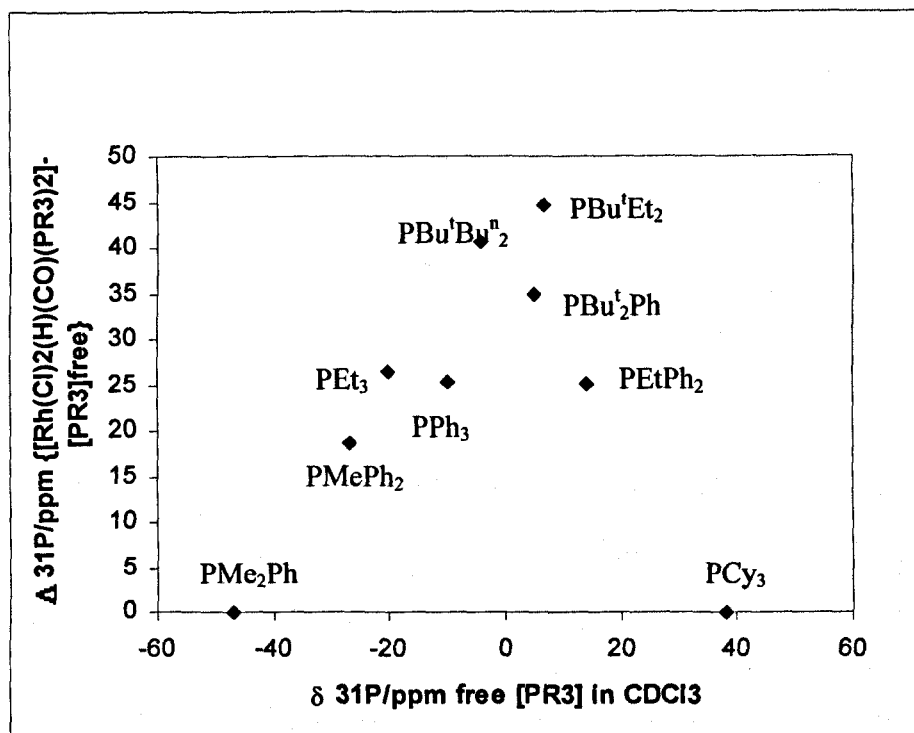


Table A3.4. Δ^* of $[\text{RhCl}_2\text{H}(\text{CO})(\text{PR}_3)_2]$ vs chemical shift in ppm of free $[\text{PR}_3]$ in CDCl_3 .

PR ₃	$\delta^{31}\text{P}$ free PR ₃ ppm	δ $[\text{RhCl}_2\text{H}(\text{CO})(\text{PR}_3)_2]$
47 PEt ₃	-20	26.5
46 PMe ₂ Ph	-47	3.59
48 PMePh ₂	-27	18.7
49 PEtPh ₂	14	25.1
36 PPh ₃	-10	25.3
50 PCy ₃	37	35
51 PBu ⁱ Et ₂	6.86	44.6
53 PBu ⁱ Bu ₂	-4.38	40.6
54 PBu ⁿ Pr ₂	-8.7	92.9

$$*\Delta = \delta^{31}\text{P/ppm} [\text{RhCl}_2\text{H}(\text{CO})(\text{PR}_3)_2] - \delta^{31}\text{P ppm} [\text{PR}_3] \text{ free in } \text{CDCl}_3$$

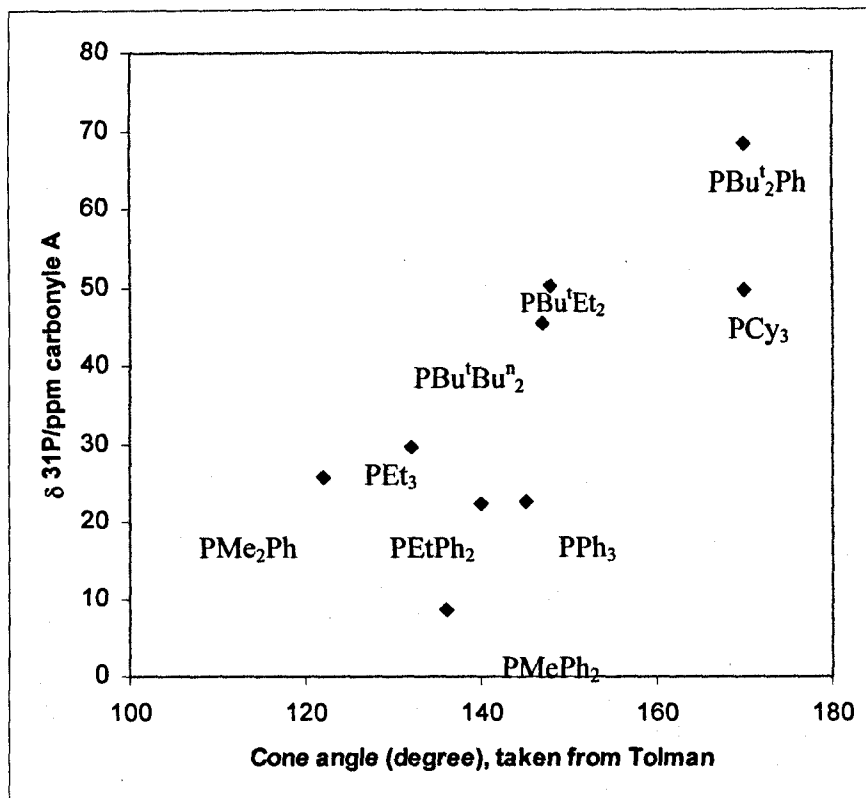


Table A3.5. Cone angle of used phosphines vs chemical shift in ppm of complexes $[\text{Rh}\{(\mu\text{-Cl})_2\text{AlCl}_2\}(\text{CO})_2(\text{PR}_3)]$, B.

PR ₃	Cone angle ¹	$\delta^{31}\text{P}$ Carbonyle B
47 PEt ₃	132	29.7
46 PMe ₂ Ph	122	25.6
48 PMePh ₂	136	8.6
49 PEtPh ₂	140	22.3
36 PPh ₃	145	22.7
50 PCy ₃	170	49.7
51 PBu ¹ Et ₂	148	50.1
52 PBu ² Ph	170	68.3
53 PBu ¹ Bu ⁿ ₂	147	45.5

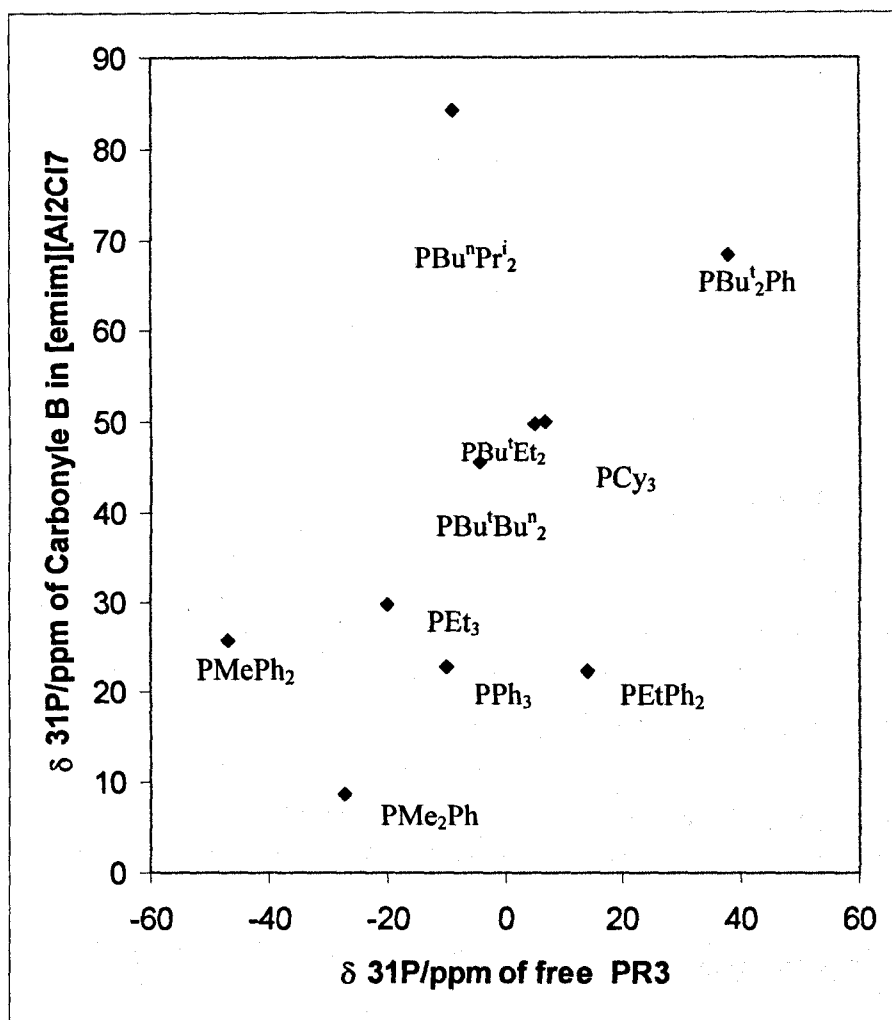


Table A3.6 Chemical shift of free phosphines vs chemical shift in ppm of complexes $[Rh\{(\mu\text{-Cl})AlCl_3\}(CO)_3(PR_3)]_B$.

PR ₃	δ ³¹ P free PR ₃ ppm	δ ³¹ P Carbonyl B
47 PEt ₃	-20	29.7
46 PMe ₂ Ph	-47	25.6
48 PMePh ₂	-27	8.6
49 PEtPh ₂	14	22.3
36 PPh ₃	-10	22.7
50 PCy ₃	37	49.7
51 PBu ^t Et ₂	6.86	50.1
52 PBu ^t ₂ Ph	37.99	68.3
53 PBu ^t Bu ⁿ ₂	-4.38	45.5

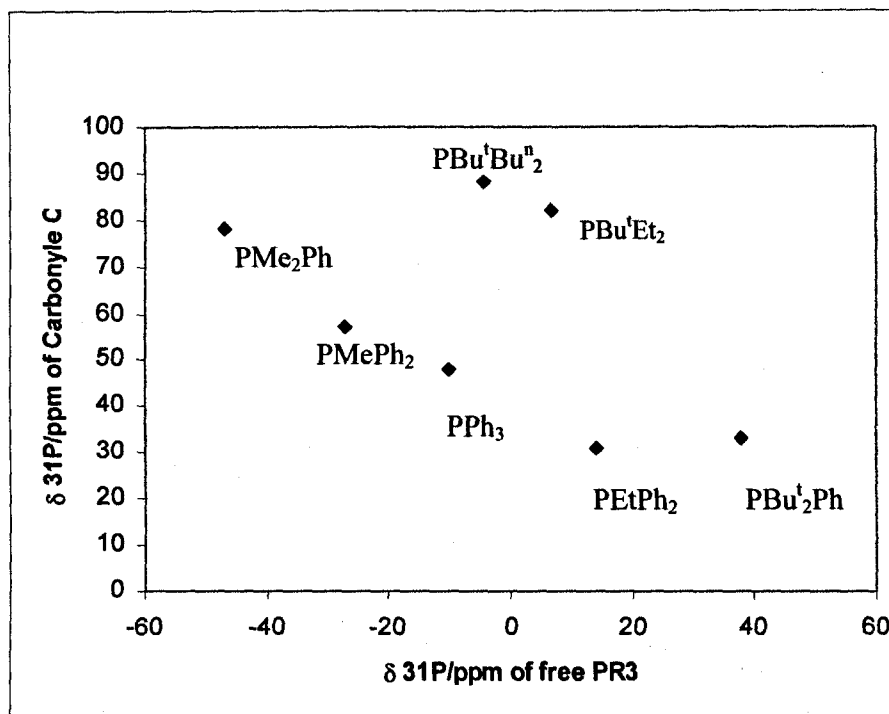


Table A3.7. Chemical shift of free phosphines vs chemical shift in ppm of complexes $[\text{Rh}\{\mu\text{-Cl}\}\text{AlCl}_3\}\text{(CO)}_3(\text{PR}_3)]$, C.

PR_3	$\delta^{31}\text{P}$ free PR_3 ppm	$\delta^{31}\text{P}$ Carbonyl C
46 PMe_2Ph	-47	31.8
48 PMePh_2	-27	30.4
49 PEtPh_2	14	45.5
36 PPh_3	-10	38.7
51 PBu^1Et_2	6.86	88.9
52 PBu^1Ph	37.99	70.2
53 $\text{PBu}^1\text{Bu}^n_2$	-4.38	84.9

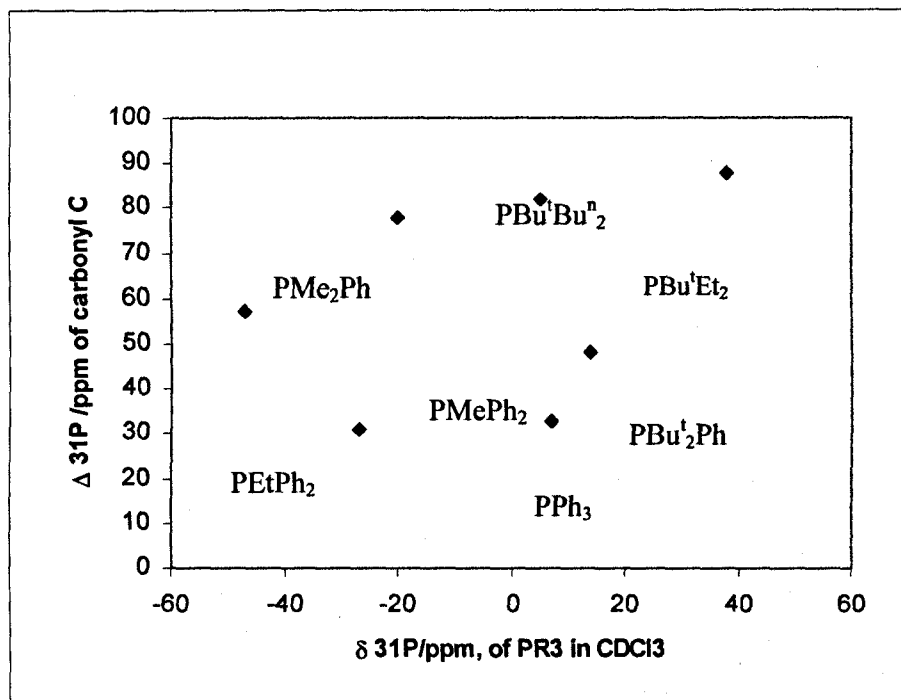


Table A3.8. Chemical shift of free PR₃ in CDCl₃ vs Δ^* in ppm of complexes $[\text{Rh}\{(\mu\text{-Cl})_2\text{AlCl}_2\}(\text{CO})_2(\text{PR}_3)]$, C.

PR ₃	Cone angle ¹	$\delta^{31}\text{P}$ Carbonyle C
46 PMe ₂ Ph	122	31.8
48 PMePh ₂	136	30.4
49 PEtPh ₂	140	45.5
36 PPh ₃	145	38.7
51 PBu ¹ Et ₂	148	88.9
52 PBu ² Ph	170	70.2
53 PBu ¹ Bu ⁿ ₂	147	84.9

$$*\Delta = \delta^{31}\text{P/ppm} [\text{Rh}\{(\mu\text{-Cl})_2\text{AlCl}_2\}(\text{CO})_2(\text{PR}_3)] \text{ in } [\text{emim}][\text{Al}_2\text{Cl}_7] - \delta^{31}\text{P/ppm free } [\text{PR}_3]$$

¹ C. A. Tolman, *Chem. Rev.*, 1977, 77, 313.

Appendix 4

*$^{31}\text{P}\{^1\text{H}\}$, ^1H and $^{103}\text{Rh}\{^1\text{H}\}$ NMR spectra of complexes **A**,
 $[\text{Rh}\{(\mu\text{-Cl})_2\text{AlCl}_2\}\{(\mu\text{-Cl})\text{AlCl}_3\}\text{H}(\text{CO})(\text{PR}_3)]$*

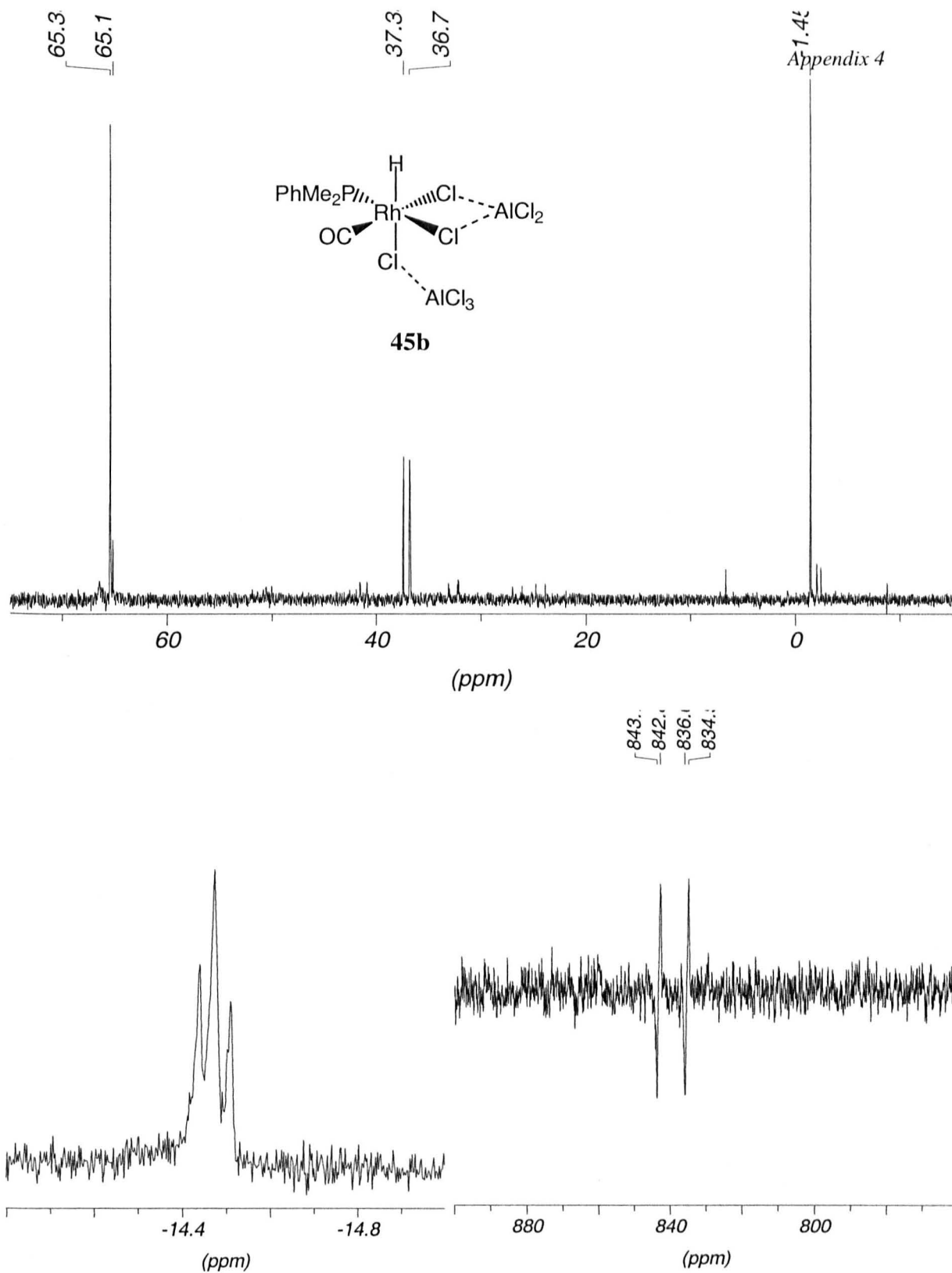


Fig. A4.1. Solution of [Rh(Cl)(CO)(PMe₂Ph)₂] in [emim][Al₂Cl₇]: a) ³¹P NMR; b) ¹H NMR; c) ¹⁰³Rh NMR.

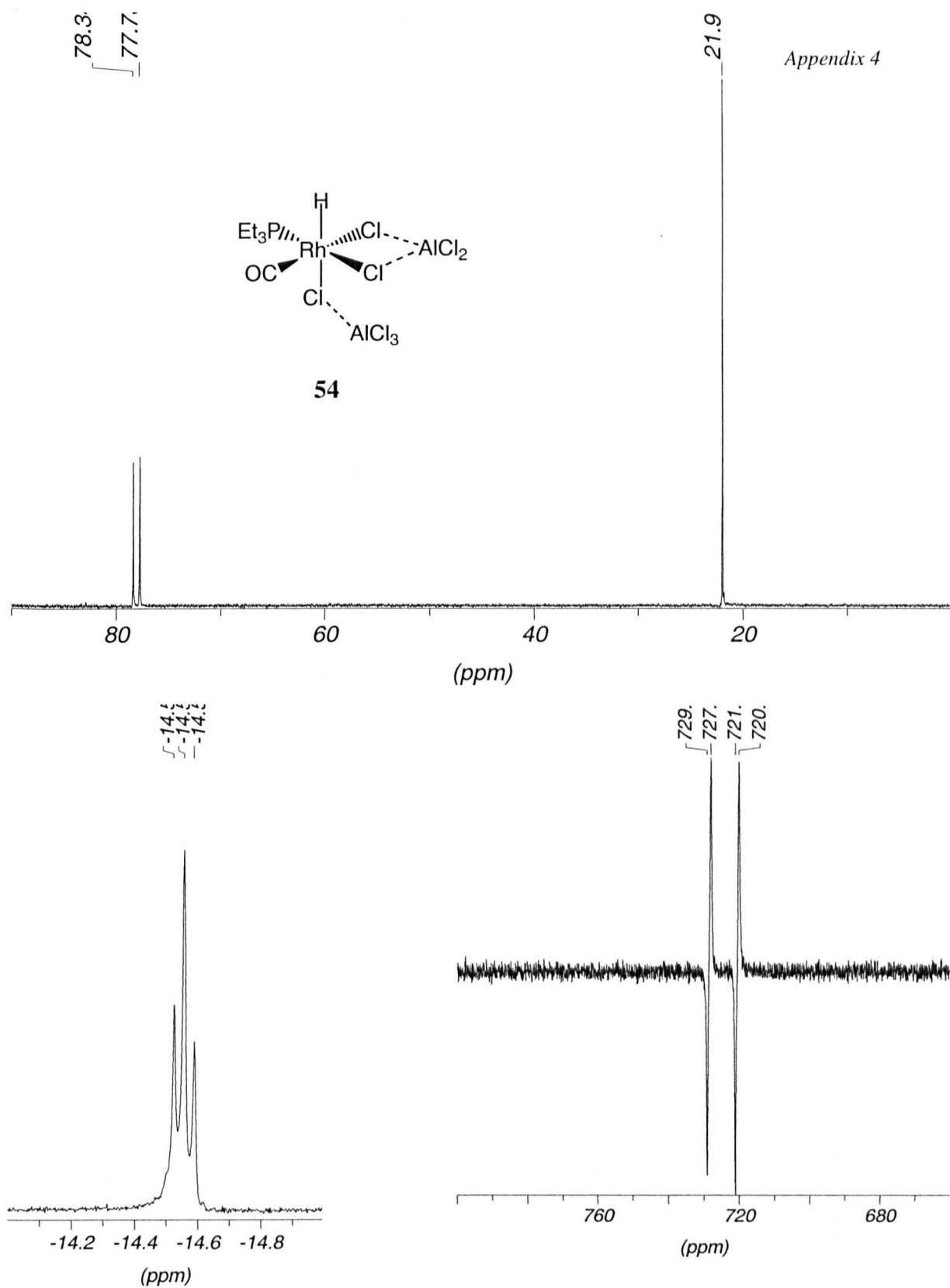


Fig. A4.2. Solution of $[\text{Rh}(\text{Cl})(\text{CO})(\text{PEt}_2)_2]$ in $[\text{emim}][\text{Al}_2\text{Cl}_7]$: a) ^{31}P NMR; b) ^1H NMR; c) ^{103}Rh NMR.

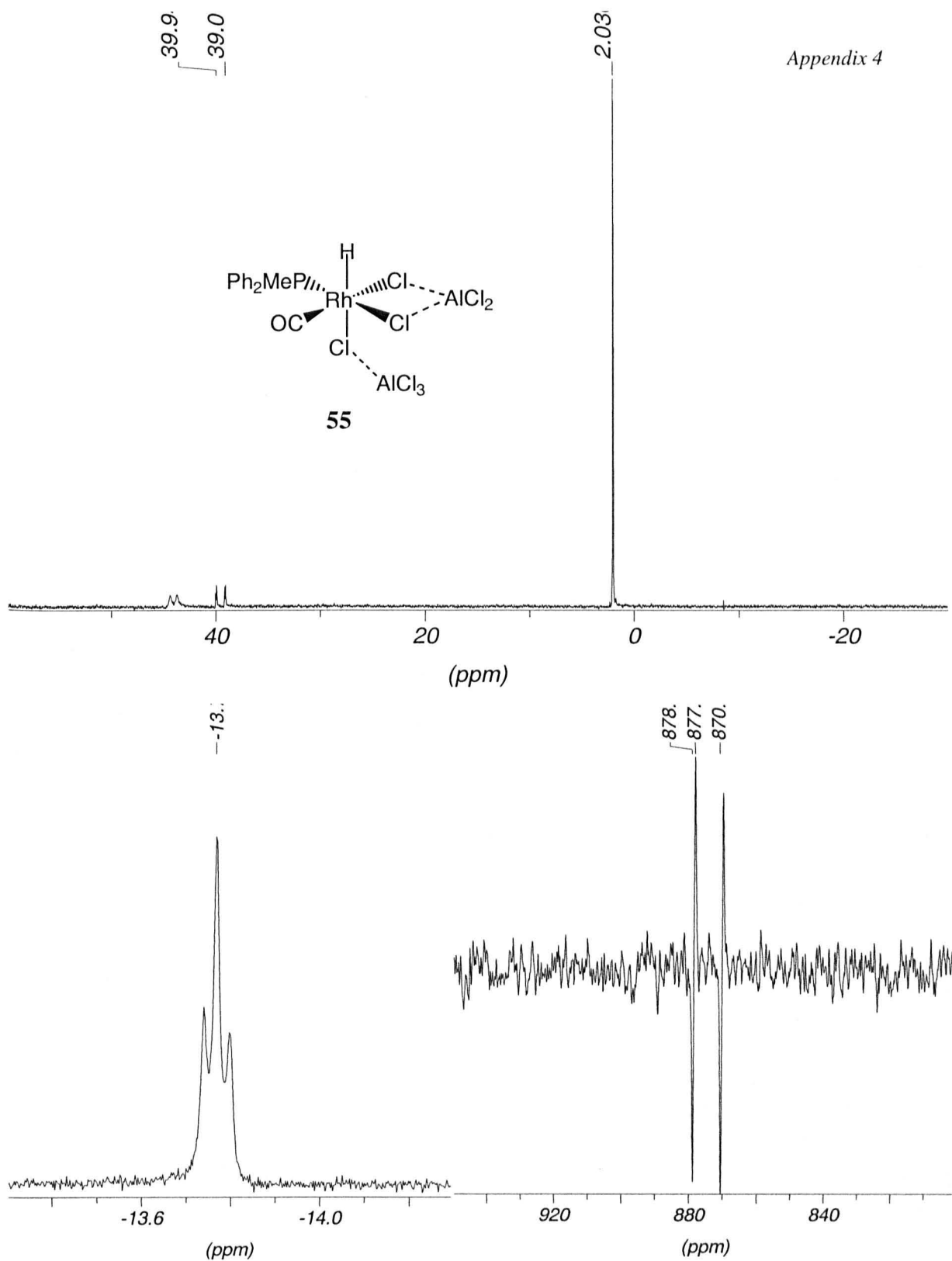


Fig. A4.3. Solution of $[\text{RhCl}(\text{CO})(\text{PMePh}_2)_2]$ in $[\text{emim}][\text{Al}_2\text{Cl}_7]$: a) ^{31}P NMR; b) ^1H NMR; c) ^{103}Rh NMR.

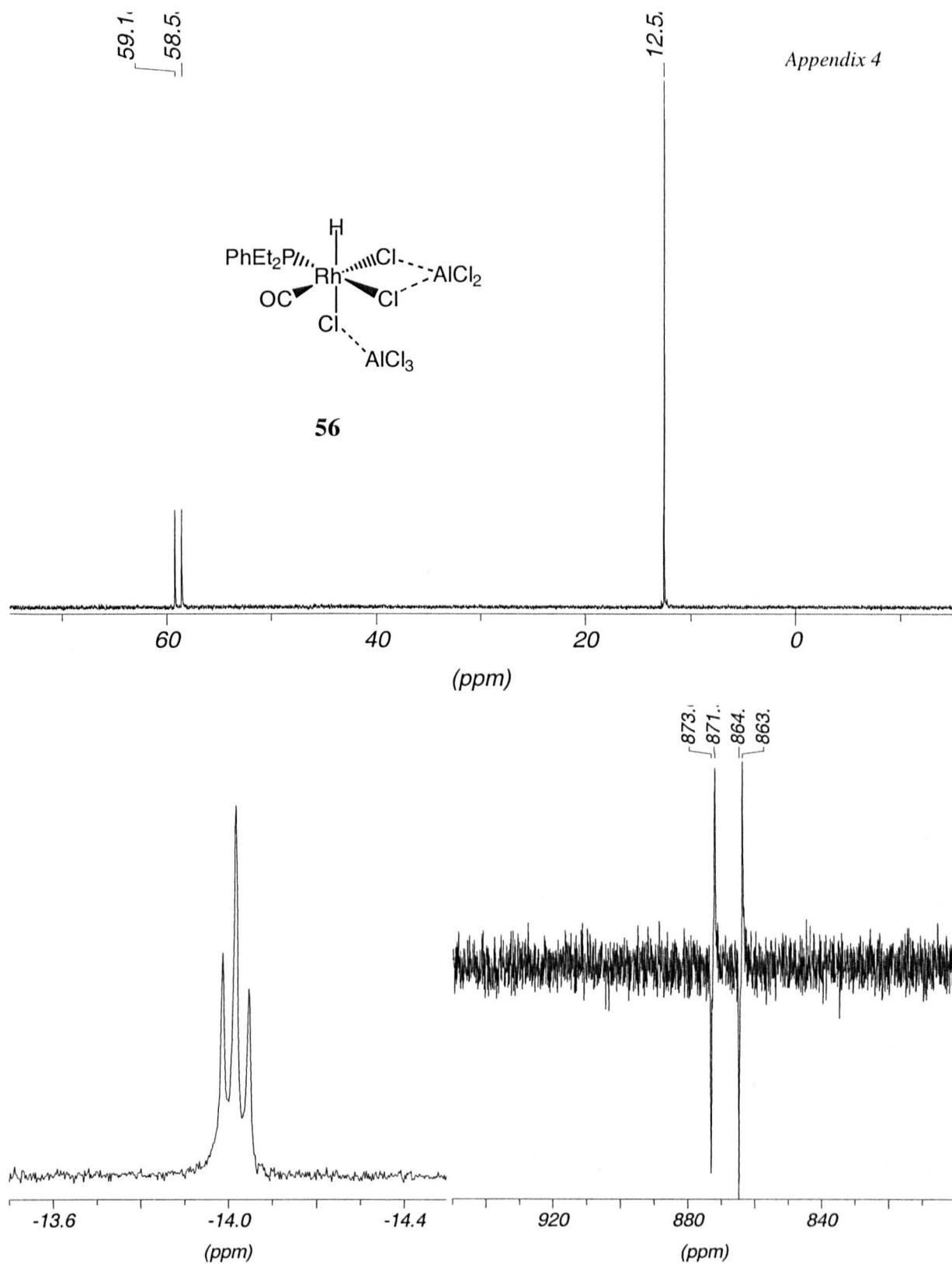


Fig. A4.4. Solution of $[\text{Rh}(\text{Cl})(\text{CO})(\text{PEt}_2\text{Ph})_2]$ in $[\text{emim}][\text{Al}_2\text{Cl}_7]$: a) ^{31}P NMR; b) ^1H NMR; c) ^{103}Rh NMR.

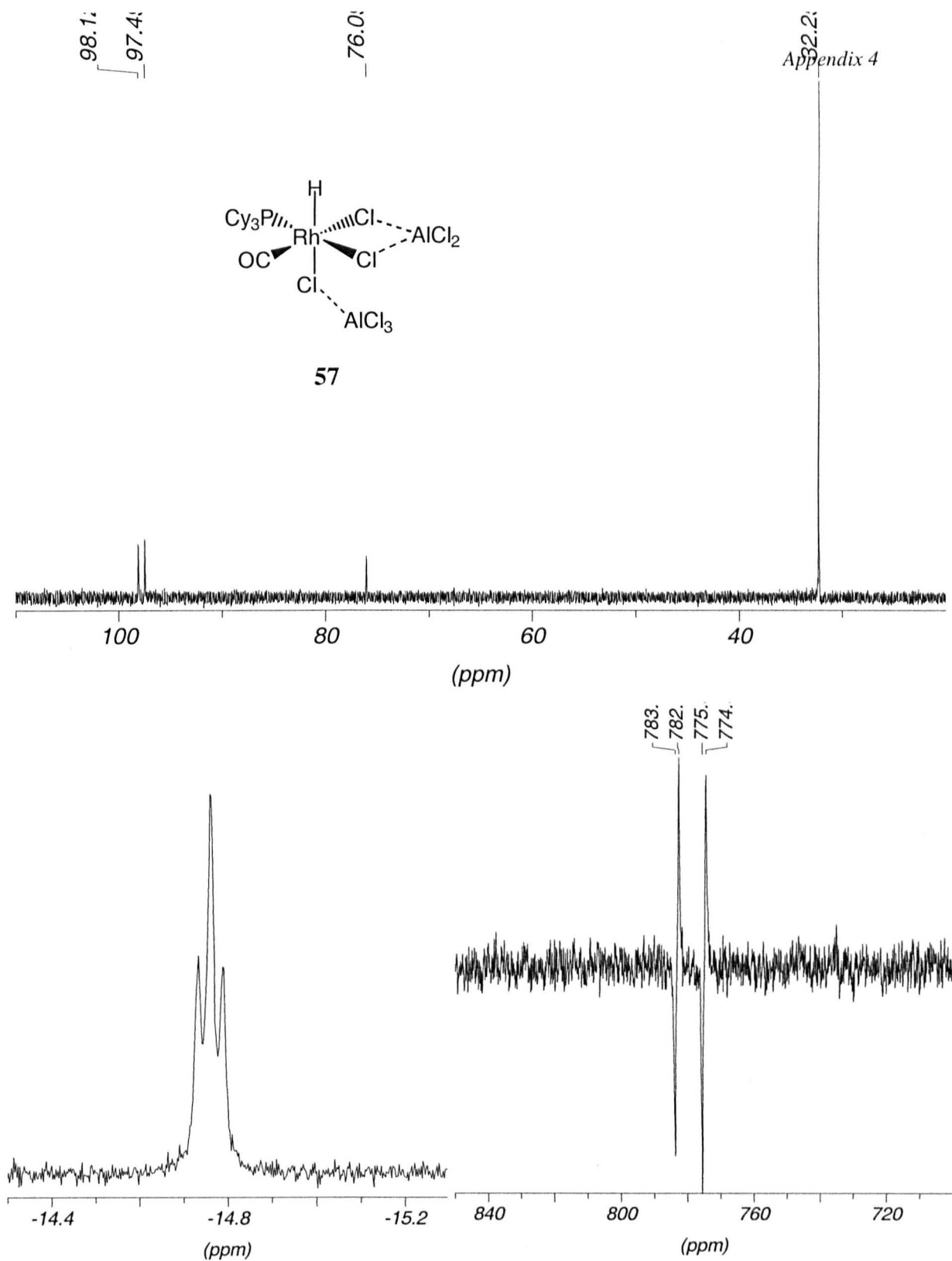


Fig. A4.5. Solution of $[\text{Rh}(\text{Cl})(\text{CO})(\text{PCy}_3)_2]$ in $[\text{emim}][\text{Al}_2\text{Cl}_7]$: a) ^{31}P NMR; b) ^1H NMR; c) ^{103}Rh NMR.

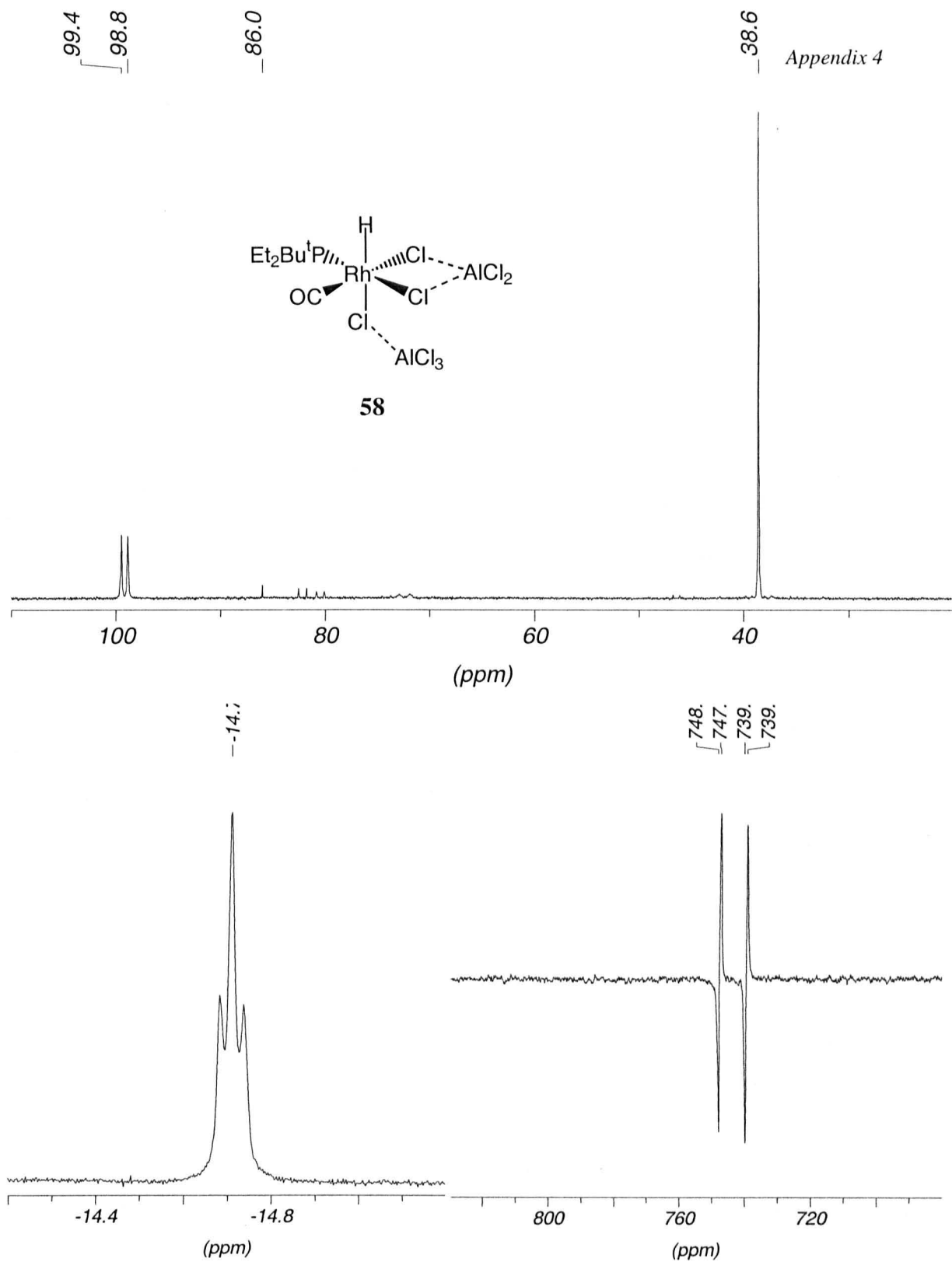


Fig. A4.5. Solution of $[\text{Rh}(\text{Cl})(\text{CO})(\text{P}^t\text{BuEt}_2)]$ in $[\text{emim}][\text{Al}_2\text{Cl}_7]$: a) ^{31}P NMR; b) ^1H NMR; c) ^{103}Rh NMR.

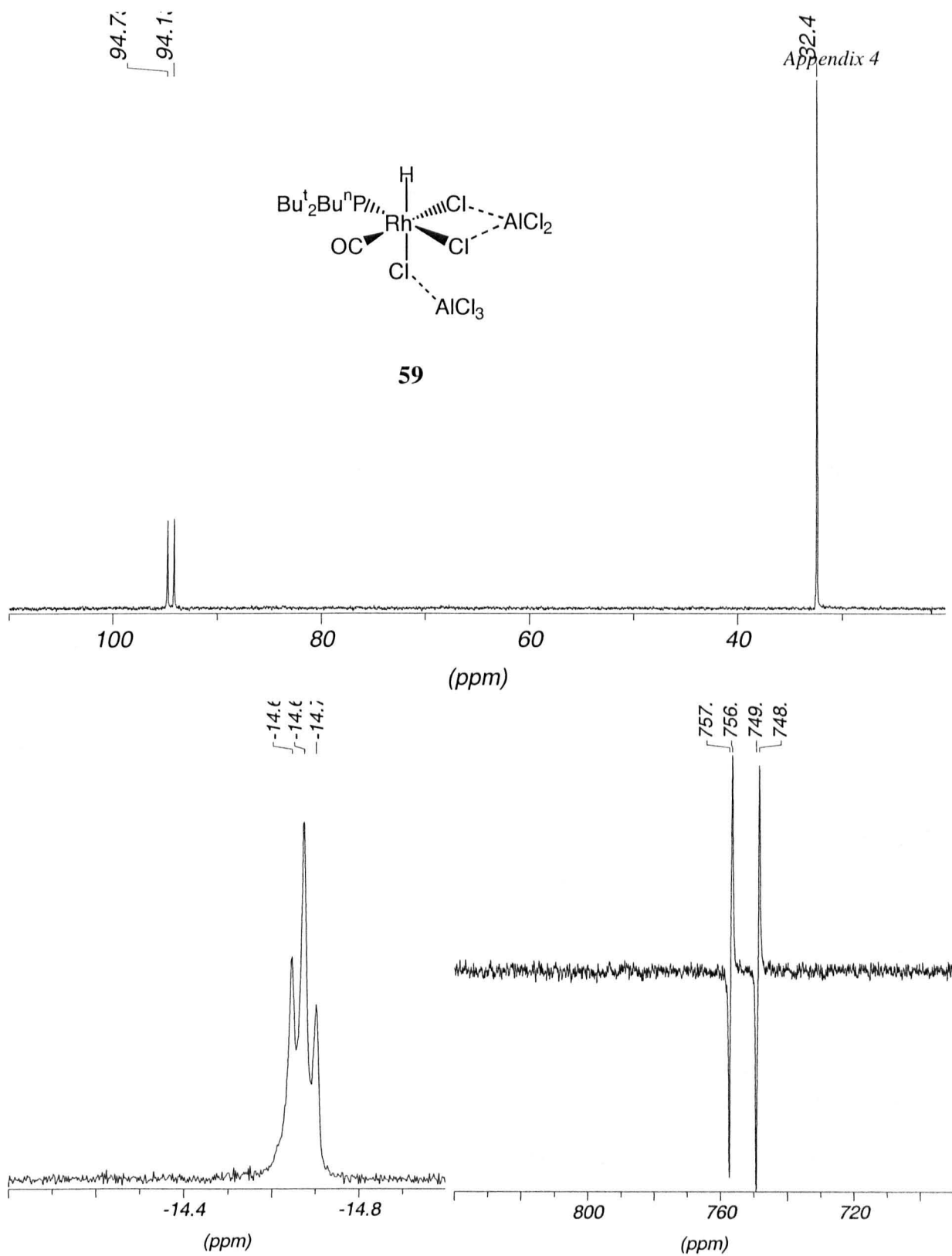


Fig. A4.6. Solution of $[\text{Rh}(\text{Cl})(\text{CO})(\text{PBu}^t\text{Bu}^2)]$ in $[\text{emim}][\text{Al}_2\text{Cl}_7]$: a) ^{31}P NMR; b) ^1H NMR; c) ^{103}Rh NMR.

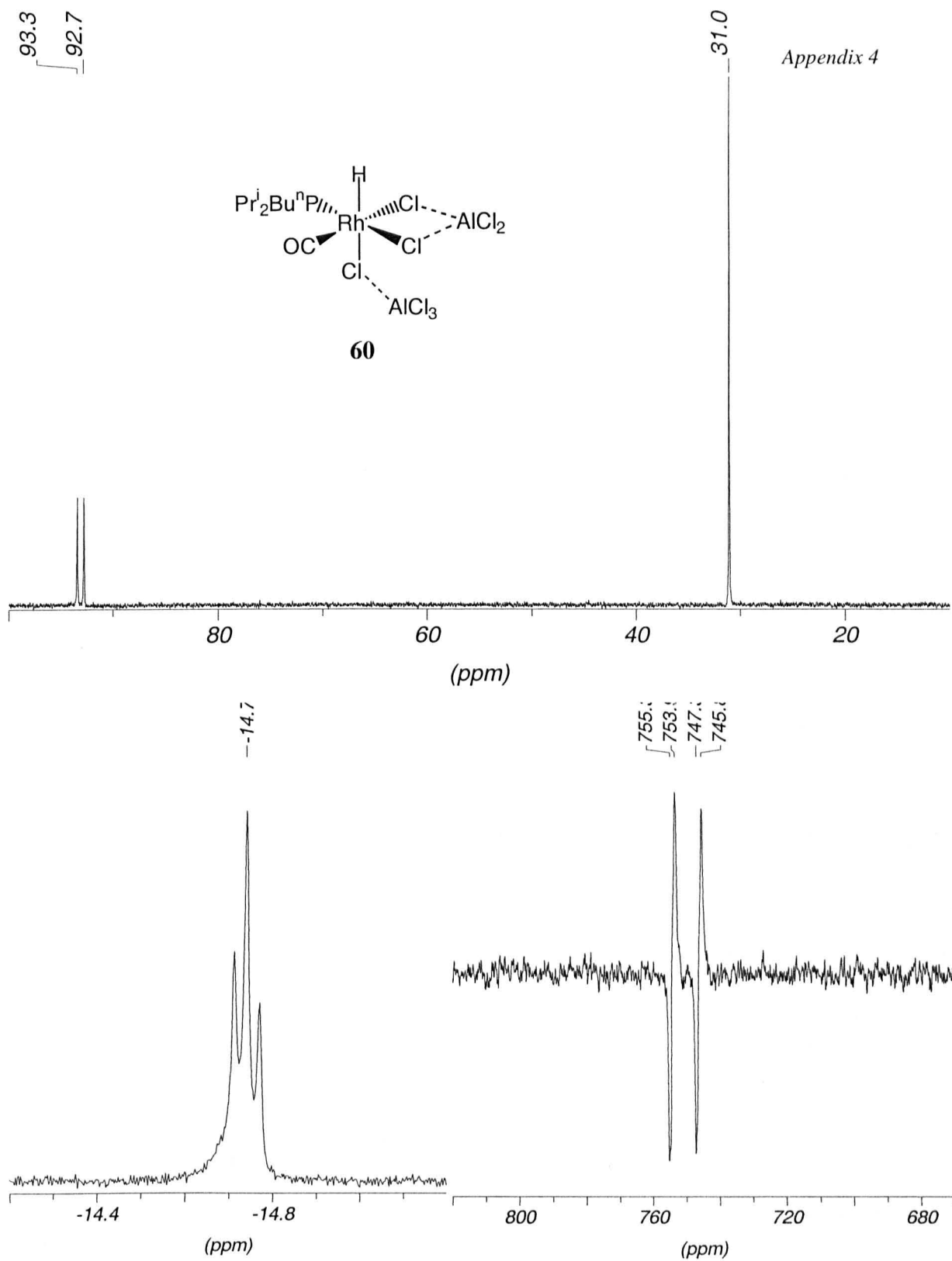


Fig. A7.7. Solution of $[\text{Rh}(\text{Cl})(\text{CO})(\text{P}^i\text{Bu}^n\text{Pr}_2)_2]$ in $[\text{emim}][\text{Al}_2\text{Cl}_7]$: a) ^{31}P NMR; b) ^1H NMR; c) ^{103}Rh NMR.